NEURO-OTOLOGY EDITOR'S PICK 2022

EDITED BY: Michael Strupp
PUBLISHED IN: Frontiers in Neurology

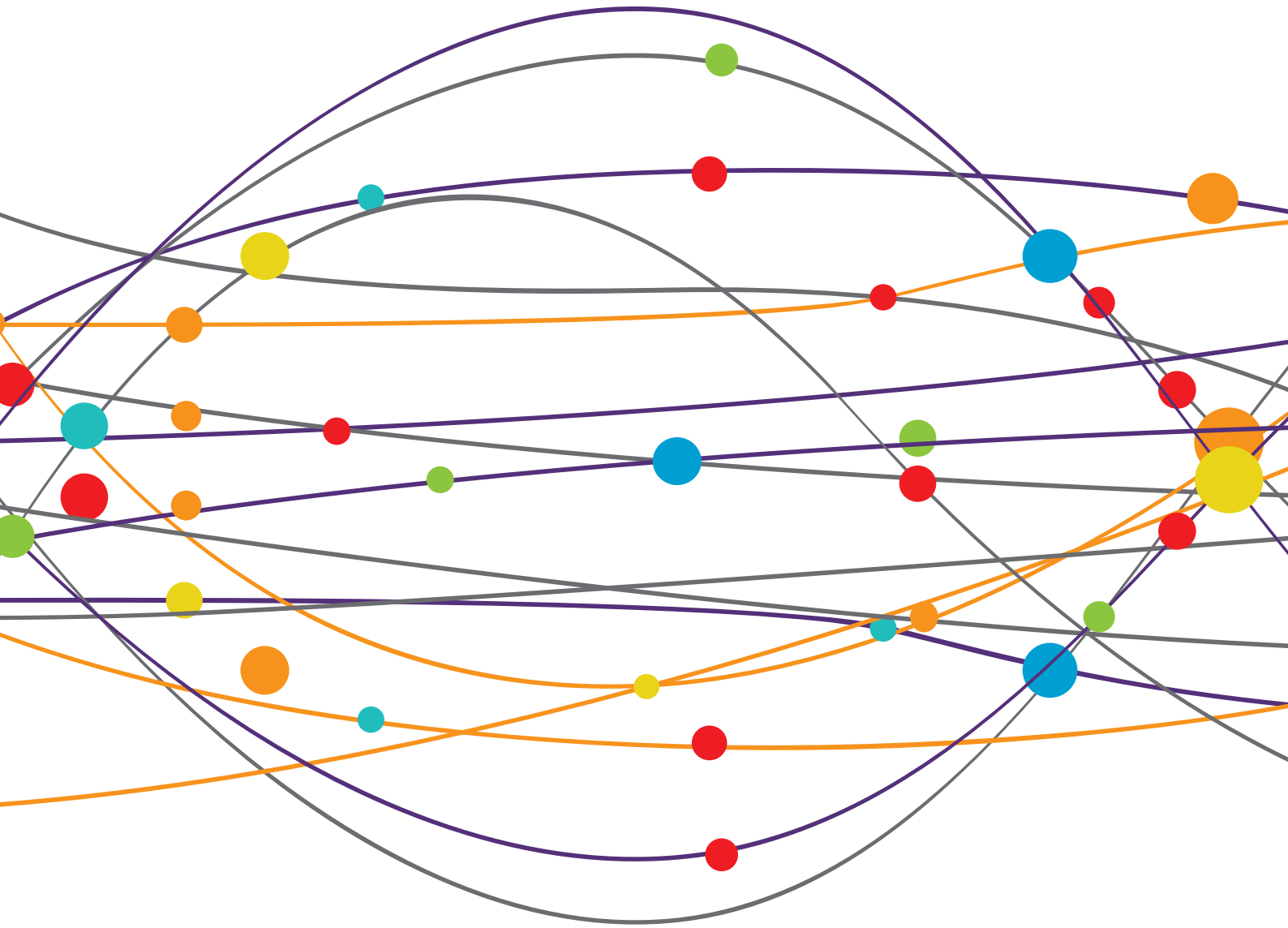

frontiers Research Topics

ISSN 1664-8714
ISBN 978-2-88976-703-8
DOI 10.3389/978-2-88976-703-8

About Frontiers

Frontiers is more than just an open-access publisher of scholarly articles: it is a pioneering approach to the world of academia, radically improving the way scholarly research is managed. The grand vision of Frontiers is a world where all people have an equal opportunity to seek, share and generate knowledge. Frontiers provides immediate and permanent online open access to all its publications, but this alone is not enough to realize our grand goals.

Frontiers Journal Series

The Frontiers Journal Series is a multi-tier and interdisciplinary set of open-access, online journals, promising a paradigm shift from the current review, selection and dissemination processes in academic publishing. All Frontiers journals are driven by researchers for researchers; therefore, they constitute a service to the scholarly community. At the same time, the Frontiers Journal Series operates on a revolutionary invention, the tiered publishing system, initially addressing specific communities of scholars, and gradually climbing up to broader public understanding, thus serving the interests of the lay society, too.

Dedication to Quality

Each Frontiers article is a landmark of the highest quality, thanks to genuinely collaborative interactions between authors and review editors, who include some of the world's best academicians. Research must be certified by peers before entering a stream of knowledge that may eventually reach the public - and shape society; therefore, Frontiers only applies the most rigorous and unbiased reviews.
Frontiers revolutionizes research publishing by freely delivering the most outstanding research, evaluated with no bias from both the academic and social point of view. By applying the most advanced information technologies, Frontiers is catapulting scholarly publishing into a new generation.

What are Frontiers Research Topics?

Frontiers Research Topics are very popular trademarks of the Frontiers Journals Series: they are collections of at least ten articles, all centered on a particular subject. With their unique mix of varied contributions from Original Research to Review Articles, Frontiers Research Topics unify the most influential researchers, the latest key findings and historical advances in a hot research area! Find out more on how to host your own Frontiers Research Topic or contribute to one as an author by contacting the Frontiers Editorial Office: frontiersin.org/about/contact

NEURO-OTOLOGY EDITOR'S PICK 2022

Topic Editor:
Michael Strupp, Ludwig Maximilian University of Munich, Germany

Citation: Strupp, M., ed. (2022). Neuro-Otology Editor's Pick 2022. Lausanne: Frontiers Media SA. doi: 10.3389/978-2-88976-703-8

Table of Contents

frontiers in Neurology

ORIGINAL RESEARCH
published: 22 January 2020
doi: 10.3389/fneur.2019.01424

Rare Variants of Putative Candidate Genes Associated With Sporadic Meniere's Disease in East Asian Population

*Eun Hye Oh[1], Jin-Hong Shin[1], Hyang-Sook Kim[1], Jae Wook Cho[1], Seo Young Choi[2], Kwang-Dong Choi[2], Je-Keun Rhee[3], Seowhang Lee[4], Changwook Lee[4] and Jae-Hwan Choi[1]**

[1] Department of Neurology, Research Institute for Convergence of Biomedical Science and Technology, Pusan National University School of Medicine, Pusan National University Yangsan Hospital, Yangsan, South Korea, [2] Department of Neurology, Pusan National University Hospital, Pusan National University School of Medicine and Biomedical Research Institute, Busan, South Korea, [3] School of Systems Biomedical Science, Soongsil University, Seoul, South Korea, [4] Department of Biological Sciences, School of Life Sciences, Ulsan National Institute of Sciences and Technology, Ulsan, South Korea

OPEN ACCESS

Edited by:
Jose Antonio Lopez-Escamez, Andalusian Autonomous Government of Genomics and Oncological Research (GENYO), Spain

Reviewed by:
Teresa Requena, University of Edinburgh, United Kingdom
Barbara Vona, University of Tübingen, Germany

***Correspondence:**
Jae-Hwan Choi
rachelbolan@hanmail.net

Specialty section:
This article was submitted to Neuro-Otology, a section of the journal Frontiers in Neurology

Received: 06 November 2019
Accepted: 31 December 2019
Published: 22 January 2020

Citation:
Oh EH, Shin J-H, Kim H-S, Cho JW, Choi SY, Choi K-D, Rhee J-K, Lee S, Lee C and Choi J-H (2020) Rare Variants of Putative Candidate Genes Associated With Sporadic Meniere's Disease in East Asian Population. Front. Neurol. 10:1424. doi: 10.3389/fneur.2019.01424

Objectives: The cause of Meniere's disease (MD) is unclear but likely involves genetic and environmental factors. The aim of this study was to investigate the genetic basis underlying MD by screening putative candidate genes for MD.

Methods: Sixty-eight patients who met the diagnostic criteria for MD of the Barany Society were included. We performed targeted gene sequencing using next generation sequencing (NGS) panel composed of 45 MD-associated genes. We identified the rare variants causing non-synonymous amino acid changes, stop codons, and insertions/deletions in the coding regions, and excluded the common variants with minor allele frequency >0.01 in public databases. The pathogenicity of the identified variants was analyzed by various predictive tools and protein structural modeling.

Results: The average read depth for the targeted regions was 1446.3-fold, and 99.4% of the targeted regions were covered by 20 or more reads, achieving the high quality of the sequencing. After variant filtering, annotation, and interpretation, we identified a total of 15 rare heterozygous variants in 12 (17.6%) sporadic patients. Among them, four variants were detected in familial MD genes (*DTNA*, *FAM136A*, *DPT*), and the remaining 11 in MD-associated genes (*PTPN22*, *NFKB1*, *CXCL10*, *TLR2*, *MTHFR*, *SLC44A2*, *NOS3*, *NOTCH2*). Three patients had the variants in two or more genes. All variants were not detected in our healthy controls ($n = 100$). No significant differences were observed between patients with and without a genetic variant in terms of sex, mean age of onset, bilaterality, the type of MD, and hearing threshold at diagnosis.

Conclusions: Our study identified rare variants of putative candidate genes in some of MD patients. The genes were related to the formation of inner ear structures, the immune-associated process, or systemic hemostasis derangement, suggesting the multiple genetic predispositions in the development of MD.

Keywords: Meniere's disease, endolymphatic hydrops, gene, whole-exome sequencing, rare variant

INTRODUCTION

Meniere's disease (MD) is a clinical syndrome that consists of episodes of spontaneous vertigo usually associated with unilateral fluctuating sensorineural hearing loss (SNHL), tinnitus and aural fullness (1). Almost 150 years have elapsed since Prosper Meniere first described the clinical entity, but unfortunately, the exact pathophysiology of this condition is yet to be fully understood. Histopathological studies in human temporal bones have found endolymphatic hydrops (EH) in most patients with MD, but the origin of the EH is unknown (2).

MD is considered a multifactorial disorder associated with the various factors including anatomical abnormalities, infections, allergens, and autoimmune disorders. Most MD cases are sporadic, but familial MD is observed in 8–10% of sporadic cases, suggesting genetic susceptibility to the development of MD (3–5). To search a candidate gene associated with MD, many approaches including linkage analysis, case-control study or the sequencing of selected genes have been previously used (6–10). A variety of common single nucleotide polymorphisms (SNPs) have been meaningfully detected in patients with MD (11–35) (**Supplementary Table 1**). Most of them were the genes related to the inflammation or regulating the ionic composition and water transport of the inner ear. However, the effect size of these common variants was small (odds ratio < 2). Furthermore, a common variant could not reflect the entire heritability of MD. Recent studies using whole-exome sequencing (WES) for Spanish families with MD have identified probably pathogenic rare variants in candidate genes including *FAM136A*, *DTNA*, *PRKCB*, *DPT,* and *SEMA3D* (36–38). Since these genes encode proteins that may be relevant to the formation or maintaining of inner ear structures, the identified rare variants are expected to account for the genetic contribution of MD, but further replicative studies in distinct populations are needed. Thus, the aim of this study was to explore the previously proposed MD-associated genes using targeted NGS to investigate the genetic basis underlying MD.

MATERIALS AND METHODS

Subjects

We recruited 68 unrelated patients with definite MD who visited a tertiary dizziness clinic from 2015 to 2018. The diagnosis of definite MD was made based on the criteria established by the Classification Committee of the Barany Society (1). All patients met the following criteria: (1) Two or more spontaneous episodes of vertigo, each lasting 20 min to 12 h, (2) Audiometrically documented low- to medium-frequency sensorineural hearing loss in the affected ear on at least one occasion before, during, or after one of the episodes of vertigo, (3) Fluctuating aural symptoms (hearing, tinnitus, or earfullness) in the affected ear, (4) Not better accounted for by another vestibular diagnosis. A brain MRI was performed to rule out any neurological lesions. The patients included 38 males and 30 females with age ranging from 28 to 89 years (mean age 60.2 $\pm$ 12.0 years). The mean age of onset was 57.5 $\pm$ 11.3 years. Most patients ($n = 63$, 93%) had a unilateral MD. Six had at least one family member with a history of MD-like symptoms. According to the phenotype, 18 (26%) were classified as delayed MD based on a previous history of sensorineural hearing loss (months or years) before the onset of vertigo episodes, while the others ($n = 50$) showed classic MD phenotype (39).

All experiments followed the tenets of the Declaration of Helsinki, and informed consents were obtained after the nature and possible consequences of this study had been explained to the participants. This study was approved by the institutional review boards of Pusan National University Yangsan Hospital.

Targeted Next-Generation Sequencing

Targeted genes were collected from the literature review. The keywords "Meniere's disease" and "gene" were used to search the MD-associated genes in PubMed, resulting in 101 papers when this study was initiated (August, 2017). After excluding the genes showing no correlation with MD, we selected 45 genes used for targeted NGS (**Supplementary Table 1**). The selected genes were largely classified into two categories as follow: (1) "familial MD gene," the pathogenic genes for familial MD identified by high-throughput sequencing (36–38); (2) "MD-associated gene," the candidate genes contributing to the development of MD demonstrated by association study or network-based study (11–35, 40). The MD gene panel was designed by the Suredesign webtool (Agilent) to cover the exons and 20 bp in the flanking regions.

Genomic DNA was extracted from the blood sample of all patients. For the generation of standard exome capture libraries, we used the Agilent SureSelect Target Enrichment protocol for Illumina paired-end sequencing library (ver. B.3, June 2015) with 1 μg input DNA. The quantification of DNA and the DNA quality was measured by PicoGreen and Nanodrop. The qualified genomic DNA sample was randomly fragmented by Covaris followed by adapter ligation, purification, hybridization, and PCR. Captured libraries were subjected to Agilent 2100 Bioanalyzer to estimate the quality and were loaded on to the Illumina HiSeq2500 (San Diego, USA) according to the manufacturer's instructions. Raw image files were processed by HCS1.4.8 for base-calling with default parameters and the sequences of each individual were generated as 100 bp paired-end reads. Sequence reads were aligned to the human reference genome sequence (GRCh37.3, hg19) using the Burrows-Wheeler Aligner (BWA, version 0.7.12). PCR duplicate reads were marked and removed with Picard tools (version 1.92). Genome Analysis Toolkit (GATK, version 2.3-9) was used for indel realignment and base recalibration. Variation annotation and interpretation analysis were performed using SnpEff (version 4.2).

Identification of Rare or Novel Variants

To identify the possible pathogenic variants, we first filtered out synonymous and non-coding variants, and extracted the variants causing non-synonymous amino acid changes, stop codons, in-frame insertions/deletions in coding regions, or changes to splice site sequences in exon/intron boundaries. Then, common variants with a minor allele frequency (MAF) > 0.01 that represented in dbSNP147, the Exome Aggregation Consortium (ExAC), gnomAD, 1,000 Genomes Project, and NHLBI GO

Exome Sequencing Project (ESP) 6500 were excluded. The pathogenicity of the non-synonymous variants was analyzed using Sorting Intolerant From Tolerant (SIFT), Likelihood Ratio Test (LRT), Polyphen2, MutationTaster, Functional Analysis Through Hidden Markov Models (FATHMM), and Combined Annotation Dependent Depletion (CADD) phred score. The higher CADD phred scores indicate that a variant is more likely to have deleterious effects (41). The strength of ectopic splicing sites created by intronic variants was evaluated by the Human Splicing Finder program. All rare and novel variants were annotated for previously reported disease-causing variants using the Human Gene Mutation Database. All variants were confirmed by Sanger DNA sequencing, and were screened in 100 normal controls.

Protein Structural Modeling

The structural modeling of missense variants of *PTPN22* (PDB accession code: 2P6X), *MTHFR* (PDB accession code: 6FCX), *NOTCH2* (PDB accession code: 2OO4) and *CXCL10* (PDB accession code: 1O80) were generated using I-TASSER server. The confidence scores (C-scores) indicating significance of threading template alignments and the convergence parameters of modeling simulation were calculated for each predicted model to estimate the quality of model (42). The calculated C-scores of *PTPN22*, *MTHFR*, *NOTCH2*, *CXCL10* were 1.61, 0.07, 0.36, 0.34, respectively. The best model was selected based on the template modeling score (TM-score) and the root mean square deviation (RMSD) value indicating proper topology of the mutant model compared to the PDB template. The optimization of predicted models was performed by PyMOL (The PyMOL Molecular Graphics System, Version 2.0 Schrödinger, LLC.), and each mutant model was aligned with that of wild type to compare three-dimensional structures.

Statistical Analyses

To investigate the association between the genetic variants and disease manifestation, we calculated the odds ratio for each variant using Fisher's exact test from the allele frequency of ExAC and gnomAD database as controls (total population and East Asian population). *P*-values were corrected for multiple testing by the total amount of variants found for each gene following Bonferroni approach. We also compared the clinical characteristics between patients with and without rare variants. Continuous variables (mean age, age of onset, and hearing threshold at diagnosis) were compared using the Mann-Whitney test, and categorical variables (sex, bilaterality, the type of MD, and the presence of family history) using Fisher's exact test. A statistical analysis was performed using SPSS software (SPSS Inc., Chicago, IL, USA) and a $p < 0.05$ was considered as significant.

RESULTS

The average read depth for the targeted regions was 1446.3-fold, and 99.4% of the targeted regions were covered by 20 or more reads, achieving the high quality of the sequencing (**Supplementary Table 2**). After variant filtering, annotation, and interpretation, we identified a total of 15 rare heterozygous variants (two novel and 13 rare variants) in 12 (17.6%) sporadic patients (**Table 1**). Among them, four variants were detected in familial MD gene, and the remaining 11 in MD-associated gene. Three patients (P-29, P-60, P-66) had the variants in two or more genes. All variants were not detected in our healthy controls ($n = 100$).

Variants in Familial MD Genes

We identified one novel and three rare heterozygous variants in three familial MD genes. Two variants were detected in *DTNA*. One was a rare variant affecting splice acceptor site located in intron 8 (P-31: c.1002-4A > G, **Figure 1A**). Human Splicing Finder predicted that this variant will alter the splice site and make new splice sites resulting in three bases longer on exon 9. Another was a nonsense variant resulting in a premature stop codon (P-66: c.2094G > A, p.W698X, **Figure 1B**). It was absent in all public database, and predicted to be deleterious by MutationTaster and CADD scores. The other rare variants were detected in *FAM136A* (P-29: c.238G > T, p.A80S, **Figure 1C**) and *DPT* (P-13: c.16C > T, p.L6F, **Figure 1D**). Both were a missense variant which a single nucleotide change results in a codon that codes for a different amino acid. Of them, the variant in *DPT* changed highly conserved amino acid and was predicted as protein-damaging potential by three prediction tools (Polyphen2, LRT, MutationTaster).

Variants in MD-Associated Genes

We identified one novel and 10 rare heterozygous variants in eight MD-associated genes. Interestingly, possibly pathogenic variants of *PTPN22* were detected in three unrelated patients. Two were truncated variants caused by premature stop codon (P-60: c.829G > T, p.E277X, **Figure 2A**) or single base deletion (P-65: c.1356delT, p.F452Lfs*3, **Figure 2B**). The nonsense variant was predicted to be deleterious by LRT, MutationTaster and CADD score. The remaining one was a missense variant with protein-damaging potential predicted by all prediction tools (P-26: c.205A > G, p.S69G, **Figure 2C**). Protein structural modeling predicted that p.S69G variant may disrupt the positions of surrounding residues (p.F68, p.N87, p.K90, and p.Q267) by steric hindrance effects, and eventually may affect the enzymatic activity of PTPN22 (**Figure 2D**).

We also detected two missense variants of *MTHFR* in three unrelated patients (P-5 and P-35: c.136C > T, p.R46W, **Figure 3A**; P-66: c.742A > G, p.I248V, **Figure 3B**). They were considered likely pathogenic by four of the prediction tools. Protein structural modeling revealed that p.R46W variant may cause breakage of salt bridges with surrounding residues (p.D188, p.D191, and p.D223), resulting in destabilizing the β-strand (β5and β6 **Figure 3C**). On the other hand, p.I248V variant showed no discernible differences when the secondary structure as well as surrounding residue orientation were analyzed.

The other five missense variants had protein-damaging potential predicted by at least one prediction tool: *SLC44A2* (P-29: c.761G > A, p.R254H, **Figure 4A**), *NOS3* (P-60: c.2207G > A, p.R736Q, **Figure 4B**), *NFKB1* (P-49: c.1799A > C, p.E600A, **Figure 4C**), *NOTCH2* (P-63: c.4688G > A, p.R1563H, **Figure 4E**), and *CXCL10* (P-29: c.85C > T, p.R29C, **Figure 4F**).

TABLE 1 | Identified rare variants in putative candidate genes associated with Meniere's disease.

Gene	mRNA	Protein	Variant effect	Patient's ID	dbSNP	ExAC MAF	gnomAD MAF	*In silico* prediction					CADD phred score
								SIFT	Polyphen	LRT	Mutation taster	FATHMM	
Familial MD genes													
DTNA	c.1002-4A > G	(–)	Aberrant splicing	P-31	rs369005625	0.00018	0.00025	(–)	(–)	(–)	(–)	(–)	21.8
DTNA	c.2094G > A	p.Trp698*	Nonsense	P-66	(–)	0	0	(–)	(–)	U	D	(–)	44
FAM136A	c.238G > T	p.Ala80Ser	Missense	P-29	rs199565792	0.00009	0.00005	T	B	N	N	(–)	18.63
DPT	c.16C > T	p.Leu6Phe	Missense	P-13	rs192608693	0.00005	0.00003	T	P	D	D	T	16.52
MD-associated genes													
PTPN22	c.205A > G	p.Ser69Gly	Missense	P-26	rs202095629	<0.00001	0	D	D	D	D	D	26.2
PTPN22	c.829G > T	p.Glu277*	Nonsense	P-60	rs72483511	<0.00001	0.00003	(–)	(–)	D	D	(–)	37
PTPN22	c.1356delT	p.Phe452Leufs*3	Deletion	P-65	(–)	0	0	(–)	(–)	(–)	(–)	(–)	(–)
NFKB1	c.1799A > C	p.Glu600Ala	Missense	P-49	rs55661548	0.00031	0.00045	T	B	N	D	T	22.5
TLR2	c.1339C > T	p.Arg447*	Nonsense	P-54	rs62323857	0.00037	0.00029	(–)	(–)	N	D	(–)	35
CXCL10	c.85C > T	p.Arg29Cys	Missense	P-29	rs11548618	0.00611	0.00608	D	D	D	D	T	25.3
MTHFR	c.136C > T	p.Arg46Trp	Missense	P-5/P-35	rs138189536	0.00022	0.00020	T	D	D	D	D	25.3
MTHFR	c.742A > G	p.Ile248Val	Missense	P-66	(–)	0.00002	0.00003	D	D	N	D	D	22.5
SLC44A2	c.761G > A	p.Arg254His	Missense	P-29	(–)	0.00002	0.00003	D	D	D	D	T	31
NOS3	c.2207G > A	p.Arg736Gln	Missense	P-60	rs544887797	0.00008	0.00010	D	D	D	D	T	33
NOTCH2	c.4688G > A	p.Arg1563His	Missense	P-63	rs76770652	0.00002	0.00002	T	B	U	D	D	22.7

MAF, minor allele frequency; MD, Meniere's disease.

Transcript ID: DTNA, NM_001198938.1; FAM136A, NM_032822.2; DPT, NM_001937.5; PTPN22, NM_015967.7; NFKB1, NM_003998.4; TLR2, NM_003264.4; CXCL10, NM_001565.4; MTHFR, NM_005957.4; SLC44A2, NM_020428.4; NOS3, NM_000603.5; NOTCH2, NM_024408.4.

SIFT- D (damaging), T (tolerated); Polyphen- D (probably damaging), P (possibly damaging), B (benign); LRT- D (deleterious), N (neutral), U (unknown); MutationTaster- D (disease_causing), N (polymorphism); FATHMM- D (deleterious), T (tolerated).

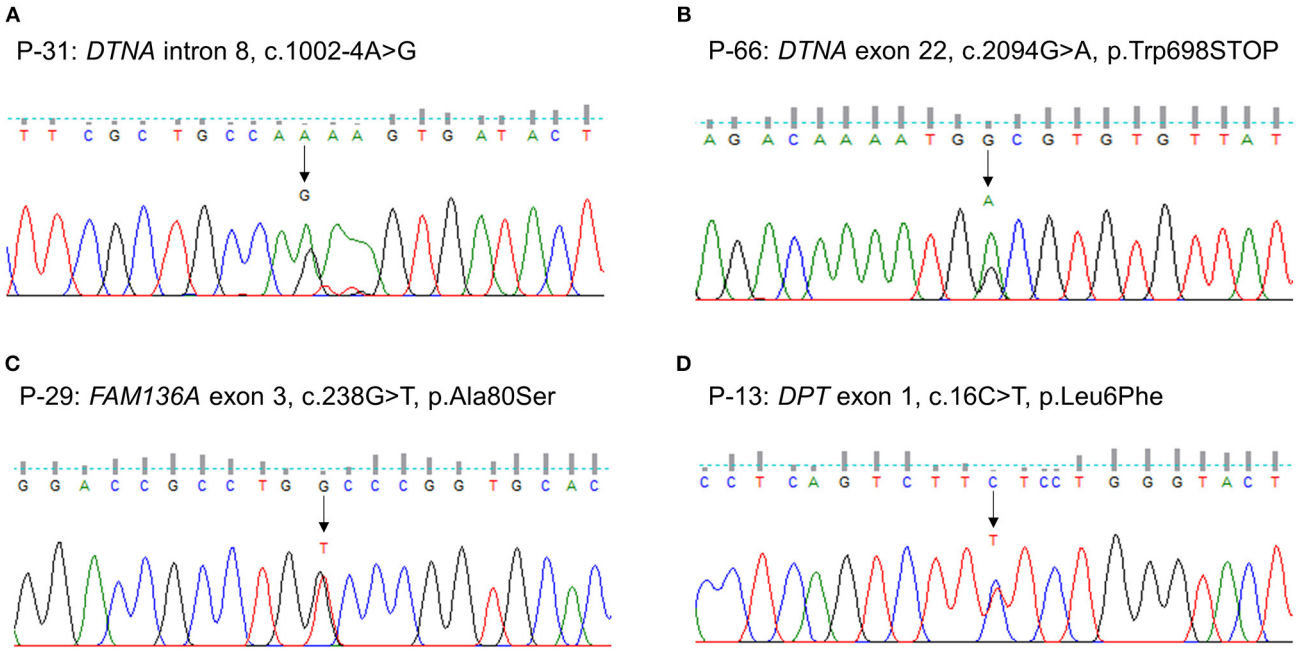

FIGURE 1 | Sequencing results of the rare variants in familial MD genes identified by targeted next-generation sequencing. The chromatograms show two rare heterozygous variants in *DTNA*: **(A)** one is a splice site variant at the 4th nucleotide of the splice acceptor site in intron 8 (c.1002-4A > G, P-31); **(B)** another is a novel nonsense variant in exon 22 causing a premature stop codon (c.2094G > A, p.W698X, P-66). The others are a heterozygous missense rare variant in exon 3 of *FAM136A* causing the substitution of alanine by serine at position 80 (c.238G > T, p.A80S, P-29) **(C)** and in exon 1 of *DPT* changing the highly conserved leucine by phenylalanine at position 6 (c.16C > T, p.L6F, P-13) **(D)**.

Protein structural modeling predicted that the p.R1563H variant in *NOTCH2* may destabilize the Lin-12/Notch repeat (LNR) domain by impairing a hydrogen bond network with surrounding residues (p.D1511, p.F1513, and p.D1515), while the p.R29C variant in *CXCL10* may cause no conformational change in overall structure. The remaining one was a nonsense variant of *TLR2* (P-54: c.1339C > T, p.R447X, **Figure 4D**), which was predicted to be deleterious by MutationTaster and CADD score.

Copy number variation (CNV) analysis using CNVkit from targeted DNA sequencing data did not reveal any pathogenic CNV in each patient.

Association Analysis of a Genetic Variant

When using the allele frequency of total population from ExAC and gnomAD database, 14 of the 15 rare variants were significantly associated with MD (unadjusted *p*-value), but eight of them showed significant association after correcting for multiple testing (Bonferroni) in both databases (**Table 2**). The genes included *DTNA*, *PTPN22*, *MTHFR*, *SLC44A2*, and *NOTCH2*. In particular, all rare variants of *PTPN22* and *MTHFR* were significantly associated with MD even after correcting for multiple testing. Compared to the allele frequency of East Asians, 10 variants were significantly associated with MD (unadjusted *p*-value) in both databases, but no significant associations were observed in all variants after correcting for multiple testing (**Table 2**).

Phenotypes of Patients With a Genetic Variant

The mean age of onset in patients with a novel/rare variant was 53 ± 11.7 years, which showed a tendency of early-onset disease rather than the patients without a genetic variant, but this was not significantly different (vs. 58.4 ± 11.1 years, $p = 0.133$, **Table 3**). Also, no significant differences were observed between the two groups in terms of sex, bilaterality, the type of MD, and hearing threshold at diagnosis (**Table 3**). Three patients with variants in two or more genes did not have distinct clinical features compared to those without variants.

DISCUSSION

To the best of our knowledge, this is the first study on extensive genetic screening with regard to putative candidate MD genes. By using targeted NGS, we identified 15 rare heterozygous variants in 11 candidate MD genes, which some of them had the pathogenic potential by *in silico* prediction or protein structural modeling. Our results highlight the genetic landscape of MD.

Over the last 20 years, many candidate genes have been proposed for MD based on the so-called "common disease-common variants" paradigm that prevailed in complex disease genetic studies (8–10). It was thought that the common variants may lead to genetic susceptibility to complex polygenic disease (43). By this approach, some SNPs associated with MD have been identified in the genes related to the inflammation or regulating

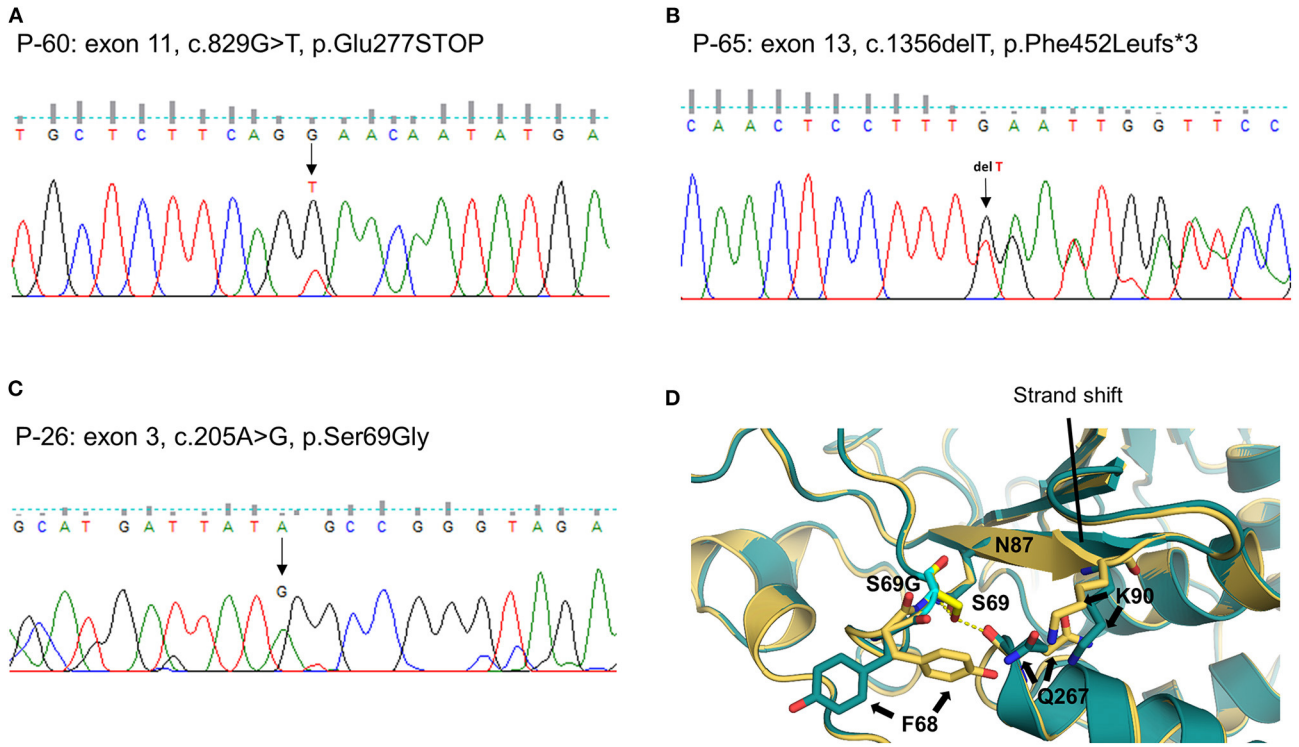

FIGURE 2 | Sequencing results and protein structural modeling of the rare variants in *PTPN22* identified by targeted next-generation sequencing. The chromatograms show three rare heterozygous variants: **(A)** one is a nonsense variant in exon 11 resulting in a premature stop codon (c.829G > T, p.E277X, P-60); **(B)** another is single base deletion in exon 13 that leads to frameshift and premature stop codon 3 amino acids downstream (c.1356delT, p.F452Lfs*3, P-65); **(C)** the other is a missense rare variant in exon 3 causing the substitution of highly conserved serine by glycine at position 69 (c.205A > G, p.S69G, P-26). Protein structural modeling predicts that p.S69G variant may affect the enzyme activity of PTPN22 by a disruption of hydrogen bonds network between p.S69 and p.N87 residues, and the steric hindrance effect resulting from the rotation of p.F68, p.Q267, and p.K90 residues **(D)**, yellow: wild type PTPN22, teal: p.S69G mutant PTPN22).

the ionic composition and water transport of the inner ear (11–35). However, most of the SNPs had small effect size with an odds ratio <2, and several variants were located in the non-coding regions of the genome. In addition, none of them would be replicated among a different ethnic group (26, 44, 45). These suggest that a common genetic variant cannot explain the entire heritability of MD and another investigation may be needed (46).

The MD has strong familial aggregation, and most of these families show an autosomal dominant mode of inheritance with incomplete penetrance (3–5). Thus, the optimal methods identifying novel genes may be a NGS technique or a massive parallel sequencing targeting for familial MD. Recent advances in molecular diagnostics have made it possible to explore the entire genome of individuals. By using WES, a Spanish group has identified novel or rare variants in the *FAM136A*, *DTNA*, *PRKCB*, *DPT*, and *SEMA3D* in several families with MD (36–38). These proteins were expressed in the neurosensorial epithelium of the crista ampullaris of the rat by immunohistochemistry. This suggests that they may play a significant role in the formation or maintaining of inner ear structures, and the identified rare variants are expected to contribute to the development of EH by the altered protein functions. In this study, we identified some rare variants of *FAM136A*, *DTNA*, and *DPT* genes in sporadic cases. Especially, one variant in *DTNA* (c.2094G > A) had highly pathogenic potential by truncating the protein. The *DTNA* encodes α-dystrobrevin (DB), a structural protein of the dystrophin-associated protein complex (36). The absence of α-DB resulted in abnormal brain capillary permeability, progressively escalating brain edema in the mouse model (47). Also, it was expressed in the vestibular system at early stages of development in mice, suggesting a relevant role in the maturation of the vestibular system (48). Although their pathogenicity should be confirmed by functional study, the rare variants in familial MD genes may have large effects on phenotype by impairing protein function, and gene-environment interactions may be strongest for rare alleles (49–51).

In addition, we detected some rare variants in the immune-associated genes including *PTPN22*, *NFKB1*, *TLR2*, and *CXCL10*. There have been growing evidences on the role of autoimmunity and immunological mechanisms in the development of MD as follows: (1) The increased prevalence of autoimmune disease among MD patients, (2) The elevated levels of autoantibodies and immunocomplexes in MD patients, (3) The association of MD with HLA-types and genetic polymorphisms, and (4) The positive response to steroid (52–54). Recent studies have found that basal levels of proinflammatory cytokines were increased in some

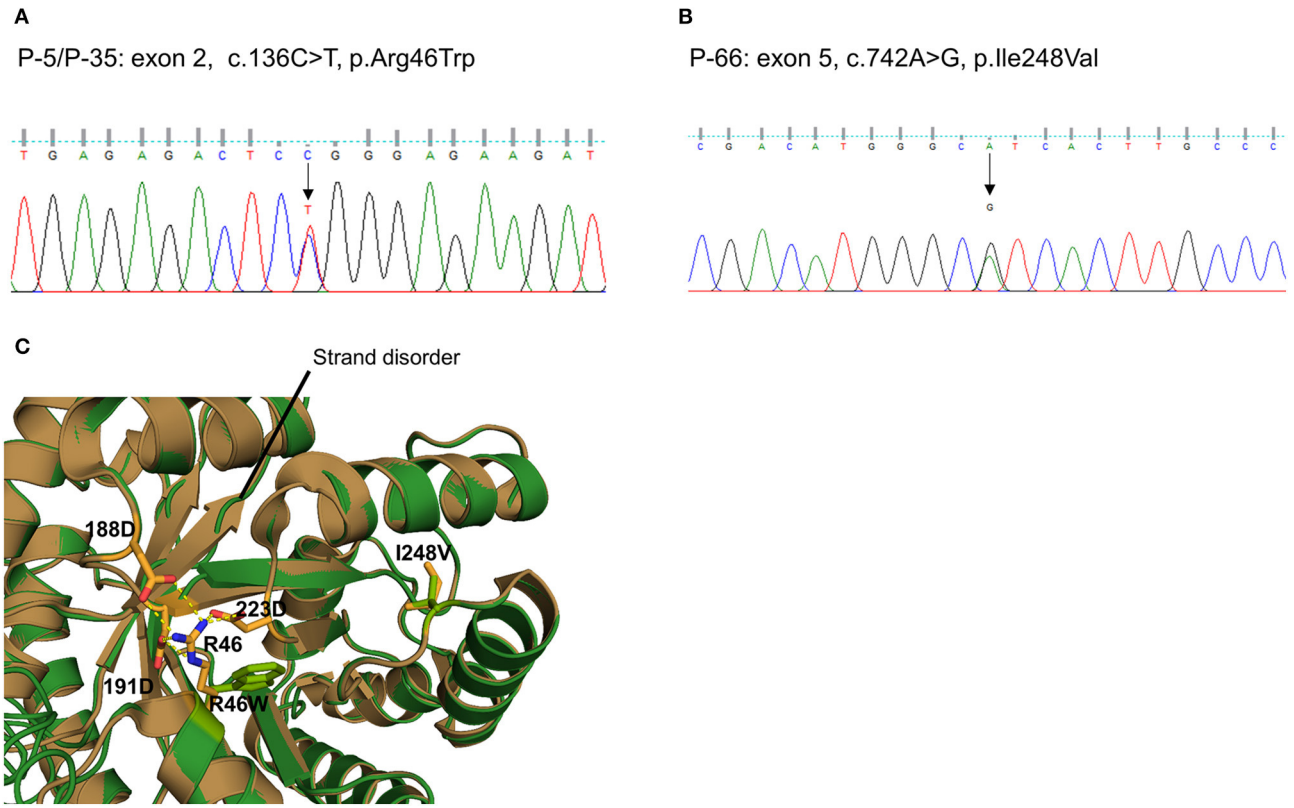

FIGURE 3 | Sequencing results and protein structural modeling of the rare variants in *MTHFR* identified by targeted next-generation sequencing. The chromatograms show two rare heterozygous variants: **(A)** one is a missense rare variant in exon 2 causing the substitution of highly conserved arginine by tryptophan at position 46 (c.136C > T, p.R46W, P-5/P-35); **(B)** another is also a missense rare variant in exon 5 causing the substitution of highly conserved isoleucine by valine at position 248 (c.742A > G, p.I248V, P-66). **(C)** Protein structural modeling shows that p.R46W variant may cause breakage of salt bridges with side chains of p.D188, p.D223, and p.D191 residues. This leads to destabilize the central β-sheet which is essential for reductase activity. On the other hands, p.I248V variant reveals no discernible differences when secondary structure as well as surrounding residue orientation are analyzed (brown: wild type MTHFR, green: p.R46W/p.I248V mutant MTHFR).

patients with MD (55, 56). Gene expression study using mRNA also demonstrated that immune-related genes such as *GSTM1*, *TMEM176A*, and *TMEM176B* were highly expressed in MD patients compared to normal controls (57). Through our study, the *PTPN22* may be of particular interest to support the immune-associated process in MD. The identified rare variants had a pathogenic potential by truncating protein or inducing structural instability. The *PTPN22* encodes lymphoid tyrosine phosphatase (LYP), which is a strong negative regulator of T cell activation, and is expressed in various immunocytes including T- and B-cells (58). It has been found to be associated with autoimmune diseases such as rheumatoid arthritis, systemic lupus erythematosus, and type 1 diabetes (59–61). A previous study also found significant association between putative functional SNP (rs2476601) and bilateral MD in the Spanish population (31). The *NFKB1* encodes a transcription factor that regulates inflammation and immune responses, and has been linked to a number of inflammatory diseases, such as autoimmune arthritis, asthma, and glomerulonephritis (15). Some allelic variants in *NFKB1* are known to modify the hearing outcome in patients with MD and unilateral SNHL (15). The *TLR2* is a member of the Toll-like receptor family, which plays a fundamental role in pathogen recognition and activation of innate immunity (40). The *CXCL10* encodes interferon gamma-induced protein 10 (IP-10), a small cytokine belonging to the CXC chemokine family (40). IP-10 is an important mediator of the inflammatory response to interferons, and has been reported to contribute to immune mediated apoptosis in the ear, inducing human presbycusis (62). All these things support the possible autoimmune etiology or immunological mechanisms in the development of MD.

For several decades, a vascular theory has been proposed as the mechanism of MD's attacks (63). The classic attacks are characterized by acute loss of vestibular response and low-tone hearing followed by an apparent recovery over hours. These unique characteristics may be explained by the differential sensitivity of inner ear tissues to transient ischemia and the excitotoxic cascade lasting several hours by ischemia/reperfusion injury (63). Most animal models demonstrated that both the endolymphatic hydrops and the impaired perfusion pressure were needed to induce MD's attacks (64, 65). Many studies have also documented an association between MD and presumed vascular disorders

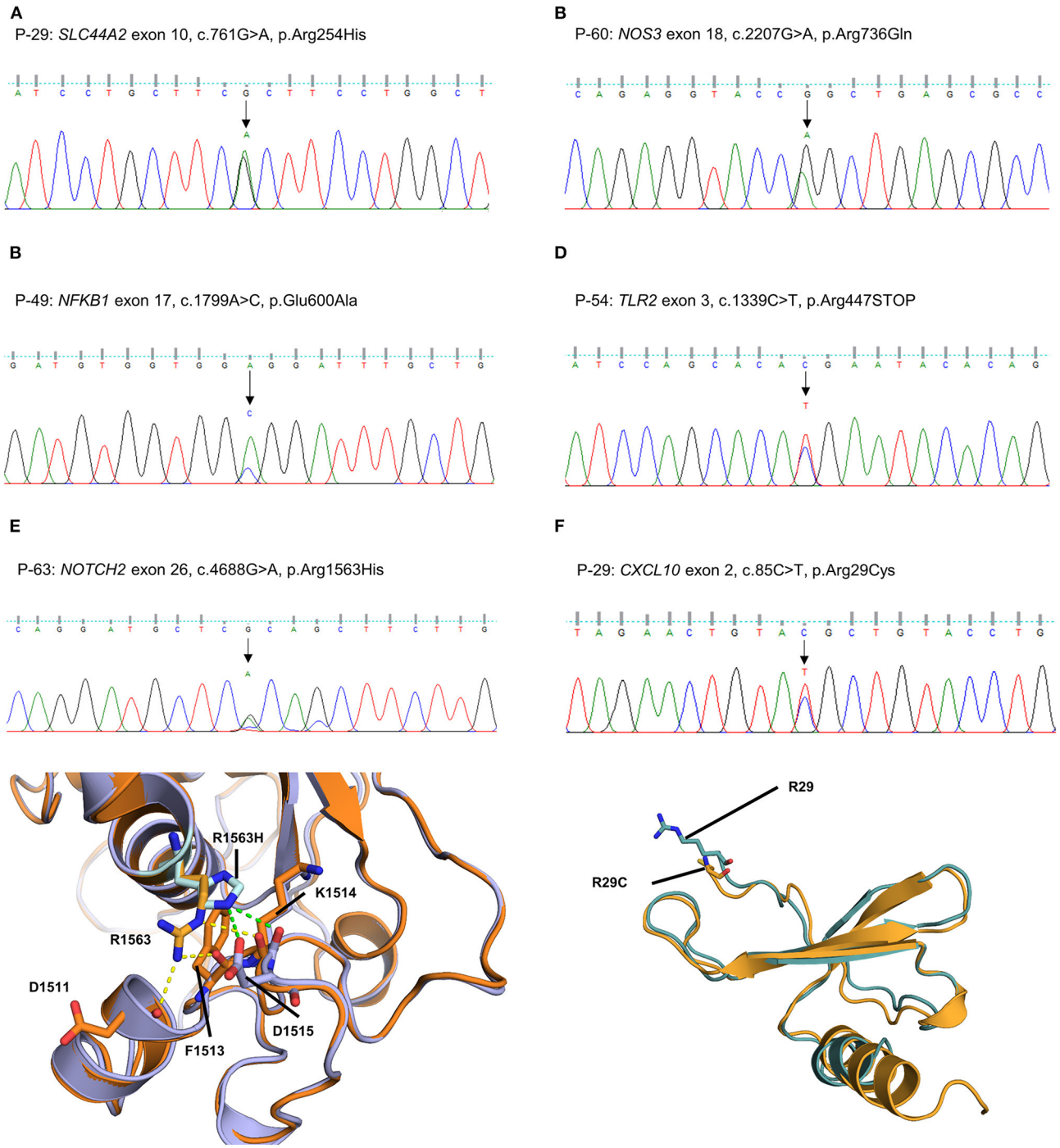

FIGURE 4 | Sequencing results and protein structural modeling of the rare variants in other MD-associated genes identified by targeted next-generation sequencing. **(A–D)** The chromatograms show a heterozygous missense rare variant in *SLC44A2* (exon 10, c.761G > A, p.R254H, P-29), *NOS3* (exon 18, c.2207G > A, p.R736Q, P-60), and *NFKB1* (exon 17, c.1799A > C, p.E600A, P-49), and a nonsense variant in exon 3 of *TLR2* causing premature stop codon (c.1339C > T, p.R447X, P-54). **(E)** P-63 has a heterozygous missense variant in exon 26 of *NOTCH2* causing the substitution of highly conserved arginine by histidine at position 1563 (c.4688G > A, p.R1563H). In protein structural modeling, p.R1563H variant may result in loss of interaction with p.D1511 and p.F1513 residues, and form new hydrogen bond network with main chain of p.K1514 residue and side chain of p.D1515 (green dash line). These impaired interactions make p.D1515 residue to lose ability to interact with a calcium ion, and eventually destabilize the Lin-12/Notch repeat domain required for regulating the NOTCH2 receptor (orange: wild type NOTCH2, purple: p.R1563H mutant NOTCH2). **(F)** P-29 had a heterozygous missense rare variant in exon 2 of *CXCL10* causing the substitution of highly conserved arginine by cystein at position 85 (c.85C > T, p.R29C). However, there is no conformational change in overall structure because the R29 residue is located at the N-terminal end and not involved in interaction with neighboring residues (teal: wild type CXCL10, orange: p.R29C mutant CXCL10).

TABLE 2 | Genetic association analysis results for rare variants.

Gene	Variant	Frequency of variant in this study	ExAC						gnomAD					
			Odd ratio, total[a]	*p*-value	Adjusted *p*-value[b]	Odd ratio, East asian[a]	*p*-value	Adjusted *p*-value[b]	Odd ratio, total[a]	*p*-value	Adjusted *p*-value[b]	Odd ratio, East asian[a]	*p*–value	Adjusted *p*–value[b]
DTNA	c.1002-4A > G	1/68	119.24 (1.5–42.4)	**0.0129**	0.1930	8.50 (0.6–18.9)	0.1654	1.0000	87.04 (1.3–36.5)	**0.0174**	0.2610	6.94 (0.4–12.2)	0.1977	1.0000
DTNA	c.2094G > A	1/68	5396.11 (1.7–1034.5)	**0.0006**	**0.0084**	384.64 (0.5–328.5)	**0.0077**	0.1155	5345.89 (1.7–1030.3)	**0.0006**	**0.0090**	442.78 (0.6–349.3)	**0.0067**	0.1005
FAM136A	c.238G > T	1/68	233.12 (1.9–59.5)	**0.0067**	0.1010	16.69 (0.6–18.9)	0.0897	1.0000	373.78 (2.2–78.6)	**0.0043**	0.0645	30.90 (0.7–26.6)	0.0511	0.7665
DPT	c.16C > T	1/68	376.81 (2.2–78.8)	**0.0043**	0.0646	26.88 (0.7–25.1)	0.0584	0.8760	692.25 (2.5–117.7)	**0.0024**	**0.0360**	57.22 (0.8–39.9)	**0.0296**	0.4440
PTPN22	c.205A > G	1/68	1707.67 (2.6–246.7)	**0.0012**	**0.0177**	125.83 (0.9–79.5)	**0.0158**	0.2370	5345.89 (1.7–1030.3)	**0.0005**	**0.0075**	442.78 (0.6–349.3)	**0.0067**	0.1005
PTPN22	c.829G > T	1/68	1791.13 (2.7–251.9)	**0.0011**	**0.0169**	127.99 (0.8–80.1)	**0.0155**	0.2325	684.10 (2.5–117.1)	**0.0025**	**0.0375**	80.36 (0.9–51.6)	**0.0222**	0.3330
PTPN22	c.1356delT	1/68	5396.11 (1.7–1034.5)	**0.0006**	**0.0084**	384.64 (0.5–328.5)	**0.0077**	0.1155	5345.89 (1.7–1030.3)	**0.0006**	**0.0090**	442.78 (0.6–349.3)	**0.0067**	0.1005
NFKB1	c.1799A > C	1/68	70.06 (1.2–32.9)	**0.0216**	0.3241	5.11 (0.4–10.1)	0.2577	1.0000	49.02 (1.1–27.9)	**0.0306**	0.4590	4.19 (0.4–9.6)	**0.0141**	0.2115
TLR2	c.1339C > T	1/68	59.18 (1.1–30.5)	**0.0255**	0.3821	54.92 (0.8–39.2)	**0.0308**	0.4620	75.26 (1.3–34.0)	**0.0201**	0.3015	49.18 (0.8–35.0)	**0.0334**	0.5010
CXCL10	c.85C > T	1/68	3.59 (0.3–8.8)	0.3427	1.0000	126.87 (0.8–79.8)	**0.0156**	0.2340	3.63 (0.3–8.8)	0.3396	1.0000	141.36 (0.9–83.6)	**0.0141**	0.2115
MTHFR	c.136C > T	2/68	163.70 (2.5–34.2)	**0.0001**	**0.0019**	13.79 (0.8–11.8)	**0.0160**	0.0019	184.44 (2.6–36.2)	**0.0001**	**0.0015**	19.17 (0.9–13.8)	**0.0087**	0.1305
MTHFR	c.742A > G	1/68	770.26 (2.6-123.3)	**0.0022**	**0.0336**	54.88 (0.8-39.1)	**0.0308**	0.2400	593.97 (2.5-103.2)	**0.0028**	**0.0420**	49.17 (0.8–35.0)	**0.0334**	0.5010
SLC44A2	c.761G > A	1/68	1079.20 (2.7–159.4)	**0.0017**	**0.0252**	76.91 (0.9–50.6)	**0.0232**	0.3480	694.64 (2.5–117.8)	**0.0025**	**0.0300**	80.40 (0.9–51.6)	**0.0222**	0.3330
NOS3	c.2207G > A	1/68	218.55 (1.8–58.4)	**0.0072**	0.1082	218.55 (1.8–58.4)	**0.0072**	0.1080	210.69 (1.8–56.5)	**0.0074**	0.1110	17.50 (0.6–19.2)	0.0855	1.0000
NOTCH2	c.4688G > A	1/68	1078.80 (2.7–159.4)	**0.0017**	**0.0252**	384.47 (0.5–328.5)	**0.0078**	0.1170	972.38 (2.6–152.3)	**0.0018**	**0.0270**	402.07 (0.5–334.9)	**0.0074**	0.1110

[a] *Odd ratios were calculated in the 95% confidence interval.*

[b] *p-value adjusted for multiple testing by the total amount of variants found for each gene following Bonferroni approach.*

The bold values denote statistical significance at the $p < 0.05$ level.

TABLE 3 | Phenotypic differences between patients with and without a genetic variant.

	Genetic variant (+), *n* = 12	Genetic variant (–), *n* = 56	*p*-value
Sex, female, *n* (%)	7 (58)	31 (55)	0.851
Age of onset, mean ± SD	53 ± 11.7	58.4 ± 11.1	0.133
Bilaterality, *n* (%)	0 (0)	5 (9)	0.576
Classic MD, *n* (%)	10 (83)	40 (71)	0.490
Hearing threshold at diagnosis (dB)[a]	49 ± 31.1	49.6 ± 24.3	0.941

[a] *Hearing threshold was defined as four pure tone average 0.5, 1, 2, and 3 kHz according to the AAO-HNS criteria.*

including migraine, sickle cell disease, Behcet's disease, and branch retinal artery occlusion (66–71). Among the identified genes in this study, several genes including *MTHFR*, *NOS3*, *SLC44A2*, and *NOTCH2* are associated with prothrombotic risk factors and various vascular disorders (72–75). The *MTHFR* encodes methylenetetrahydrofolate reductase which catalyzes the conversion of 5,10-methylenetetrahydrofolate to 5-methyltetrahydrofolate, a co-substrate for homocystein remethylation to methionine (29). Specific polymorphisms in *MTHFR* (rs1801131, rs1801133) have been proposed as predisposing inherited vascular risk factors in the development of MD and sudden SNHL (29, 76, 77). The *NOS3* encodes a nitric oxide synthase 3, which is responsible for the generation of nitric oxide (NO), a vasodilator in the vascular endothelium (13). NOS3 is also located in the inner and outer hair cells, and a polymorphism of *NOS3* (rs1799983) was significantly associated with the risk of sudden SNHL and MD (13). The *SLC44A2* encodes a choline transporter-like protein 2 (CTL2) which plays a role in choline transport or uptake with CTL1 (32). Two polymorphisms in *SLC44A2* (rs2288904, rs9797861) were linked to venous thrombosis, coronary artery disease, and stroke, and rs2288904 was associated with severity of MD (32). Furthermore, *in vivo* binding of anti-SLC44A2 antibody induced hearing loss in mice and guinea pigs (78, 79). Thus, their genetic deficiency may cause the increased permeability of vascular endothelial cells, oxidative stress response, and increased vascular resistance, resulting in thrombosis and disturbance of micro-circulation in the inner ear (32).

Although the diagnostic criteria established by the Classification Committee of the Barany Society may improve the accuracy in clinical diagnosis of MD, the phenotypic heterogeneity is observed and some patients may have co-morbid conditions with MD, such as migraine or autoimmune disorders (39). Recent study suggests that an enrichment of rare variants in hearing loss genes such as *GJB2*, *SLC26A*, or *USH1G* may contribute to explain these phenotypic heterogeneities (80). Our patients in this study also showed a broad phenotypic spectrum regarding the onset age, clinical subgroups, and hearing threshold at diagnosis, and some had an accumulation of rare variants in two or more MD genes. Although we confined our gene panel to putative candidate genes associated with MD, our results also suggest the additive effect of several rare variants in the variable expressivity of MD phenotype. Alternatively, the burden of copy number variation can help understand phenotypic heterogeneity (81). Further studies may be needed to confirm these theories.

This study has potential limitations. Despite the extensive genetic screening using NGS, more than 80% of our patients did not have any likely pathogenic variant in putative candidate MD genes. This low detection rate may be due to a high proportion of sporadic cases in our study. Or, the unknown genes or additional factors including epigenetic and environmental modification are likely to contribute to the development of MD (46). We also did not perform functional study determining pathogenicity of our variants. Indeed, several variants in our study were predicted to be benign by *in silico* prediction tools, or affect only some isoforms of a gene. Despite the rarity and putative pathogenicity of the variants, establishing the pathogenicity may be difficult without a functional study, especially in sporadic cases. With regard to variants of familial MD gene, we could not determine if they were *de novo* mutations because of parental death. Finally, our panel did not include the *GSTM1* or *histamine H4 receptor* genes, which have recently been suggested as a possible candidate gene of MD (57, 82). All of these should be considered when interpreting our results.

In conclusion, we identified rare variants of putative candidate genes in some of MD patients. The identified genes were related to the formation of inner ear structures, the immune-associated process, or systemic hemostasis derangement, suggesting the multiple genetic predispositions in the development of MD. Since there are still many MD patients without genetic variants, further assessments for the candidate genes will be needed.

DATA AVAILABILITY STATEMENT

The raw data supporting the conclusions of this manuscript will be made available by the authors, without undue reservation, to any qualified researcher.

ETHICS STATEMENT

All experiments followed the tenets of the Declaration of Helsinki, and informed consents were obtained after the nature and possible consequences of this study had been explained to the participants. This study was approved by the institutional review boards of Pusan National University Yangsan Hospital.

AUTHOR CONTRIBUTIONS

EO analyzed and interpreted the data and wrote the manuscript. J-HS and H-SK perfomed the experiment. SC, K-DC, J-KR, and JC analyzed and interpreted the data. SL and CL interpreted the data and revised the manuscript. J-HC contributed to the design and conceptualization of the study, and revised the manuscript.

FUNDING

This research was supported by Research Institute for Convergence of Biomedical Science and Technology Grant (30-2018-016), Pusan National University Yangsan Hospital.

SUPPLEMENTARY MATERIAL

The Supplementary Material for this article can be found online at: https://www.frontiersin.org/articles/10.3389/fneur.2019.01424/full#supplementary-material

REFERENCES

1. Lopez-Escamez JA, Carey J, Chung WH, Goebel JA, Magnusson M, Mandala M, et al. Diagnostic criteria for Meniere's disease. *J Vestib Res*. (2015) 25:1–7. doi: 10.3233/VES-150549
2. Rauch SD, Merchant SN, Thedinger BA. Meniere's syndrome and endolymphatic hydrops: double-blind temporal bone study. *Ann Otol Rhinol Laryngol*. (1989) 98:873–83. doi: 10.1177/000348948909801108
3. Requena T, Espinosa-Sanchez JM, Cabrera S, Trinidad G, Soto-Varela A, Santos-Perez S, et al. Familial clustering and genetic heterogeneity in Meniere's disease. *Clin Genet*. (2014) 85:245–52. doi: 10.1111/cge.12150
4. Morrison AW, Bailey ME, Morrison GA. Familial Meniere's disease: clinical and genetic aspects. *J Laryngol Otol*. (2009) 123:29–37. doi: 10.1017/S0022215108002788
5. Lee JM, Kim MJ, Jung J, Kim HJ, Seo YJ, Kim SH. Genetic aspects and clinical characteristics of familial Meniere's disease in a South Korean population. *Laryngoscope*. (2015) 125:2175–80. doi: 10.1002/lary.25207
6. Klar J, Frykholm C, Friberg U, Dahl N. A Meniere's disease gene linked to chromosome 12p12.3. *Am J Med Genet B Neuropsychiatr Genet*. (2006) 141b:463–7. doi: 10.1002/ajmg.b.30347
7. Arweiler-Harbeck D, Horsthemke B, Jahnke K, Hennies HC. Genetic aspects of familial Meniere's disease. *Otol Neurotol*. (2011) 32:695–700. doi: 10.1097/MAO.0b013e318216074a
8. Frejo L, Giegling I, Teggi R, Lopez-Escamez JA, Rujescu D. Genetics of vestibular disorders: pathophysiological insights. *J Neurol*. (2016) 263 (Suppl. 1):S45–53. doi: 10.1007/s00415-015-7988-9
9. Roman-Naranjo P, Gallego-Martinez A, Lopez Escamez JA. Genetics of vestibular syndromes. *Curr Opin Neurol*. (2018) 31:105–10. doi: 10.1097/WCO.0000000000000519
10. Requena T, Espinosa-Sanchez JM, Lopez-Escamez JA. Genetics of dizziness: cerebellar and vestibular disorders. *Curr Opin Neurol*. (2014) 27:98–104. doi: 10.1097/WCO.0000000000000053
11. Teggi R, Lanzani C, Zagato L, Delli Carpini S, Manunta P, Bianchi G, et al. Gly460Trp alpha-adducin mutation as a possible mechanism leading to endolymphatic hydrops in Meniere's syndrome. *Otol Neurotol*. (2008) 29:824–8. doi: 10.1097/MAO.0b013e318180a4b1
12. Nishio N, Teranishi M, Uchida Y, Sugiura S, Ando F, Shimokata H, et al. Polymorphisms in genes encoding aquaporins 4 and 5 and estrogen receptor α in patients with Ménière's disease and sudden sensorineural hearing loss. *Life Sci*. (2013) 92:541–6. doi: 10.1016/j.lfs.2013.01.019
13. Teranishi M, Uchida Y, Nishio N, Kato K, Otake H, Yoshida T, et al. Polymorphisms in genes involved in the free-radical process in patients with sudden sensorineural hearing loss and Ménière's disease. *Free Radic Res*. (2013) 47:498–506. doi: 10.3109/10715762.2013.793319
14. Yazdani N, Mojbafan M, Taleba M, Amiri P, Nejadian F, Amoli MM. Sex-specific association of RANTES gene−403 variant in Meniere's disease. *Eur Arch Otorhinolaryngol*. (2015) 272:2221–5. doi: 10.1007/s00405-014-3151-y
15. Cabrera S, Sanchez E, Requena T, Martinez-Bueno M, Benitez J, Perez N, et al. Intronic variants in the NFKB1 gene may influence hearing forecast in patients with unilateral sensorineural hearing loss in Meniere's disease. *PLoS ONE*. (2014) 9:e112171. doi: 10.1371/journal.pone.0112171
16. Teggi R, Colombo B, Trimarchi M, Bianco M, Manfredi A, Corti A. Altered chromogranin a circulating levels in Meniere's Disease. *Dis Markers*. (2015) 2015:643420. doi: 10.1155/2015/643420
17. Vrabec JT, Liu L, Li B, Leal SM. Sequence variants in host cell factor C1 are associated with Meniere's disease. *Otol Neurotol*. (2008) 29:561–6. doi: 10.1097/MAO.0b013e318168d23b
18. Khorsandi MT, Amoli MM, Borghei H, Emami H, Amiri P, Amirzargar A, et al. Associations between HLA-C alleles and definite Meniere's Disease. *Iranian J Allergy Asthma Immunol*. (2011) 10:119–22. doi: 10.02/ijaai.119122
19. Melchiorri L, Martini A, Rizzo R, Berto A, Adinolfi E, Baricordi OR. Human leukocyte antigen-A, -B, -C and -DR alleles and soluble human leukocyte antigen class I serum level in Meniere's disease. *Acta Otolaryngol Suppl*. (2002) 548:26–9. doi: 10.1080/00016480260094938
20. Meng X, Lian N, Yang Z, Liu C, Tang L. An association study of histocompatibility leukocyte antigen-class II with Meniere's disease. *Zhonghua Er Bi Yan Hou Ke Za Zhi*. (2001) 36:25–7.
21. Lopez-Escamez JA, Vilchez JR, Soto-Varela A, Santos-Perez S, Perez-Garrigues H, Aran I, et al. HLA-DRB1*1101 allele may be associated with bilateral Meniere's disease in southern European population. *Otol Neurotol*. (2007) 28:891–5. doi: 10.1097/MAO.0b013e3180dca1cc
22. Koo JW, Oh SH, Chang SO, Park MH, Lim MJ, Yoo TJ, et al. Association of HLA-DR and type II collagen autoimmunity with Meniere's disease. *Tissue Antigens*. (2003) 61:99–103. doi: 10.1034/j.1399-0039.2003.610112.x
23. Kawaguchi S, Hagiwara A, Suzuki M. Polymorphic analysis of the heat-shock protein 70 gene (HSPA1A) in Ménière's disease. *Acta Otolaryngol*. (2008) 128:1173–7. doi: 10.1080/00016480801901675
24. Furuta T, Teranishi M, Uchida Y, Nishio N, Kato K, Otake H, et al. Association of interleukin-1 gene polymorphisms with sudden sensorineural hearing loss and Ménière's disease. *Int J Immunogenet*. (2011) 38:249–54. doi: 10.1111/j.1744-313X.2011.01004.x
25. Doi K, Sato T, Kuramasu T, Hibino H, Kitahara T, Horii A, et al. Ménière's disease is associated with single nucleotide polymorphisms in the human potassium channel genes, KCNE1 and KCNE3. ORL *J Otorhinolaryngol Relat Spec*. (2005) 67:289–93. doi: 10.1159/000089410
26. Hietikko E, Kotimäki J, Okuloff A, Sorri M, Männikkö M. A replication study on proposed candidate genes in Ménière's disease, and a review of the current status of genetic studies. *Int J Audiol*. (2012) 51:841–5. doi: 10.3109/14992027.2012.705900
27. Gazquez I, Moreno A, Aran I, Soto-Varela A, Santos S, Perez-Garrigues H, et al. MICA-STR A.4 is associated with slower hearing loss progression in patients with Meniere's disease. *Otol Neurotol*. (2012) 33:223–9. doi: 10.1097/MAO.0b013e31824296c8
28. Yazdani N, Khorsandi A, Shtiani MT, Zarandy MM, Mohammadi SJ, Ghazavi H, et al. Association between MIF gene variation and Meniere's disease. *Int J Immunogenet*. (2013) 40:488–91. doi: 10.1111/iji.12058
29. Huang Y, Teranishi M, Uchida Y, Nishio N, Kato K, Otake H, et al. Association between polymorphisms in genes encoding methylenetetrahydrofolate reductase and the risk of Ménière's disease. *J Neurogenet*. (2013) 27:5–10. doi: 10.3109/01677063.2013.770510
30. Lopez-Escamez JA, Moreno A, Bernal M, Perez-Garrigues H, Santos-Perez S, Soto-Varela A, et al. Poly(ADP-ribose) polymerase-1 (PARP-1) spanning promoter region confer protection to bilateral Meniere's disease. *Acta Otolaryngol*. (2009) 129:1222–5. doi: 10.3109/00016480802684080
31. Lopez-Escamez JA, Saenz-Lopez P, Acosta L, Moreno A, Gazquez I, Perez-Garrigues H, et al. Association of a functional polymorphism of PTPN22 encoding a lymphoid protein phosphatase in bilateral Meniere's disease. *Laryngoscope*. (2010) 120:103–7. doi: 10.1002/lary.20650
32. Nair TS, Kommareddi PK, Galano MM, Miller DM, Kakaraparthi BN, Telian SA, et al. SLC44A2 single nucleotide polymorphisms, isoforms, and expression: association with severity of Meniere's disease? *Genomics*. (2016) 108:201–8. doi: 10.1016/j.ygeno.2016.11.002
33. Requena T, Gazquez I, Moreno A, Batuecas A, Aran I, Soto-Varela A, et al. Allelic variants in TLR10 gene may influence bilateral affectation and clinical course of Meniere's disease. *Immunogenetics*. (2013) 65:345–55. doi: 10.1007/s00251-013-0683-z

34. Greco A, Gallo A, Fusconi M, Marinelli C, Macri GF, De Vincentiis M. Meniere's disease might be an autoimmune condition? *Autoimmunity Reviews.* (2012) 11:731–8. doi: 10.1016/j.autrev.2012.01.004
35. Teggi R, Zagato L, Delli Carpini S, Citterio L, Cassandro C, Albera R, et al. Genetics of ion homeostasis in Ménière's Disease. *Eur Arch Otorhinolaryngol.* (2017) 274:757–63. doi: 10.1007/s00405-016-4375-9
36. Requena T, Cabrera S, Martin-Sierra C, Price SD, Lysakowski A, Lopez-Escamez JA. Identification of two novel mutations in FAM136A and DTNA genes in autosomal-dominant familial Meniere's disease. *Hum Mol Genet.* (2015) 24:1119–26. doi: 10.1093/hmg/ddu524
37. Martín-Sierra C, Requena T, Frejo L, Price SD, Gallego-Martinez A, Batuecas-Caletrio A, et al. A novel missense variant in PRKCB segregates low-frequency hearing loss in an autosomal dominant family with Meniere's disease. *Hum Mol Genet.* (2016) 25:3407–15. doi: 10.1093/hmg/ddw183
38. Martín-Sierra C, Gallego-Martinez A, Requena T, Frejo L, Batuecas-Caletrío A, Lopez-Escamez JA. Variable expressivity and genetic heterogeneity involving DPT and SEMA3D genes in autosomal dominant familial Meniere's disease. *Eur J Hum Genet.* (2017) 25:200–7. doi: 10.1038/ejhg.2016.154
39. Frejo L, Martin-Sanz E, Teggi R, Trinidad G, Soto-Varela A, Santos-Perez S, et al. Extended phenotype and clinical subgroups in unilateral Meniere disease: a cross-sectional study with cluster analysis. *Clin Otolaryngol.* (2017) 42:1172–80. doi: 10.1111/coa.12844
40. Li L, Wang Y, An L, Kong X, Huang T. A network-based method using a random walk with restart algorithm and screening tests to identify novel genes associated with Menière's disease. *PLoS ONE.* (2017) 12:e0182592. doi: 10.1371/journal.pone.0182592
41. Rentzsch P, Witten D, Cooper GM, Shendure J, Kircher M. CADD: predicting the deleteriousness of variants throughout the human genome. *Nucleic Acids Res.* (2019) 47:D886–94. doi: 10.1093/nar/gky1016
42. Yang J, Zhang Y. Protein structure and function prediction using I-TASSER. *Curr Protoc Bioinform.* (2015) 52:1–15. doi: 10.1002/0471250953.bi0508s52
43. Reich DE, Lander ES. On the allelic spectrum of human disease. *Trends Genet.* (2001) 17:502–10. doi: 10.1016/S0168-9525(01)02410-6
44. Li YJ, Jin ZG, Xu XR. Variants in the KCNE1 or KCNE3 gene and risk of Meniere's disease: a meta-analysis. *J Vestib Res.* (2016) 25:211–8. doi: 10.3233/VES-160569
45. Campbell CA, Della Santina CC, Meyer NC, Smith NB, Myrie OA, Stone EM, et al. Polymorphisms in KCNE1 or KCNE3 are not associated with Meniere disease in the Caucasian population. *Am J Med Genet A.* (2010) 152a:67–74. doi: 10.1002/ajmg.a.33114
46. Gazquez I, Lopez-Escamez JA. Genetics of recurrent vertigo and vestibular disorders. *Curr Genomics.* (2011) 12:443–50. doi: 10.2174/138920211797248600
47. Lien CF, Mohanta SK, Frontczak-Baniewicz M, Swinny JD, Zablocka B, Górecki DC. Absence of glial α-dystrobrevin causes abnormalities of the blood-brain barrier and progressive brain edema. *J Biol Chem.* (2012) 287:41374–85. doi: 10.1074/jbc.M112.400044
48. Lien CF, Vlachouli C, Blake DJ, Simons JP, Górecki DC. Differential spatio-temporal expression of alpha-dystrobrevin-1 during mouse development. *Gene Expr Patterns.* (2004) 4:583–93. doi: 10.1016/j.modgep.2004.01.015
49. Eichler EE, Flint J, Gibson G, Kong A, Leal SM, Moore JH, et al. Missing heritability and strategies for finding the underlying causes of complex disease. *Nat Rev Genet.* (2010) 11:446–50. doi: 10.1038/nrg2809
50. Lettre G. Rare and low-frequency variants in human common diseases and other complex traits. *J Med Genet.* (2014) 51:705–14. doi: 10.1136/jmedgenet-2014-102437
51. Saint Pierre A, Génin E. How important are rare variants in common disease? *Brief Funct Genomics.* (2014) 13:353–61. doi: 10.1093/bfgp/elu025
52. Tomoda K, Suzuka Y, Iwai H, Yamashita T, Kumazawa T. Menière's disease and autoimmunity: clinical study and survey. *Acta Otolaryngol Suppl.* (1993) 500:31–4. doi: 10.3109/00016489309126174
53. Filipo R, Mancini P, Nostro G. Ménière's disease and autoimmunity. *Ann N Y Acad Sci.* (1997) 830:299–305. doi: 10.1111/j.1749-6632.1997.tb51900.x
54. Kim SH, Kim JY, Lee HJ, Gi M, Kim BG, Choi JY. Autoimmunity as a candidate for the etiopathogenesis of Meniere's disease: detection of autoimmune reactions and diagnostic biomarker candidate. *PLoS ONE.* (2014) 9:e111039. doi: 10.1371/journal.pone.0111039
55. Frejo L, Gallego-Martinez A, Requena T, Martin-Sanz E, Amor-Dorado JC, Soto-Varela A, et al. Proinflammatory cytokines and response to molds in mononuclear cells of patients with Meniere disease. *Sci Rep.* (2018) 8:5974. doi: 10.1038/s41598-018-23911-4
56. Flook M, Frejo L, Gallego-Martinez A, Martin-Sanz E, Rossi-Izquierdo M, Amor-Dorado JC, et al. Differential proinflammatory signature in vestibular migraine and meniere disease. *Front Immunol.* (2019) 10:1229. doi: 10.3389/fimmu.2019.01229
57. Sun Y, Zhang D, Sun G, Lv Y, Li Y, Li X, et al. RNA-sequencing study of peripheral blood mononuclear cells in sporadic Ménière's disease patients: possible contribution of immunologic dysfunction to the development of this disorder. *Clin Exp Immunol.* (2018) 192:33–45. doi: 10.1111/cei.13083
58. Mustelin T, Alonso A, Bottini N, Huynh H, Rahmouni S, Nika K, et al. Protein tyrosine phosphatases in T cell physiology. *Mol Immunol.* (2004) 41:687–700. doi: 10.1016/j.molimm.2004.04.015
59. Begovich AB, Carlton VE, Honigberg LA, Schrodi SJ, Chokkalingam AP, Alexander HC, et al. A missense single-nucleotide polymorphism in a gene encoding a protein tyrosine phosphatase (PTPN22) is associated with rheumatoid arthritis. *Am J Hum Genet.* (2004) 75:330–7. doi: 10.1086/422827
60. de Lima SC, Adelino JE, Crovella S, de Azevedo Silva J, Sandrin-Garcia P. PTPN22 1858C > T polymorphism and susceptibility to systemic lupus erythematosus: a meta-analysis update. *Autoimmunity.* (2017) 50:428–34. doi: 10.1080/08916934.2017.1385774
61. Lee YH, Rho YH, Choi SJ, Ji JD, Song GG, Nath SK, et al. The PTPN22 C1858T functional polymorphism and autoimmune diseases–a meta-analysis. *Rheumatology.* (2007) 46:49–56. doi: 10.1093/rheumatology/kel170
62. Dong Y, Li M, Liu P, Song H, Zhao Y, Shi J. Genes involved in immunity and apoptosis are associated with human presbycusis based on microarray analysis. *Acta Otolaryngol.* (2014) 134:601–8. doi: 10.3109/00016489.2014.880795
63. Foster CA, Breeze RE. The Meniere attack: an ischemia/reperfusion disorder of inner ear sensory tissues. *Med Hypotheses.* (2013) 81:1108–15. doi: 10.1016/j.mehy.2013.10.015
64. Takumida M, Akagi N, Anniko M. A new animal model for Meniere's disease. *Acta Otolaryngol.* (2008) 128:263–71. doi: 10.1080/00016480701497436
65. Kimura R. Experimental endolymphatic hydrops. In: Harris JP, editor. *Meniere's Disease*. The Hague: Kugler publications; 1999. p. 115–24.
66. Lee H, Lopez I, Ishiyama A, Baloh R. Can migraine damage the inner ear? *Arch Neurol.* (2000) 57:1631–4. doi: 10.1001/archneur.57.11.1631
67. Lee H, Whitman GT, Lim JG, Yi SD, Cho YW, Ying S, et al. Hearing symptoms in migrainous infarction. *Arch Neurol.* (2003) 60:113–6. doi: 10.1001/archneur.60.1.113
68. Marcus RE, Lee YM. Inner ear disorders in a family with sickle cell thalassemia. *Arch Otolaryngol.* (1976) 102:703–5.
69. Schwanitz HJ, Knop J, Bonsmann G. Behcet disease with inner ear involvement. *Zeitschrift fur Hautkrankheiten.* (1984) 59:1173–4.
70. Brama I, Fainaru M. Inner ear involvement in Behcet's disease. *Arch Otolaryngol.* (1980) 106:215–7. doi: 10.1001/archotol.1980.00790280023004
71. Recupero SM, Abdolrahimzadeh R, Occhiuto S, Tripodi A. G, Branch retinal artery occlusion in a young woman with Meniere's disease. *Ophthalmologica.* (1998) 212:77–9.
72. Liew SC, Gupta ED. Methylenetetrahydrofolate reductase (MTHFR) C677T polymorphism: epidemiology, metabolism and the associated diseases. *Eur J Med Genet.* (2015) 58:1–10. doi: 10.1016/j.ejmg.2014.10.004
73. Tilburg J, Adili R, Nair TS, Hawley ME, Tuk DC, Jackson M, et al. Characterization of hemostasis in mice lacking the novel thrombosis susceptibility gene Slc44a2. *Thromb Res.* (2018) 171:155–9. doi: 10.1016/j.thromres.2018.09.057
74. Oliveira-Paula GH, Lacchini R, Tanus-Santos JE. Clinical and pharmacogenetic impact of endothelial nitric oxide synthase polymorphisms on cardiovascular diseases. *Nitric Oxide.* (2017) 63:39–51. doi: 10.1016/j.niox.2016.08.004
75. Rasheed MA, Kantoush N, Abd El-Ghaffar N, Farouk H, Kamel S, Ibrahim AA, et al. Expression of JAZF1, ABCC8, KCNJ11and Notch2 genes and vitamin D receptor polymorphisms in type 2 diabetes, and their association with microvascular complications. *Ther Adv Endocrinol Metab.* (2017) 8:97–108. doi: 10.1177/2042018817708910

76. Shu J, Yin S, Tan AZ, He M. Association between the methylenetetrahydrofolate reductase gene C677T polymorphism and sudden sensorineural hearing loss: a meta-analysis. *Eur Arch Otorhinolaryngol*. (2015) 272:2267–74. doi: 10.1007/s00405-014-3198-9
77. Uchida Y, Sugiura S, Ando F, Shimokata H, Nakashima T. Association of the C677T polymorphism in the methylenetetrahydrofolate reductase gene with sudden sensorineural hearing loss. *Laryngoscope*. (2010) 120:791–5. doi: 10.1002/lary.20809
78. Nair TS, Prieskorn DM, Miller JM, Dolan DF, Raphael Y, Carey TE. KHRI-3 monoclonal antibody-induced damage to the inner ear: antibody staining of nascent scars. *Hear Res*. (1999) 129:50–60. doi: 10.1016/S0378-5955(98)00220-2
79. Nair TS, Raphael Y, Dolan DF, Parrett TJ, Perlman LS, Brahmbhatt VR, et al. Monoclonal antibody induced hearing loss. *Hear Res*. (1995) 83:101–13. doi: 10.1016/0378-5955(94)00194-U
80. Gallego-Martinez A, Requena T, Roman-Naranjo P, Lopez-Escamez JA. Excess of rare missense variants in hearing loss genes in sporadic meniere disease. *Front Genet*. (2019) 10:76. doi: 10.3389/fgene.2019.00076
81. Girirajan S1, Rosenfeld JA, Coe BP, Parikh S, Friedman N, Goldstein A, et al. Phenotypic heterogeneity of genomic disorders and rare copy-number variants. *N Engl J Med*. (2012) 367:1321–31. doi: 10.1056/NEJMoa1200395
82. Qin D, Zhang H, Wang J, Hong Z. Histamine H4 receptor gene polymorphisms: a potential contributor to Meniere disease. *BMC Med Genomics*. (2019) 12:71. doi: 10.1186/s12920-019-0533-4

Conflict of Interest: The authors declare that the research was conducted in the absence of any commercial or financial relationships that could be construed as a potential conflict of interest.

frontiers in Neurology

ORIGINAL RESEARCH
published: 29 May 2020
doi: 10.3389/fneur.2020.00470

Identification of New Biomarkers of Posturo-Locomotor Instability in a Rodent Model of Vestibular Pathology

*Emna Marouane[1,2], Guillaume Rastoldo[1], Nada El Mahmoudi[1], David Péricat[1], Christian Chabbert[1], Vincent Artzner[2] and Brahim Tighilet[1]**

[1] Aix Marseille Université-CNRS, Laboratoire de Neurosciences Sensorielles et Cognitives, LNSC UMR 7260, Equipe Physiopathologie et Thérapie des Désordres Vestibulaires, Marseille, France, [2] BIOSEB SAS, Vitrolles, France

The vestibular system plays a crucial role in maintaining postural balance. Unilateral vestibular lesions result in a typical syndrome characterized by postural imbalance, altered locomotor patterns and gaze stabilization, as well as cognitive and neurovegetative disorders. One of the main difficulties encountered in the development of new anti-vertigo drugs is the lack of sensitivity in the evaluation of this syndrome. Qualitative assessments of the vestibular syndrome have been developed, but methods of conducting quantitative evaluations are critically lacking. Recently, assessments with a dynamic weight-bearing device (DWB®, Bioseb) revealed postural alterations in rats subjected to unilateral vestibular neurectomy (UVN). Our team is evaluating a new version of this device capable of quantifying additional parameters of postural and locomotor equilibrium. The objective of this study was to use this device to assess these new posturo-locomotor parameters in a rat model of a vestibular pathology. The biomarkers measured by this device are as follows: the barycenter, the support surface and the weight distribution of the rats when they were moving or stationary. Before UVN, the rats showed a symmetric distribution of their weight along the lateral axis. In the acute phase after UVN on the left side, the rats distributed more weight on the right side than on the left side and then distributed more weight on the left side. These results corroborate those presented in our previous study. The support surface of the rats increased between 1 day and 30 days after UVN, and the barycenter distribution reflected the weight distribution. In addition, our results show smaller changes in the weight distributions when the animals are moving compared with when they are stationary in the acute phase after UVN. This study provides new information on the static and dynamic postural balance patterns observed after unilateral vestibular loss in rats. These data are relevant because they objectively quantify the posturo-locomotor component of vestibular syndrome as well as the compensatory strategies used after vestibular loss. These results may guide the development of rehabilitation protocols for vestibular patients and the validation of pharmacological compounds favoring the restoration of equilibrium.

Keywords: vestibular compensation, posturo-locomotor instability, vestibular syndrome, automated analyses method, rodent model of vestibular pathology

OPEN ACCESS

Edited by:
Andreas Zwergal, Ludwig Maximilian University of Munich, Germany

Reviewed by:
Paul Smith, University of Otago, New Zealand
Vincenzo Marcelli, Local Health Authority Naples 1 Center, Italy

***Correspondence:**
Brahim Tighilet
brahim.tighilet@univ-amu.fr

Specialty section:
This article was submitted to Neuro-Otology, a section of the journal Frontiers in Neurology

Received: *12 March 2020*
Accepted: *29 April 2020*
Published: *29 May 2020*

Citation:
Marouane E, Rastoldo G, El Mahmoudi N, Péricat D, Chabbert C, Artzner V and Tighilet B (2020) Identification of New Biomarkers of Posturo-Locomotor Instability in a Rodent Model of Vestibular Pathology. Front. Neurol. 11:470. doi: 10.3389/fneur.2020.00470

INTRODUCTION

The vestibular system is a sensory-motor system that plays a crucial role in postural control, locomotion, gaze stabilization and space orientation (1) (**Figure 1A**). Unilateral damage of this system leads to a vestibular syndrome involving posturo-locomotor, oculomotor, perceptual-cognitive and vegetative disorders (**Figure 1B**), which have a significant impact on patients' daily lives. The prevalence of this syndrome is high: an epidemiological study recently conducted on data from 70,000,000 patients in Germany estimated that the prevalence is 6.5% (2). However, preclinical studies lack reliable methods of evaluation to precisely quantify the vestibular syndrome, its evolution over time and the effect of different therapies on the kinetics of individuals with vestibular syndrome (3). In a rodent model, the consequences of unilateral vestibular injury are essentially assessed qualitatively by various scales that address several vestibular symptoms (e.g., circling, tumbling, retropulsion, or head-tilting) (4–7). These different scales describe the overall kinetics of the syndrome, and the disorders are most severe during the first 3 days after injury (a post-lesional critical period) and then decrease in severity until baseline values are restored (vestibular compensation) [(8) for review]. However, these scales remain subjective; it is therefore necessary to design new evaluation paradigms for the objective and parametric quantification of the vestibular syndrome. For several years, in human clinical practice, posturography has been commonly used for the assessment of postural vestibular disorders (9). The utilization of force platforms that record the movements of the patient's center of pressure and provide an estimate of the energy required for postural stabilization has proven to be a particularly sensitive and relevant diagnostic tool for the vestibular syndrome (10–13). Under different experimental conditions (static, dynamic, open and closed eyes), posturography allows a global evaluation of postural vestibular deficits. It is also a valuable tool for evaluating the effects of different vestibular therapies (pharmacological and rehabilitative) on the quality and timing of postural functional recovery (14).

This study aimed to identify new parameters to objectively quantify posturo-locomotor deficits in our rat model of unilateral vestibular neurectomy (UVN).

The first quantitative study conducted on the vestibular syndrome in rodents is relatively recent (6). The use of a weight distribution evaluation device (DWB®, Bioseb) to identify the bearing forces of the different limbs of animals has revealed severe alterations in the weight distributions in rats that have undergone unilateral vestibular neurectomy (UVN). With an advanced version of this device (DWB2®, Bioseb), we can differentiate static and dynamic vestibular behavior in our animal model and extract new data, such as the coordinates of the animal's limbs, at any time. To migrate from an evaluation that is essentially qualitative, in this study, we designed a new method of quantitative analysis based on parametric measurements. For the first time, we have demonstrated a postural imbalance following a vestibular lesion using parameters similar to those used in human clinical practice, such as plots of the position of the animal's barycenter under static condition (statokinesiograms), the surfaces of the 90% confidence ellipses of these statokinesiograms (15), the speed of displacement of the barycenter, and the speed of the barycenter as a function of the sway area (SFA: Speed as a Function of the Area), which yields estimates of the energy used for postural stabilization (16). Other behavioral phenotype characteristics of unilateral vestibular injuries were analyzed: the weight distribution on the medial lateral axis, the time spent by the animal leaning on its abdomen, and the number of laps performed during the circling periods. These data are consistent with those from our previous studies (6) and provide new information on the postural equilibrium pattern observed after vestibular loss in rats.

This parametric approach yields improved sensitivity in the evaluation of posturo-locomotor deficits following unilateral vestibular lesions. It will likely become an essential preclinical tool that is used to test the effectiveness of antivertiginous compounds or rehabilitation protocols on posturo-locomotor function recovery after vestibular loss.

MATERIALS AND METHODS

Animals

The experiments were performed on 16 Long Evans male rats of 10–12 weeks old (250/300 g) originating from our own breeding, from parents arising from Charles River (St Germain sur l'Arbresle, France). All experiments were performed in accordance with the National Institutes of Health's Guide for Care and Use of Laboratory Animals (NIH Publication no. 80–23) revised in 1996 for the UK Animals (Scientific Procedures) Act of 1986 and associated guidelines or the Policy on Ethics approved by the Society for Neuroscience in November 1989 and amended in November 1993 and under the veterinary's supervision and the National Ethical Committee's control (French Agriculture Ministry Authorization: B13-055-25). Present study was specifically approved by Neurosciences Ethic Committee N°71 from the French National Committee of animal experimentation. Every attempt was made to minimize both the number and the suffering of animals used in this experiment. The animals were housed in a large confined space with 12–12 h diurnal light variations with free access to water and food. They were housed at the Fédération 3C (Center Saint-Charles, Aix-Marseille University) animal facility.

The 16 animals were divided into two groups: SHAM group ($n = 7$) and UVN group ($n = 9$). See below for the details of procedures used for surgery.

Study Design

The behavioral investigations were carried out in 2 parts (**Figure 2**): a first quantitative evaluation of the syndrome with the DWB2®, and a second qualitative evaluation of the syndrome following the same scale as the one detailed in Péricat et al. (5). The rats were manipulated for 5 days before the preoperative session. During that period, a quantitative analysis of the postural parameters (reference values) was performed with the DWB2®. All the rats then underwent surgery before being assessed during the acute stage (post-lesion days 1, 2, and 3) and the vestibular

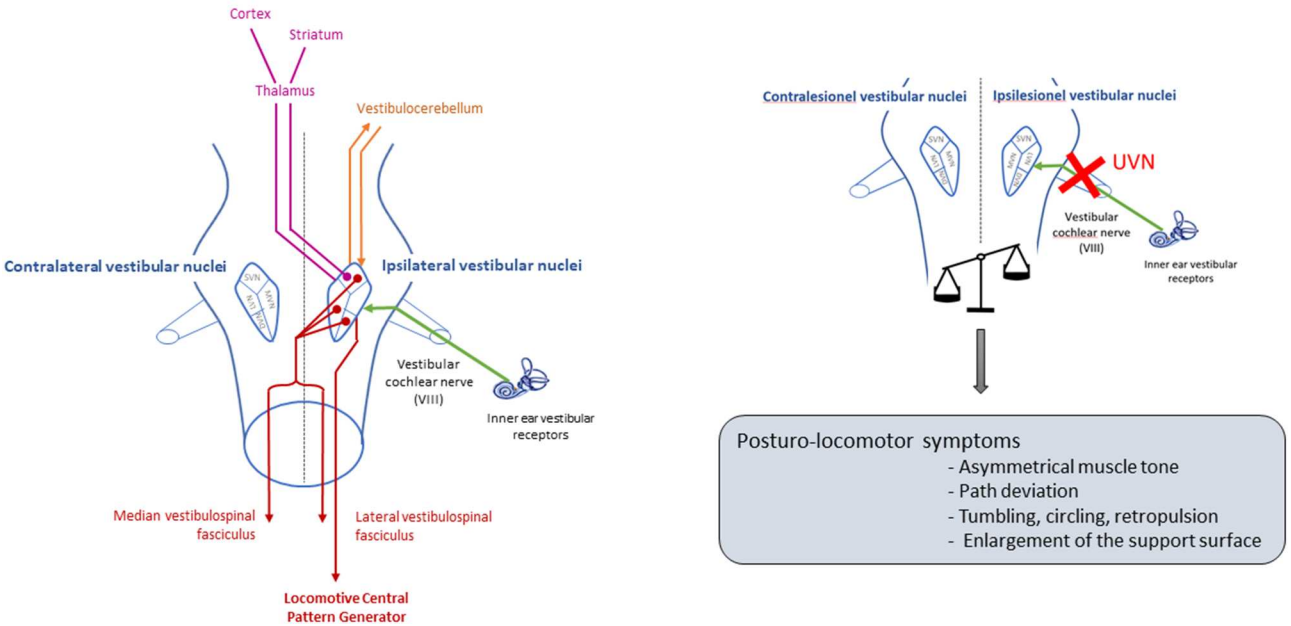

FIGURE 1 | Pathways involved in posturo-locomotor function of the vestibular system, and deficits after unilateral vestibular neurectomy. **(A)** The vestibular nerve transmits information from peripheral vestibular receptors to the four vestibular nuclei located in the brain stem [medial vestibular nucleus (MVN), lateral vestibular nucleus (LVN), superior vestibular nucleus (SVN) and inferior vestibular nucleus (DVN)]. The vestibular nuclei then project toward various structures involved in the control of posturo-locomotor function: the spinal cord (17), the cerebellum (18), the striatum (19) and different cortical zones such as the motor cortex (20). The medial vestibulospinal fasciculus sends ipsi and contralateral projections to motoneurons of the neck muscles, allowing head stabilization, while the lateral vestibulospinal fasciculus projects ipsilaterally to the trunk and leg muscles, allowing anti-gravitary muscle tone, and to the locomotor CPG responsible for automatic locomotion coordination. The vestibular nuclei receive and transmit information to the vestibulocerebellum, involved in posture control, and via a thalamic relay, the vestibular nuclei project toward the striatum which is involved in locomotion control. The vestibular nuclei therefore constitute a central relay for the control of posture and locomotion, and a unilateral vestibular loss that induces electrophysiological imbalance between the homologous vestibular nuclei will generate a characteristic posturo-locomotor syndrome that affects each level of the neural network described above. **(B)** UVN will cause an electrophysiological asymmetry between homologous vestibular nuclei (21). Due to all the pathways previously described, this electrophysiological asymmetry will lead to various posture-locomotor symptoms.

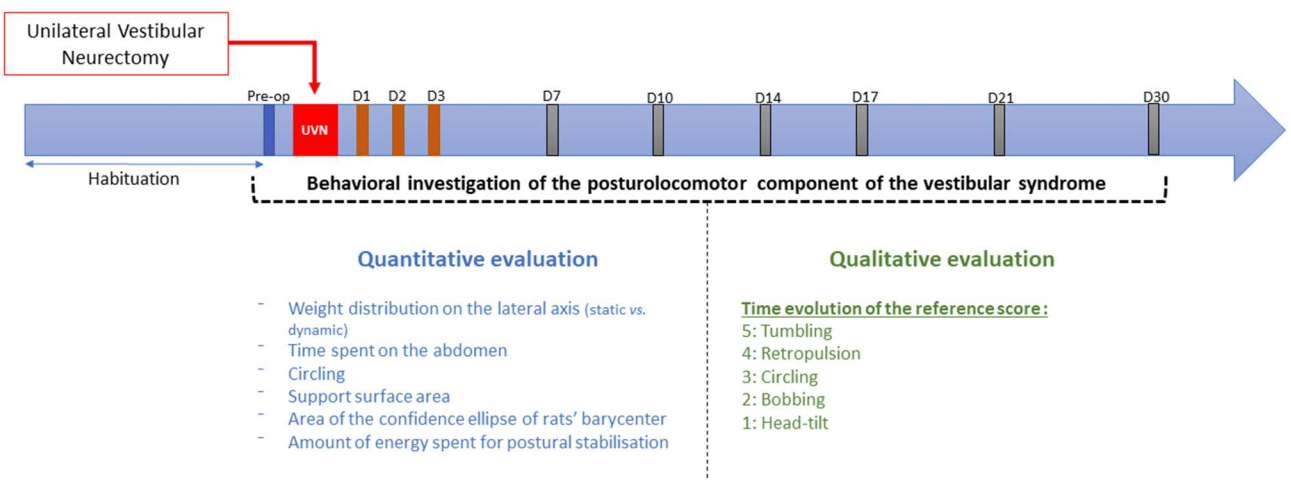

FIGURE 2 | Study design. Details of the procedure used to evaluate quantitatively and qualitatively the vestibular syndrome before and after unilateral vestibular neurectomy. Behavioral investigation of the posturolocomotor component of the vestibular syndrome was made in a first preoperative session (serving as a reference value) and then at 1, 2, 3, 7, 10, 14, 17, 21, and 30 post-lesioned days (D). Two types of evaluation were carried: a first quantitative evaluation detailed in this study and a qualitative evaluation based on previous paper (5).

syndrome compensated stage (post-lesion days 7, 10, 14, 17, 21, and 30).

Surgery

The UVN was performed on nine rats following the surgical procedure previously reported in the literature (5). The rats were placed in the induction box and left for 5 min (isoflurane concentration 4%). Once they were deeply anesthetized, they were intubated and, during the surgery, the anesthesia was maintained at an isoflurane concentration of 3%. A tympanic bulla approach gave access to the vestibular nerve: the cervical muscular planes were dissected leading to the tympanic bulla, which was widely drilled to expose the stapedial artery and the promontory containing the cochlea. The cochlea was drilled, exposing the cochlear nerve. The cochlear nerve meatus was enlarged with a needle leading to the vestibulocochlear nerve, which was sectioned at its entry into the brainstem after aspiration of the Scarpa's ganglion. The wound was closed using a stapler. Before the animal awakened, a solution of Ringer Lactate (Virbac; 10 ml/kg) was injected subcutaneously to reduce the dehydration resulting from the rats' inability to drink normally due to the lesion. Buprenorphine (Buprecare®; 0.05 mg/kg) was given 30 min before the surgery.

In another 7 sham rats, surgery was stopped at the opening of the tympanic bulla.

Qualitative Evaluation of the Vestibular Syndrome

The vestibular syndrome induced in the rat after UVN is characterized by typical symptoms previously described in various species [rat UVN model: (5), mice UVN model: (4), cat UVN model: (7)]. These symptoms usually include tumbling, retropulsion, circling, bobbing and head-tilt which are all present in the acute phase of the syndrome and progressively disappear following vestibular compensation.

For this study, we used the same scale as the one previously reported (5). It is a cumulative scale where a score is assigned to each symptom, based on its severity (tumbling: 5, retropulsion: 4, circling: 3, bobbing: 2, head-tilt: 1).

Quantitative Evaluation of the Vestibular Syndrome

Analysis Device

The second version of the dynamic weight-bearing (DWB2®) device (Bioseb, Vitrolles, France) was used to evaluate the postural instability of rodents following unilateral vestibular loss. This apparatus has previously been described for the assessment of postural instabilities in the same model of vestibular loss (6). It consists of a Plexiglas chamber (25 × 25 cm) with a floor covered by a 2,000 force sensors plate. The weight passed through each part of the body in contact with the ground was assessed automatically in each sensor at a sampling frequency of 30 Hz. A high frequency camera was directed at the side of the enclosure to assist with data analysis. Both the sensors and the camera were connected to a computer using the latest DWB2 software version available at the time (v2.0.60). The software was configured as follows: part of the animal body is detected if it activates at least 2 pixels and if the weight in the central pixel is 0.7 g minimum, with at least 1 adjacent pixel recording 0.3 g. This new version allows us to distinguish periods when the animal is static or dynamic by applying a mobility threshold of 700 ms—if each area in contact with the sensors is stationary for at least 700 ms, the animal is considered static, otherwise it is dynamic. Using the software, the operator then manually identified each paw (front left, front right, rear left, and rear right) and the areas in contact with the ground, which are identified as "Other zones" (tail, abdomen, head …) with the support of the video.

Each animal could move freely in the arena for 5 min in each pre-operative and post-operative session. The pre-operative session was recorded the day before the surgery, and then the time course of the syndrome was studied on days 1, 2, 3, 7, 10, 14, 17, 21, and 30 post-UVN (**Figure 2**).

Data Analysis

The software performed a first automatic analysis of the acquisition file. This analysis involves the identification of the paw that activated each group of ground sensors. Following that, an experimenter checked the analyses and made corrections when necessary. Sequences where a paw cannot be clearly identified were removed from the analyses.

With this analysis, we could identify many parameters calculated automatically by the software (e.g., the weight distribution on each paw) as well as the support applied by each identified area of the animal's body in contact with the ground sensors (in grams) and the mean coordinates of these areas (in cm).

With the help of the software and home-made programs developed on Scilab (open-source software), different biomarkers were extracted, for static and dynamic phenotypes.

Static and Dynamic Parameters

The weight distributed on lateral axis during the acquisition allowed us to determine how the animal distributes its weight between his left and right paws in order to find its balance. This parameter had been investigated previously (6), but without distinguishing the static condition from the dynamic condition. This parameter was expressed as a percentage of the animal weight applied on the left limbs and right limbs at the day of acquisition.

By analogy with humans who use canes to gain postural stability, we tried to determine whether our rodent model had adopted a similar strategy by adding a support point on the ground. To that end, we quantified the average time the animals spent with their abdomen on the ground sensors, during static and dynamic periods. To do so, we calculated the time spent with another part of the body, with coordinates between the animal's four legs.

Dynamic Parameters

Circling is a phenotype specific to unilateral vestibular loss. This behavior happens when the rat starts to circle around its axis. We quantified this circling behavior by counting the number of fast laps performed during an acquisition. By tracking each front paw separately, we were able to quantify the deviation angle θ of

each step made by the animal (Equations 1, 2). To do so, we used coordinates of the front paws during dynamic periods – FRx, FLx, FRy, and FLy are, respectively, the coordinates of the front right and front left paw on the X axis and on the Y axis. When the cumulative sum of θ was equal to 360° or −360°, it meant that the animal had made 1 complete lap with one paw, respectively, to the left or to the right. To distinguish the circling from the thigmotaxis (a specific behavior whereby the animal stays close to the walls of an arena during exploration), a 500 ms filter was applied over the duration of the supports of each leg. We then calculated the average of the number of laps obtained with the front left and right paws to quantify the number of laps made by circling during one acquisition.

$$\theta_{FR} = \tan^{-1}\left(FRy_{n+1}, FRx_{n+1}\right) - \tan^{-1}\left(FRy_{n}, FRx_{n}\right) \quad (1)$$

$$\theta_{FL} = \tan^{-1}\left(FLy_{n+1}, FLx_{n+1}\right) - \tan^{-1}\left(FLy_{n}, FLx_{n}\right) \quad (2)$$

Static Parameters

The support surface area is a sensitive parameter used to assess static postural instability in several models of unilateral vestibular loss [cats: (7), rats: (22)]. It was calculated by measuring the surface delimited by the four legs of rats while they were static during a session, using coordinates of each paws in the ground sensors. The maximum value for each acquisition was used to quantify instability moments.

Posturographic phenotypes

Previously, recorded data from the first version of this device (DWB® Bioseb SAS) were used to model the fine postural disruptions of UVN rats (6). To do that, the mean position of the barycenter was estimated with the help of the weight applied on each paw. Here, the use of paws coordinates allowed us to calculate a true barycenter of the bearing forces applied by the paws on the ground sensors (Equations 3, 4). The position of the barycenter was calculated at each period when the animal was stationary and on its four paws.

$$Barx = \frac{FLx*FLw + FRx*FRw + RLx*RLw + RRx*RRw}{FLw + FRw + RLw + RRw} \quad (3)$$

$$Bary = \frac{FLy*FLw + FRy*FRw + RLy*RLw + RRy*RRw}{FLw + FRw + RLw + RRw} \quad (4)$$

Based on the coordinates of the rat's barycenter over time, we were able to trace the statokinesigram of each acquisition. The statokinesigrams show the trajectories in 2D of the barycenter and the center of gravity of each paw every time the calculation is performed. The coordinates of the barycenter have also allowed us to use finer and more precise postural parameters already used in human clinical practice, such as the body sway area (body's balancing zone) [(15): Human, (13): Human, (23): mouse model]. These coordinates allowed us to quantify the postural stability and locomotion speed of our rat model as a function of the sway area (SFA) in order to estimate the energy spent by the rat to stabilize its posture (16). Indeed, on the same surface, the barycenter can cover a more or less long distance. This parameter is used in clinical posturology to estimate the energy a patient spent when he is on a force platform. In human clinical studies, the time the subject spends in a stationary position on a force platform is controlled. Here, we have chosen to use the speed of movement of the barycenter in order to avoid the variable durations of the static postures.

Body sway was evaluated by measuring the area of the confidence ellipse that includes 90% of the barycenter. With this classical method, we eliminate 10% of the extreme points to suppress postural sway values that were possibly due to quasi voluntary movements. This calculation was made when rats were static and on their four paws. An average weighted by the duration of each of these moments is then established for each acquisition.

Statistical Analysis

For each of the parameters evaluated on the two groups of rats (UVN and SHAM groups) the recorded values are expressed as average + SEM. To test the effect of UVN, we performed analysis of variance (Two-way ANOVA with repeated measures). For *post-hoc* analyses, Dunnett's tests were performed to compare values at each post-operative time with pre-operative values, and Tukey-Kramer multiple comparison tests to compare the results obtained between UVN group and SHAM group and between static and dynamic conditions. The Tukey-Kramer multiple comparison test is adapted for comparison of samples of different size.

In order to avoid interindividual differences in postural parameters due to small differences in weight or foot placement between rats, all postural parameters were expressed as normalized data. Each result obtained by the animals was normalized with the result they individually obtained during the preoperative condition.

Pearson correlations were also calculated between the quantitative parameters and the parameters from the qualitative scoring scale in order to see or not similarities in their kinetics. These results give us the Pearson correlation coefficient r (no correlation if close to 0, low if between 0.3 and 0.5 and high if >0.5), and the significance of the correlation p (**Table 1**).

RESULTS

This study analyses the longitudinal effects of a sudden and unilateral suppression of vestibular information on different posturo-locomotor biomarkers: [1] the weight distribution on the lateral axis and the time the animals spend leaning on their abdomen, in static and dynamic condition, [2] the number of turns performed in circling periods (behavior), [3] the maximum support surface area and posturographic parameters such as body sway and the amount of energy spent to stabilize (SFA), studied when the animal is static on its four paws. The results obtained in the UVN group are compared with preoperative values to observe the effects of the vestibular lesion, and with a SHAM group in order to avoid post-surgical effects or possible habituation effects to the task not visible under preoperative conditions.

TABLE 1 | Correlations between the results of qualitative behavioral assessment and the results of quantitative behavioral assessment of vestibular syndrome.

Biomarkers used in the present study	Pearson r	*P*
Maximum support surface area	**0.36**	**0.0004***
Time spent in the abdomen, static periods	**0.3459**	**0.0008***
Time spent in the abdomen, dynamic periods	**0.3542**	**0.0006***
Left circling	**0.5592**	**<0.0001***
Right circling	0.1504	0.157
Amount of energy spent to stabilize	0.1686	0.1121
Body sway area	−0.03676	0.7309
Weight distribution on right limbs, static periods	**0.3782**	**0.0002***
Weight distribution on left limbs, static periods	**−0.3782**	**0.0002***
Weight distribution on right limbs, dynamic periods	0.2149	0.042*
Weight distribution on left limbs, dynamic periods	−0.2149	0.042*

The parameters tested during this study are listed in the first column. In the second column the Pearson correlation coefficients r are listed, and in the third column their degree of significance. The parameters in bold are those correlated with the qualitative scale (low but significant correlations) ($p < 0.05$).*

Static and Dynamic Parameters

Weight Distribution Along the Lateral Axis

The results for this parameter are shown in **Figure 3**. Before the unilateral vestibular lesion, the UVN group distributed its weight symmetrically between the right and left sides (static right % = 50.9 ± 1.3; static left % = 49.1 ± 1.3; dynamic right % = 51 ± 0.9; dynamic left % = 49 ± 0.9). At the first post-lesion day, no significant differences were observed on dynamic laterality parameters compared with preoperative values, or between the UVN group and the SHAM group. Nevertheless, in the UVN group, under static conditions, significant differences appeared between left and right limbs ($p < 0.0001$) and with the preoperative condition ($p < 0.05$). On the 2nd post-lesion day, significant differences still existed in the UVN group, in static condition, between left and right limbs ($p < 0.05$). No other differences were observed on days 2 and 3 post-lesion. From 1 week to 1 month after UVN, rats significantly shift their weights to the left limbs (D7: $p < 0.001$, D10–D30: $p < 0.0001$), with no difference between static and dynamic conditions. During this period, significant differences were also observed between the UVN group and the SHAM group (D7: $p < 0.05$, D10–D30: $p < 0.0001$).

During all post-lesion delays, under static and dynamic conditions, we can observe that the SHAM group had a symmetric weighting distribution between the right and left limbs (right % between 47.2 ± 2 and 51.2 ± 1.4 and left % between 48.8 ± 1.3 and 52.8 ± 2).

Time Spent Leaning on the Abdomen

Whatever the analysis time, the sham group never places its abdomen on the floor sensors as shown in **Figure 3D**. However, the abdomen of the UVN group animals is detected by the ground sensors from the first day after UVN (**Figure 3C**). At the first day post-UVN, significant differences are observed compared with the SHAM group ($p < 0.005$ and $p < 0.0001$ in static and dynamic condition; respectively) and with the preoperative condition for static ($p < 0.001$) and dynamic ($p < 0.0001$) conditions. During the 2nd and 3rd post-lesion days, some animals continue to lean on their abdomen for short periods of time but with no significant differences. The animals in the UVN group regain a posture without support on their abdomen from the 7th day postlesion.

Dynamic Parameters

In order to have an objective quantification of the circling behavior observed in our vestibular syndrome model (5) and in several other disease models (24), we counted the number of complete turns performed with rapid leg support during all post-lesion days (**Figure 4**).

Concerning the number of right-hand turns, no significant difference is observed between the SHAM and UVN groups. The SHAM group performs on average <2 fast laps per session during all analyzed delays, and the UVN group performed a maximum of 2.3 ± 0.7 fast laps to the right at 7th day postlesion.

Significant differences are observed in the number of left laps circling at postlesion days 1, 3, and 7. These differences are observed between the UVN and the SHAM groups (D1: $p < 0.0001$, D3: $p < 0.05$, D7: $p < 0.001$) and with the preoperative values for the UVN group (D1: $p < 0.0001$, D3: $p < 0.05$, D7: $p < 0.001$).

Static Parameters

Maximum Support Surface Area

The support surface area has been used in several animal models [(7) in cats, (22) in rats] to quantify postural instability following unilateral vestibular loss. Nevertheless, these data were acquired in the rat UVN model after reactivation of the vestibular syndrome by stimulation of the otolith system [(5) for more information]. Here, in order to quantify the postural instability, we have chosen to select the maximum surface area of the polygon during a session, which reflects instability periods of the animal.

The results obtained reveal a little variability in the SHAM group; the data normalized with the preoperative condition are between 0.8 and 1.2 (**Figure 5**). Nevertheless, from the first post-lesion day, the maximum value of the support surface area increases significantly in the UVN group compared both to the preoperative time (from day1 to day 7: $p < 0.0001$; day 10 and day 17: $p < 0.05$; day 14, day 21 and day 30 : $p < 0.0001$), and compared to the SHAM group (from day 1 to day 14 : $p < 0.0001$, from day 17 to day 30 : $p < 0.05$).

Posturographic Parameters

Statokinesiograms

The calculation of the position of the barycenter at a frequency of 30 Hz, at each moment, when the animal is on its four paws and stationary, allowed us to trace the average positions of the paws and the position of the barycenter of each animal at each session. These statokinesiograms show us different postural patterns depending on the group of rats and the post-lesion time, including a greater dispersion of the barycenter point cloud at several post-lesion days (**Figure 6**). We then these

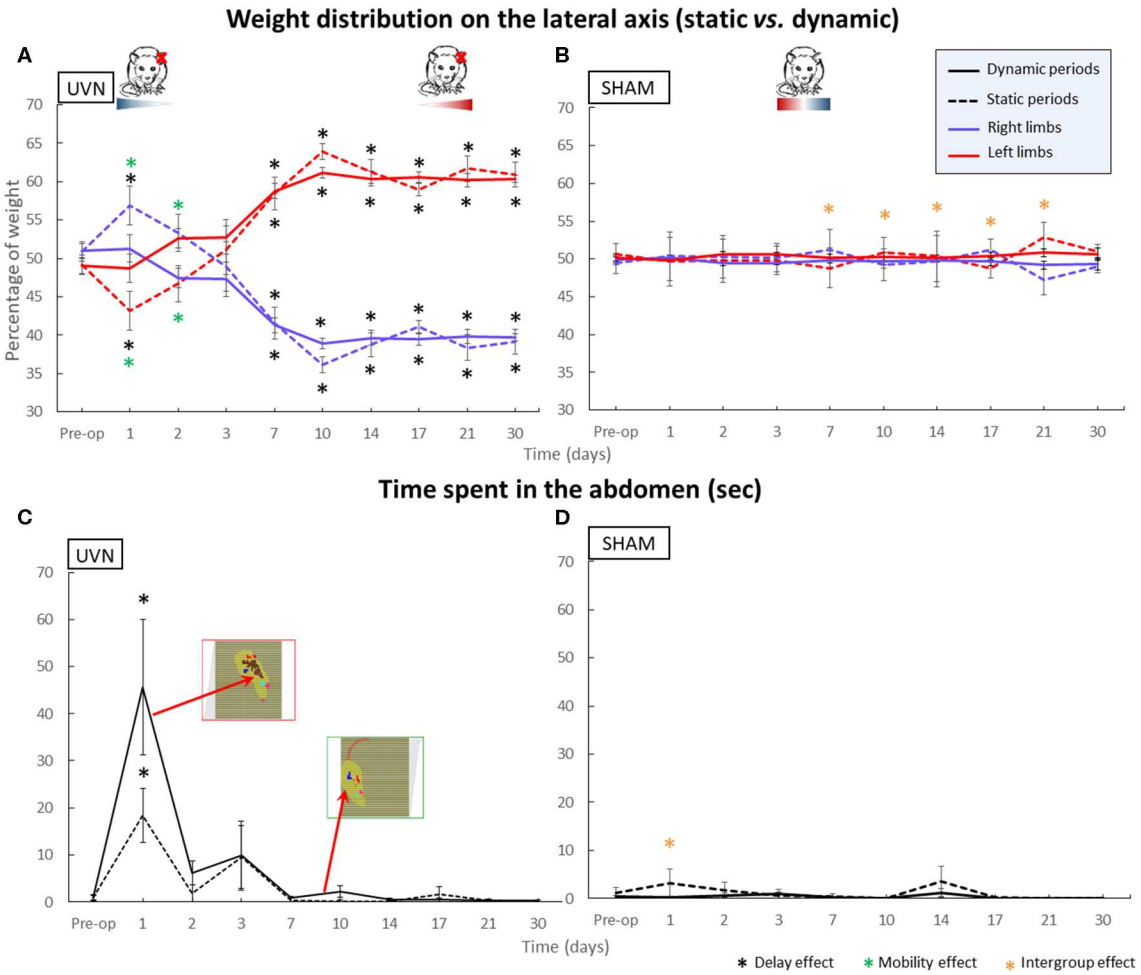

FIGURE 3 | Parameters discriminating between static and dynamic behavior. Within A. The weight distribution on the lateral axis and in B. the time spent on the abdomen. **(A)** The weight distribution on the lateral axis shows asymmetric kinetics in the UVN group. Rats correctly distribute their weight between right and left limbs during the preoperative session and then switch more weight to their right limbs in static condition at day 1 & day 2 post-UVN ($p < 0.05$) while the dynamic weight distribution remains symmetrical. During the compensated period, UVN animals significantly distribute more weight on their left limbs whatever the static or dynamic condition. **(B)** SHAM animals always have a symmetrical weight distribution. The geometric shapes in color under the rat drawings indicate the amount of weight distribution on the left (red) and right (blue) paws in the UVN and SHAM group rats. **(C)** The UVN group spends significantly more time on their abdomen at day 1 postlesion compared to the preoperative session ($0.0001 < p < 0.001$) and compared to the SHAM group [static ($p < 0.005$) and dynamic ($p < 0.0001$)], with more time overall leaning on his abdomen in dynamic condition. **(D)** This behavior is never observed in the SHAM group. Standard errors of the mean are reported as vertical lines. Delay effect refers to significative differences with the preoperative condition; mobility effect means that a significative difference was found between static and dynamic condition; intergroup effect means that a significative difference was found between UVN and SHAM group (*$p < 0.05$).

plots to quantify the body sway and the energy expended to stabilize it (SFA).

Estimation of the energy spent to stabilize

The results from the quantification of the energy expended to stabilize the posture (**Figure 7A**) show a significant difference on the first post-lesion day between the SHAM and UVN groups ($p < 0.01$) and with the preoperative condition for the UVN group ($p < 0.001$). No significant difference was observed at the preoperative time, and from the 2nd to the 30th post-lesion day between the two tested groups.

Quantification of postural instability

The results from the body sway (**Figure 7B**) show a significant gradual increase in this parameter beginning the 3rd postlesion day and persisting until the 30th postlesion day in the UVN group, indicating a progressive postural instability. The surface of the confidence ellipse at 90% of the barycenter doubles from postlesion D3 to postlesion D30 and remains significantly different with the preoperative time. No significant variation in this parameter is observed in the SHAM group, whose surface area of the normalized confidence ellipse remains close to 1.

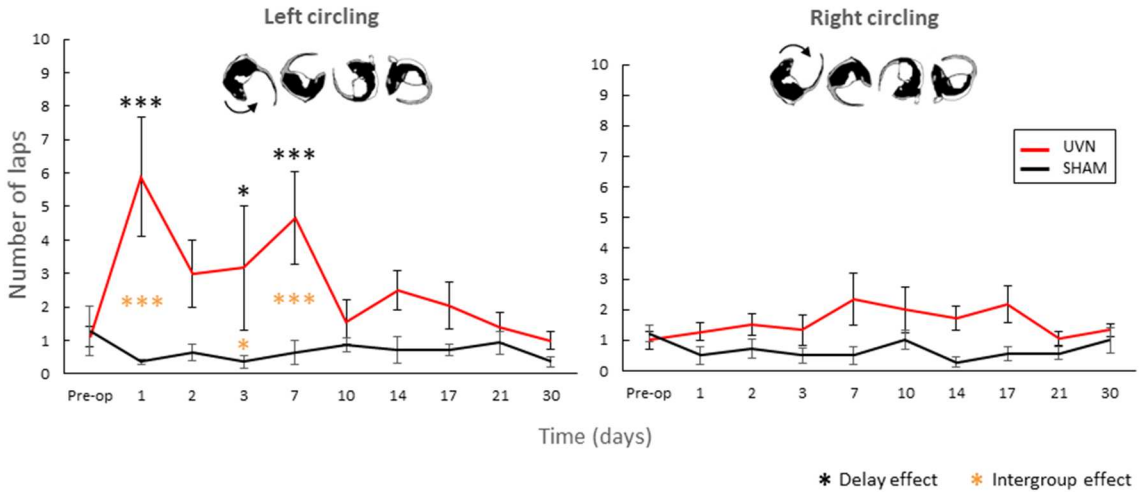

FIGURE 4 | Quantification of the circling behavior. The UVN group performed significantly more left circling at D1, D3, and D7 compared to the preoperative period and the SHAM group ($0.05 < p < 0.0001$). Concerning the number of right-hand turns, no significant difference is observed between the SHAM and UVN groups. This circling behavior is never observed in the SHAM group. Standard errors of the mean are reported as vertical lines. Delay effect refers to significative differences with the preoperative condition; intergroup effect means that a significative difference was found between UVN and SHAM group (*$p < 0.05$; ***$p < 0.001$).

Statistical Correlations Between the Two Methods for Analyzing the Posturo-Locomotor Syndrome Following Unilateral Vestibular Suppression

The results from the qualitative vestibular syndrome assessment scale used in the same rodent model [(5), **Figure 8A**] describe the kinetics of vestibular syndrome. The disorders are expressed at their peak during the first 3 days after UVN, then gradually decrease at the 7th post lesion day to stabilize at a score of 2 on average at the 30th postlesion day (**Figure 8B**).

Correlations were made between the quantitative and qualitative parameters in the UVN (**Table 1**). Low ($0.35 < r < 0.38$) but highly significant ($p < 0.001$) correlations exist between the results of the qualitative scale and the quantitative parameters: maximum support surface area, time spent in the abdomen (static and dynamic periods), weight distribution on left limbs (static periods). The left circling quantitative parameter is strongly and significantly correlated with the qualitative scoring ($r = 0.56$; $p < 0.0001$). The weight distribution quantitative parameter on the left legs is inversely correlated to the qualitative scale ($r = -0.38$; $p < 0.0002$).

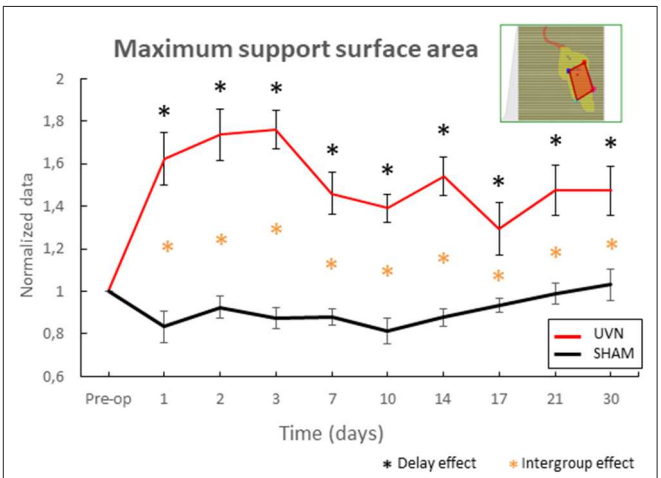

FIGURE 5 | Automatic quantification of the maximum support surface area, a biomarker of postural instability. This parameter reveals instability following surgery in the NVU group at critical and compensated periods. Note that from the first post-lesion day to the last acquisition day, the maximum value of the support surface area of the sustentation polygon increases significantly in the UVN group compared to the preoperative time ($0.05 < p < 0.0001$), and compared to the SHAM group ($0.05 < p < 0.0001$). Standard errors of the mean are reported as vertical lines. Delay effect refers to significative differences with the preoperative condition; intergroup effect means that a significative difference was found between UVN and SHAM group (*$p < 0.05$).

DISCUSSION

This study provides new information on the postural balance patterns observed in a rodent model of acute vestibular peripheral pathology (UVN rat model). We quantify for the first-time postural parameters, such as those analyzed in human clinical studies in the field of posturology. Plots of the position of the animals' barycenter under static conditions (stabilograms), the surface of the 90% ellipse of confidence of these stabilograms, the speed of displacement of the barycenter, and the speed of the barycenter as a function of the sway area (SFA) provide estimates of the energy used for postural stabilization. In addition, two new vestibular behavioral phenotypes are also quantified for the first time in this study: the time spent by the animal leaning

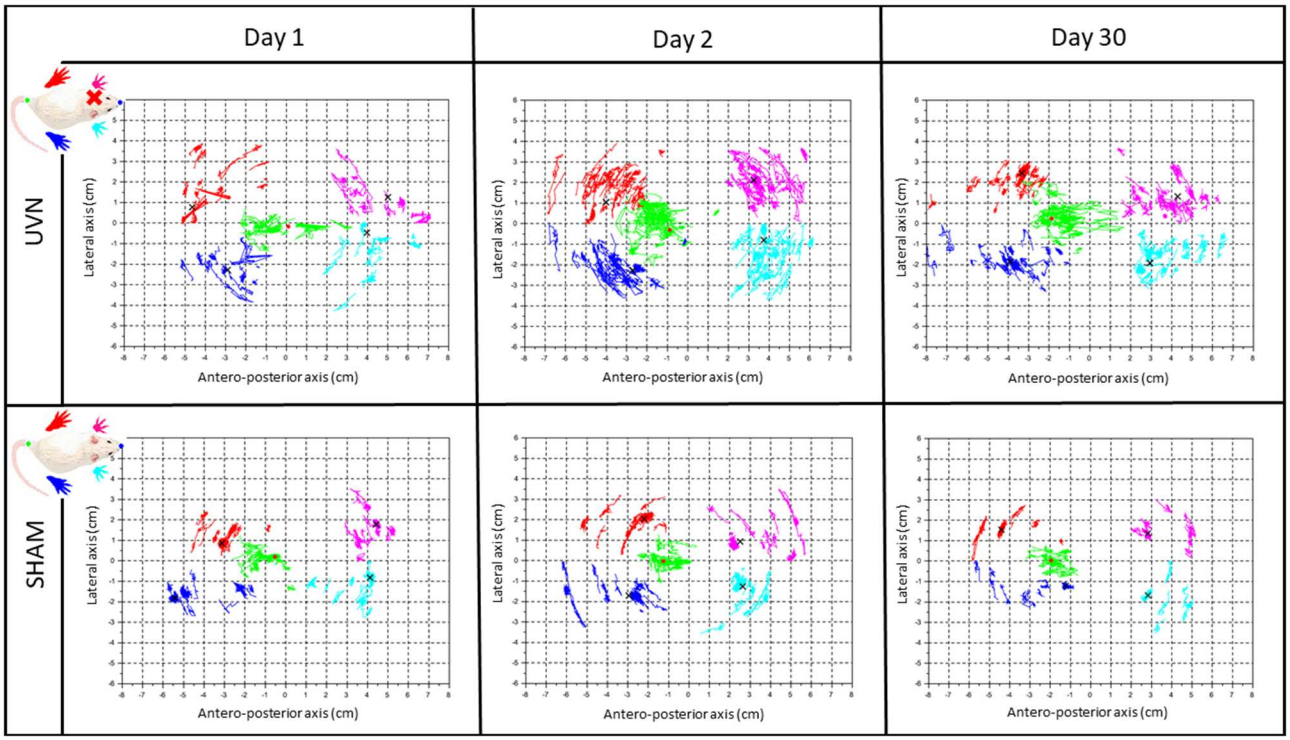

FIGURE 6 | The rodent stabilogram, a representative illustration of the kinetics of barycenter and paws positions. Plot of the successive positions of the legs and the barycentre at each moment when the animal is stationary with its 4 paws placed on the sensors during a 5-min acquisition. The first line of the table gathers the stabilograms of a representative UVN rat at different post-UVN days (Day 1, Day 2, and Day 30), the second line gathers the stabilograms of a representative SHAM rat at these same post-UVN days times. For each stabilogram, the antero-posterior axis is on the abscissa and the lateral axis on the ordinate. The dark blue, red, light blue and pink dot clouds are the traces of the average positions, respectively, of the right rear paws, left rear paws, right front, and left front paws during a session at each moment when the animal is static on its four legs. The green point cloud is the trace of the successive positions of the barycentre calculated at each of these moments. The different black crosses represent the average position of the legs during an entire session. The red dot represents the average position of the barycentre during a session. The pattern of stabilograms appears stable in SHAM rats, compared to the UVN group where the pattern appears more instable at the three representative post-UVN days.

on its abdomen and the number of laps performed during the circling behavior. This was done through a newly automated and parametric analysis method that is independent but correlated with the qualitative scales that are traditionally used (4, 5, 25).

These new postural biomarkers have allowed us to differentiate static behavior from dynamic behavior, to automatically quantify circling in a unilateral vestibular lesion model (behavior usually noted in qualitative score scales), and to focus precisely on the postural disorders inherent to our rodent model of unilateral vestibular pathology.

Static and Dynamic Behavioral Parameters

Based on the impact of vestibular loss on the weight distribution on the lateral axis, we have suggested a strategy for postural rebalancing during the acute phase of vestibular syndrome. Indeed, at D1 and D2 postlesion, animals exhibit good dynamic balance because they distribute their weight symmetrically, whereas this distribution is asymmetric with more weight applied on the ipsilesional side under static conditions. The control of locomotion is managed by a very large network (26). These neural networks are located in the spinal cord and form the central pattern generators (CPGs) of locomotion. These CPGs, through the action of a pacemaker neural network (27), are able to initiate rhythmic motor control in the absence of sensory feedback. Rats have 2 CPGs: one at the cervical level for the control of the rhythmicity of the front limbs and one at the lumbar level for the control of the rhythmicity of the movements of the trunk and hindlimbs (28). Thus, once motor control is initiated and in the absence of external disturbances, the CPGs generate an automatic rhythm for walking. Under static conditions, the information obtained from the hair cells of the peripheral vestibular receptors located mainly in the saccule and utricle becomes essential to maintain anti-gravity muscle tone during rest (29). Thus, during the acute phase of vestibular syndrome (the critical period of 1–3 days postlesion), when the animal is stationary, UVN causes asymmetry in the anti-gravity muscle tone, with a decrease on the ipsilateral side due to the absence of gravity information from the deafferented side. This asymmetry in muscle tone is probably responsible for the larger weight distribution on the right-side paws and the use of the abdomen for support as a postural stabilization strategy. Weight rebalancing under dynamic conditions can also occur due to the contribution of other sensory modalities, thus supporting

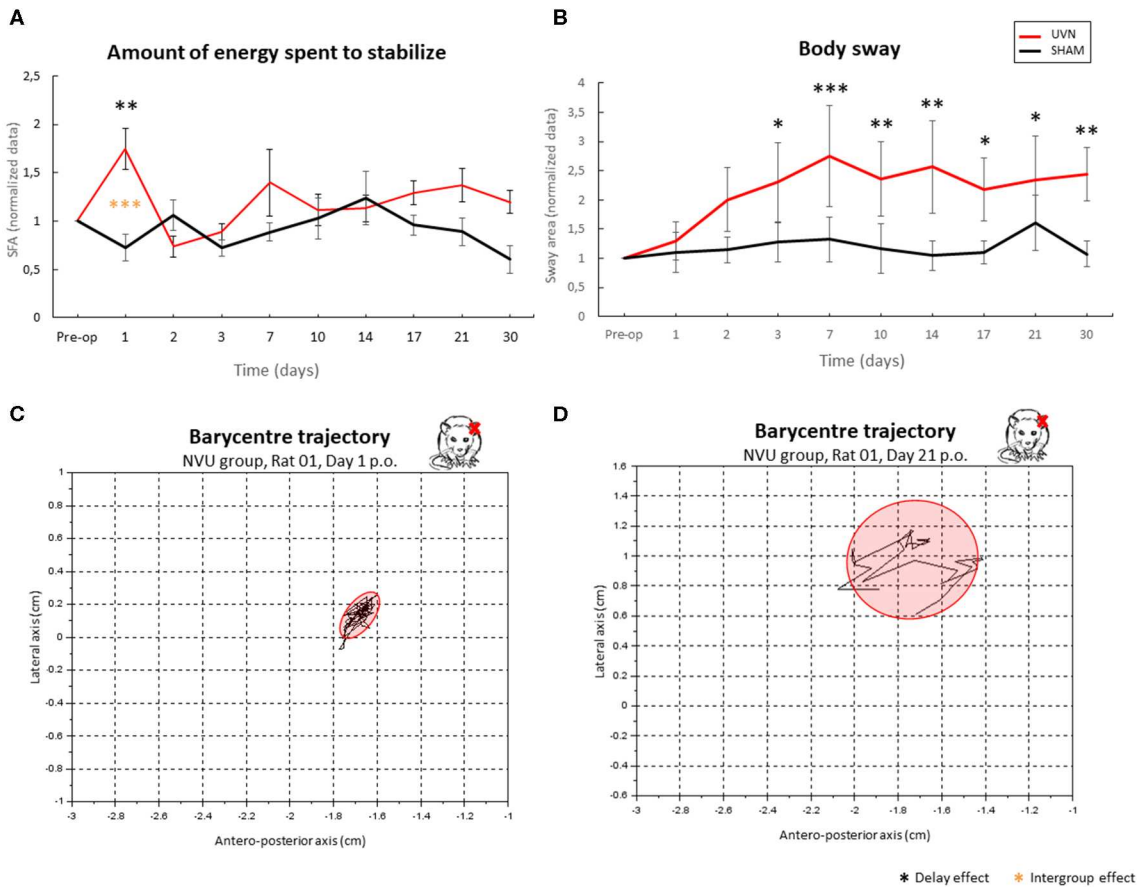

FIGURE 7 | Use of posturographic parameters to quantify postural instability in a UVN rodent model. **(A)** quantification of the energy spent for posture stabilization. **(B)** body sway. **(C,D)** examples of barycentre plots observed in a representative NVU rat in acute **(C)** and compensated **(D)** period. The NVU group spends significantly more energy to stabilize on the first day post-UVN ($p < 0.001$); this energy is quantified by a ratio between the velocity of the barycentre and the surface of the confidence ellipse. It then stabilizes from D2 to D30 and becomes similar to that of the SHAM group, in which there is little variation at any time. The body-sway **(B)** is significantly higher in UVN rats from D3 to D30 and remains stable in SHAM rats. In **(C)**, we can see the representation of the displacement of the barycentre as well as its confidence ellipse at a time when the animal spends a lot of energy stabilizing its posture: the animal is stable but the displacement of its barycentre shows efforts spent to concentrate the position of its barycentre in the surface of the ellipse. In **(D)**, the same parameters are represented at a compensated delay: the animal is unstable (high surface area of confidence ellipse), and the dispersion of the path of its barycentre shows little effort applied to restrict the movement of the barycentre in a small area, that underlies a new postural strategy. Delay effect refers to significative differences with the preoperative condition; intergroup effect means that a significative difference was found between UVN and SHAM group (*$p < 0.05$; **$p < 001$; ***$p < 0.001$).

the sensory substitution phenomenon observed in patients after vestibular neurectomy (13). Indeed, during locomotion, plantar information and visual flow can augment the sensory inputs and thus contribute to the rebalancing of electrophysiological activity between the two vestibular nuclei (VN), which is known to be the key parameter of vestibular compensation (30). During locomotion, the activity of spinal cord CPGs take control of the locomotor system and also contribute to the restoration of electrophysiological homeostasis of the VN since these spinal neural networks project directly onto the VN (31) (**Figure 1A**). This postural readjustment is also observed under dynamic conditions in patients. An increase in walking speed leads to a decrease in the gait deviations observed in vestibular patients (32).

In addition, the data from the UVN group's abdominal exposure time indicate that during this critical period (from 1 to 3 days postlesion), animals place their abdomen on the ground sensors. This behavior was not observed during the other postlesion days or in the SHAM group. We can also observe that they use their abdomen as a support, especially in dynamic conditions. We hypothesize that UVN rats use their abdomen to maintain dynamic balance, and this part of the body acts as a new support point used to promote stability, especially under dynamic conditions. The same type of behavior is found in humans, as people with poor balance tend to lean on a cane.

From the 7th day postlesion, the animals distribute much more weight on the ipsilesional side, which is consistent with the results previously published (6) and reflects muscle tone recovery on the ipsilesional side. Nevertheless, the animals in the UVN group maintained this weight distribution asymmetry on the lateral axis until the 30th day after UVN. It can be assumed that this weight asymmetry in favor of the injured side may explain the

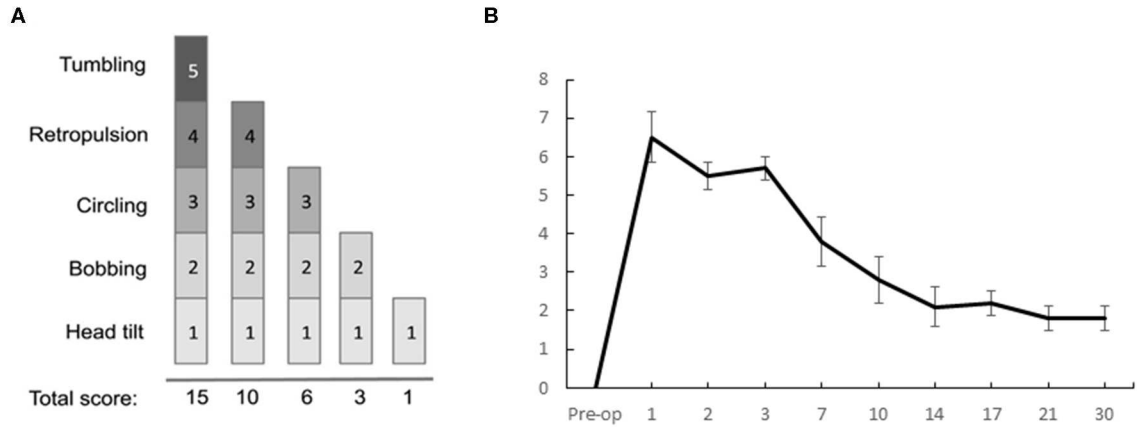

FIGURE 8 | Qualitative evaluation of the posturo-locomotor components of the vestibular syndrome. **(A)** Illustration of the evaluation grid used to conduct the analysis. **(B)** Results of the qualitative evaluation of the UVN group at the different delays of the study: we can observe a critical period when the disorders are at their peak from D1 to D3, then a period when the disorders gradually compensate each other, with a progressive decrease in the score from D7 to D30.

body's inclination and the deviation of the locomotor trajectory on the side of vestibular loss, as observed in patients after UVN (13, 32, 33).

It can also be noted that this weight asymmetry appears as early as 7 days postlesion, which coincides with the time at which the animals stopped the abdomen, support on the ground sensors. Although the animals no longer used their abdomen because they recovered muscle tone in their limbs, their weight redistribution pattern on the lateral axis was different from that observed in the preoperative period. The animals were able to compensate but not fully recover to preoperative levels after experiencing vestibular loss.

Dynamic Parameter

Circling refers to rapid rotational behavior that is observed in different disease models (4, 5, 7, 24). This phenotype is common to rodent models of various pathologies with cerebral asymmetry (Parkinson's disease, schizophrenia, depression or anxiety). A similar behavior has been observed in humans: in the absence of visual information, they exhibit a circular deviation to the right or left in their locomotor pattern (34). The authors of this article suggest that this phenomenon may be related to an asymmetry in non-pathological vestibular information.

In the literature, the most common hypothesis explaining circling is a dopaminergic imbalance in the striatal pathways (19). However, the VN project massively toward the thalamic parafascicular nucleus, which in turn projects directly toward the striatum (**Figure 1A**). It is recognized that this vestibulo-thalamo-striatal pathway is essential for the control of posture and leg movements (35). Thus, circling may be a result of a striatal electrophysiological imbalances resulting from electrophysiological imbalances that are observed in the VN after unilateral vestibular loss (**Figure 1B**). Similarly, its disappearance may be linked to a rebalancing of the electrical activity in the striatum. Indeed, it is well-demonstrated in the literature that vestibular syndrome is the result of electrophysiological asymmetry between homologous VN, characterized as low spontaneous electrical activity on the deafferented side and high activity on the intact side. Studies in the literature also indicate that restoring the electrophysiological balance between the two opposing VN is the key parameter for postural, locomotor and gaze stabilization function recovery (30, 36–41). In addition, the reticulospinal pathway is modulated by vestibular, visual and proprioceptive information. According to the model proposed by Deliagina et al. (42), UVN causes an imbalance in the electrophysiological activity recorded in the reticular formation, resulting in locomotor imbalances, which has been shown to result in rolling behaviors in lamprey. Circling behavior may thus represent a behavioral phenotype typical of an alteration in the excitation vs. inhibition balance of a heterogeneous neural network including, among others, VN, the striatum, the reticular formation and locomotor CPGs.

Static Parameters: Posturology

The support surface area is usually measured in animal models of vestibular pathology to assess static postural deficits following unilateral vestibular lesions (7, 22). In rats, this parameter is usually used in situations in which the syndrome is reactivated. In the present study, the support surface was calculated in a spontaneous situation of instability (the maximum value per session was selected). Our results show that the area of the support surface became significantly larger and reached the maximum size during the acute period, which is 1–3 days postlesion. This area gradually decreased but remained significantly wider postoperatively compared with preoperatively. These results indicate persistent postlesion postural instability but provide little information on the fine kinetics of vestibular syndrome. Posturology assessments provide more information about the static deficits observed in our rodent model. This used in human clinical practice for the diagnosis and evaluation of postural disorders and for the assessment of instability. Statokinesiograms are shown here for the first time

in rats under ecological conditions, without any restraint, unlike in other studies (23, 43). In this study, postural parameters are automatically studied when an animal voluntarily immobilizes itself, which reduces the need to retrain animals subjected to a stressful model of pathology (25). The analysis of the barycenter was carried out when the animal was at rest on its 4 paws, and 10% of the extreme values were excluded so that the barycenter positions where the animal started a voluntary movement were not included in the dataset.

Body sway was also analyzed for the first time in an automated way in rats, and the results indicate that instability increases gradually after vestibular loss, reaching a peak at D7, and remains high until 1 month after UVN. These data are comparable to those obtained in patients after the same type of vestibular lesion (UVN), which show an increase in body sway that is maintained over time (13). In another study, Deveze et al. (14) observed posturographic deficits in vestibular patients, which were also maintained over the long term without rehabilitation. In addition, a similar analysis showed that body sway is a good posturo-locomotor phenotypic biomarker when used for the differentiation of different neurodegenerative diseases (23).

The energy expended for postural stabilization increases sharply on the first day after UVN and then normalizes. It seems logical that the level of energy expenditure is highest during the peak of the severity of vestibular syndrome. According to the qualitative analysis, the postural disorder is the most severe on the first day postlesion, when behaviors such as circling and tumbling are observed (5, 6). Restoring postural balance to compensate for these deficits certainly requires a considerable amount of energy and effort. The energy parameter has never been studied in animals subjected to unilateral vestibular loss. A study in vestibular patients using the wavelet method showed the same results; vestibular loss patients spent more energy maintaining balance than control subjects (12). This parameter is therefore a good tool to assess the difficulty of an animal suffering from postural disorders of different origins in maintaining balance.

The posturo-locomotor deficits observed in the acute phase are probably due to the excitability imbalance between the two homologous VN (**Figure 1B**). It is the electrophysiological asymmetry between VN that induces an asymmetry in muscle tone that is responsible for postural imbalances. Conversely, it can be assumed that the restoration of certain postural biomarkers (time spent on the abdomen, circular behavior, SFA) in the period in which compensatory behaviors are developed results from the restoration of electrophysiological homeostasis between the VN (21). Nevertheless, changes in some biomarkers (ipsilateral weight distribution, body sway) lead to the development of a new postural strategy expressed during the period in which compensatory behaviors are developed. These biomarkers cannot be estimated by an experimenter and have therefore never been included in the qualitative assessment scales for vestibular syndrome. Persistent long-term postural locomotor disorders have also been clinically identified in vestibular patients.

In this study, we provide the results of a new way of quantifying the posture-locomotor deficits associated with vestibular lesions and the compensatory strategies adopted. We highlighted new parameters that can be considered finer biomarkers of postural and locomotor alterations following vestibular loss. These data corroborate the phenomenon of vestibular compensation, which is well-described in the literature, and also highlight the presence of persistent balance disorders in vestibular lesioned rats. The focus of pre-clinical therapies should therefore be to resolve these persistent disorders in rodent models, thus leading to improvements in postural balance during the period in which compensatory behaviors are developed. This parametric approach is more sensitive than traditional methods in the evaluation of unilateral vestibular syndrome in rodents, so it is anticipated that it will become an essential evaluation tool used to test the efficacy of anti-vertigo compounds or rehabilitation protocols on the kinetics and the quality of restoration of posture-locomotor balance after vestibular loss.

DATA AVAILABILITY STATEMENT

The datasets generated for this study are available on request to the corresponding author.

ETHICS STATEMENT

The animal study was reviewed and approved by French Agriculture Ministry Authorization: B13-055-25. Neuroscience Ethic Committee N°71 from the French National Committee of animal experimentation.

AUTHOR CONTRIBUTIONS

EM and BT: conceptualization and writing—original draft. EM, NE, and GR: data curation. EM, VA, DP, and BT: formal analysis. BT and CC: funding acquisition. EM, BT, NE, GR, DP, and VA: investigation. EM, BT, DP, and VA: methodology. BT: project administration. BT and VA: supervision and validation. EM, BT, and CC: writing—review & editing.

FUNDING

This project was funded by the CIFRE program of the French National Agency for Technological Research (ANRT—CIFRE agreement No. 2017/0189). The Ministère de l'Enseignement Supérieur et de la Recherche and the CNRS (UMR 7260 AMU and CNRS) was also supported this study.

ACKNOWLEDGMENTS

We would like to thank Yves Cazals for his help in the analysis; Elodie Mansour for the animal care and Aïcha Marouane for the English correction.

REFERENCES

1. Angelaki DE, Cullen KE. Vestibular system: the many facets of a multimodal sense. *Annu Rev Neurosci.* (2008) 31:125–50. doi: 10.1146/annurev.neuro.31.060407.125555
2. Hulse RS, Biesdorf A, Hormann K, Stuck B, Erhart M, Hulse M, et al. Peripheral vestibular disorders: an epidemiologic survey in 70 million individuals. *Otol Neurotol.* (2019) 40:88–95. doi: 10.1097/MAO.0000000000002013
3. Chabbert C. Principles of vestibular pharmacotherapy. *Handbook of Clin Neurol.* (2018) 137:207–18. doi: 10.1016/B978-0-444-63437-5.00014-5
4. Cassel R, Bordiga P, Pericat D, Hautefort C, Tighilet B, Chabbert C. New mouse model for inducing unilateral vestibular deafferentation syndrome. *J Neurosci Methods.* (2018) 293:128–35. doi: 10.1016/j.jneumeth.2017.09.002
5. Péricat D, Farina A, Agavnian-Couquiaud E, Chabbert C, and Tighilet B. Complete and irreversible unilateral vestibular loss: a novel rat model of vestibular pathology. *J Neurosci Methods.* (2017) 283:83–91. doi: 10.1016/j.jneumeth.2017.04.001
6. Tighilet B, Péricat D, Frelat A, Cazals Y, Rastoldo G, Boyer F, et al. Adjustment of the dynamic weight distribution as a sensitive parameter for diagnosis of postural alteration in a rodent model of vestibular deficit. *PLoS ONE.* (2017) 12:e0187472. doi: 10.1371/journal.pone.0187472
7. Tighilet B, Leonard J, Bernard-Demanze L, Lacour M. Comparative analysis of pharmacological treatments with N-acetyl-DL-leucine (Tanganil) and its two isomers (N-acetyl-L-leucine and N-acetyl-D-leucine) on vestibular compensation: behavioral investigation in the cat. *Eur J Pharmacol.* (2015) 769:342–9. doi: 10.1016/j.ejphar.2015.11.041
8. Lacour M, Helmchen C, Vidal PP. Vestibular compensation : the neuro-otologist's best friend. *J Neurol.* (2016) 263:S54–64. doi: 10.1007/s00415-015-7903-4
9. Gagey PM, Toupet M. Orthostatic postural control in vestibular neuritis: a stabilometric analysis. *Ann Otol Rhinal Laryngol.* (1991) 100:971–5. doi: 10.1177/000348949110001204
10. Lacour M, Borel L. Vestibular control of posture and gait. *Arch Ital Biol.* (1993) 131:2–3.
11. Furman JM. Role of posturography in the management of vestibular patients. *Otolaryngol Head Neck Surg.* (1995) 112:8–15. doi: 10.1016/S0194-5998(95)70300-4
12. Young LR, Bernard-Demanze L, Dumistrescu M, Magnan J, Borel L, Lacour M. Postural performance of vestibular loss patients under increased postural threat. *J Vestib Res.* (2012) 22:129–38. doi: 10.3233/VES-2012-0449
13. Lacours M, Barthelemy J, Borel L, Magnan L, Zerri C, Chays A, et al. Sensory strategies in human postural control before and after unilateral vestibular neurotomy. *Exp Brain Res.* (1997) 115:300–10. doi: 10.1007/PL00005698
14. Deveze A, Bernard-Demanze L, Xavier F, Lavieille J-P, Elziere M. Vestibular compensation and vestibular rehabilitation. Current concepts and new trends. *Clin Neurophysiol.* (2014) 44:49–57. doi: 10.1016/j.neucli.2013.10.138
15. Takagi A, Fujimara E, Suehiro S. A new method of statokinesigram area mesurement: application of a statistically calculated ellipse. vestibular and visual control on posture and locomotor equilibrium. In: *7th Int. Symp. Int. Soc.* Posturography, Houston, Tex. (1985). p. 74–79 doi: 10.1159/000410306
16. Norre ME, Forrez G, Beckers A. Vestibulospinal findings in two syndromes with spontaneous vertigo attacks. *Ann Otol Rhinol Laryngol.* (1989) 98:191–5. doi: 10.1177/000348948909800305
17. Kasumacic N, Glover JC, Perreault MC. Segmental patterns of vestibular-mediated synaptic inputs to axial and limb motoneurons in the neonatal mouse assessed by optical recording. *J Physiol.* (2010) 588:4905–25. doi: 10.1113/jphysiol.2010.195644
18. Voogd J, Glickstein M. The anatomy of cerebellum. *Trends Cogn Sci.* (1998) 2:307–13. doi: 10.1016/S1364-6613(98)01210-8
19. Stiles L, Smith PF. The vestibular-basal ganglia connection: balancing motor control. *Brain Res.* (2015) 1597:180–8. doi: 10.1016/j.brainres.2014.11.063
20. Lopez C. The vestibular system: balancing more than just the body. *Curr Opin Neurol.* (2016) 29:74–83. doi: 10.1097/WCO.0000000000000286
21. Ris L, Godaux E. Neuronal activity in the vestibular nuclei after contralateral or bilateral labyrinthectomy in the alert guinea pig. *J Neurophysiol.* (1998) 80:2352–67. doi: 10.1152/jn.1998.80.5.2352
22. Liberge M, Manrique C, Bernard-Demanze L, Lacour M. Changes in TNFα, NFκB and MnSOD protein in the vestibular nuclei after unilateral vestibular deafferentation. *J Neuroinflamm.* (2010) 7:91. doi: 10.1186/1742-2094-7-91
23. Hutchinson D, Ho V, Dodd M, Dawson HN, Zumwalt AC, Schmitt D, et al. Quantitative measurement of postural sway in mouse models of human degenerative disease. *Neuroscience.* (2007) 148:825–32. doi: 10.1016/j.neuroscience.2007.07.025
24. Loscher W. Abnormal circling behavior in rat mutants and its relevance to model specific brain dysfunctions. *Neurosci Behav Rev.* (2009) 34:31–49. doi: 10.1016/j.neubiorev.2009.07.001
25. Tighilet B, Manrique C, Lacour M. Stress axis plasticity during vestibular compensation in the adult cat. *Neuroscience.* (2009) 160:716–30. doi: 10.1016/j.neuroscience.2009.02.070
26. Mackinnon CD. Sensorimotor anatomy of gait, balance, and falls. *Handbook Clin Neurol.* (2018) 159:3–26. doi: 10.1016/B978-0-444-63916-5.00001-X
27. Harris-Warrick RM. General principles of rythmogenesis in central pattern networks. *Prog Brain Res.* (2010) 187:213–22. doi: 10.1016/B978-0-444-53613-6.00014-9
28. Falgairolle M, Cazalets JR. Metachronal coupling between spinal neuronal networks during locomotor activity in newborn rat. *J Physiol.* (2007) 580:87–102. doi: 10.1113/jphysiol.2006.115709
29. Mathews MA, Camp AJ, Murray AJ. Reviewing the role of the efferent vestibular system in motor and vestibular circuits. *Front Physiol.* (2017) 8:552. doi: 10.3389/fphys.2017.00552
30. Lacour M, Tighilet B. Plastic events in the vestibular nuclei during vestibular compensation: the brain orchestration of a "deafferentation" code. *Restor Neurol Neurosci.* (2010) 28:19–35. doi: 10.3233/RNN-2010-0509
31. Beliez L. *Mécanismes spinaux et supraspinaux impliqués dans le couplage entre les réseaux locomoteurs et posturaux* (thesis). Université de Bordeaux, France (2014).
32. Borel L, Harlay F, Lopez C, Magnan J, Chays A, Lacour M. Walking performance of vestibular-defective patients before and after unilateral vestibular neurotomy. *Behav Brain Res.* (2004) 150:191–200. doi: 10.1016/S0166-4328(03)00257-2
33. Borel L, Harlay F, Magnan J, Chays A, Lacour M. Deficits and recovery of head and trunk orientation and stabilization after unilateral vestibular loss. *Brain.* (2002) 125:880–94. doi: 10.1093/brain/awf085
34. Bestaven E, Guillaud E, Cazalets JR. Is "circling" behavior in humans related to postural asymmetry? *PLoS ONE.* (2012) 7:e43861. doi: 10.1371/journal.pone.0043861
35. Lopez C, Blanke O. The thalamocortical vestibular system in animals and humans. *Brain Res Rev.* (2011) 67:119–46. doi: 10.1016/j.brainresrev.2010.12.002
36. Smith PF, Curthoys IS. Neuronal activity in the contralateral medial vestibular nucleus of the guinea pig following unilateral labyrinthectomy. *Brain Res.* (1988) 444:295–307. doi: 10.1016/0006-8993(88)90938-9
37. Smith PF, Curthoys IS. Neuronal activity in the ipsilateral medial vestibular nucleus of the guinea pig following unilateral labyrinthectomy. *Brain Res.* (1988) 444:308–19. doi: 10.1016/0006-8993(88)90939-0
38. Smith PF Curthoys IS. Mechanisms of recovery following unilateral labyrinthectomy: a review. *Brain Res Brain Res Rev.* (1989) 14:155–80. doi: 10.1016/0165-0173(89)90013-1
39. Ris L, de Waele C, Serafin M, Vidal PP, Godaux E. Neuronal activity in the ipsilateral vestibular nucleus following unilateral labyrinthectomy in the alert guinea pig. *J Neurophysiol.* (1995) 74:2087–99. doi: 10.1152/jn.1995.74.5.2087
40. Zennou-Azogui Y, Borel L, Lacour M, Ez-Zaher L, Ouaknine M. Recovery of head postural control following unilateral vestibular neurectomy in the cat: neck muscle activity and neuronal correlates in the Deiter's

nuclei. *Acta Oto-laryngol Suppl.* (1993) 509:1–19. doi: 10.3109/00016489309130556

41. Dutia MB. Mechanisms of vestibular compensation: recent advances. *Curr Opin Otolaryngol Head Neck Surg.* (2010) 18:420–4. doi: 10.1097/MOO.0b013e32833de71f
42. Deliagina TG, Orlovsky GN, Zelenin PV, Beloozerova IN. Neural bases of postural control. *Physiology*. (2006) 21:216–25. doi: 10.1152/physiol.00001.2006
43. Funato T, Sato Y, Fujiki S, Sato Y, Aoi S, Tsuchiya K, et al. Postural control during quiet bipedal standing in rats. *PLoS ONE.* (2017)12:e0189248. doi: 10.1371/journal.pone.0189248

Conflict of Interest: The authors declare that the research was conducted in the absence of any commercial or financial relationships that could be construed as a potential conflict of interest.

frontiers in Neurology

SYSTEMATIC REVIEW
published: 29 May 2020
doi: 10.3389/fneur.2020.00225

The Relationship of Tinnitus Distress With Personality Traits: A Systematic Review

Juliëtte J. C. M. van Munster[1,2*†], *Wouter H. van der Valk*[1†], *Inge Stegeman*[3,4], *Arno F. Lieftink*[3] *and Adriana L. Smit*[3,4]

[1] *Department of Otorhinolaryngology and Head & Neck Surgery, Leiden University Medical Center, Leiden University, Leiden, Netherlands,* [2] *Department of Neurosurgery, Leiden University Medical Center, Leiden University, Leiden, Netherlands,* [3] *Department of Otorhinolaryngology and Head & Neck Surgery, University Medical Center Utrecht, Utrecht, Netherlands,* [4] *Brain Center Rudolf Magnus, University Medical Center Utrecht, Utrecht, Netherlands*

Objectives: An association between tinnitus distress with anxiety and depression is described in literature. A similar relationship might exist between tinnitus distress and personality traits, especially since associations between personality traits and other chronic diseases are already revealed. In this systematic review, we aim to investigate whether personality is a risk factor for tinnitus distress.

Design: We searched PubMed and EMBASE databases from inception up to December 31, 2018 for articles on the association between tinnitus distress and personality. Two researchers screened titles, abstracts, and full texts for eligibility. Directness of evidence and risk of bias were assessed. From the included studies, study characteristics and outcome data of tinnitus distress and personality traits were extracted.

Results: A total of 323 unique articles were screened of which 11 cross-sectional studies were eligible for critical appraisal and were used for data extraction. Including study populations were heterogenous, and studies scored high to moderate risk of bias. Nine out of 11 articles showed an association between tinnitus distress and the personality of neuroticism.

Conclusions: By limitations in the methodology of included studies, the evidence on specific personality traits as a risk factor for tinnitus distress is inconclusive. Some evidence on a positive association with neuroticism is identified. To draw conclusions about causal relations, these further studies should be of longitudinal design in a cohort setting. These studies should assess tinnitus distress using validated questionnaires with multiple personality dimensions and validated questionnaires to assess personality traits.

Keywords: tinnitus, tinnitus distress, personality traits, five-factor model, neuroticism

OPEN ACCESS

Edited by:
Agnieszka J. Szczepek, Charité – Universitätsmedizin Berlin, Germany

Reviewed by:
Heike Argstatter, Deutsches Zentrum für Musiktherapieforschung, Germany
Grant Searchfield, The University of Auckland, New Zealand

****Correspondence:***
Juliëtte J. C. M. van Munster
j.j.c.m.van_munster@lumc.nl

[†] These authors have contributed equally to this work

Specialty section:
This article was submitted to Neuro-Otology, a section of the journal Frontiers in Neurology

Received: *06 November 2019*
Accepted: *10 March 2020*
Published: *29 May 2020*

Citation:
van Munster JJCM, van der Valk WH, Stegeman I, Lieftink AF and Smit AL (2020) The Relationship of Tinnitus Distress With Personality Traits: A Systematic Review. Front. Neurol. 11:225. doi: 10.3389/fneur.2020.00225

INTRODUCTION

Tinnitus is the presence of a buzzing or tinkling sound in one or both ears without an acoustic external source to the head and can be associated with a reduction in health-related quality of life (1–3). Growing evidence shows that many cases of tinnitus are associated with de-afferentation of the central auditory structures due to aging, noise exposure, otologic injury, or other causes. The prevalence of tinnitus varies widely, depending on the used methodology,

selected population, and definition of tinnitus. For that reason, the prevalence of the adult population experiencing tinnitus is estimated to be 10–25% (4). Where only 1–7% of the adult tinnitus population seems to struggle with bothersome tinnitus, others experience this symptom without any difficulties, which underlines the heterogeneity of the experienced disease (4). This heterogeneity is not only the experienced diversity in the tinnitus itself (e.g., lateralization, temporal course, sound characteristics) but also due to differences in tinnitus-related problems such as sleep and concentration difficulties and accompanying co-morbidities. Tinnitus-related distress is diverse and can be described as a complex phenomenon associated with negative appraisal, selective attention, safety behaviors, beliefs, and a distorted perception of tinnitus (5, 6). Thereby, it is not surprising that the individual needs of patients for tinnitus-related healthcare are various (4, 7).

So far, it is unclear to what extent psychopathological disorders are predisposing to tinnitus complaints, do aggravate symptoms, or refrain patients from tinnitus relief by diverse tinnitus therapies (8–10). The same might be argued for possible influences of personality traits (10) whereby personality can be defined as the characteristic pattern of thinking, feeling, and behaving of an individual (11). Early appearance of personality after birth indicates that personality is partly genetic determined (12, 13). Many studies have investigated the association between personality and diseases, for instance, between personality and the development of cardiovascular disease and cancer (14–17). A similar relationship could exist between personality characteristics and tinnitus. In the cognitive tinnitus model, it is assumed that tinnitus provokes distress in persons who hold overly negatively thoughts about it, thereby motivating maintaining factors. Subsequently, patients gain a distorted perception of their tinnitus. In 2014, Mucci et al. analyzed the relationship between tinnitus and personality by reviewing the literature from 1968 to 2012 (5, 18). They concluded that tinnitus is associated with several personality characteristics, especially on neuroticism, though a clear distinction between tinnitus perception and tinnitus distress was not made and the quality of data was not assessed. Personality characteristics in patients with more distress might differ from others without high distress levels. A scoping review by Durai et al. in 2016 found associations between tinnitus distress and multiple personality traits such as high neuroticism and low extraversion (19). Still, this review has important limitations due to the scoping method: relevant studies may not have been identified, and a quality assessment was not performed.

To measure personality traits, a wide range of questionnaires can be used. Some questionnaires focus on specific personality traits (19) where other questionnaires are based on models dividing personality into dimensions, for instance, three (Eysenck's theory) or five dimensions [the five-factor model (FFM): the "Big Five"] (19, 20). The variance between factors in the FFM is substantial compared to the variance of other personality inventories (21), and thereby, the FFM adopted a prominent position in the field of personality assessment (22). Assessing personality traits by a validated instrument in tinnitus patients might contribute to a better understanding about the relationship between both. As differences in personality traits can influence tinnitus-related distress and the response on different tinnitus treatments, which is especially important for tinnitus patients with severe complaints of tinnitus, this insight might be of benefit to understand the disease and treatment outcome. Therefore, we aim to investigate whether personality is a risk factor for tinnitus distress by a systematic review of the literature.

TABLE 1 | Eligibility criteria.

Inclusion criteria
Studies that correlated tinnitus distress with personality characteristics
Participants ≥18 years of age
Exclusion criteria
Studies that correlated tinnitus with psychiatric disease or pathological personality
Studies on personality characteristics in patients with hearing loss, dizziness, or chronic disease
Validation studies of a questionnaire
Reviews or case reports
Studies investigating a therapy for tinnitus

MATERIALS AND METHODS

Search Strategy

We searched PubMed and Embase to access records, which analyzed the relationship between tinnitus distress and personality up to December 2018. PubMed was searched by entering the following search criteria in PubMed: [personal*(Title/Abstract)] AND {[tinnitus (MeSH Terms)] OR tinnitus (Title/Abstract)}. A similar search strategy was used to search Embase. The Preferred Reporting Items for Systematic Reviews and Meta-analysis (PRISMA) was used as a writing guideline (23).

Study Selection

After removal of duplicates, two researchers (JM and WV) independently screened titles and abstracts of searched articles. Eligible full text articles were retrieved through the databases and by emailing the authors. Full text eligibility was determined by the in- and exclusion criteria listed in **Table 1**. We included studies if they included adults with tinnitus that correlated tinnitus distress with personality characteristics. With tinnitus distress, terms such as tinnitus loudness, annoyance, and handicap were also included. When there was a different opinion on eligibility, the two reviewers tried to reach consensus. Studies investigating a therapy for tinnitus were excluded since interventions can change personality traits (24). The third and fifth author (IS and AS) were consulted if no unanimity was achieved.

Data Collection

Two researchers (JM and WV) extracted data regarding study design, study population, group size, setting, questionnaires

TABLE 2 | Correlation between non-FFM personality questionnaires and the FFM personality traits based on the literature.

Questionnaire	FFM neuroticism	FFM extraversion	FFM openness	FFM agreeableness	FFM conscientiousness	References
EPI-Neuroticism	Neuroticism	–	–	–	–	(35)
EPQ	Neuroticism	Extraversion	–	Psychoticism (R)	Psychoticism (R)	(35)
FMPS	Mistakes, standards, parent criticism	–	Parent criticism, doubts	Parent expectations (R)	Standards (R), doubts, organization	(33)
FPI-R	Life satisfaction (R) Excitability Strain Somatic complaints Emotionality	Inhibitedness (R) Extraversion Achievement orientation Aggressiveness	Openness	Social orientation Aggressiveness (R)	Need for achievement	(36)
MMPI	Hypochondriasis Depression Psychasthenia	Social introversion (R)	Masculine/feminine (R)	Paranoia (R)	Psychopathic deviate (R)	(37)
MPQ	PEM (R), NEM	PEM (R)	Constraint (R)	NEM (R)	PEM, constraint	(26)
TCI	Harm avoidance Self-directedness (R)	Harm avoidance (R) Persistence	Self-transcendence	Cooperativeness Reward Dependence	Self-directedness Persistence Novelty Seeking (R)	(28, 31)

Different personality questionnaires and their domains were compared and correlated to the personality traits of the FFM. Reverse correlations are depicted by (R). EPI, Eysenck Personality Inventory; EPQ, Eysenck Personality Questionnaire; FMPS, Frost Multidimensional Perfectionism Scale; FPI-R, Freiburger Personlichkeitsinventar; MMPI, Minnesota Multiphasic Personality Inventory; MPQ, Multidimensional Personality Questionnaire; NEM, Negative Emotionality superfactor; TCI, Temperament and Character Inventory; PEM, Positive Emotionality superfactor.

regarding tinnitus distress and personality, and outcomes of the evaluation concerning tinnitus distress and personality. Primary outcome was the relationship between tinnitus distress and personality traits, as described by the FFM. The FFM is a taxonomy of five traits: neuroticism, extraversion, openness, agreeableness, and conscientiousness (25). The Big Five Personality Dimensions Scale, the NEO Five-Factor Inventory (NEO-FFI), and the Big Five Inventory (BFI) are based on the FFM. When included trials used personality trait questionnaires not based on the FFM categorization, these personality traits were matched to the FFM categories. For this, the literature was searched to find a correlation between the non-FFM personality trait category and the traits as defined and scored by the FFM (26–34). Those associations and stratifications between FFM personality traits and non-FFM traits are described in **Table 2**. Mean scores of the questionnaires including standard deviations and *P*-values were distracted from the articles when available. When a *t*-test was used, the *F*-ratio and *P*-value were documented.

Risk of Bias

Critical appraisal of selected studies regarding risk of bias (RoB) was performed by two researchers (WV and JM), using the Newcastle–Ottawa Quality Assessment Scale, using different assessment scales for cohort studies and for case-control studies (38). This instrument is divided into three subdomains concerning the bias in selection, comparability, and exposure. Each subdomain consists of one to four categories of potential bias. A study can be awarded one or two stars depending on each item within the categories. Selection can be awarded with a maximum of four stars, comparability with a maximum of two stars, and outcome with a maximum of three stars. The more stars were earned, the lower the risk of bias of the study was rated.

RESULTS

Study Selection

Our flow chart of the study selection, including reasons for exclusion of articles, is shown in **Figure 1**. After removal of duplicates, 323 unique records were identified. Of these, 255 articles were excluded based on title and abstract screening. After reading the full text of 68 articles, 11 articles were eligible for critical appraisal.

Risk of Bias and Quality Assessment

Critical appraisal of the 11 articles is outlined in **Table 3**. None of the studies were awarded with the maximal amount of nine stars; the range is between three and six stars. The majority used a selected group of tinnitus patients by including them from outpatient clinics (40, 41, 43, 44, 46–49). Furthermore, none of the case-control studies did provide information about non-respondents, and all cohort studies were of cross-sectional study design hindering the assessment of adequate follow-up. In addition, the majority of studies did not correctly control for confounding factors (40, 41, 43–49). Together, this limits the number of stars awarded for all subdomains. Only two studies used a representative cohort of patients with tinnitus out of the general population; however, these studies used a single question of tinnitus distress in contrast to validated multi-item questionnaires (45, 50).

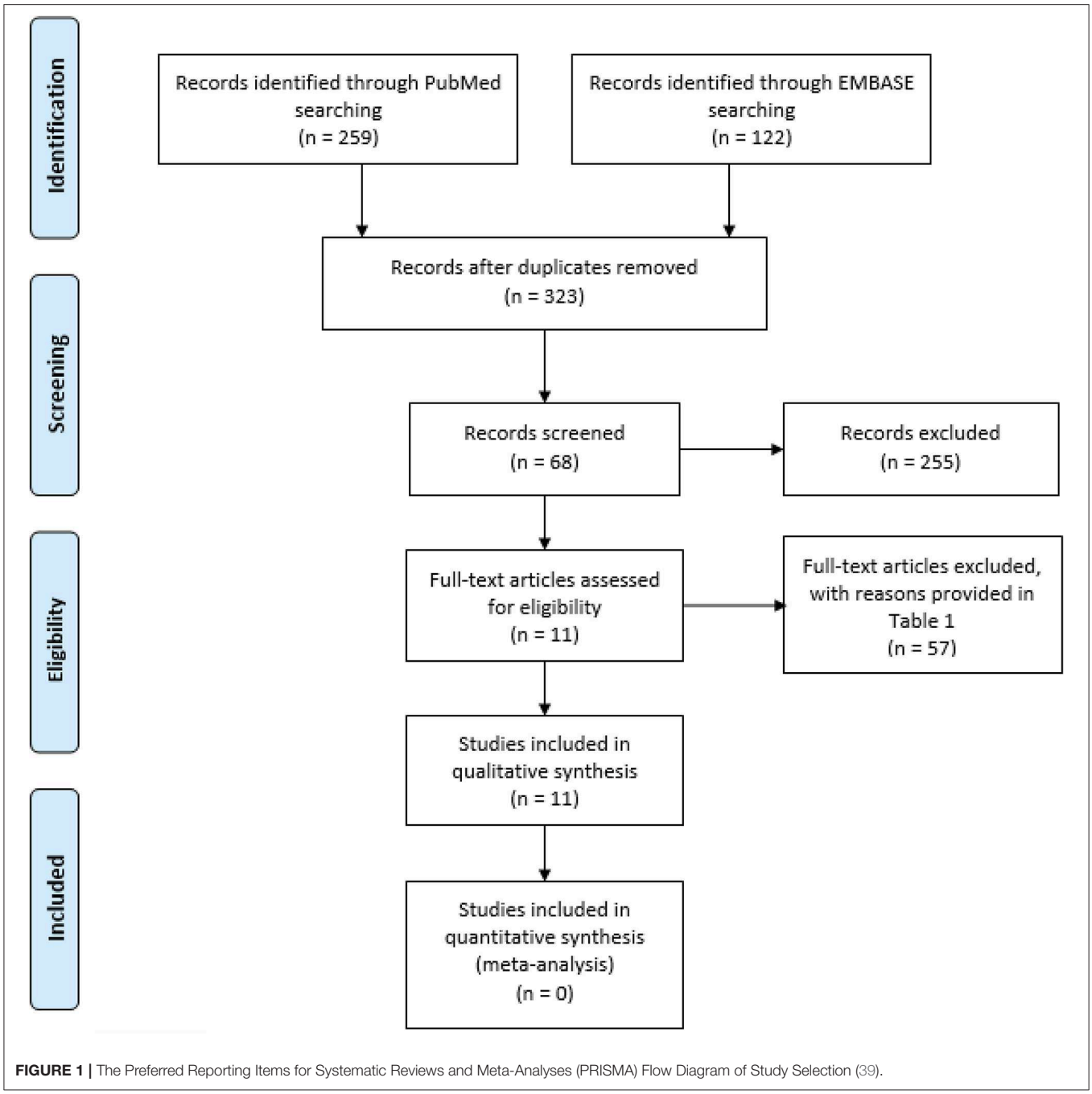

FIGURE 1 | The Preferred Reporting Items for Systematic Reviews and Meta-Analyses (PRISMA) Flow Diagram of Study Selection (39).

Characteristics of Studies

There was a large heterogeneity in tinnitus questionnaires and personality questionnaires to measure tinnitus distress and personality traits, respectively, in the included studies. Because of this heterogeneity, no meta-analysis could be performed. Therefore, a descriptive analysis of the included articles is provided. All but three (42, 45, 50) studies included patients who visited the tinnitus department or Ear-, Nose-, Throat (ENT), which leads to a specific patient selection. The two cohort studies included patients from large-population studies in Dunedin (New Zealand) and the United Kingdom (UK) (45, 50) and assessed personality traits in a cross-sectional manner.

Synthesis of the Results

Extensive descriptions of the articles and outcomes are presented in **Table 4**.

Tinnitus Distress and Personality Traits

A majority (9 out of 11 studies) of the included studies showed one or more associations (both positive and negative) between

TABLE 3 | Risk of bias assessment using the Newcastle–Ottawa Quality Assessment Scale.

References	Selection (Max. ****)	Comparability (Max. **)	Outcome (Max. ***)	Total number of stars[b]
Adami Dehkordi et al. (40)[a]	***		**	*****
Andersson et al. (41)	**		*	***
Durai et al. (42)[a]	***	**	*	******
Gerber et al. (43)	*		**	***
Langguth et al. (44)	**		*	***
McCormack et al. (45)	***			***
Meric et al. (46)	**	**	*	*****
Salviati et al. (47)	**		*	***
Strumila et al. (48)	**		*	***
Weber et al. (49)	**		*	***
Welch and Dawes (50)	***	**		*****

[a] *Newcastle–Ottawa Quality Assessment Scale for case-control studies was used.*
[b] *A maximum of nine stars could be earned in total and implies the lowest Risk of Bias.*

tinnitus distress and personality (41, 44–47, 49, 50). Two out of 11 articles studied the association between tinnitus distress and the FFM personality traits by usage of the NEO five-factor inventory (44) or a short version of the Big Five Personality dimensions scale (48). Of those, Langguth et al. did find a negative association between scores on the Tinnitus Handicap Inventory (THI) and consciousness (correlation coefficient $= -0.367$, $p = 0.003$), and a positive association between tinnitus distress on the Tinnitus Questionnaire (TQ) and neuroticism (correlation coefficient $= 0.276$, $p = 0.028$) (44). Furthermore Strumila et al. (48) stated that high THI scores did not predict high scores on any of the personality traits, but neuroticism did influence distress of tinnitus perception ($p < 0.001$, standardized coefficient 0.38).

The other nine studies used non-FFM-based questionnaires to assess personality traits in similar domains to the FFM division (40–43, 45–47, 49, 50). To be able to make a comparison, we converted these outcomes of personality traits to the FFM personality traits when a comparison between both was described in literature, as stated previously (**Tables 2**, **5**). One study found a positive association between bothersome tinnitus and neuroticism [odds ratio (95% CI) $= 4.11$ (3.69–4.58), $p < 0.001$] using the EPI-neuroticism questionnaire (45). Eight of nine non-FFM-based studies indicated a positive correlation between neuroticism and increased tinnitus distress, including the New Zealand study, which represents a sample of the general population (**Table 5**) (40–42, 45–47, 49, 50). For the other categories of personality traits (extraversion, openness, agreeableness, and consciousness), we found no conclusive results about an association with tinnitus distress.

DISCUSSION

In the present review, we studied personality traits as a risk factor for tinnitus distress, in which 11 cross-sectional studies with a high degree of heterogeneity in methods and outcomes were included. Owing to heterogeneity in the reported personality traits, it was not possible to perform a meta-analysis. Of the FFM, neuroticism was the only trait with a positive relationship with tinnitus distress in multiple studies. The association between neuroticism and tinnitus distress is in line with previous findings about emotional health and tinnitus: tinnitus distress shows close relationships with factors related to emotional health, and emotional health may be prognostic for the development of tinnitus distress (51, 52). One could argue that patients with more severe complaints of tinnitus are indeed more likely to have a neurotic personality, since neuroticism is described as the tendency to experience negative emotions. However, neuroticism is also associated with psychopathological symptoms of depression and anxiety (53), which complicates the causality of this association, since anxiety and depression are more prevalent among tinnitus patients (8, 19, 54). Moreover, both tinnitus and personality are potentially influenced by genetic factors (55, 56). Interestingly, of the FFM traits, the strongest associations were revealed between genetic variants and neuroticism (56–58). One of these studies used the same prospective cohort in the United Kingdom as the study of McCormack et al. (45) of which results were included in this systematic review. Indeed, this study found a positive association between neuroticism and tinnitus.

Several major limitations of this systematic review must be mentioned. Most of the studies included a selected population of tinnitus patients visiting an ENT department, audiological clinic, or tinnitus clinics and, thus, are not necessarily representative of the general population. For instance, headache-prone individuals have found to differ in personality profiles when comparing institutionalized patients to non-institutionalized controls from outside the clinic (59). Potentially, help-seeking tinnitus patients might differ in personality from non-help-seeking tinnitus patients. Owing to the selected sample of tinnitus patients used in the included studies in our review, generalization of outcomes is hindered. Moreover, most studies are prone to bias as scored by the Newcastle–Ottawa Quality Assessment Scale. For instance, confounders in the relation between personality traits and tinnitus distress exist, but not all studies described or analyzed these potential confounding factors such as gender (41, 48, 50). Additionally, as many different questionnaires were used to assess the personality traits, we used previously described correlations to convert the personality domains out of these questionnaires into the FFM categorization, to be able to compare outcomes of different studies. To our knowledge, however, this method is not validated nor described previously.

For all these reasons, the evidence we present in this systematic review about the relationship between personality and tinnitus is inconclusive. The aim of our review was to assess personality as a risk factor for tinnitus distress. Longitudinal cohort studies are needed to assess the causality of personality in tinnitus, address the limitations, and reveal additional potential confounders in this relationship.

TABLE 4 | Summary of studies on personality characteristics in tinnitus patients according to tinnitus distress.

References	Questionnaires (personality, tinnitus)	Study design	Study population	Sample number (Tinnitus number)	Outcomes
Andersson et al. (41)	HADS, ISI, FMPS TRQ	Case series Cross-sectional	Tinnitus patients visiting the Audiology Department	256 (256)	Severity of tinnitus was correlated with Concern over Mistakes, Personal Standards, Parental Expectations, Parental Criticism, Doubts about Action and Organization ($p < 0.05$)
Adami Dehkordi et al. (40)	EPQ TET, TSI	Case control Cross-sectional	Patients with idiopathic tinnitus from the ENT Department and matched, healthy non-tinnitus volunteers from patients' family	66 (33)	No associations between the TSI, the 1–10 Tinnitus Scale Score and any of the personality traits were found
Durai et al. (42)	MPQ TFI	Case control Cross-sectional	Tinnitus sufferers recruited from the University of Auckland Tinnitus Research Volunteer Database Non-tinnitus sufferers recruited via the University of Auckland Hearing and Tinnitus database, posters, and social media	215 (61)	Within tinnitus sufferers, stress reaction scores were negatively correlated with constraint ($r = -0.365$, $p = 0.004$) and social closeness/positive emotionality ($r = -0.296$, $p = 0.02$) and positively correlated with alienation scores/negative emotionality ($r = 0.406$, $p = 0.001$) Total TFI scores was significantly negatively correlated with social closeness ($r = -0.312$, $p < 0.001$) The tinnitus group had lower levels of self-control scores (mean = 12.70, SD = 4.15) and social closeness scores (mean = 8.46, SD = 3.57) than controls (respectively, mean = 13.76, SD = 3.26; mean = 10.11, SD = 4.06) and higher alienation scores (mean = 3.48, SD = 3.87) than controls (mean = 10.11, SD = 4.06)
Gerber et al. (43)	MMPI, scaling method to assess severity of stress events by Homes and Rahe 26-item questionnaire designed to obtain a subjective measure of tinnitus severity (not validated)	Case series Cross-sectional	Male tinnitus patients referred to the Audiology Clinic with subjective tinnitus as a primary complaint	45 (45)	Severity of tinnitus was not related to stress events or differences on the MMPI profile
Langguth et al. (44)	NEO-FFI, BDI THI, TQ	Case series Cross-sectional	Patients with tinnitus for at least 6 months, visiting the Tinnitus Clinic	72 (72)	High tinnitus handicap was correlated with low agreeableness ($p = 0.003$), but not with neuroticism, extraversion, openness, and conscientiousness High tinnitus severity was correlated with high neuroticism ($p = 0.028$), but not with extraversion, openness, agreeableness, and conscientiousness
McCormack et al. (45)	EPI-Neuroticism Single question concerning tinnitus annoyance	Cohort Cross-sectional	Tinnitus, and non-tinnitus participants, aged 40 to 69 years, recruited from the UK Biobank Dataset	172.621 (27.964)	Neuroticism had a stronger association with bothersome tinnitus [4.11 (OR 95% CI 3.69–4.58); $p < 0.001$] than tinnitus presence [OR 2.11 (95% CI 2.00–2.22); $p < 0.001$]
Meric et al. (46)	French short MMPI TRQ, THQ, STSS scale	Case series Cross-sectional	Tinnitus patients visiting the ENT Department	281 (281)	Increasing tinnitus impact and handicap were correlated with paranoia, psychasthenia, schizophrenia, and hypochondriasis ($p < 0.0001$). No association was present for mania
Salviati et al. (47)	VRS, SCL90-R, TCI THI	Case series Cross-sectional	Tinnitus patients from the Tinnitus Center of the Department of Sense Organs	239 (239)	Tinnitus handicap was associated with all psychopathological dimensions (somatization, obsessive–compulsive, anxiety, depression, sensitivity, hostility, phobic anxiety, paranoid ideation, psychoticism; $p < 0.001$) Harm avoidance and self-directedness were also correlated with tinnitus handicap ($p < 0.004$), but not with reward dependence ($p = 0.88$), novelty seeking ($p = 0.90$), persistence ($p = 0.70$), cooperativeness ($p = 0.32$), and self-transcendence ($p = 0.21$)

(Continued)

TABLE 4 | Continued

References	Questionnaires (personality, tinnitus)	Study design	Study population	Sample number (Tinnitus number)	Outcomes
Strumila et al. (48)	HADS, short version of Big Five Personality Dimensions Scale and sociodemographic questions THI, VAS of tinnitus severity	Case series Cross-sectional	Tinnitus sufferer recruited via internet	212 (212)	Tinnitus severity was not correlated with personality traits [in mean (SD)]: - Extraversion mean 26.49 (5.13) - Agreeableness 26.46 (5.13) - Consciousness 26.33 (4.02) - Neuroticism 18.55 (5.45) - Openness 21.39 (5.32)
Weber et al. (49)	FPI-R, BDI TQ	Case series Cross-sectional	Adult, tinnitus patients visiting the ENT Department	121 (121)	Based on tinnitus severity, patients differed in - Life satisfaction ($F = 5.497$; $p = 0.001$), lower if increasing severity - Excitability ($F = 5.151$; $p = 0.002$), higher if increasing severity - Aggressiveness ($F = 3.483$; $p = 0.018$), higher if increasing severity - Stress ($F = 10.846$; $p < 0.001$), higher if increasing severity - Physical complaints ($F = 12.876$; $p < 0.001$), higher if increasing severity - Health concerns ($F = 3.610$; $p = 0.015$), higher if increasing severity - Emotionality ($F = 12.708$; $p < 0.001$), higher if increasing severity
Welch and Dawes (50)	MPQ Single question concerning tinnitus annoyance	Cohort Cross-sectional	Tinnitus and non-tinnitus participants born between April 1972 and March 1973 from a birth cohort of Dunedin (New Zealand's South Island)	970 (437)	Based on amount of tinnitus, personality differed significantly: Positive emotionality [$F_{(2.946)} = 3.675$; $p = 0.026$] - Social closeness lower in groups with more tinnitus [$F_{(2.946)} = 13.242$; $p < 0.001$] - Well-being, social potency, and achievement did not differ Negative emotionality [$F_{(2.946)} = 12.810$; $p < 0.001$] - Stress reaction [$F_{(2.946)} = 9.144$, $p < 0.001$] higher in groups with more tinnitus - Alienation higher in groups with more tinnitus (Wald = 12.206; p<0.001) - Aggression did not differ Constraint [$F_{(2.946)} = 5.516$; $p = 0.004$] - Self-control lower in groups with more tinnitus [$F(2.946) = 4.752$; $p = 0.009$] - Harm avoidance or Traditionalism did not differ Based on the annoyance of tinnitus, personality differed significantly: Positive emotionality [$F_{(2.424)} = 3.010$, $p = 0.050$] - Social closeness lower in patients more tinnitus distress [$F_{(2.424)} = 3.471$; $p = 0.032$] - Well-being lower in groups with more annoyance (Wald = 6.579, $p = 0.010$) - Social potency or achievement did not differ Negative emotionality [$F_{(2,424)} = 6.039$, $p = 0.003$) higher in groups with more annoyance. Annoyance was not related to constraint [$F_{(2.424)} = 1.722$, $p = 0.180$].

Secondary outcome on tinnitus distress, annoyance, or severity on personality characteristics in tinnitus patients per publication (first author, year of publication). Per publication, the used tinnitus and personality questionnaires used are depicted; if underlined, they assessed personality traits. Study design and information on the included populations are shown. The outcomes show results of tinnitus distress in relation to personality traits in tinnitus patients. BDI, Beck Depression Inventory; EPI, Eysenck Personality Inventory; EPQ, Eysenck Personality Questionnaire; FMPS, Frost Multidimensional Perfectionism Scale; FPI-R, Freiburger Personlichkeitsinventar; HADS, Hospital Anxiety and Depression Scale; ISI, Insomnia Severity Index; MMPI, Minnesota Multiphasic Personality Inventory; MPQ, Multidimensional Personality Questionnaire; NEO-FFI, NEO Five-Factor Inventory; SCL-90-R, Symptom Checklist-90-Revised; STSS, Subjective Tinnitus Severity Scale; TCI, Temperament and Character Inventory; TET, Tinnitus Evaluation Test; TFI, Tinnitus Functional Index; THI, Tinnitus Handicap Inventory; THQ, Tinnitus Handicap Questionnaire; TQ, Tinnitus Questionnaire; TRQ, Tinnitus Reaction Questionnaire; TSI, Tinnitus Severity Index; VAS, Visual Analog Scale; VRS, Stress-Related Vulnerability Scale.

TABLE 5 | Association of personality trait outcomes to tinnitus distress.

FFM	Association between tinnitus distress and personality		
	Positive association	**Negative association**	**No association found**
Neuroticism	Neuroticism (44)*(45) Positive emotionality (42, 50) Negative emotionality (42) Parental criticism (41) Concerns over mistakes (41) Hypochondriasis (46) Depression (46) Psychasthenia (46) Harm avoidance (47) Self-directedness (47) Life satisfaction (49) Excitability (49) Strain (49) Somatic complaints (49) Emotionality (49)		Neuroticism (48)* Neuroticism (40) Hypochondria (43) Depression (43) Psychasthenia (43)
Extraversion	Aggressiveness (49)	Social introversion (46) Social closeness (50) Positive emotionality (42, 50)	Extraversion (44, 48)* Extraversion (40) Social introversion (43) Wellbeing, social potency, achievement (50)
Openness	Constraint (50) Parental criticism (41) Doubts about Action (41)	Masculinity/Femininity (46)	Openness (44, 48)* Harm avoidance and traditionalism (50) Masculine/feminine (43)
Agreeableness	Parental expectations (41)	Agreeableness (48)* Negative emotionality (42)	Psychoticism (40) Agreeableness (44)* Negative emotionality Paranoia (46) Aggressiveness (49) Paranoia (43)
Consciousness	Personal standards (41) Doubts about action (41)	Consciousness (44, 48)* Constraint (42) Positive emotionality (42) Self-control (50)	Psychoticism (40) Positive emotionality (50) Harm avoidance and traditionalism (50) Psychopathic deviate (43, 46)

** Personality traits as measured using the FFM personality traits. Other personality traits are "translated" according to **Table 2** and clustered under the corresponding FFM personality traits.*

The potential relationship of tinnitus distress with neuroticism may affect the success of specific tinnitus treatments, making the execution of high-quality studies on this topic of eminent importance. For example, cognitive behavioral treatment (CBT) targets the emotional reactivity and (dysfunctional) behavioral mechanisms. Studies assessing tinnitus outcome after CBT treatment show a reduction in disease-related distress and increased daily life functioning in individuals with subjective tinnitus (60–62). Interestingly, FFM personality can affect the tinnitus outcome after CBT treatment as demonstrated by Kleinstauber et al. in a clinical trial (63). Therefore, one should not only consider tinnitus distress (64) but also individual characteristics as personality traits to tailor tinnitus treatment for this heterogenous group of patients.

CONCLUSION

We endeavored to present the evidence on the relationship between tinnitus distress and personality traits in this systematic review. Owing to limitations in the methodology of included studies, the evidence on specific personality traits as a risk factor for tinnitus distress is inconclusive. Some evidence on a positive association with neuroticism is identified. To draw conclusions about causal relations, future studies should be of longitudinal design in a cohort setting. These studies should assess tinnitus distress using validated questionnaires with multiple personality dimensions and validated questionnaires to assess personality traits.

DATA AVAILABILITY STATEMENT

The datasets generated for this study are available on request to the corresponding author.

AUTHOR CONTRIBUTIONS

This study was conceived and designed by JM, WV, IS, and AS. All authors contributed to acquisition, analysis, and interpretation of data. The drafting of the manuscripts was performed by JM and WV. Critical revision of the manuscript for important intellectual content as well as study supervision was performed by AS, IS, and AL.

REFERENCES

1. Henry JA, Dennis KC, Schechter MA. General review of tinnitus: prevalence, mechanisms, effects, and management. *J Speech Lang Hear Res*. (2005) 48:1204–35. doi: 10.1044/1092-4388(2005/084)
2. Nondahl DM, Cruickshanks KJ, Dalton DS, Klein BE, Klein R, Schubert CR, et al. The impact of tinnitus on quality of life in older adults. *J Am Acad Audiol*. (2007) 18:257–66. doi: 10.3766/jaaa.18.3.7
3. Prestes R, Daniela G. Impact of tinnitus on quality of life, loudness and pitch match, and high-frequency audiometry. *Int Tinnitus J*. (2009) 15:134–8.
4. Bauer CA. Tinnitus. *N Engl J Med*. (2018) 378:1224–31. doi: 10.1056/NEJMcp1506631
5. Mckenna L, Handscomb L, Hoare DJ, Hall DA. A scientific cognitive-behavioral model of tinnitus: novel conceptualizations of tinnitus distress. *Front Neurol*. (2014) 5:196. doi: 10.3389/fneur.2014.00196
6. Brüggemann P, Szczepek AJ, Rose M, Mckenna L, Olze H, Mazurek B. Impact of multiple factors on the degree of tinnitus distress. *Front Hum Neurosci*. (2016) 10:341. doi: 10.3389/fnhum.2016.00341
7. Nemholt SS, Schmidt JH, Wedderkopp N, Baguley DM. Prevalence of tinnitus and/or hyperacusis in children and adolescents: study protocol for a systematic review. *BMJ Open*. (2015) 5:e006649. doi: 10.1136/bmjopen-2014-006649
8. Geocze L, Mucci S, Abranches DC, Marco MA, Penido Nde O. Systematic review on the evidences of an association between tinnitus and depression. *Braz J Otorhinolaryngol*. (2013) 79:106–11. doi: 10.5935/1808-8694.20130018
9. Pinto PC, Marcelos CM, Mezzasalma MA, Osterne FJ, De Melo Tavares De Lima MA, Nardi AE. Tinnitus and its association with psychiatric disorders: systematic review. *J Laryngol Otol*. (2014) 128:660–4. doi: 10.1017/S0022215114001030
10. Trevis KJ, Mclachlan NM, Wilson SJ. A systematic review and meta-analysis of psychological functioning in chronic tinnitus. *Clin Psychol Rev*. (2018) 60:62–86. doi: 10.1016/j.cpr.2017.12.006
11. Andersen AM, Bienvenu OJ. Personality and psychopathology. *Int Rev Psychiatr*. (2011) 23:234–47. doi: 10.3109/09540261.2011.588692
12. Thomas A, Chess S, Zrull JP, Chairman DO. Temperament and development. *J Am Acad Child Psychiatr*. (1978) 17:732–3. doi: 10.1016/S0002-7138(09)61026-8
13. Cloninger CR, Svrakic DM, Przybeck TR. A psychobiological model of temperament and character. *Arch Gen Psychiatr*. (1993) 50:975–90. doi: 10.1001/archpsyc.1993.01820240059008
14. Eysenck HJ. Personality, cancer and cardiovascular disease: a causal analysis. *Personal Individual Differ*. (1985) 6:535–56. doi: 10.1016/0191-8869(85)90003-0
15. Eysenck HJ. Psychosocial factors, cancer, and ischaemic heart disease. *BMJ*. (1992) 305:457–9. doi: 10.1136/bmj.305.6851.457
16. Eysenck HJ. Prediction of cancer and coronary heart disease mortality by means of a personality inventory: results of a 15-year follow-up study. *Psychol Rep*. (1993) 72:499–516. doi: 10.2466/pr0.1993.72.2.499
17. Eysenck HJ. Personality and coronary heart disease. *Br J Hosp Med*. (1994) 52:120.
18. Mucci S, Geocze L, Abranches DC, Antunez AE, Penido Nde O. [Systematic review of evidence on the association between personality and tinnitus]. *Braz J Otorhinolaryngol*. (2014) 80:441–7. doi: 10.1016/j.bjorl.2014.05.031
19. Durai M, Searchfield G. Anxiety and depression, personality traits relevant to tinnitus: a scoping review. *Int J Audiol*. (2016) 55:605–15. doi: 10.1080/14992027.2016.1198966
20. Vorkapić ST. The significance of preschool teacher's personality in early childhood education: analysis of eysenck's and big five dimensions of personality. *Int J Psychol Behav Sci*. (2012) 2:28–37. doi: 10.5923/j.ijpbs.20120202.05
21. O'connor BP. A quantitative review of the comprehensiveness of the five-factor model in relation to popular personality inventories. *Assessment*. (2002) 9:188–203. doi: 10.1177/10791102009002010
22. Hoekstra H, Ormel J, Fruyt F. *NEO-PI-R/NEO-FFI Big Five Persoonlijkheidsvragenlijst*. Amsterdam: Hogrefe Publishing (2007).
23. Moher D, Liberati A, Tetzlaff J, Altman DG. Preferred reporting items for systematic reviews and meta-analyses: the PRISMA statement. *BMJ*. (2009) 339:b2535. doi: 10.1136/bmj.b2535
24. Roberts BW, Luo J, Briley DA, Chow PI, Su R, Hill PL. A systematic review of personality trait change through intervention. *Psychol Bull*. (2017) 143:117–41. doi: 10.1037/bul0000088
25. McCrae RR, John OP. An introduction to the five-factor model and its applications. *J Pers*. (1992) 60:175–215. doi: 10.1111/j.1467-6494.1992.tb00970.x
26. Church AT. Relating the tellegen and five-factor models of personality structure. *J Pers Soc Psychol*. (1994) 67:898–909. doi: 10.1037/0022-3514.67.5.898
27. Eysenck HJ. *Five-Factor Model*. (2001) Available online at: http://www.personalityresearch.org/bigfive/eysenck.html (accessed Febuary 18, 2020).
28. MacDonald DA, Holland D. Examination of relations between the NEO personality inventory-revised and the temperament and character inventory. *Psychol Rep*. (2002) 91:921–30. doi: 10.2466/pr0.2002.91.3.921
29. Hoekstra H, Ormel J, Fruyt F. *Handleiding NEO-PI-R en NEO-FFI Persoonlijkheidsvragenlijsten* Amsterdam: Hogrefe Publishing (2007).
30. Rushton JP, Irwing P. A general factor of personality (GFP) from the multidimensional personality questionnaire. *Personal Indivi Differ*. (2009) 47:571–6. doi: 10.1016/j.paid.2009.05.011
31. Capanna C, Struglia F, Riccardi I, Daneluzzo E, Stratta P, Rossi A. Temperament and character inventory-R (TCI-R) and big five questionnaire (BFQ): convergence and divergence. *Psychol Rep*. (2012) 110:1002–6. doi: 10.2466/02.03.09.PR0.110.3.1002-1006
32. Howard S, Hughes BM. Construct, concurrent and discriminant validity of type D personality in the general population: associations with anxiety, depression, stress and cardiac output. *Psychol Health*. (2012) 27:242–58. doi: 10.1080/08870446.2011.603423
33. Briley DA, Domiteaux M, Tucker-Drob EM. Achievement-relevant personality: relations with the big five and validation of an efficient instrument. *Learn Individ Differ*. (2014) 32:26–39. doi: 10.1016/j.lindif.2014.03.010
34. Lars. *Das Freiburger Persönlichkeitsinventar*. (2015) Available online at: http://www.typentest.de/blog/2015/11/das-freiburger-personlichkeitsinventar/ (accessed Febuary 18, 2020).
35. Costa PT, McCrae RR. Four ways five factors are basic. *Personal Individ Differ*. (1992) 13:653–65. doi: 10.1016/0191-8869(92)90236-I
36. Borkenau P, Ostendorf F. Untersuchungen zum fünf-faktoren-modell der persönlichkeit und seiner diagnostischen erfassung. [Investigations of the five-factor model of personality and its assessment]. *Zeitschrift Differ Diagnosti Psychol*. (1989) 10:239–51.
37. Cortina JM, Doherty ML, Schmitt N, Kaufman G, Smith RG. The big five personality factors in the IPI and MMPI: predictors of police performance. *Person Psychol*. (1992) 45:119–40. doi: 10.1111/j.1744-6570.1992.tb00847.x
38. Wells G, O'Connell D, Peterson J, Welch V, Losos M, Tugwell P, et al. *The Newcastle-Ottawa Scale (NOS) For Assessing the Quality of Nonrandomised Studies in Meta-analyses*. (2000) Available: http://www.ohri.ca/programs/clinical_epidemiology/oxford.asp
39. Moher D, Liberati A, Tetzlaff J, Altman DG, The PRISMA Group. Preferred reporting items for systematic reviews and meta-analyses: the PRISMA statement. *PLoS Med*. (2009) 6:e1000097. doi: 10.1371/journal.pmed1000097
40. Adami Dehkordi M, Javanbakht M, Sarfarazi Moghadam S, Meshkat M, Abolbashari S. Personality traits in patients with subjective idiopathic tinnitus. *Iran J Otorhinolaryngol*. (2015) 27:369–75. doi: 10.22038/IJORL.2015.4791
41. Andersson G, Airikka M-L, Buhrman M, Kaldo V. Dimensions of perfectionism and tinnitus distress. *Psychol Health Med*. (2005) 10:78–87. doi: 10.1080/13548500512331315389
42. Durai M, O'Keeffe MG, Searchfield GD. The personality profile of tinnitus sufferers and a nontinnitus control group. *J Am Acad Audiol*. (2017) 28:271–82. doi: 10.3766/jaaa.15103
43. Gerber KE, Nehemkis AM, Charter RA, Jones HC. Is tinnitus a psychological disorder? *Int J Psychiatr Med*. (1985) 15:81–7. doi: 10.2190/E59L-2PRU-GPAE-VJ8B
44. Langguth B, Kleinjung T, Fischer B, Hajak G, Eichhammer P, Sand PG. Tinnitus severity, depression, and the big five personality traits. *Prog Brain Res*. (2007) 166:221–5. doi: 10.1016/S0079-6123(07)66020-8
45. McCormack A, Edmondson-Jones M, Fortnum H, Dawes P, Middleton H, Munro KJ, et al. The prevalence of tinnitus and the relationship with

neuroticism in a middle-aged UK population. *J Psychosom Res*. (2014) 76:56–60. doi: 10.1016/j.jpsychores.2013.08.018
46. Meric C, Gartner M, Collet L, Chery-Croze S. Psychopathological profile of tinnitus sufferers: evidence concerning the relationship between tinnitus features and impact on life. *Audiol Neurootol*. (1998) 3:240–52. doi: 10.1159/000013796
47. Salviati M, Bersani FS, Terlizzi S, Melcore C, Panico R, Romano GF, et al. Tinnitus: clinical experience of the psychosomatic connection. *Neuropsychiatr Dis Treat*. (2014) 10:267–75. doi: 10.2147/NDT.S49425
48. Strumila R, Lengvenyte A, Vainutiene V, Lesinskas E. The role of questioning environment, personality traits, depressive and anxiety symptoms in tinnitus severity perception. *Psychiatr Q*. (2017) 88:865–77. doi: 10.1007/s11126-017-9502-2
49. Weber JH, Jagsch R, Hallas B. [The relationship between tinnitus, personality, and depression]. *Z Psychosom Med Psychother*. (2008) 54:227–40. doi: 10.13109/zptm.2008.54.3.227
50. Welch D, Dawes PJ. Personality and perception of tinnitus. *Ear Hear*. (2008) 29:684–92. doi: 10.1097/AUD.0b013e318177d9ac
51. D'Amelio R, Archonti C, Schol S, Falkai P, Plinkert PK, Delb W. [Psychological distress associated with acute tinnitus]. *Hno*. (2004) 52:599–603. doi: 10.1007/s00106-003-0944-5
52. Wallhausser-Franke E, Delb W, Balkenhol T, Hiller W, Hormann K. Tinnitus-related distress and the personality characteristic resilience. *Neural Plast*. (2014) 2014:370307. doi: 10.1155/2014/370307
53. Muris P, Roelofs J, Rassin E, Franken I, Mayer B. Mediating effects of rumination and worry on the links between neuroticism, anxiety and depression. *Personal Individ Differ*. (2005) 39:1105–11. doi: 10.1016/j.paid.2005.04.005
54. Pattyn T, Van Den Eede F, Vanneste S, Cassiers L, Veltman DJ, Van De Heyning P, et al. Tinnitus and anxiety disorders: a review. *Hear Res*. (2016) 333:255–65. doi: 10.1016/j.heares.2015.08.014
55. Lo MT, Hinds DA, Tung JY, Franz C, Fan CC, Wang Y, et al. Genome-wide analyses for personality traits identify six genomic loci and show correlations with psychiatric disorders. *Nat Genet*. (2017) 49:152–6. doi: 10.1038/ng.3736
56. Maas IL, Brüggemann P, Requena T, Bulla J, Edvall NK, Hjelmborg JVB, et al. Genetic susceptibility to bilateral tinnitus in a Swedish twin cohort. *Gene Med*. (2017) 19:1007–12. doi: 10.1038/gim.2017.4
57. Okbay A, Baselmans BM, De Neve JE, Turley P, Nivard MG, Fontana MA, et al. Genetic variants associated with subjective well-being, depressive symptoms, and neuroticism identified through genome-wide analyses. *Nat Genet*. (2016) 48:624–33. doi: 10.1038/ng.3552
58. Smith DJ, Escott-Price V, Davies G, Bailey ME, Colodro-Conde L, Ward J, et al. Genome-wide analysis of over 106 000 individuals identifies 9 neuroticism-associated loci. *Mol Psychiatr*. (2016) 21:749–57. doi: 10.1038/mp.2016.49
59. Ziegler DK, Paolo AM. Headache symptoms and psychological profile of headache-prone individuals: a comparison of clinic patients and controls. *Arch Neurol*. (1995) 52:602–6. doi: 10.1001/archneur.1995.00540300076016
60. Martinez-Devesa P, Perera R, Theodoulou M, Waddell A. Cognitive behavioural therapy for tinnitus. *Cochrane Database Syst Rev*. (2010) 9:Cd005233. doi: 10.1002/14651858.CD005233.pub3
61. Hesser H, Weise C, Westin VZ, Andersson G. A systematic review and meta-analysis of randomized controlled trials of cognitive-behavioral therapy for tinnitus distress. *Clin Psychol Rev*. (2011) 31:545–53. doi: 10.1016/j.cpr.2010.12.006
62. Cima RFF, Mazurek B, Haider H, Kikidis D, Lapira A, Norena A, et al. A multidisciplinary European guideline for tinnitus: diagnostics, assessment, and treatment. *HNO*. (2019) 67:10–42. doi: 10.1007/s00106-019-0633-7
63. Kleinstauber M, Weise C, Andersson G, Probst T. Personality traits predict and moderate the outcome of Internet-based cognitive behavioural therapy for chronic tinnitus. *Int J Audiol*. (2018) 57:538–44. doi: 10.1080/14992027.2018.1432902
64. Van De Heyning P, Gilles A, Rabau S, Van Rompaey V. Subjective tinnitus assessment and treatment in clinical practice: the necessity of personalized medicine. *Curr Opin Otolaryngol Head Neck Surg*. (2015) 23:369–75. doi: 10.1097/MOO.0000000000000183

Conflict of Interest: The authors declare that the research was conducted in the absence of any commercial or financial relationships that could be construed as a potential conflict of interest.

frontiers in Neurology

ORIGINAL RESEARCH
published: 05 June 2020
doi: 10.3389/fneur.2020.00505

Quantitative Evaluation of a New Posturo-Locomotor Phenotype in a Rodent Model of Acute Unilateral Vestibulopathy

*Guillaume Rastoldo[1], Emna Marouane[1], Nada El Mahmoudi[1], David Péricat[1], Audrey Bourdet[1], Elise Timon-David[1], Olivier Dumas[2], Christian Chabbert[1] and Brahim Tighilet[1]**

[1] Aix Marseille Université-CNRS, Laboratoire de Neurosciences Sensorielles et Cognitives, LNSC UMR 7260, Equipe Physiopathologie et Thérapie des Désordres Vestibulaires, Groupe de Recherche Vertige (GDR#2074), Marseille, France, [2] Société Française de Kinésithérapie Vestibulaire, Lyon, France

Vestibular pathologies are difficult to diagnose. Existing devices make it possible to quantify and follow the evolution of posturo-locomotor symptoms following vestibular loss in static conditions. However, today, there are no diagnostic tools allowing the quantitative and spontaneous analysis of these symptoms in dynamic situations. With this in mind, we used an open-field video tracking test aiming at identifying specific posturo-locomotor markers in a rodent model of vestibular pathology. Using Ethovision XT 14 software (Noldus), we identified and quantified several behavioral parameters typical of unilateral vestibular lesions in a rat model of vestibular pathology. The unilateral vestibular neurectomy (UVN) rat model reproduces the symptoms of acute unilateral peripheral vestibulopathy in humans. Our data show deficits in locomotion velocity, distance traveled and animal mobility in the first day after the injury. We also highlighted alterations in several parameters, such as head and body acceleration, locomotor pattern, and position of the body, as well as "circling" behavior after vestibular loss. Here, we provide an enriched posturo-locomotor phenotype specific to full and irreversible unilateral vestibular loss. This test helps to strengthen the quantitative evaluation of vestibular disorders in unilateral vestibular lesion rat model. It may also be useful for testing pharmacological compounds promoting the restoration of balance. Transfer of these novel evaluation parameters to human pathology may improve the diagnosis of acute unilateral vestibulopathies and could better follow the evolution of the symptoms upon pharmacological and physical rehabilitation.

Keywords: posture, locomotor activity, vestibular compensation, unilateral vestibular lesion, vestibular syndrome, behavior, ethovision

OPEN ACCESS

Edited by:
Paul Smith,
University of Otago, New Zealand

Reviewed by:
Andreas Zwergal,
Ludwig Maximilian University of Munich, Germany
Sung Huhn Kim,
Yonsei University, South Korea

***Correspondence:**
Brahim Tighilet
brahim.tighilet@univ-amu.fr

Specialty section:
This article was submitted to Neuro-Otology, a section of the journal Frontiers in Neurology

Received: *21 February 2020*
Accepted: *07 May 2020*
Published: *05 June 2020*

Citation:
Rastoldo G, Marouane E, El Mahmoudi N, Péricat D, Bourdet A, Timon-David E, Dumas O, Chabbert C and Tighilet B (2020) Quantitative Evaluation of a New Posturo-Locomotor Phenotype in a Rodent Model of Acute Unilateral Vestibulopathy. Front. Neurol. 11:505. doi: 10.3389/fneur.2020.00505

INTRODUCTION

Unilateral vestibular neurectomy (UVN) induces characteristic vestibular syndrome, composed of oculomotor, posturo-locomotor, and cognitive deficits in a rodent model. These vestibular disorders occur as a result of alterations in the vestibulo-oculomotor and vestibulo-spinal reflexes, as well as in vestibulo-cortical and vestibulo-cerebellar pathways. In humans, as in animals,

vestibular syndrome can be split into several phases of different amplitudes depending on the type, stage, and severity of peripheral damage (1). In the UVN model, vestibular syndrome is particularly severe as a result of the massive imbalance in neuronal activity between the ipsilateral and contralateral vestibular nuclei (2, 3). The acute phase of vestibular syndrome in the UVN rodent model lasts several hours but may extend to days and is characterized by static and dynamic disorders (posturo-locomotor and oculomotor symptoms) in their most severe forms. This is followed by a partially compensated phase in which spontaneous resting activity recovers in neurons of the vestibular nuclei ipsilateral to the lesion. This leads to a full disappearance of the static disorders. However, some dynamic deficits remain poorly compensated and never fully disappear. These data are well-documented in several reviews (1, 4–10).

The vestibular nuclei directly impact postural control through two major descending pathways to the spinal cord: the lateral and the medial vestibulospinal tracts (**Figure 1**). The medial vestibulospinal tract (MVST) is mainly composed of axons from the medial vestibular nucleus and, to a lesser extent, fibers from the lateral and descending (inferior) vestibular nucleus. This tract descends bilaterally and innervates the upper cervical regions of the spinal cord that innervate the upper-body musculature, particularly the neck musculature, essential for stabilizing the head in static or dynamic conditions (12–14). The lateral vestibulospinal tract (LVST) is composed mainly of axons from neurons in the lateral vestibular nucleus (Deiter's nucleus), with some contribution from the inferior vestibular nuclei. This tract descends ipsilaterally and innervates the entire length of the spinal cord, modulating the extensor musculature of the body. The LVST mainly terminates on interneurons in Rexed's laminae VII and VIII in the forelimb and hindlimb segments of the spinal cord. Rexed's VII laminae are also an important site for reticulospinal and corticospinal pathway termination. Thus, the vestibulospinal pathways are well-positioned to modulate the reflex responses to anticipated or imposed body displacements (15–17).

Current examinations of patients with vestibular loss generally involve assessment of the vestibulo-ocular reflex (VOR) (18) and vestibulo-spinal reflex with standing balance studies [(19–21), for review see Cohen (22)]. However, standing and walking are different motor functions. A patient's gait can be measured with a gyroscope system that records trunk sway (23) or with tests of walking balance such as the Tandem walking test (24, 25) or the 10-Meter Walk test (26). In most cases, walking balance tests are not useful for screening people for vestibular impairments but can be useful in vestibular rehabilitation in patients with known diagnoses (24). Among the large number of studies that have investigated postural and ocular reflex deficits after acute unilateral vestibular loss in rats, only a few have thoroughly investigated locomotor activity (27–29) (Porter et al., 1990). Furthermore, the analysis is restricted to velocity, distance traveled, or spatial exploration behavior. The present study was designed to further decipher new parameters for quantitative evaluation of posturo-locomotor syndrome and its compensation over time. We evaluated the spontaneous posturo-locomotor activity of the rat in an open field using up-to-date animal video tracking software and correlated these data with those obtained in a human clinic in vestibular pathology.

MATERIALS AND METHODS

Animals and Experimental Protocols

Sixteen adult long evans rats (250–300 g) were used for this study. All experiments were performed in accordance with the National Institutes of Health's Guide for Care and Use of Laboratory Animals (NIH Publication no. 80-23) revised in 1996 for the UK Animals (Scientific Procedures) Act of 1986 and associated guidelines or the Policy on Ethics approved by the Society for Neuroscience in November 1989 and amended in November 1993 and under the veterinary and National Ethical Committee supervision (French Agriculture Ministry Authorization: B13-055-25). Present study was specifically approved by Neurosciences Ethic Committee N°71 from the French National Committee of animal experimentation. Every attempt was made to minimize both the number and the suffering of animals used in this experiment. Rats had free access to food and water and were housed individually under a constant 12 h light. Animals were divided into 2 groups as follow: a sham operated group ($n = 8$ female), a unilateral vestibular neurectomy (uvn) group ($n = 4$ male and $n = 4$ female).

Unilateral Vestibular Neurectomy

Animals were submitted to a left-side vestibular nerve section ($n = 8$) following the surgical procedure previously reported in the literature (30). Thirty minutes after a subcutaneous injection of buprenorphine (Buprecare®; 0.02 mg/kg), the rats were placed in the induction box and left for 5 min (isoflurane concentration 4%). Once they were deeply anesthetized, they were intubated and, during the surgery, the anesthesia was maintained at an isoflurane concentration of 3%. A tympanic bulla approach gave access to the vestibular nerve: the cervical muscular planes were dissected leading to the tympanic bulla, which was widely drilled to expose the stapedial artery and the promontory containing the cochlea. The cochlea was drilled, exposing the cochlear nerve. The cochlear nerve meatus was enlarged with a needle leading to the vestibulocochlear nerve, which was sectioned at its entry into the brainstem after aspiration of the Scarpa's ganglion. The wound was closed using a stapler. Before awakening the animal, a solution of Ringer Lactate (Virbac; 10 ml/kg) was administered subcutaneously in order to alleviate the dehydration resulting from the inability of the animal to drink normally as a result of the injury. For the sham operated group ($n = 8$), surgery was stopped at the opening of the tympanic bulla.

The successfulness of the surgery is attested at the behavioral level by the presence of a characteristic vestibular syndrome and at the histological level by the observation under optical microscopy of the full section of the 8th cranial nerve between Scarpa ganglion and vestibular nuclei from the brainstem [see Péricat et al. (30) for details].

Open Field for Video Tracking

Animals were individually placed in an open field (80 × 80 × 40 cm). Their behavior was recorded for 10 min using a

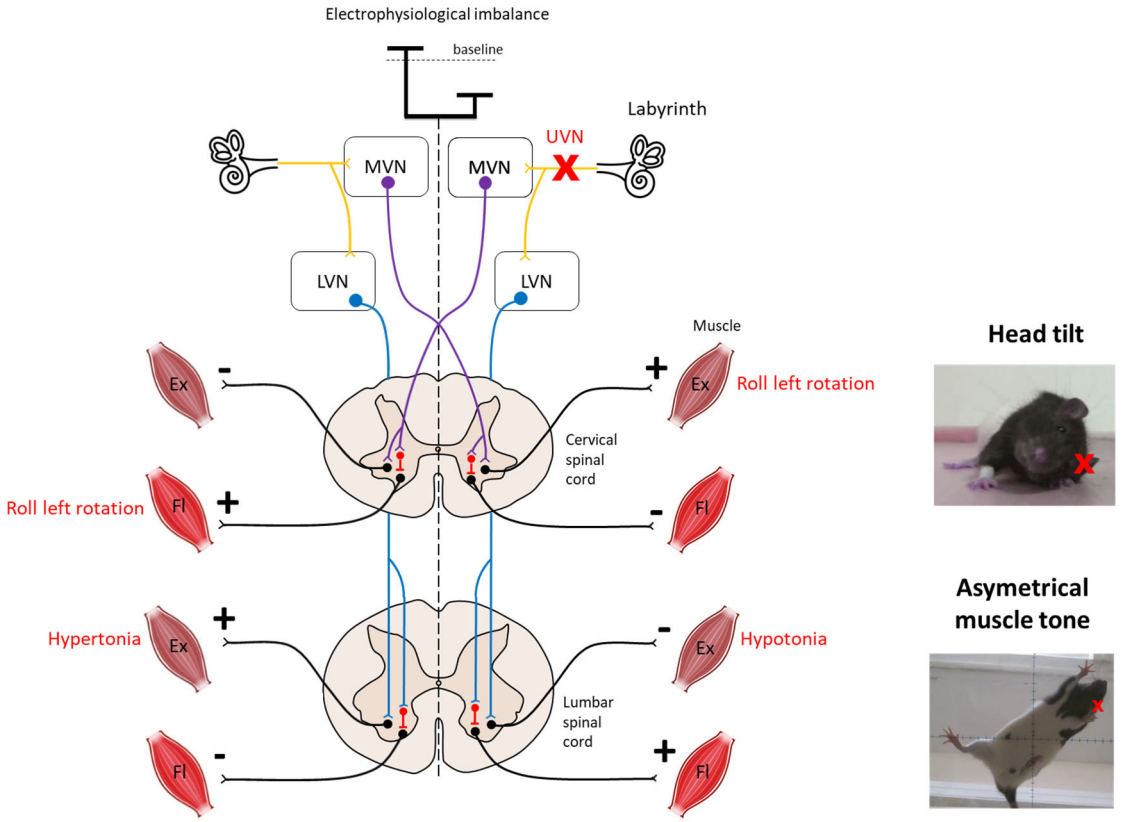

FIGURE 1 | Overview of vestibulospinal reflexes to support the head tilt and hypotonia observed after unilateral vestibular neurectomy. The medial vestibulo-spinal tract (purple) is primarily composed of axons from the medial vestibular nucleus (MVN) and mainly projects contralaterally to the cervical spinal cord to mediate the vestibulocollic reflex. The lateral vestibulospinal tracts (blue) is primarily composed of axons from the lateral vestibular nucleus (LVN) and projects ipsilaterally to the entire length of the spinal cord to influence the extensor musculature of the body involved in balance. Both tracts exert excitatory effects on extensor motoneurons with some inhibitory effects on flexor motoneurons in normal condition. Left unilateral vestibular neurectomy (UVN) induces a electrophysiological imbalance between homologous vestibular nuclei. Loss of activity in the ipsilateral vestibular nucleus induces hypotonia of the lumbar extensor muscles via the lateral vestibulospinal tract. In contrast, the increase in activity in the contralateral lateral vestibular nucleus induces hypertonia of the extensor muscles opposite to the lesion as observed on the picture. Left UVN induces a head tilted (rolled) to the left side (see picture). Extensor activity is induced on the side to which the head is inclined, and flexor activity is induced on the opposite side via the medial vestibulospinal tract (11). Ex, Extensor muscle; Fl, Flexor muscle; LVN, Lateral vestibular nucleus; MVN, Medial vestibular nucleus.

digital camera and analyzed with EthoVision™ XT 14 software (Noldus) (**Figure 2**). The surfaces of the open field were cleaned thoroughly between trials. To minimize stress, the room was lit as dimly as possible while allowing us to clearly discern the rats. At the beginning of the session, the rat was placed on the right side of the field, head in front of the wall. A first acquisition was done the day before the lesion, serving as a reference value, and then acquisitions were performed at days (D) 1, 2, 3, 7, 10, 14, 21, and 30 post-lesion.

Detection and Behavioral Analysis

We used the dynamic subtraction method. Ethovision™ automatically detected the following body-points throughout the recordings: nose point, center point, and tail base of each animal (as shown in **Figure 2** and in **Figures 6F** and **7F** for the recall).

We used 3 analysis profile for 19 variables we selected for analysis (**Table 1**). The first profile does not use a filter and all data were analyzed (No filter—All data). The second profile uses the minimal distance moved (MDM) smoothing method to filter out small movements (<0.7 cm) of the subject's center point that are caused by random noise and all data were analyzed (MDM—All data). The third profile uses the MDM smoothing method and analyzed only selected track segments while the animal is in motion (MDM—Moving).

"Duration not moving" of rats was calculated with an average interval of 3 samples and a threshold of 2.00 cm/s for start and 1.75 cm/s for stop velocity. "Duration highly mobile, mobile and immobile" were calculated with an average interval of 3 samples and a threshold for highly mobile above 5%, mobile between 1 and 5% and immobile below 1%. "Global mobility" is the sum of the % of highly mobile and mobile. "Frequency for high and low acceleration" were calculated with an average interval of 3 samples with a threshold for high acceleration above 50 cm/s^2 and exclude instances shorter than 0.20 s. "Mean positive and negative accelerations" were calculated by selecting with a filter only acceleration above 0 cm/s^2 or under 0 cm/s^2 on the data. Velocity for the nose point and center point was calculated with an average interval of 3 sample. "Multi condition" with the

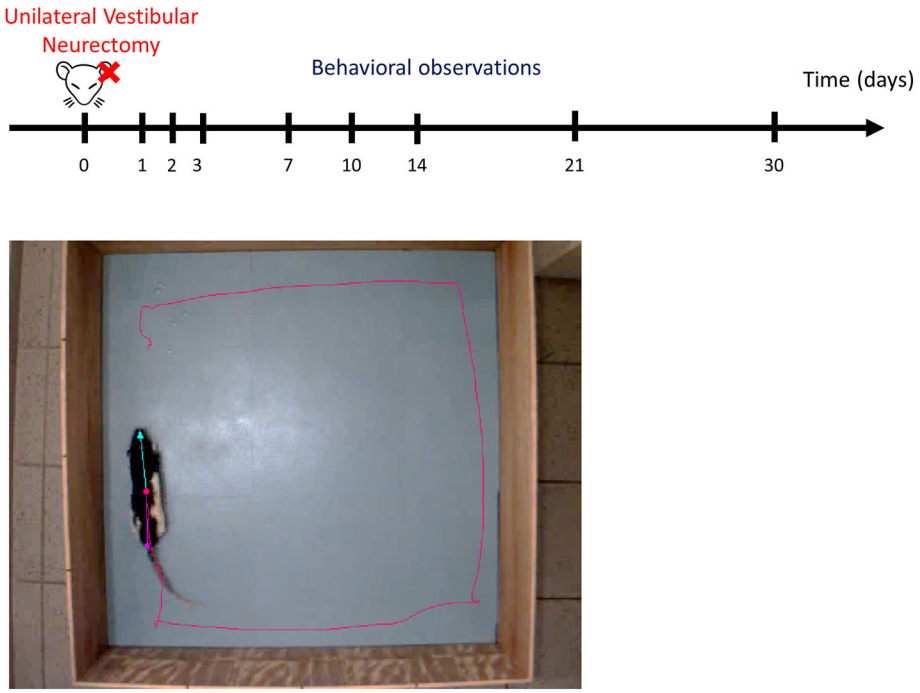

FIGURE 2 | Experimental protocol. Upper part: schematic representation of behavioral observation in video-tracking to evaluate the time course of functional recovery at different post-UVN days. Behavioral analyses were made the day before the lesion, serving as a reference value, and then were performed at days (D) 1, 2, 3, 7, 10, 14, 21, and 30 post-lesion. Lower part: screenshot of the video recording used in the analysis. Ethovision^{TM} automatically detect the following body points throughout the recordings: nose point (blue triangle), center point (red circle), and tail base (purple square) of each animal. The red line illustrates the plot of the center point while the animal is moving. Each animal allowed to explore the open field for 10 min. The open field is a square of 80 × 80 cm.

TABLE 1 | Variables measured with Ethovision XT 14.

Variable	Body point	Filter—segment	Measurement	Unit
Movement	Center point	No filter—all data	Duration not moving	%
Mobility state	Whole body	No filter—all data	Duration highly mobile	%
Mobility state	Whole body	No filter—all data	Duration mobile	%
Mobility state	Whole body	No filter—all data	Global mobility (sum of Highly mobile and Mobile)	%
Mobility state	Whole body	No filter—all data	Duration Immobile	%
Acceleration state (body)	Center point	No filter—all data	Frequency for High and Low Accelerations	
Acceleration state (head)	Nose point	No filter—all data	Frequency for High and low Accelerations	
Positive acceleration	Center point	No filter—all data	Mean	cm/s^2
Negative acceleration	Center point	No filter—all data	Mean	cm/s^2
Relative body angle	Center, nose and tail base point	MDM—all data	Mean	°
Velocity (head)	Nose point	MDM—all data	Mean and Maximum	cm/s
Cephalic nystagmus (bobbing)	Nose point	MDM—all data	Frequency of velocity for the nose point ≥ 100 cm/s	
Distance moved	Center point	MDM—when moving	Total	cm
Velocity (body)	Center point	MDM—when moving	Mean and Maximum	cm/s
Body axis rotation CW	Center to nose point	MDM—when moving	Frequency	
Body axis rotation CCW	Center to nose point	MDM—when moving	Frequency	
Body points rotation CW	Center point	MDM—when moving	Frequency	
Body points rotation CCW	Center point	MDM—when moving	Frequency	
Absolute meander	Center point	MDM—when moving	Mean	°/cm

CW, clockwise (contralesional)°; CCW, counterclockwise (ipsilesional); MDM, Minimal Distance Moved.

variable: "Velocity" for the nose point ≥100 cm/s (averaged over 3 samples) allow us to calculate the frequency of velocity for the nose point ≥100 cm/s. Velocity for the nose point ≥100 cm/s was associated with a cephalic nystagmus behavior when recorded. To select the track segments when the animal is in motion, we selected for every trial recorded in EthoVision™ the track-segments where the animal was moving (thresholds of 2.00 cm/s for start and 1.75 cm/s for stop velocity). "Body axis rotation" has been set to count every 1 rotation with a threshold of 30° allowing us to calculate when the animal is spinning around its own axis. "Body point rotation" has been set to count every 1 rotation with a threshold of 50° with a minimum distance moved of 2 cm allowing us to calculate the rotation in the open field when the animal walks around in circle.

Statistical Analysis

The statistical analyses were evaluated by one-way repeated-measures ANOVA followed by a simple contrast to compare the postoperative time with the pre-operative time for each group (JASP). Difference between the Sham and NVU group were evaluated by two-way repeated measures ANOVA. If significant effect were found, *post-hoc* Bonferroni was performed (GraphPad, Prism). Results were considered significant at $p < 0.05$.

RESULTS

Effect of UVN on Rat Activity and Spatial Exploration

Unilateral vestibular neurectomy (UVN) produced significant changes in posturo-locomotor activity of rats in the open field (**Figure 3A**). UVN rats showed significant decreased in the total distance moved the first 3 days after UVN (Preop: 5897.88 ± 303.68; Day 1: 1,034 ± 308, $p < 0.001$; Day 2: 2,969 ± 419, $p < 0.01$; Day 3: 3,601 ± 530, $p < 0.05$). From day 7 until day 30, the mean distance traveled by lesioned rats was significantly increased relative to that observed before UVN (Day 7: 8,209 ± 1,314, $p < 0.05$; Day 10: 10,127 ± 1,418, $p < 0.001$; Day 14: 10,475 ± 1,125, $p < 0.001$; Day 21: 9,633 ± 1,081, $p < 0.001$; Day 30: 10,222 ± 1,141, $p < 0.001$; **Figure 3B**) and significantly differed from the Sham group (Day 7: $p < 0.01$; Day 10: $p < 0.001$; Day 14: $p < 0.001$; Day 21: $p < 0.001$; Day 30: $p < 0.001$). The average distance moved of rat from the Sham group was not significantly different to that observed before the sham lesion.

Meander, defined as tortuous/winding movement (**Figure 3D**) was significantly increased at day 1 (Preop: 2.98 ± 0.1; Day 1: 12.42 ± 5.19, $p < 0.001$) post-lesion and was significantly different from the Sham group (Day 1: $p < 0.001$). From day 2 until day 30, the meander of lesioned rats was no longer significantly different to that observed before UVN (**Figure 3C**). The meander of the Sham group was not significantly different to that observed before the sham lesion.

Mobility of UVN and Sham Rats

The software discriminates between movement and mobility. Movement is a discrete variable, related to the center-point, with two possible states: "Moving" and "Not moving" (**Figure 4A**). The state "Moving" relates to states when running mean velocity exceeds 2.00 cm/s (start velocity). This state remains until the running mean velocity drops below 1.75 cm/s (stop velocity). It becomes "Not moving" until the running mean velocity reaches the start velocity again. Mobility can be defined as the degree of movement of an animal's body and is calculated 100% independent of movement of the coordinates identified as the center-point (or the nose/tail point).

The % of time not moving or in immobility of UVN rats followed the same time course. It increased significantly the first 3 days after UVN with a maximum value at day 1 (Preop: 23.09 ± 2.06; Day 1: 72.83 ± 4.69, $p < 0.001$; Day 2: 45.41 ± 3.78, $p < 0.001$; Day 3: 36.92 ± 3.36, $p < 0.001$; for % of time not moving and, Preop: 9.86 ± 1.39; Day 1: 61.56 ± 5.18, $p < 0.001$; Day 2: 35.09 ± 3.85, $p < 0.001$; Day 3: 24.37 ± 3.33, $p < 0.001$; for % of time in immobility) and returned to control values from day 7 until day 30 (**Figures 4B,C**). Interestingly, the difference between UVN and Sham groups differed for the % of time not moving or in immobility. Indeed, the % of time not moving was significantly different at pre-operative time (Pre-op: $p < 0.05$) and at days 1 (Day 1: $p < 0.001$), 7 (Day 7: $p < 0.001$), 10 (Day 10: $p < 0.001$), 14 (Day 14: $p < 0.001$), 21 (Day 21: $p < 0.001$), and 30 (Day 30: $p < 0.001$). Conversely, the % of time in immobility, which was not significantly different at pre-operative time, significantly differed at day 1 (Day 1: $p < 0.001$) and day 2 (Day 2: $p < 0.01$). These differences are due to the method of calculation of these two parameters (see above).

Mobility of the animal can be separated in % of time highly mobile (above 5% of change in area detected) and in % of time mobile (between 1 and 5% of change). The % of time highly mobile of UVN rats is the mirror curve of the % of time in immobility: decreased significantly the first 3 days after UVN with a maximum at day 1 (Preop: 54.44 ± 2.87; Day 1: 12.65 ± 3.71, $p < 0.001$; Day 2: 34.29 ± 4.06, $p < 0.001$; Day 3: 39.59 ± 4.25, $p < 0.001$) but was significantly increased from day 7 until day 30 (Day 7: 65.18 ± 5.16, $p < 0.01$; Day 10: 65.21 ± 4.71, $p < 0.01$; Day 14: 65.62 ± 3.44, $p < 0.01$; Day 21: 61.87 ± 3.61, $p < 0.05$; Day 30: 62.73 ± 4.41, $p < 0.05$). The % of time highly mobile between the Sham and the UVN group was significantly different on days 1, 7, 10, 14, 21, 30 (D1: $p < 0.001$; D7: $p < 0.001$; D10: $p < 0.001$; D14: $p < 0.001$; D21: $p < 0.001$; D30: $p < 0.001$; **Figure 4D**).

The % of time mobile of UVN rats decreased significantly at day 1 and day 2 (Preop: 35.68 ± 1.79; Day 1: 25.75 ± 2.91, $p < 0.01$; Day 2: 30.60 ± 1.67, $p < 0.01$) and then return to control value at day 3 but decreased once again from day 7 to day 30 (Day 7: 25.88 ± 3.97, $p < 0.01$; Day 10: 23.08 ± 3.46, $p < 0.001$; Day 14: 22.64 ± 2.31, $p < 0.001$; Day 21: 24.92 ± 2.05, $p < 0.001$; Day 30: 25.85 ± 3.22, $p < 0.001$). The same results was obtained when we compare the Sham and the UVN group (D1: $p < 0.01$; D2: $p < 0.01$; D7: $p < 0.001$; D10: $p < 0.001$; D14: $p < 0.001$; D21: $p < 0.001$; D30: $p < 0.001$; **Figure 4E**).

Global mobility (sum of highly mobile and mobile) of UVN rats significantly decreased the first 3 days after UVN (Preop: 91.12 ± 4.66; Day 1: 38.41 ± 5.18, $p < 0.001$; Day 2: 64.90 ± 3.85, $p < 0.001$; Day 3: 75.61 ± 3.31, $p < 0.001$) and then returned to control values from day 7 until day 30 (**Figure 4F**). Interestingly,

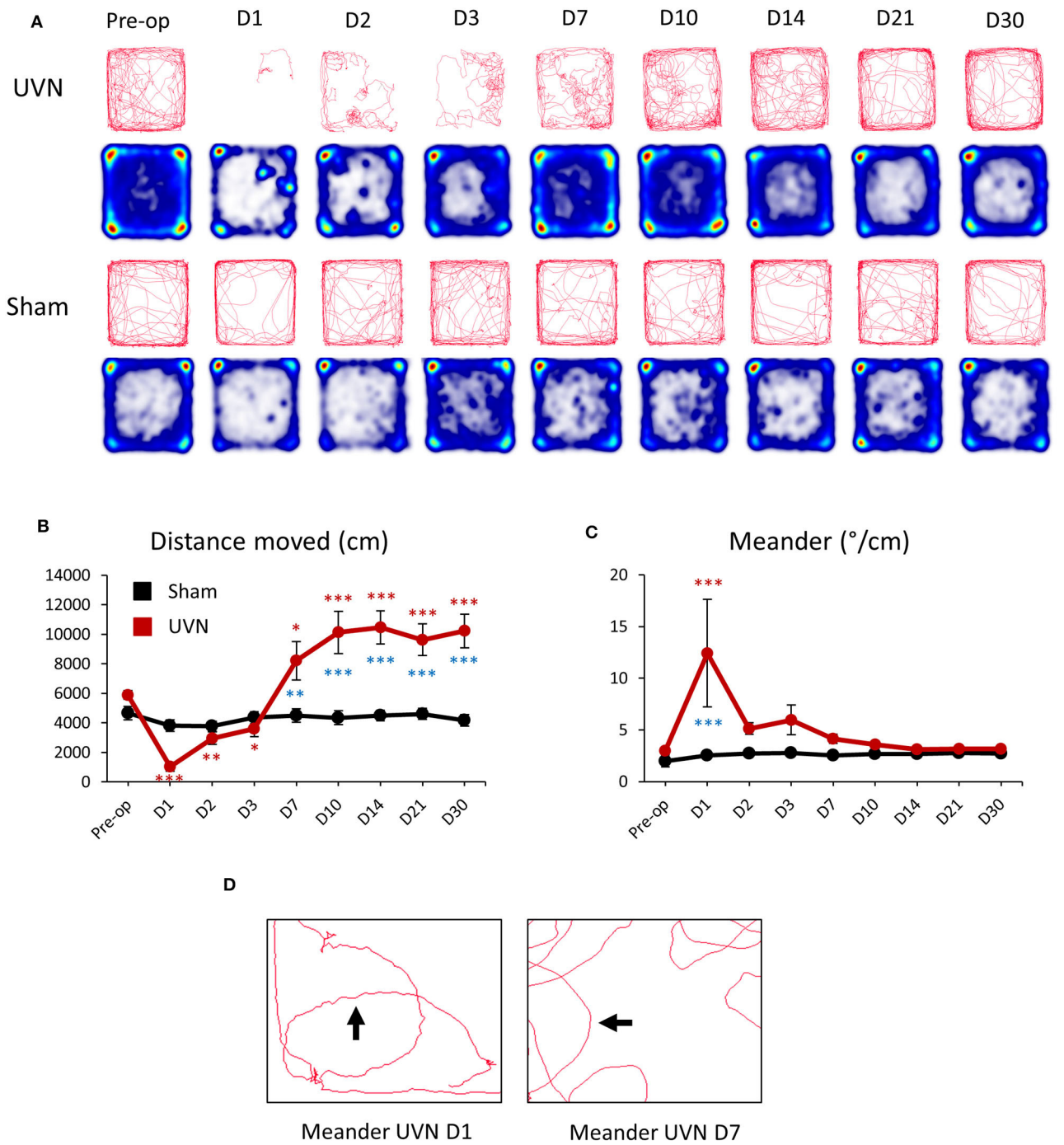

FIGURE 3 | Effect of UVN on rat activity and spatial exploration in an open field. **(A)** Movement tracing and spatial exploration pattern (Heatmaps) of UVN and Sham rats in an open field over the 10 min analysis period. Heatmaps indicate the cumulative time at place (blue to red scale increasing duration). **(B)** Curve illustrating the mean postoperative recovery of the distance moved by rats on the open-field in the two experimental group of rats (Sham in black and UVN in red). **(C)** Curve illustrating the mean postoperative recovery of meander by rats on the open-field in the two experimental group of rats (Sham in black and UVN in red). Data represent mean ± SEM; $^{*}P < 0.05$, $^{**}P < 0.01$, $^{***}P < 0.001$. **(D)** Zoom on the movement tracing of a UVN rat 1 and 7 days after the surgery. Meander is defined as "the change in direction of movement of a subject relative to the distance moved by that subject and provides an indication of how convoluted the subject's trajectory is." As observed on the movement tracing by rats 1 day after the surgery the trajectory (arrow) of the animal is more "tortuous" compared to the trajectory of the same rat seven days after UVN. A significant difference from the pre-operative value is indicated by * in black for the SHAM group. A significant difference from the pre-operative value is indicated by * in red for the UVN group. A significant difference between the SHAM and the UVN group is indicated with * in blue.

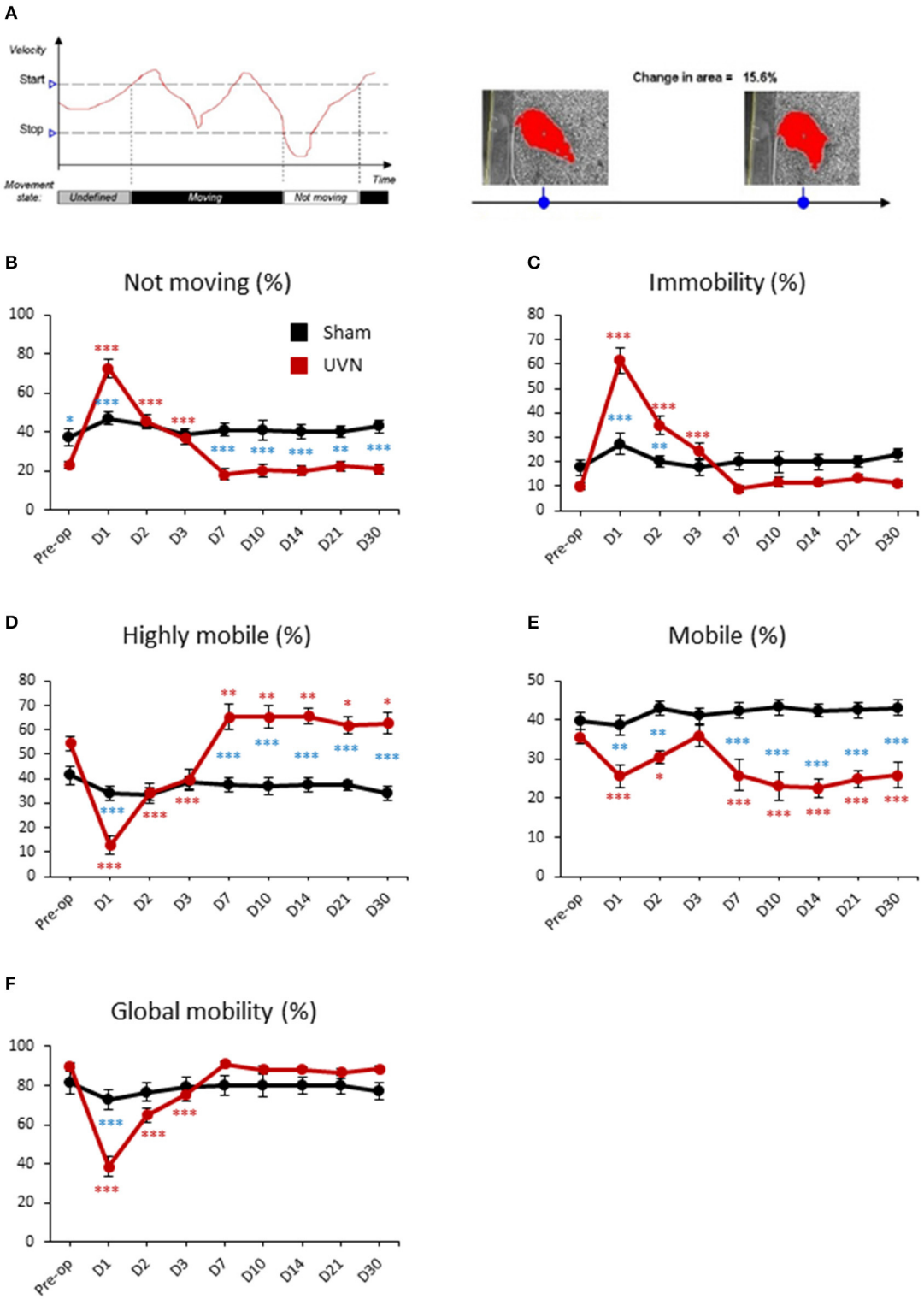

FIGURE 4 | Mobility of UVN and Sham rats in the open field. **(A)** Illustration of the variable movement (on left) and mobility (on right). In the following example for movement, because the velocity initially lies between the Stop velocity and the Start velocity, the state is undefined. When velocity exceeds the Start velocity value, Movement is given the value "Moving." When velocity drops below the Stop velocity value, Movement is given the value "Not moving." Mobility can be defined as the degree of movement of an animal's body independent of spatial displacement of the center or any other body point, which is measured by Movement. The calculation of mobility does not use the x,y coordinates of the animal. Mobility is calculated 100% independent of movement of the coordinates identified as the center-point (or

(Continued)

FIGURE 4 | the nose/tail point). **(B)** Curves illustrating the kinetics of the % of time when the animal is not moving for UVN (red) and Sham (black) group. **(C)** Curves illustrating the kinetics of the % of time when the animal is immobile for UVN (red) and Sham (black) group. **(D)** Curves illustrating the kinetics of the % of time when the animal is highly mobile for UVN (red) and Sham (black) group. **(E)** Curves illustrating the kinetics of the % of time when the animal is mobile for UVN (red) and Sham (black) group. **(F)** Curves illustrating the kinetics of the % of time when the animal is either mobile or highly mobile (global mobility) for UVN (red) and Sham (black) group. Data represent mean ± SEM; $^{*}P < 0.05$, $^{**}P < 0.01$, $^{***}P < 0.001$. A significant difference from the pre-operative value is indicated by * in black for the SHAM group. A significant difference from the pre-operative value is indicated by * in red for the UVN group. A significant difference between the SHAM and the UVN group is indicated with * in blue.

the sham and the UVN groups significantly differed at day 1 (D1: $p < 0.001$) only.

For all parameters analyzed, the Sham group did not significantly differ from that observed before the sham lesion.

Rotations Frequencies of UVN and Sham Rats

Animal's rotations were analyzed through monitoring both the rotations of rats around their body axis and the circling travel in the arena (**Figure 5A**). The animal's rotations can be analyzed in body axis rotation and in arena rotation. Body axis rotation quantifies if the rat is spinning around its own axis while arena rotation quantifies if the rat walks around the arena in circle (**Figure 5A**). Before the lesion UVN rats rotated 4.25 ± 0.97 times on themselves (body axis rotation) on the clockwise (contralesional) direction and 3.25 ± 0.55 times on the counterclockwise (ipsilesional) direction. After UVN the mean number of contralesional body axis rotation increased significantly at day 2 and 3 (Day 2: 12.62 ± 4.09, $p < 0.05$; Day 3: 17.25 ± 5.64, $p < 0.001$). From day 7 until day 30 the mean number of contralesional body axis rotations of UVN rats was no longer significantly different to that observed before the lesion. The Sham group rotated on themselves (body axis rotation) significantly less on the contralesional side compare to the UVN group at day 2 and day 3 (Day 2: $p < 0.05$; Day 3: $p < 0.001$). Similar results were obtained for the ipsilesional body axis rotation from day 7 to day 30 compare to the UVN group (Day 7: $p < 0.001$; Day 10: $p < 0.001$; Day 14: $p < 0.001$; Day 21: $p < 0.001$; Day 30: $p < 0.001$; **Figure 5B**). Conversely, the mean number of ipsilesional body axis rotation after UVN increased significantly from day 7 until day 30 (Day 7: 24.62 ± 6.49, $p < 0.001$; Day 10: 25.19 ± 6.27, $p < 0.001$; Day 14: 22.37 ± 5.54, $p < 0.001$; Day 21: 20.25 ± 4.79, $p < 0.001$; Day 30: 22.5 ± 5.24, $p < 0.001$; **Figure 5D**). The number of body axis rotation in either ipsilesional or contralesional side was not significantly affected by the sham surgery nor the postoperative time.

Before the lesion, UVN rats rotated 13 ± 1.13 times in the arena on the clockwise (contralesional) direction and 11 ± 1.06 on the counterclockwise (ipsilesional) direction. One day after UVN the mean number of arena rotations on the contralesional direction decreased significantly to 4.87 ± 1.28 ($p < 0.05$) and decreased insignificantly to 3.75 ± 1.30 ($p = 0.115$) on the ipsilesional direction due to the incapacity of UVN rats to move properly 1 day after the lesion. From day 2 until day 30, arena rotations of UVN rats on the contralesional direction did not significantly differed relative to that observed before the lesion. However, the contralesional arena rotations of the Sham group were significantly reduced at day 3 and 7 compared to the UVN group (Day 3: $p < 0.01$; Day 7: $p < 0.01$; **Figure 5C**). Conversely, the ipsilesional arena rotations of UVN rats was not affected by the lesion the first 3 postoperative days but increased significantly from day 7 to day 30 (Day 7: 28.75 ± 5.54, $p < 0.001$; Day 10: 31.25 ± 5.32, $p < 0.001$; Day 14: 27.37 ± 4.66, $p < 0.001$; Day 21: 25.12 ± 3.50, $p < 0.001$; Day 30: 31.62 ± 3.85, $p < 0.001$). Furthermore, the ipsilesional arena rotations of the UVN group were significantly increased from day 7 to day 30 compared to the Sham group (Day 7: $p < 0.001$; Day 10: $p < 0.001$; Day 14: $p < 0.001$; Day 21: $p < 0.001$; Day 30: $p < 0.001$; **Figure 5E**).

The number of arena rotations in either ipsilesional or contralesional side was not significantly affected by the sham surgery nor postoperative time for the Sham group.

Locomotor Velocity of UVN and Sham Rats

The mean velocity of the head (calculated from the nose-point) and the body (calculated from the center-point) of UVN rats was 14.50 ± 0.61 cm/s and 17 ± 0.53 cm/s before UVN. These values significantly decreased at day 1 and day 2 for the head velocity (Day 1: 3.61 ± 0.91, $p < 0.001$; Day 2: 8.94 ± 0.93, $p < 0.001$) and over the first 3 days after lesion for the body velocity (Day 1: 8.45 ± 0.80, $p < 0.001$; Day 2: 11.27 ± 0.79, $p < 0.001$; Day 3: 12 ± 1.17, $p < 0.001$). From day 7 until day 30, the mean head velocity of the UVN rats significantly increased (Day 7: 22.41 ± 2.43, $p < 0.001$; Day 10: 24.68 ± 2.46, $p < 0.001$; Day 14: 24.82 ± 2.02, $p < 0.001$; Day 21: 23.54 ± 2.19, $p < 0.001$; Day 30: 24.08 ± 2.29, $p < 0.001$). On the other hand, the mean velocity of the body of UVN rats was significantly increased from day 10 to day 30 (Day 10: 23.90 ± 2.38, $p < 0.001$; Day 14: 25.02 ± 1.90, $p < 0.001$; Day 21: 25.11 ± 2.08, $p < 0.001$; Day 30: 25.44 ± 2.13, $p < 0.001$; **Figures 6A,C**).

The mean velocity of the head or the body was not significantly affected by the sham surgery nor postoperative time for the Sham group.

Maximum head and body velocities during vestibular compensation evolved differently than the mean velocity. Maximum head velocity of UVN rats was not impaired after UVN during the first 3 days but increased significantly from day 7 to day 30 compare to pre-operative values (Preop: 114.83 ± 5.23; Day 7: 145.78 ± 5.67, $p < 0.01$; Day 10: 145.09 ± 3.03, $p < 0.01$; Day 14: 138.99 ± 3.85, $p < 0.05$; Day 21: 153.62 ± 11.90, $p < 0.001$; Day 30: 141.40 ± 6.78, $p < 0.01$; **Figure 6B**). Conversely, maximum body velocity of UVN rats was 77.02 ± 3.20 cm/s before UVN and significantly decreased with a peak at day 1 (29.64 ± 2.39, $p < 0.001$) until day 7 post-lesion (Day 2: 35.29 ± 2.26, $p < 0.001$; Day 3: 36.47 ± 3.79, $p < 0.001$; Day 7: 56.69 ± 4.70, $p < 0.001$). From day 10 until day 30, the maximum body velocity of the lesioned rats was

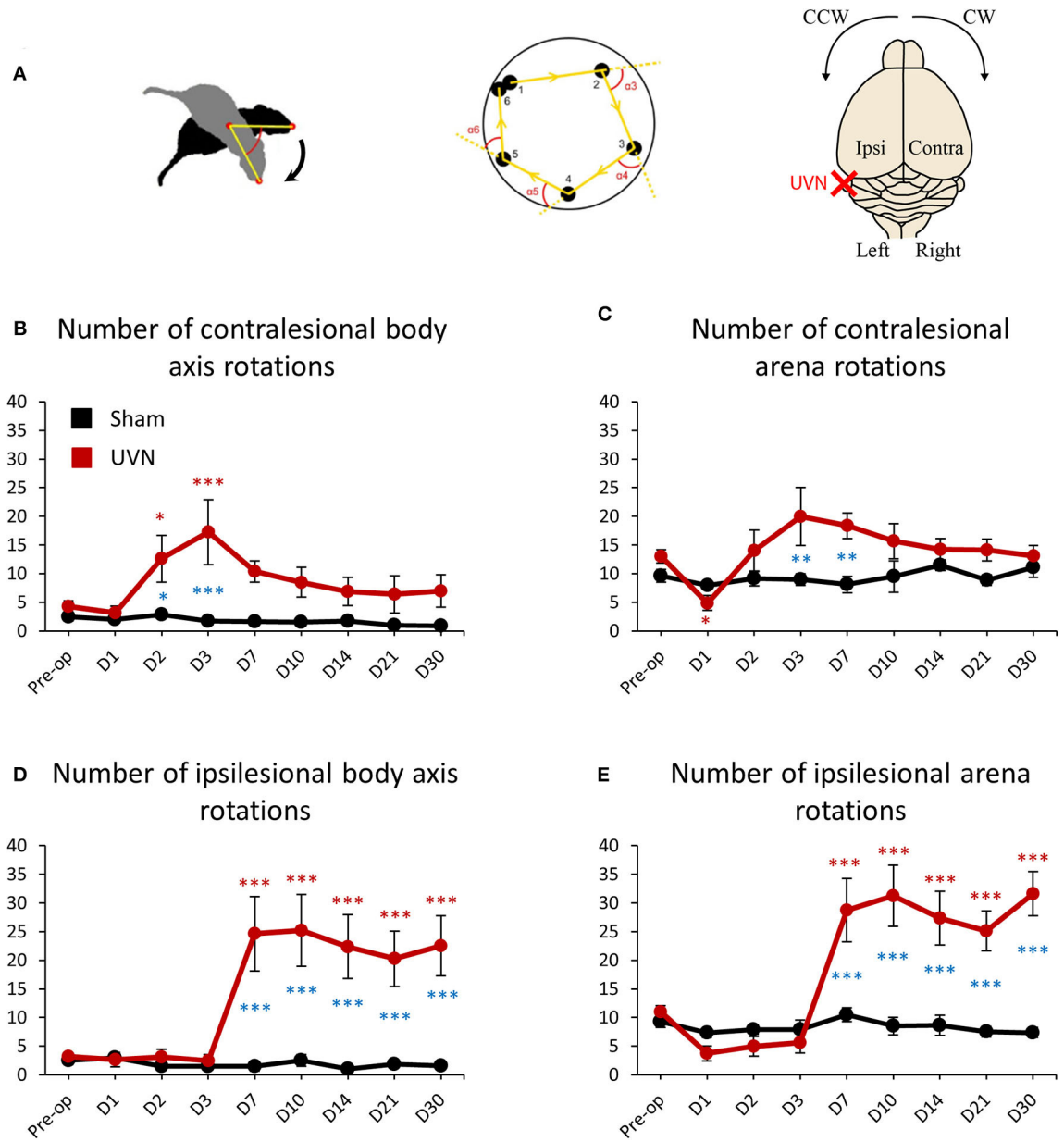

FIGURE 5 | Rotation frequencies of UVN and Sham rats in the open field. **(A)** Illustration of body axis rotation (left part), arena rotation (middle part) and illustration of the contralateral and ipsilateral hemispheres regarding the lesion and turning direction (right part). A rotation in a counterclockwise (CCW) direction is a ipsilesional rotation and vice versa for clockwise (CW) rotations. Body axis rotation is a method used to quantify if the rat is spinning around its own axis. Arena rotation is suitable for when animal walks around in circles (middle part). **(B)** Curves illustrating the kinetics of body axis rotation frequencies on the intact side (contralesional rotations) of UVN (red) and Sham (black) group. **(C)** Curves illustrating the kinetics of arena rotation frequencies on the intact side (contralesional rotations) of UVN (red) and Sham (black) group. **(D)** Curves illustrating the kinetics of body axis rotation frequency on the lesioned side (ipsilesional rotation) of UVN (red) and Sham (black) group. **(E)** Curves illustrating the kinetics of Arena rotation frequency on the lesioned side (ipsilesional rotations) of UVN (red) and Sham (black) group. Data represent mean ± SEM; $^{*}P < 0.05$, $^{**}P < 0.01$, $^{***}P < 0.001$. A significant difference from the pre-operative value is indicated by * in black for the SHAM group. A significant difference from the pre-operative value is indicated by * in red for the UVN group. A significant difference between the SHAM and the UVN group is indicated with * in blue.

no longer significantly different to that observed before UVN (**Figure 6D**). Maximum head velocity of the UVN group was significantly increased compared to the Sham group at day 7, 10, 21 and 30 post-lesion (Day 7: $p < 0.001$; Day 10: $p < 0.001$; Day 21: $p < 0.01$; Day 30: $p < 0.01$) and the maximum head velocity was not significantly affected by the sham surgery nor postoperative time (**Figure 6B**). Conversely, the maximum body velocity of the Sham group was significantly increased from day

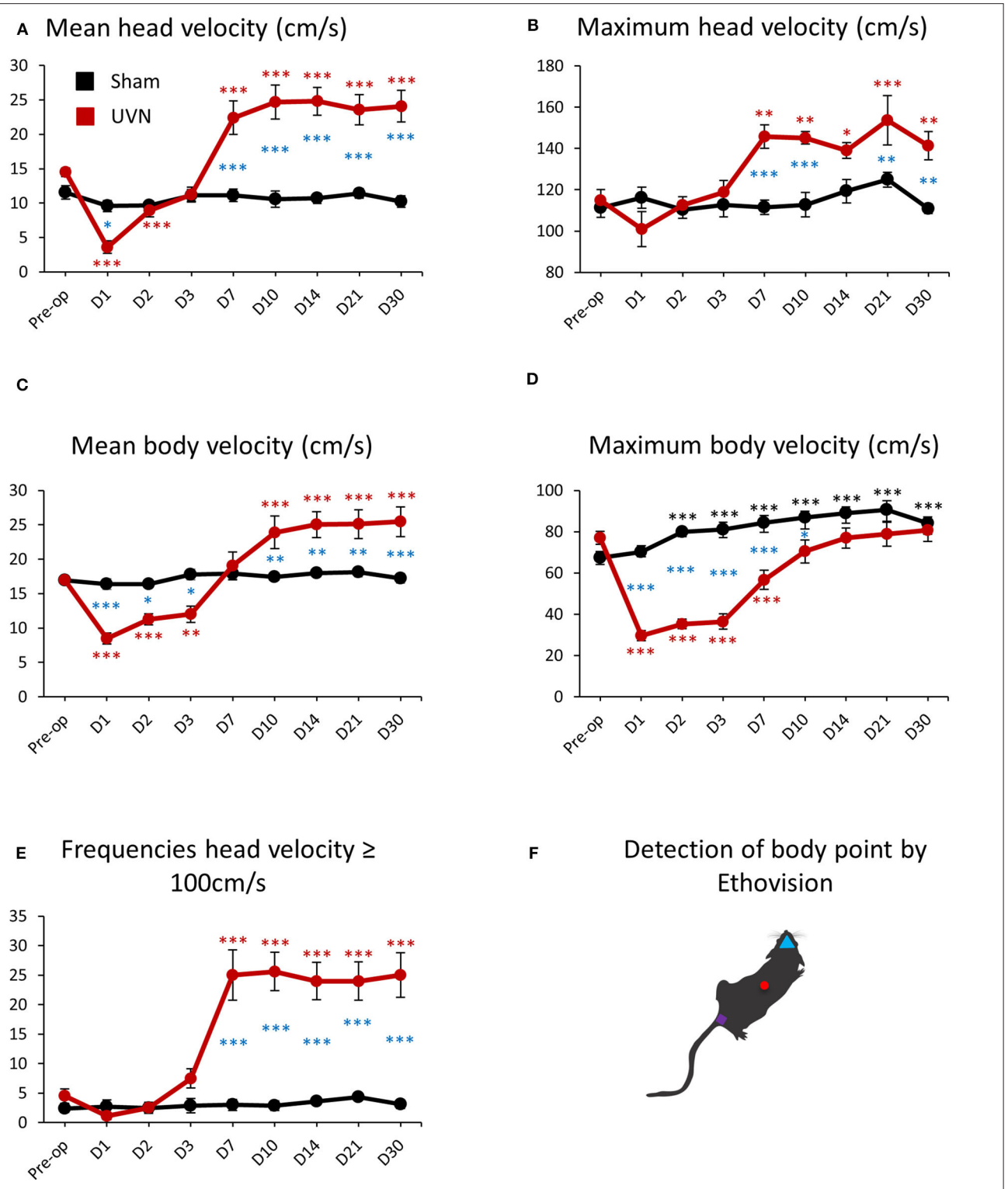

FIGURE 6 | Locomotor velocity of UVN and Sham rats in the open field. **(A)** Curves illustrating the kinetics of the mean velocity (cm/s) of the head (calculated from the nose point) for UVN (red) and Sham (black) group. **(B)** Curves illustrating the kinetics of the maximum velocity (cm/s) of the head for UVN (red) and Sham (black) group. **(C)** Curves illustrating the kinetics of the mean velocity (cm/s) of the body (calculated from the center-point) for UVN (red) and Sham (black) group. **(D)** Curves illustrating the kinetics of the maximum velocity (cm/s) of the body for UVN (red) and Sham (black) group. **(E)** Curves illustrating the kinetics of the frequencies of the velocity of the head superior or equal to 100 cm/s, linked to the bobbing behavior (cephalic nystagmus) for UVN (red) and Sham (black) group. Bobbing behavior is defined when the velocity for the nose point is ≥ 100 cm/s. **(F)** illustration of the detection of body point by Ethovision™ throughout the recordings: nose point (blue

(Continued)

FIGURE 6 | triangle), center point (red circle), and tail base (purple square) of each animal. Data represent mean ± SEM; *$P < 0.05$, **$P < 0.01$, ***$P < 0.001$. A significant difference from the pre-operative value is indicated by * in black for the SHAM group. A significant difference from the pre-operative value is indicated by * in red for the UVN group. A significant difference between the SHAM and the UVN group is indicated with * in blue.

2 to day 30 post-lesion compared to the pre-operative value (Day 2: 79.94 ± 2.89, $p < 0.001$; Day 3: 81.01 ± 3.52, $p < 0.001$; Day 7: 84.37 ± 3.48, $p < 0.001$; Day 10: 87 ± 2.83, $p < 0.001$; Day 14: 88.91 ± 3.01, $p < 0.001$; Day 21: 90.59 ± 4.39, $p < 0.001$; Day 30: 84.18 ± 3.05, $p < 0.001$, **Figure 6D**). The maximum body velocity of UVN rats was significantly decreased compared to the Sham group during the first 10 days post-lesion (Day 1: $p < 0.001$; Day 2: $p < 0.001$; Day 3: $p < 0.001$; Day 7: $p < 0.001$; Day 10: $p < 0.05$).

The increased head velocity from day 7 to day 30 for the UVN group was correlated with the appearance of cephalic nystagmus (bobbing) induced by the lesion (**Video 1**). Indeed, we could quantify the frequencies of bobbing with a high-pass filter to calculate the number of times the head (nose point) velocity exceeds 100 cm/s. As shown on **Figure 6E**, in physiologic condition, the software detected a few numbers of times when the head velocity exceeded 100 cm/s (Preop: 4.5 ± 1.21) because the rat can reach these values without being associated to bobbing behavior. However, the numbers of times for which the head velocity exceeded 100 cm/s did not change (between 2 and 4 detection) for the Sham group over time but bobbing frequencies on the UVN group increased significantly from day 7 to day 30 post-lesion (Day 7: 25 ± 4.25, $p < 0.001$; Day 10: 25.62 ± 3.24, $p < 0.001$; Day 14: 24 ± 3.16, $p < 0.001$; Day 21: 24 ± 3.24, $p < 0.001$; Day 30: 25 ± 3.79, $p < 0.001$; **Figure 6E**) and was correlated with the increased of maximum head velocity (see **Figure 6B**).

Acceleration of UVN and Sham Rats

Total number of accelerations of the rats can be separated in high (above 50 cm/s^2) and low (below 50 cm/s^2) accelerations for both the body and head. UVN rats performed an average of 107.37 ± 5.93 high accelerations (**Figure 7A**) and 771 ± 15.42 low accelerations (**Figure 7B**) of the head (calculated from the nose point) before the lesion. High accelerations of the head of UVN rats almost disappeared at day 1 (17.75 ± 4.34, $p < 0.001$), slowly recovered at day 2 (46.12 ± 7.65, $p < 0.001$) and increased significantly from day 7 to day 30 post-lesion (Day 7: 169.25 ± 16.75, $p < 0.001$; Day 10: 193.56 ± 20.11, $p < 0.001$; Day 14: 200 ± 19.17, $p < 0.001$; Day 21: 188.12 ± 21.56, $p < 0.001$; Day 30: 194 ± 20.94, $p < 0.001$; **Figure 7A**). Low acceleration of the head of UVN rats significantly decreased at day 1 and day 2 post-lesion (Day 1: 438.12 ± 42.12, $p < 0.001$; Day 2: 636.87 ± 27.85, $p < 0.001$) and recovered pre-operative values from day 3 until day 30 (**Figure 7B**). While the number of high accelerations of the head of the Sham group was significantly lower compared to the UVN group from day 7 to day 30 (Day 7: $p < 0.001$; Day 10: $p < 0.001$; Day 14: $p < 0.001$; Day 21: $p < 0.001$; Day 30: $p < 0.001$; **Figure 7A**), the number of low accelerations of the head is only significantly different from the UVN group at day 1, day 7 and day 10 (Day 1: $p < 0.001$; Day 7: $p < 0.001$; Day 10: $p < 0.05$; **Figure 7B**).

UVN rats performed an average of 88.87 ± 7.31 high (**Figure 7C**) and 379.5 ± 26.56 low body accelerations (**Figure 7D**) calculated from the center point, before the lesion. High body accelerations almost disappeared during the first 3 days post-lesion (Day 1: 0.87 ± 0.74, $p < 0.001$; Day 2: 4.12 ± 1.49, $p < 0.001$; Day 3: 11.5 ± 4.61, $p < 0.001$) and increased significantly from day 10 to day 30 (Day 10: 134.43 ± 24.33, $p < 0.001$; Day 14: 156.25 ± 22.50, $p < 0.001$; Day 21: 146.12 ± 24.07, $p < 0.001$; Day 30: 156.5 ± 23.66, $p < 0.001$; **Figure 7C**). Low body accelerations of UVN rats significantly decreased the first 3 days post-lesion (Day 1: 86.12 ± 20.63, $p < 0.001$; Day 2: 221.87 ± 33.06, $p < 0.001$; Day 3: 262.87 ± 38.69, $p < 0.001$) and increased significantly from day 7 until day 30 (Day 7: 533.87 ± 45.80; Day 10: 515.81 ± 34.40, $p < 0.001$; Day 14: 502.5 ± 22.20, $p < 0.001$; Day 21: 490.87 ± 28.40, $p < 0.001$; Day 30: 491.12 ± 29.38, $p < 0.001$; **Figure 7D**). While the number of high body accelerations of the Sham group significantly differed from those of the UVN group at day 3, 14, and 30 post-lesion (Day 3: $p < 0.01$; Day 14: $p < 0.01$ Day 30: $p < 0.01$; **Figure 7C**), the number of low body accelerations significantly differed before the lesion and at day 1, 7, 10, 14, 21, and 30 post-lesion (Preop: $p < 0.05$; Day 1: $p < 0.01$ Day 7: $p < 0.001$; Day 10: $p < 0.001$; Day 14: $p < 0.001$; Day 21: $p < 0.001$; Day 30: $p < 0.001$; **Figure 7D**).

By averaging positive accelerations of UVN animals we found that rats before lesion had a mean acceleration of 49.37 ± 2.04 cm/s^2 in. We also found the same recovery kinetics after UVN than the frequencies of high body acceleration with two phases: a significant decrease in the mean positive accelerations during the first 3 days after injury (Day 1: 19.08 ± 2.02, $p < 0.001$; Day 2: 30.87 ± 2.32, $p < 0.001$; Day 3: 33.49 ± 2.47, $p < 0.001$) followed by a second phase with an increase from day 10 to day 30 (Day 10: 61.97 ± 5.56, $p < 0.001$; Day 14: 63.42 ± 4.42, $p < 0.001$; Day 21: 63.29 ± 5.07, $p < 0.001$; Day 30: 65.02 ± 5.43, $p < 0.001$; **Figure 7E**).

All acceleration parameters investigated was not significantly affected by the sham surgery nor postoperative time for the Sham group.

Posture of UVN and Sham Rats

Body torsion of the rats before UVN was 0.35° ± 0.74, so the rat's body is straight. UVN produced a significative change in posture on day 7 post-lesion with a mean body torsion of 6.17° ± 1.03 (toward the intact side) compared to pre-operative value (**Figure 8**), from day 7 to day 30 the mean body torsion was maintained between 4 and 4.9 without significant effect. One day after the surgery UVN rats bent their body significantly on the ipsilesional side compared to the Sham group (Day 1: $p < 0.05$).

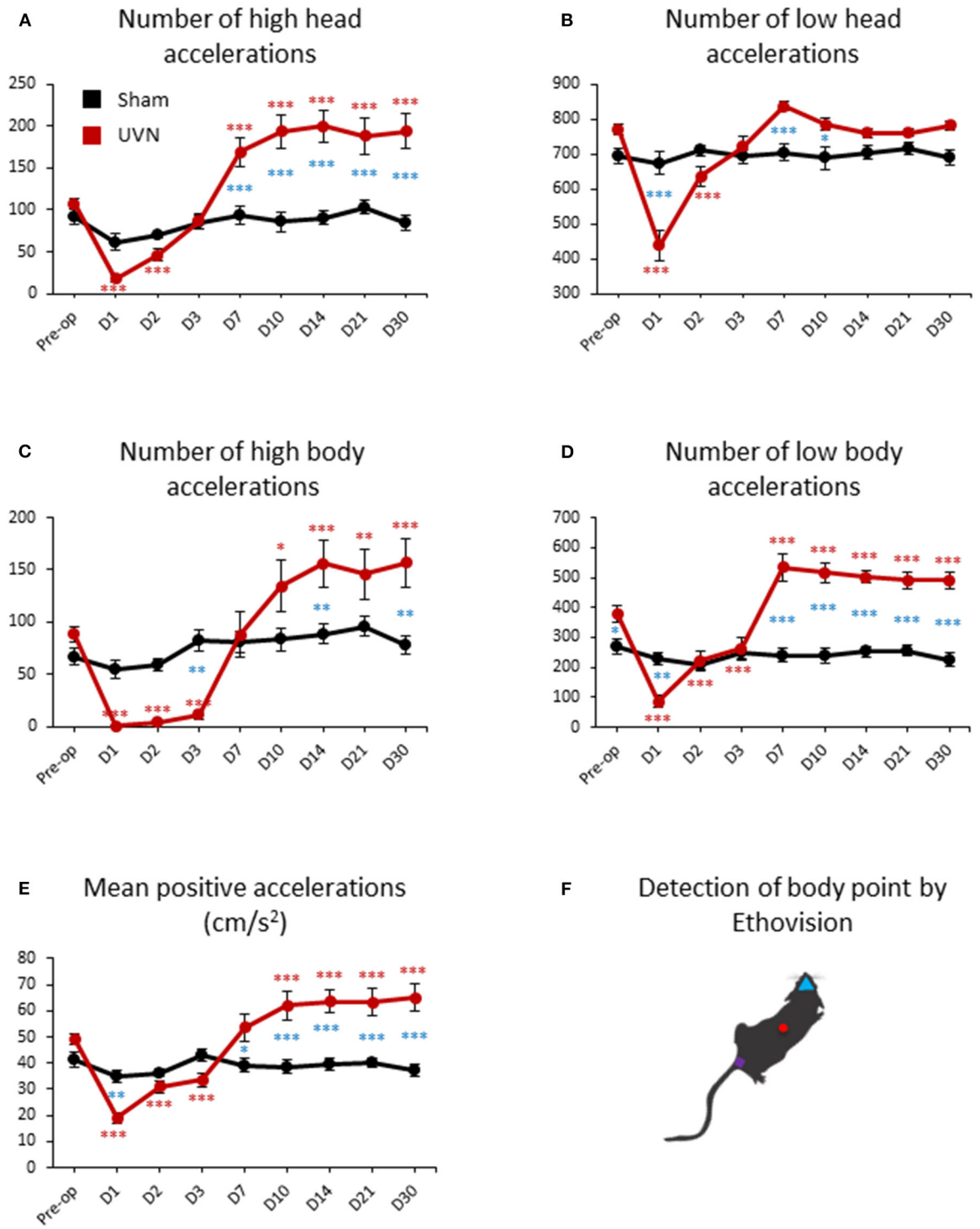

FIGURE 7 | Acceleration of UVN and Sham rats in the open field. **(A)** Curves illustrating the kinetics of the mean number of high acceleration of the nose-point (above 50 cm/s^2) for UVN (red) and Sham (black) group. **(B)** Curves illustrating the kinetics of the mean number of low acceleration of the nose-point (below 50 cm/s^2) for UVN (red) and Sham (black) group. **(C)** Curves illustrating the kinetics of the mean number of high acceleration of the center point (above 50 cm/s^2) for UVN (red) and Sham (black) group. **(D)** Curves illustrating the kinetics of the mean number of low acceleration of the center point (below 50 cm/s^2) for UVN (red) and Sham (black) group. **(E)** Curves illustrating the mean positive accelerations of the rat (cm/s^2) for UVN (red) and Sham (black) group. **(F)** Illustration of the detection of body point by Ethovision^{TM} throughout the recordings: nose point (blue triangle), center point (red circle) and tail base (purple square) of each animal. Data represent mean ± SEM; $^*P < 0.05$, $^{**}P < 0.01$, $^{***}P < 0.001$. A significant difference from the pre-operative value is indicated by * in black for the SHAM group. A significant difference from the pre-operative value is indicated by * in red for the UVN group. A significant difference between the SHAM and the UVN group is indicated with * in blue.

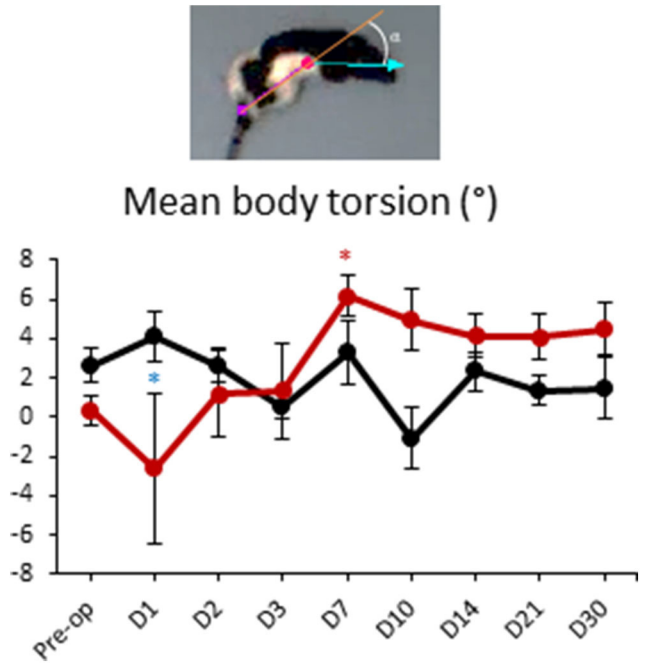

FIGURE 8 | Posture of UVN and Sham rats in the open-field. Curves illustrating the mean body torsion of UVN (red) and Sham (black). Data represent mean ± SEM; *$P < 0.05$. A significant difference from the pre-operative value is indicated by * in black for the SHAM group. A significant difference from the pre-operative value is indicated by * in red for the UVN group. A significant difference between the SHAM and the UVN group is indicated with * in blue.

The mean body torsion was not significantly affected by the sham surgery nor by the postoperative time for the Sham group.

DISCUSSION

Locomotion, Exploration, and Velocity of UVN Rats

Our data showed a significant decrease in the total distance moved and the body velocity during the first 3 days after unilateral vestibular neurectomy (UVN). This phase was followed by a significant increase from day 7 or 10 until day 30 in the distance moved and body velocity, respectively. We demonstrated a significant increase in the meander (sinuous trajectory of the animal) only the first day post-UVN. Certain parameters, such as velocity, were compensated within 7 days post-UVN. These results corroborate those of Lindner et al. (29) in a chemical model of unilateral labyrinthectomy. In this model, rats demonstrated a significant increase in their velocity above baseline after day 7.

Locomotion is an automated behavior generated at the spinal level by the central pattern generator of locomotion (15). However, in response to external factors, the nervous system updates the spinal pattern generator based on multisensory feedback, such as visual, somatosensory or vestibular inputs. In addition to purely vestibular information, vestibular nucleus neurons also receive visual and somatosensory inputs (15, 31), which are required for postural and locomotion control (12, 32). The vestibular nuclei influence motoneurons in the spinal cord through two descending tracts: the medial vestibulospinal and, in prime position to influence the locomotor pattern, the lateral vestibulospinal tract (33). Indeed, the activity of Deiter's neurons is modulated during treadmill locomotion in the cats (34).

Our results from an animal model of vestibular pathology align with observations obtained in vestibular patients subjected to the same type of vestibular deafferentation. Indeed, curative unilateral vestibular neurotomy in vestibular defect patients affects both gait and walking performance and reduces the mean walking velocity (35, 36). These functional parameters are also affected in patients with vestibular disorders (37–40). The slow walking speed of vestibular defect patients can be explained by the reduction in the sensation of imbalance induced by the gain asymmetry of the vestibulo-ocular reflex (VOR) and thus may be a behavioral strategy employed by the subjects to avoid imbalance and fall.

Regarding the velocity parameter, we also demonstrated a time recovery difference in UVN animals between mean and maximum body velocity: the maximum body velocity of the animals had recovered at day 10, compared a recovery to baseline for the mean body velocity at day 7, followed by an increase above the baseline level after day 7. We can assume that after vestibular loss, the priority of the animal is first to move correctly at a medium speed before being able to move faster. In fact, the higher the speed of head movement, the stronger the asymmetry felt in the vestibulo-ocular and vestibulo-spinal pathways. How can the increase in body velocity between day 10 and day 30 post-UVN be explained? Inspired by the observation of a dog with acute unilateral vestibulopathy, Brandt et al. (37) demonstrated that patients with acute vestibulopathy run with less deviation to the affected side than during walking. They suggested that when running, the automatic spinal locomotor program suppresses destabilizing vestibular input. This compensatory behavior may be an option in vestibular defect rats. One possibility is that the rats increase their walking velocity to stabilize their balance (observed between day 10 and day 30). This strategy of increasing walk speed is found in cycling practice, where at low speed, the balance is more precarious than at high speed. If vestibular patients do not run, it is because they consider that their condition probably does not allow them to; it is an avoidance strategy. Indeed, the vestibular contribution to gait variability, which is a predictive marker for falls, declines with faster walking and running (41). Therefore, their balance would be better when running because dynamic balance strategies are different at low and high speeds (41–45).

Regarding the distance moved parameter, we demonstrated an increase exploration of the UVN rats between day 7 and day 30 after the lesion in line with the increase in body velocity. We have two interpretations to these data:

1 The mathematical explanation with a simple formula "Speed = Distance / Time", informs us that if animals increase their speed without changing the analysis time (10 min) or mobility time (**Figure 4**), then an increase in velocity is correlated with an increase in distance traveled.

2 An alternative explanation for the increased exploration in the open field may also be due to a spatial disorientation. The head maps (**Figure 3**) show a higher probability of being in the center of the open field for UVN rats (especially on day 7 to 14 post UVN), which is a kind of non-physiological behavior for rats. Spatial disorientation has been described after unilateral vestibular lesions (46–48) and could explain the increased exploration observed in UVN rats.

Head Velocity

Interestingly, we found in rats that the mean head velocity recovered faster than the mean walking velocity (day 3 for the head and day 7 for the body velocity). When we looked at the maximum velocity, this recovery was even more obvious: the maximum head velocity was not altered the first days after the vestibular lesion, while maximum walking velocity was impaired and only recovered 10 days after UVN. According to our data, rats, unlike humans, are able to maintain high head velocities during the first few days after UVN while the vestibular syndrome is at its peak. In humans, unlike in rats, the eye has a fovea. A shift of the image onto the fovea is a source of visual discomfort known as oscillopsia. Vestibular patients tend to hold their head still in order to maintain the stability of the visual scene and therefore strongly decrease the speed of head movements in order to avoid this discomfort (49). This behavior is supported by the inability of humans to maintain equilibrium with unstable vision. For head velocities $>100°$/s, ocular fixation is no longer sufficient to stabilize the image and the VOR takes over. However, unilateral vestibular impairment systematically leads to an alteration of the VOR, causing oscillopsia and thus, instability of the visual scene. Living animals without fovea, such as rats (50), also have the ability to fix and stabilize the eye and have far fewer saccades of the eye than humans. It can be assumed that they are also much less disturbed by image shifts on the retina and thus at oscillopsia. Thus, in the rat, it is not the visual syndrome that is predominant but the posturo-locomotor syndrome. In the rat, retinal slip is not very problematic, and rats can mobilize the head sooner than the body. This behavior obviously requires the implementation of more complex substitution strategies because of the necessity to stabilize its center of gravity as well. We assume that the priority for the animal is first to stabilize its head (and therefore its velocity) before stabilizing its body locomotion. Indeed, when walking in the open field, turns are anticipated by directing the gaze and tilting the head relative to the headings. Eventually, the trunk follows the direction of the head movement (51).

We noticed that the mean head velocity increased between the 3rd and 7th day after UVN, a delay directly linked with the emergence of cephalic nystagmus or "bobbing" (**Video 1**). Bobbing in rodents with vestibular deficits refers to rapid and abnormal intermittent head and neck sweeping (movements). This is the first time that we automatically quantified this specific bobbing behavior along with the head velocity. During the video analysis of the rat in the open field, we noticed that the head velocity during bobbing was always >100 cm/s. Bobbing in humans is not observed or is poorly documented, but head oscillations are increased after UVN in patients (35). We suggest that bobbing is the result of vestibulo-nucal control asymmetry resulting from vestibulo-colic reflex impairment induced by UVN. Indeed, the axons of the medial vestibulospinal tract that target the motoneurons of the cervical spinal cord contribute to head stabilization (13, 16).

Acceleration

The head and body accelerations of a rat during free locomotion were quantified for the first time in an automated manner. This measurement is important because it is done under "ecological conditions," i.e., in spontaneous and not imposed conditions. It is important to remember that the otolith organs, the utricle and saccule, detect linear acceleration and not velocity. We showed that acceleration in UVN rats mimics the kinetics observed for velocity. The kinetics of the acceleration parameters differ depending on whether we are dealing with the head or body segment. The number of high body accelerations (above 50 cm/s^2) recovers more slowly the first 3 days post-UVN than that of low accelerations (below 50 cm/s^2). For the velocity, the number of high and low head accelerations recovers differently than the body accelerations. These data are correlated with the displacement profile of UVN rats: if the rats move less during the acute phase of the syndrome (day 1 to day 3 post-UVN), this reduces the number of high and low body accelerations. Furthermore, increases in mean head velocity from day 7 to day 30 related to bobbing behavior are also correlated with an increased number of high head accelerations but not low accelerations at the same postlesional delay. Interestingly, we showed almost a complete disappearance of high accelerations of the body in the first post-lesion days with just a slight increase at day 3 (only 11 high accelerations on day 3 on average compared to 88 in the control condition). This result suggests that it is too difficult for a moving animal to accelerate above 50 cm/s^2 after the induction of vestibular lesion.

By averaging only the positive accelerations (and thus suppressing decelerations or negative accelerations), we can follow the kinetics of the mean positive acceleration of UVN rats during vestibular compensation. We found that the rats had a mean acceleration of 50 cm/s^2 when they moved freely before vestibular lesions. For the mean body velocity, the mean acceleration of the UVN rats was reduced until day 7 and then increased above the baseline level after day 7. We also noticed a more important variability from day 7 to day 30 for the mean acceleration and the frequencies of high body accelerations. Since the variation in these parameters was weak before the injury, we can assume that the increase in variability once the animal compensated for the vestibular loss was due to a deficit in acceleration detection. The contralesional utricle and saccule may not be sufficient to properly detect accelerations, resulting in fluctuating accelerations during animal movements. One of the first studies on the perception of linear acceleration in humans reported that thresholds for the detection of linear acceleration in bilateral vestibular loss subjects were nearly 10 times higher than those in control subjects (52). Conversely, Gianna et al. (53) found that the detection of whole-body acceleration in patients with bilateral vestibular loss overlapped with the results from control subjects, but they found high inter-subject variability. On the other hand, the perception of linear acceleration in unilateral

labyrinthectomized patients varies according to the orientation of the head (54). The sensitivity of the patient was reduced only when the patient lay with the damaged side downwards.

Circling and Rotations

First, it is important to differentiate between a specific circling behavior observed after a unilateral vestibular deficit and rotations performed by the animal. The circling behavior induced by a unilateral vestibular deficit is defined when the animal runs in one direction in a circular pattern that occasionally becomes violent (**Video 2**). Usually, animals with a unilateral vestibular lesion run with a circling behavior in the ipsilesional direction. The term "run" is important here because the circling behavior is faster than a typical rotation performed by the animal (i.e., body axis rotation, **Video 3**), for example, when he is in a corner and wants to turn back. There is a limit to detecting the rotation of an animal around its own axis when using an automatic system. Some of the rotations detected with Ethovision^{TM} were just rotations made for exploring the environment, while other rotations were linked to the circling behavior caused by the UVN. Therefore, we detected an increase in body axis rotations on the contralesional side (clockwise direction) at day 2 and day 3 for 3 rats, while circling behaviors on the contralesional side of a unilateral vestibular lesion were never observed. Another limitation in the observations of circling behaviors is the influence of the size of the environment in which the animal is analyzed. We noticed that the rats did not exhibit circling behaviors during the first 3 days after UVN in an open field of 80 × 80 cm but did demonstrate circling behaviors in their home cages or in a device of 25 × 25 cm (55). The size of the environment required to observe circling behaviors is therefore important to note for future experiments and discussion of the results.

We demonstrated that rats increased the number of body axis rotations on the ipsilesional side from day 7 to day 30 in correlation with an increase in the number of arena rotations in the same direction. While some body axis rotations detected with video tracking came from rats exhibiting circling behaviors subsequent to UVN, the arena rotations can be interpreted as a bias in the exploratory behavior of the UVN rats. Rats prefer to explore their environment by rotating ipsilaterally to their lesion rather than in the opposite direction. This preferred sense of ipsilesional exploration can be explained by the UVN inducing an asymmetry of muscle tone (56), an increase in weight applied to the ipsilesional paw (55), an ipsilesional shift of their environment on the retina (57), or an ipsilesional path deviation (36). Another possibility comes from a model of vestibular compensation in lampreys (58). The opposite and symmetrical activity of both the left and right groups of reticulospinal neurons allow the lamprey to swim straight. Reticulospinal neurons in the lamprey receive vestibular input from the contralateral side and project to the spinal cord. Thus, unilateral loss of vestibular input causes inactivation of reticulospinal neurons on the contralateral side. This inactivation impairs the symmetrical activity of the left and right groups of reticulospinal neurons and provokes ipsilesional rotation of the lamprey (58).

There is evidence that Parkinson's disease is associated with dysfunction of the vestibular system [for review see Smith (59)]. Eugène et al. (60) studied circling behaviors in vestibular deficient KCNE1 mutant mice and reported that they were associated with increased tyrosine hydroxylase expression—a marker for DA synthesis—in the striatum ipsilateral to the direction of circling. In a model of Parkinson's disease, the lack of dopamine on the injured side leads to rotations by the animal to the ipsilateral side to the lesion. Evidence from animal studies strongly suggests that vestibular input is transmitted to the basal ganglia and to the striatum in particular (59). Thus, circling behaviors could be the result of a striatal electrophysiological imbalance resulting from the electrophysiological imbalance observed in the vestibular nuclei after unilateral vestibular loss. At the behavioral level, unilateral 6-hydroxydopamine lesions cause postural asymmetry (head torsion) and unilateral akinesia in rats. These behavioral disorders are perceptible when intrastriatal dopamine levels are reduced by at least 70% (61, 62). Head torsion and hypotonia are also observed in the UVN model.

The circling behaviors observed in the rodent model after unilateral vestibular loss are not reported in vestibular patients, but there is a deviation of the gait on the lesion side in humans with no full-circle walking. Indeed, the "star walk" or "blind walk" test requires the patient to close his or her eyes and take the same number of steps forward and backward in a straight line several times in a row. Since the deviation in the walk is always in the same direction (and is not corrected by sight since the patient keeps his or her eyes closed), the patient draws a star as he walks (63). When the injury is unilateral, the deviation of the gait is on the lesion side. A similar result can be obtained with the Fukuda test (64).

Body Tilt and Posture in UVN and Sham Rats

When we analyzed the mean body angle of the animals during the 10 min of video tracking, we noticed that the rats tilted their body on average by 4° on the contralesional side from day 7 and never compensated. X-ray radiography of the guinea pig was performed to investigate the vestibular control on posture of animals with selective lesions on the horizontal and anterior ampullary nerves, the utricular and saccular maculae, and the posterior semicircular canal ampulla (65). Four to seven hours after a unilateral lesion of the horizontal semicircular canal nerve, the authors also found head rotation and bending of the body toward the lesioned side. Interestingly, 3 of the 8 rats in our UVN group bent their body toward the lesioned side by an average of 14° 1 day after the lesion was induced. In our experiment, the mean body tilts were calculated while the rats moved around in the open field and explored their environment, while in Vidal's study, X-ray photographs were taken while the rats were still. Surprisingly, the authors did not notice postural changes with a unilateral anterior canal nerve lesion and proposed that anterior canal afferent information is distributed bilaterally to the spinal cord to describe their results. Unilateral otolith lesions sparing the semicircular canals induced a side tilt of the head-neck ensemble toward the side of the lesion but did not produce inclination

about the vertical axis of the body. It appears that cutting the entire vestibular nerve is necessary to induce long-term postural changes in animals.

Trunk orientation in humans after UVN varies if the subject's eyes are open or closed: the trunk deviates toward the operated side until day 90 in the eyes closed condition, and the posture reverses toward the intact side until day 30 in the eyes open condition (35). This postural reversal can be related to modifications in reference frames that the patients base themselves on (66). Since the vertical visual reference of the patient is perceived as tilted toward the intact side, the trunk deviation in the same direction may result from an alignment of the patient's body with respect to the vertical visual reference they perceive.

To explain the inclination of the body on the contralesional side in our UVN rats, we proposed, as in humans, that the inclination of the rat's body on the contralesional side can be related to a subjective vertical deviation of the rat to the operated side. Thus, an inclination of the body on the contralesional side would compensate for the visual vertical reference they perceive. The increase in weight applied on the ipsilateral paws following the lesion from day 7 to day 30 (55) may also be correlated with the inclination of the body on the contralateral side from day 7 to day 30 observed in this study.

Acute Phase and Compensated Phase of Posturo-Locomotor Symptoms in UVN Rats

The meander, % of time that the animal was immobile or not moving, number of contralesional body axis and arena rotations, mean head and body velocities, maximum body velocity and number of low head accelerations were impaired during the first week after unilateral vestibular lesion and then compensated (i.e., returned to baseline level). However, the distance moved, % of time that the animal was mobile or highly mobile, number of body axis and arena rotations toward the ipsilesional side, mean and maximum head velocity, mean body velocity, bobbing frequencies, number of high head, and body accelerations, number of low body accelerations, mean positive accelerations and mean body torsion on the contralesional side never returned to baseline level. This clearly shows an acute phase (first week post-UVN) of the vestibular syndrome and a compensated phase (after the first week post-UVN) in which some parameters are fully compensated, and others are not. Data from the literature regarding vestibular compensation report that "static deficits (those present in the absence of body movement) fully compensate while dynamic deficits (those present when body is moving) remain poorly compensated" (1, 67). We show in the present study that this assumption is not a dogma since certain parameters, such as maximum body velocity, did not follow this observation. Indeed, the maximum body velocity, which is clearly observable when the body is moving, fully compensated. These original results concerning the kinetics of compensation for static and dynamic vestibular deficits could be due to the use of a fine and automated analysis device.

Permanent Vestibular Loss Leading to the Expression of an Overcompensated Posturo-Locomotor Phenotype: Neurophysiological Correlates

The restoration of activity in deafferented vestibular nuclei has been shown to contribute to the restoration of vestibular functions (9). Interestingly, the restoration of spontaneous activity in deafferented lateral vestibular nucleus was not complete 4 months after UVN in cats (68) but was completely restored in the same nucleus 1 week after unilateral labyrinthectomy in guinea pigs (69). The authors indicated that this discrepancy could be explained as a difference in species rather than in the nature of the vestibular deafferentation. Given the phylogenetic proximity, the rat could have kinetics of restoration of vestibular nuclei (VN) activity comparable to that of the guinea pig. At the behavioral level, several posturo-locomotor parameters, such as the velocity of the body and the head, return to baseline levels between 7 and 10 days after UVN, exceed their baseline level after this period and reach a plateau that is maintained until 1 month after UVN. This new behavioral profile can be considered a "post-locomotor overcompensated phenotype."

The return to electrophysiological homeostasis between the two homologous VN is a priority for vestibular functional recovery. It results from both intrinsic mechanisms expressed in deafferented vestibular nuclei and extrinsic mechanisms involving other central nervous system structures, such as a reweighting of other sensory modalities, with an increase in visual, tactile, or proprioceptive weight (70–75). The return to electrophysiological balance in the VN does not reflect the compensation of posturo-locomotor parameters since they significantly exceed their baseline level. These data indicate that in addition to the restoration of spontaneous activity, other mechanisms could explain this "overcompensated behavioral phenotype." The nature of the evoked activity of the deafferented vestibular nuclei could be implicated. In fact, an increase in the sensitivity of neurons in the VN to dynamic stimuli could explain this overcompensated behavioral phenotype. A change in the sensitivity of neuronal responses to bidirectional rotations has been observed in the vestibular nuclei in cats after unilateral labyrinthectomy (76). This indicates the emergence of a new electrophysiological expression of vestibular nuclei after vestibular loss, probably underlying this "overcompensated behavioral phenotype." The priority of this new electrophysiological profile within the deafferented vestibular environment is not to restore the vestibular function as it was before the injury but to allow the animal to find a "new" posturo-locomotor balance.

Clinical Relevance

Balance tests like tandem walking or walking with head turns are not useful for screening people for vestibular impairments but may be useful for assessing vestibular rehabilitation over time among patients with known diagnoses (24). Consistent to Cohen's study and based on our results, it can be assumed that the evaluation of both mean and maximum locomotor

velocity could be useful in assessing vestibular compensation in human clinical practice. In view of our results concerning the acceleration parameter, it would also be interesting to take this factor into account in vestibular deficient patients at different stages of the pathology, which could give us information on the level of compensation achieved by the patient. Like we said if vestibular patients do not run, it is because they consider that their condition probably does not allow them to; it is an avoidance strategy. By encouraging them during vestibular rehabilitation to accelerate and increase their locomotor velocity, it is possible that this psychological lock will disappear, and that patients will adapt to a faster walking and a more secure gait. The trajectory of the patient during his displacements can also be evaluated and be similar to what we measure with the "meander." A possible limitation is the difficulty to have baseline data from the patient prior to vestibular impairment.

CONCLUSION

The numerous cellular and molecular rearrangements that take place in the adult vestibular nuclei in the days following permanent unilateral vestibular loss suggest that the vestibular compensation phenomenon recruits plasticity mechanisms similar to those observed during the critical developmental period. Indeed, during a 1-week time window after UVN, there is a an increase in the level of BDNF, a strong cellular proliferation, a glial reaction, and a downregulation of KCC2 associated with an excitatory action of GABA (8, 77, 78). At the behavioral level, impairment and recovery of certain parameters is observed during the same critical 7-day period following UVN. This acute posturo-locomotor phenotype reminds us of the developmental strategies used for walk acquisition. Injury to the adult vestibular system induces a transient reactivation of developmental mechanisms at both the behavioral and cellular levels. This suggests that compensation for gait and postural balance in the vestibulo-lesioned rat is a form of sensorimotor relearning involving both interdependent cellular mechanisms and behavioral strategies.

DATA AVAILABILITY STATEMENT

The datasets generated for this study are available on request to the corresponding author.

ETHICS STATEMENT

The animal study was reviewed and approved by French Agriculture Ministry Authorization: B13-055-25 Approved by Neurosciences Ethic Committee N°71 from the French National Committee of animal experimentation.

AUTHOR CONTRIBUTIONS

GR and BT designed the experiment. GR, EM, NE, AB, ET-D, and DP programmed the experiment. GR, EM, NE, and AB recorded the data. GR and BT analyzed the data. GR, BT, CC, and OD drafted the manuscript. All authors reviewed the manuscript.

ACKNOWLEDGMENTS

We thank Elodie Mansour for taking care of the animals and Abdessadek El Ahmadi for expertise in statistical analysis.

SUPPLEMENTARY MATERIAL

The Supplementary Material for this article can be found online at: https://www.frontiersin.org/articles/10.3389/fneur.2020.00505/full#supplementary-material

REFERENCES

1. Lacour M, Helmchen C, Vidal PP. Vestibular compensation: the neuro-otologist's best friend. *J Neurol*. (2016) 263:54–64. doi: 10.1007/s00415-015-7903-4
2. Dutheil S, Lacour M, Tighilet B. Neurogenic potential of the vestibular nuclei and behavioural recovery time course in the adult cat are governed by the nature of the vestibular damage. *PLoS ONE*. (2011) 6:e22262. doi: 10.1371/journal.pone.0022262
3. Precht W, Shimazu H, Markham CH. A mechanism of central compensation of vestibular function following hemilabyrinthectomy. *J Neurophysiol*. (1966) 29:996–1010. doi: 10.1152/jn.1966.29.6.996
4. Darlington CL, Smith PF. Molecular mechanisms of recovery from vestibular damage in mammals: recent advances. *Prog Neurobiol*. (2000) 62:313–25. doi: 10.1016/S0301-0082(00)00002-2
5. Darlington CL, Dutia MB, Smith PF. The contribution of the intrinsic excitability of vestibular nucleus neurons to recovery from vestibular damage: recovery from vestibular damage: role of vestibular nucleus. *Eur J Neurosci*. (2002) 15:1719–27. doi: 10.1046/j.1460-9568.2002.02024.x
6. Dieringer N. "Vestibular compensation": neural plasticity and its relations to functional recovery after labyrinthine lesions in frogs and other vertebrates. *Prog Neurobiol*. (1995) 46:97–129. doi: 10.1016/0301-0082(94)00063-N
7. Dutia MB. Mechanisms of vestibular compensation: recent advances. *Curr opin Otolaryngol Head Neck. Surg*. (2010) 18:420–4. doi: 10.1097/MOO.0b013e32833de71f
8. Lacour M, Tighilet B. Plastic events in the vestibular nuclei during vestibular compensation: the brain orchestration of a "deafferentation" code. *Restor Neurol Neurosci*. (2010) 28:19–35. doi: 10.3233/RNN-2010-0509
9. Smith PF, Curthoys IS. Mechanisms of recovery following unilateral labyrinthectomy: a review. *Brain Res Rev*. (1989) 14:155–80. doi: 10.1016/0165-0173(89)90013-1
10. Smith PF, Darlington CL. Neurochemical mechanisms of recovery from peripheral vestibular lesions (vestibular compensation). *Brain Res Rev*. (1991) 16:117–33. doi: 10.1016/0165-0173(91)90001-O
11. Hain TC, Helminski JO. Chapter 1: Anatomy and physiology of the normal vestibular system. 3rd ed. In: Herdman SJ, Clendaniel RA, editors. *Vestibular Rehabilitation*. Philadelphia, PA: F.A. Davis Company (2007). p. 2–18.
12. Vidal PP, Cullen K, Curthoys IS, Du Lac S, Holstein G, Idoux E, et al. The vestibular system. In: Paxinos G, editor. *The Rat Nervous System*. London: Elsevier (2015). p. 805–64. doi: 10.1016/B978-0-12-374245-2.00028-0
13. Wilson VJ, Maeda M. Connections between semicircular canals and neck motorneurons in the cat. *J Neurophysiol*. (1974) 37:346–57. doi: 10.1152/jn.1974.37.2.346
14. Wilson VJ, Yoshida M. Comparison of effects of stimulation of deiters' nucleus and medial longitudinal fasciculus on neck, forelimb, and hindlimb

motoneurons. *J Neurophysiol*. (1969) 32:743–58. doi: 10.1152/jn.1969.32.5.743
15. MacKinnon CD. Sensorimotor anatomy of gait, balance, and falls. In: *Handbook of Clinical Neurology*. Elsevier (2018). p. 3–26.
16. McCall AA, Miller DM, Yates BJ. Descending influences on vestibulospinal and vestibulosympathetic reflexes. *Front Neurol.* (2017) 8:112. doi: 10.3389/fneur.2017.00112
17. Mihailoff GA, Haines DE (editors). Chapter 24: Motor system I: peripheral sensory, brainstem, and spinal influence on anterior horn neurons. In: *Fundamental Neuroscience for Basic and Clinical Applications*. Philadelphia, PA: Elsevier (2018). p. 346–59. doi: 10.1016/B978-0-323-39632-5.00024-4
18. Navari E, Cerchiai N, Casani AP. Assessment of vestibulo-ocular reflex gain and catch-up saccades during vestibular rehabilitation. *Otol Neurotol.* (2018) 39:E1111–7. doi: 10.1097/MAO.0000000000002032
19. Deveze A, Bernard-Demanze L, Xavier F, Lavieille J-P, Elziere M. Vestibular compensation and vestibular rehabilitation. Current concepts and new trends. *Neurophysiol Clin.* (2014) 44:49–57. doi: 10.1016/j.neucli.2013.10.138
20. Devèze A, Montava M, Lopez C, Lacour M, Magnan J, Borel L. Vestibular compensation following vestibular neurotomy. *Eur Ann Otorhinolaryngol Head Neck Dis*. (2015) 132:197–203. doi: 10.1016/j.anorl.2015.04.003
21. Visser JE, Carpenter MG, van der Kooij H, Bloem BR. The clinical utility of posturography. *Clin Neurophysiol.* (2008) 119:2424–36. doi: 10.1016/j.clinph.2008.07.220
22. Cohen HS. A review on screening tests for vestibular disorders. *J Neurophysiol*. (2019) 122:81–92. doi: 10.1152/jn.00819.2018
23. Allum JHJ, Scheltinga A, Honegger F. The effect of peripheral vestibular recovery on improvements in vestibulo-ocular reflexes and balance control after acute unilateral peripheral vestibular loss. *Otol Neurotol*. (2017) 38:E531–8. doi: 10.1097/MAO.0000000000001477
24. Cohen HS, Mulavara AP, Peters BT, Sangi-Haghpeykar H, Bloomberg JJ. Tests of walking balance for screening vestibular disorders. *J Vestib Res*. (2012) 22:95–104. doi: 10.3233/VES-2012-0443
25. Cohen HS, Stitz J, Sangi-Haghpeykar H, Williams SP, Mulavara AP, Peters BT, et al. Tandem walking as a quick screening test for vestibular disorders: tandem walking for vestibular screening. *Laryngoscope*. (2018) 128:1687–91. doi: 10.1002/lary.27022
26. Tramontano M, Bergamini E, Iosa M, Belluscio V, Vannozzi G, Morone G. Vestibular rehabilitation training in patients with subacute stroke: a preliminary randomized controlled trial. *NeuroRehabilitation*. (2018) 43:247–54. doi: 10.3233/NRE-182427
27. Chen ZP, Zhang XY, Peng SY, Yang ZQ, Wang YB, Zhang YX, et al. Histamine H1 receptor contributes to vestibular compensation. *J Neurosci*. (2019) 39:1350–18. doi: 10.1523/JNEUROSCI.1350-18.2018
28. Ito J, Nakajima K, Mori S. Postnatal changes in locomotor movements after labyrinthectomy in rats. *Neurosci Res*. (1998) 32:343–7. doi: 10.1016/S0168-0102(98)00101-1
29. Lindner M, Gosewisch A, Eilles E, Branner C, Krämer A, Oos R, et al. Ginkgo biloba extract EGb 761 improves vestibular compensation and modulates cerebral vestibular networks in the rat. *Front Neurol*. (2019) 10:147. doi: 10.3389/fneur.2019.00147
30. Péricat D, Farina A, Agavnian-Couquiaud E, Chabbert C, Tighilet B. Complete and irreversible unilateral vestibular loss: a novel rat model of vestibular pathology. *J Neurosci Methods*. (2017) 283:83–91. doi: 10.1016/j.jneumeth.2017.04.001
31. McCall AA, Miller DM, DeMayo WM, Bourdages GH, Yates BJ. Vestibular nucleus neurons respond to hindlimb movement in the conscious cat. *J Neurophysiol*. (2016) 116:1785–94. doi: 10.1152/jn.00414.2016
32. Niklasson M, Tham R, Larsby B, Eriksson B. The influence of visual and somatosensory input on the vestibulo-oculomotor reflex of pigmented rats. *J Vestib Res*. (1990) 1:251–62.
33. Witts EC, Murray AJ. Vestibulospinal contributions to mammalian locomotion. *Curr Opin Physiol.* (2019) 8:56–62. doi: 10.1016/j.cophys.2018.12.010
34. Orlovsky GN. Activity of vestibulospinal neurons during locomotion. *Brain Res*. (1972) 46:85–98. doi: 10.1016/0006-8993(72)90007-8
35. Borel L, Harlay F, Magnan J, Chays A, Lacour M. Deficits and recovery of head and trunk orientation and stabilization after unilateral vestibular loss. *Brain*. (2002) 125:880–94. doi: 10.1093/brain/awf085
36. Borel L, Harlay F, Lopez C, Magnan J, Chays A, Lacour M. Walking performance of vestibular-defective patients before and after unilateral vestibular neurotomy. *Behav Brain Res*. (2004) 150:191–200. doi: 10.1016/S0166-4328(03)00257-2
37. Brandt T, Strupp M, Benson J. You are better off running than walking with acute vestibulopathy. *Lancet*. (1999) 354:746. doi: 10.1016/S0140-6736(99)03179-7
38. Buchanan JJ, Horak FB. Vestibular loss disrupts control of head and trunk on a sinusoidally moving platform. *J Vestib Res*. (2001) 11:371–89.
39. Cohen HS, Sangi-Haghpeykar H. Walking speed and vestibular disorders in a path integration task. *Gait Posture*. (2011) 33:211–3. doi: 10.1016/j.gaitpost.2010.11.007
40. Mamoto Y, Yamamoto K, Imai T, Tamura M, Kubo T. Three-dimensional analysis of human locomotion in normal subjects and patients with vestibular deficiency. *Acta Otolaryngol*. (2002) 122:495–500. doi: 10.1080/00016480260092282
41. Dietrich H, Heidger F, Schniepp R, MacNeilage PR, Glasauer S, Wuehr M. Head motion predictability explains activity-dependent suppression of vestibular balance control. *Sci Rep*. (2020) 10:668. doi: 10.1038/s41598-019-57400-z
42. Dietrich H, Wuehr M. Strategies for gaze stabilization critically depend on locomotor speed. *Neuroscience*. (2019) 408:418–29. doi: 10.1016/j.neuroscience.2019.01.025
43. Fabre-Adinolfi D, Parietti-Winkler C, Pierret J, Lassalle-Kinic B, Frère J. You are better off running than walking revisited: does an acute vestibular imbalance affect muscle synergies?. *Hum Mov Sci*. (2018) 62:150–60. doi: 10.1016/j.humov.2018.10.010
44. Jahn K, Strupp M, Schneider E, Dieterich M, Brandt T. Differential effects of vestibular stimulation on walking and running: *Neuroreport*. (2000) 11:1745–8. doi: 10.1097/00001756-200006050-00029
45. MacNeilage PR, Glasauer S. Quantification of head movement predictability and implications for suppression of vestibular input during locomotion. *Front Comput Neurosci*. (2017) 11:47. doi: 10.3389/fncom.2017.00047
46. Jacob P-Y, Poucet B, Liberge M, Save E, Sargolini F. Vestibular control of entorhinal cortex activity in spatial navigation. *Front Integr Neurosci*. (2014) 8:38. doi: 10.3389/fnint.2014.00038
47. Péruch P, Borel L, Gaunet F, Thinus-Blanc G, Magnan J, Lacour M. Spatial performance of unilateral vestibular defective patients in nonvisual versus visual navigation. *J Vestib Res*. (1999) 9:37–47.
48. Zheng Y, Darlington CL, Smith PF. Impairment and recovery on a food foraging task following unilateral vestibular deafferentation in rats. *Hippocampus*. (2006) 16:368–78. doi: 10.1002/hipo.20149
49. Renga V. Clinical evaluation of patients with vestibular dysfunction. *Neurol Res Int.* (2019) 2019:3931548. doi: 10.1155/2019/3931548
50. Meier PM, Reinagel P. Rats and humans differ in processing collinear visual features. *Front Neural Circuits*. (2013) 7:197. doi: 10.3389/fncir.2013.00197
51. Imai T, Moore ST, Raphan T, Cohen B. Interaction of the body, head, and eyes during walking and turning. *Exp Brain Res.* (2001) 136:1–18. doi: 10.1007/s002210000533
52. Walsh EG. Role of the vestibular apparatus in the perception of motion on a parallel swing. *J Physiol.* (1961) 155:506–13. doi: 10.1113/jphysiol.1961.sp006643
53. Gianna C, Heimbrand S, Gresty M. Thresholds for detection of motion direction during passive lateral whole-body acceleration in normal subjects and patients with bilateral loss of labyrinthine function. *Brain Res Bull*. (1996) 40:443–7. doi: 10.1016/0361-9230(96)00140-2
54. Walsh EG. Perception of linear motion following unilateral labyrinthectomy: variation of threshold according to the orientation of the head. *J Physiol.* (1960) 153:350–7. doi: 10.1113/jphysiol.1960.sp006538
55. Tighilet B, Péricat D, Frelat A, Cazals Y, Rastoldo G, Boyer F, et al. Adjustment of the dynamic weight distribution as a sensitive parameter for diagnosis of postural alteration in a rodent model of vestibular deficit. *PLoS ONE*. (2017) 12:e0187472. doi: 10.1371/journal.pone.0187472
56. Zennou-Azogui Y, Borel L, Lacour M, Ez-Zaher L, Ouaknine M. Recovery of head postural control following unilateral vestibular neurectomy in the

cat: neck muscle activity and neuronal correlates in deiters' nuclei. *Acta Otolaryngol*. (1993) 113:5–19. doi: 10.3109/00016489309130556
57. Halmagyi GM, Curthoys IS, Cremer PD, Henderson CJ, Todd MJ, Staples MJ, et al. The human horizontal vestibulo-ocular reflex in response to high-acceleration stimulation before and after unilateral vestibular neurectomy. *Exp Brain Res.* (1990) 81:479–90. doi: 10.1007/BF02423496
58. Pavlova EL. Vestibular compensation in lampreys: restoration of symmetry in reticulospinal commands. *J Exp Biol.* (2004) 207:4595–603. doi: 10.1242/jeb.6247
59. Smith PF. Vestibular functions and parkinson's disease. *Front Neurol.* (2018) 9:1085. doi: 10.3389/fneur.2018.01085
60. Eugène D, Deforges S, Vibert N, Vidal P-P. Vestibular critical period, maturation of central vestibular neurons, and locomotor control. *Ann NY Acad Sci*. (2009) 1164:180–7. doi: 10.1111/j.1749-6632.2008.03727.x
61. Hefti F, Melamed E, Sahakian BJ, Wurtman RJ. Circling behavior in rats with partial, unilateral nigro-striatal lesions: effect of amphetamine, apomorphine, and DOPA. *Pharmacol Biochem Behav.* (1980) 12:185–8. doi: 10.1016/0091-3057(80)90353-6
62. Zigmond MJ, Strlcker EM. Current topics T. Parkinson's disease studies with an animal model. *Life Sci*. (1984) 35:5–18. doi: 10.1016/0024-3205(84)90147-4
63. Nyabenda A, Briart C, Deggouj N, Gersdorff M. A normative study of the vestibulospinal and rotational tests. *Adv Physiother*. (2004) 6:122–9. doi: 10.1080/14038190310012052
64. Cohen HS, Sangi-Haghpeykar H, Ricci NA, Kampangkaew J, Williamson RA. Utility of stepping, walking, and head impulses for screening patients for vestibular impairments. *Otolaryngol Head Neck Surg.* (2014) 151:131–6. doi: 10.1177/0194599814527724
65. Vidal PP, Wang DH, Graf W, de Waele C. Chapter 22: Vestibular control of skeletal geometry in the guinea pig: a problem of good trim? In: Allum JHJ, Allum-Mecklenburg DJ, Harris FP, Probst R, editors. *Progress in Brain Research*. Amsterdam; London; New York, NY; Tokyo: Elsevier (1993). p. 229–43. doi: 10.1016/S0079-6123(08)62282-7
66. Borel L, Lopez C, Péruch P, Lacour M. Vestibular syndrome: a change in internal spatial representation. *Neurophysiol Clin.* (2008) 38:375–89. doi: 10.1016/j.neucli.2008.09.002
67. Tighilet B, Chabbert C. Adult neurogenesis promotes balance recovery after vestibular loss. *Prog Neurobiol.* (2019) 174:28–35. doi: 10.1016/j.pneurobio.2019.01.001
68. Xerri C, Gianni S, Manzoni D, Pompeiano O. Central compensation of vestibular deficits. I response characteristics of lateral vestibular neurons to roll tilt after ipsilateral labyrinth deafferentation. *J Neurophysiol.* (1983) 50:428–48. doi: 10.1152/jn.1983.50.2.428
69. Ris L, de Waele C, Serafin M, Vidal PP, Godaux E. Neuronal activity in the ipsilateral vestibular nucleus following unilateral labyrinthectomy in the alert guinea pig. *J Neurophysiol*. (1995) 74:2087–99. doi: 10.1152/jn.1995.74.5.2087
70. Deliagina T. Vestibular compensation in lampreys: impairment and recovery of equilibrium control during locomotion. *J Exp Biol*. (1997) 200:1459–71.
71. Igarashi M, Alford BR, Watanabe T, Maxian PM. Role of neck proprioceptors for the maintenance of dynamic bodily equilbrium in the squirrel monkey. *Laryngoscope*. (1969) 79:1713–27. doi: 10.1288/00005537-196910000-00003
72. Lacour M, Barthelemy J, Borel L, Magnan J, Xerri C, Chays A, et al. Sensory strategies in human postural control before and after unilateral vestibular neurotomy. *Exp Brain Res.* (1997) 115:300–10. doi: 10.1007/PL00005698
73. Medendorp WP, Alberts BBGT, Verhagen WIM, Koppen M, Selen LPJ. Psychophysical evaluation of sensory reweighting in bilateral vestibulopathy. *Front Neurol.* (2018) 9:377. doi: 10.3389/fneur.2018.00377
74. Thompson LA, Haburcakova C, Goodworth AD, Lewis RF. An engineering model to test for sensory reweighting: nonhuman primates serve as a model for human postural control and vestibular dysfunction. *J Biomech Eng*. (2018) 140:011008. doi: 10.1115/1.4038157
75. Tjernström F, Fransson P-A, Kahlon B, Karlberg M, Lindberg S, Siesjö P, et al. Different visual weighting due to fast or slow vestibular deafferentation: before and after schwannoma surgery. *Neural Plast*. (2019) 2019:1–11. doi: 10.1155/2019/4826238
76. Chan YS, Shum DKY, Lai CH. Neuronal response sensitivity to bidirectional off-vertical axis rotations: a dimension of imbalance in the bilateral vestibular nuclei of cats after unilateral labyrinthectomy. *Neuroscience*. (1999) 94:831–43. doi: 10.1016/S0306-4522(99)00374-7
77. Dutheil S, Watabe I, Sadlaoud K, Tonetto A, Tighilet B. BDNF signaling promotes vestibular compensation by increasing neurogenesis and remodeling the expression of potassium-chloride cotransporter KCC2 and GABAA receptor in the vestibular nuclei. *J Neurosci.* (2016) 36:6199–212. doi: 10.1523/JNEUROSCI.0945-16.2016
78. Tighilet B, Brezun JM, Dit Duflo Sylvie G, Gaubert C, Lacour M. New neurons in the vestibular nuclei complex after unilateral vestibular neurectomy in the adult cat: reactive neurogenesis in adult vestibular lesioned cats. *Eur J Neurosci.* (2007) 25:47–58. doi: 10.1111/j.1460-9568.2006.05267.x

Conflict of Interest: The authors declare that the research was conducted in the absence of any commercial or financial relationships that could be construed as a potential conflict of interest.

frontiers in Neurology

ORIGINAL RESEARCH
published: 11 September 2020
doi: 10.3389/fneur.2020.00997

From Acute to Chronic Tinnitus: Pilot Data on Predictors and Progression

Veronika Vielsmeier[1], Ryan Santiago Stiel[2], Pingling Kwok[1], Berthold Langguth[3] and Martin Schecklmann[3]*

[1] Department of Otorhinolaryngology, University of Regensburg, Regensburg, Germany, [2] Department of Otorhinolaryngology, Klinikum St. Elisabeth Straubing GmbH, Straubing, Germany, [3] Department of Psychiatry and Psychotherapy, University of Regensburg, Regensburg, Germany

Little is known about the transition from acute tinnitus to chronic tinnitus. By means of this study, we are attempting to close this gap by presenting prospective pilot data of patients with acute tinnitus, followed by tracking their condition's trajectory over a period of 6 months. Forty-nine patients presenting with acute tinnitus (duration < 28 days) were recruited in two clinics. We recorded demographic and clinical tinnitus-related data as well as data on personality, health, treatments, and life-style, during patients' first appearance in the clinic and again three and 6 months thereafter. Standard audiograms were performed at the first and the second visit. Nine (18.4%) patients showed full remission of their tinnitus. These patients differed from patients with a chronic course of tinnitus by shorter tinnitus duration, lower fear-related hyperacusis, higher proportion of female gender, increased ear pressure, and lower levels of alcohol consumption. Among the patients with a chronification of tinnitus, there was no change in tinnitus characteristics. However, their tinnitus distress improved moderately over time. These preliminary data are in line with earlier studies that have shown that only a small proportion of those patients presenting in the clinic with acute tinnitus experience a full remission. The results of this study can be of service in deducing hypotheses for the transition from acute to chronic tinnitus and in developing designs for interventional studies.

Keywords: acute tinnitus, chronic tinnitus, questionnaire, causes for progression, predictors

OPEN ACCESS

Edited by:
Jose Antonio Lopez-Escamez, Andalusian Autonomous Government of Genomics and Oncological Research (GENYO), Spain

Reviewed by:
Yu-Chen Chen, Nanjing Medical University, China
Alessandra Fioretti, European Hospital, Italy

****Correspondence:***
Veronika Vielsmeier
veronika.vielsmeier@ukr.de

Specialty section:
This article was submitted to Neuro-Otology, a section of the journal Frontiers in Neurology

Received: *04 June 2020*
Accepted: *29 July 2020*
Published: *11 September 2020*

Citation:
Vielsmeier V, Santiago Stiel R, Kwok P, Langguth B and Schecklmann M (2020) From Acute to Chronic Tinnitus: Pilot Data on Predictors and Progression. Front. Neurol. 11:997. doi: 10.3389/fneur.2020.00997

INTRODUCTION

Subjective chronic tinnitus has a high prevalence, affecting 10–15% of adults worldwide (1, 2), and is responsible for high costs for health care systems (3). Research on chronic tinnitus has been growing during the last decade.

Several hypotheses about risk factors for developing chronic or decompensated tinnitus exist. Hearing impairment can be found in almost all patients with chronic tinnitus (4, 5). However, not every patient with hearing difficulty has tinnitus, meaning that hearing impairment may be a required but not sufficient risk factor. For example, Muhlmeier et al. published a study including 113 patients with acute idiopathic sudden sensorineural hearing loss. Here, tinnitus loudness decreased rapidly in cases of mild-moderate hearing loss and tinnitus had completely resolved in two-thirds of the patients after 3 months. In contrast, when tinnitus is associated with severe-profound hearing loss, it improved significantly less (6). Also, temporomandibular joint or neck pathologies are discussed as moderators for tinnitus (7).

Additional comorbidities such as depression (8), anxiety (8), hyperacusis (9), and personality traits such as neuroticism (10), are discussed as determining factors for the development of decompensated tinnitus, resulting in patients seeking for help. Anxiety disorders in tinnitus patients seem to be associated with more psychosocial stress (11). Other studies could show that low resilience is associated with low emotional health and distressing tinnitus (12). D'Amelio et al. described a high correlation between the degree of depression on one side and the dysfunctional coping with stress and emotional distress caused by tinnitus on the other side, frequently present in acute tinnitus cases (13).

Most findings on risk factors for chronic or decompensated tinnitus are based on cross-sectional and retrospective datasets or specific populations. Up to now, prospective and longitudinal studies are sparse. Overall, the transition and progression from acute to chronic tinnitus has not been sufficiently addressed.

We were only able to identify two studies investigating the course of acute tinnitus. One study followed the trajectory of tinnitus over 6 months (14). There, 10 out of 44 patients showed full recovery. Tinnitus-attributed sleep disturbance, anxiety, and life satisfaction, each assessed at first investigation, independently predicted tinnitus distress at the second assessment 6 months later in patients with a chronic course of tinnitus. These three variables together predicted 56% of the variance of tinnitus distress at the time of the second assessment. This is in accordance with a follow-up study of patients with tinnitus after 2 years, showing that severe tinnitus suffering was associated with a higher likelihood of anxiety disorders, more psychosocial stress and lower global assessment of function scores (11).

The second observational study on the development of acute tinnitus over time showed that almost 90% of participants developed chronic tinnitus, only five out of 41 patients showed complete remission after 6 months (15). Aspects of mental health like level of depression and anxiety at the beginning of tinnitus seem to be predicting a higher level of tinnitus decompensation after 6 months (15).

The prevalence data of these two prospective studies are in contrast to a retrospective study by Forti et al. of 269 patients who were treated with Tinnitus Retraining Therapy and sound generators, 26% did not use the sound generator in a mean time of 49 (+-16,89) months of follow-up, because their tinnitus apparently was no longer a problem (16).

In sum, data on the progression of acute tinnitus are limited, and the focus seems to be on the prediction of tinnitus worsening and not on predictors for tinnitus remission; or studies are based on a specific sub-group of patients with sudden hearing loss. Thus, we performed a two-center observational survey to evaluate possible predictors for tinnitus remission and investigate the transition from acute to chronic tinnitus during a time interval of 6 months after onset.

MATERIALS AND METHODS

We included 50 patients presenting in either one of two clinics of Otorhinolaryngology in Eastern Bavaria (Regensburg, Straubing), beginning from October 2013, with a duration of acute tinnitus of up to 28 days. For this work, acute tinnitus was defined by a tinnitus duration below 28 days, with the intention of investigating the transition from acute to chronic tinnitus. There is heterogeneity of definition of acute (<3 months), subacute (<6 months), and chronic tinnitus (>6 months but also >3 months) in the literature (15, 17). However, as we were interested in the transition from one stage to the other, we restricted our inclusion criteria to the very acute duration of tinnitus and decided to conduct the follow-up visits 3 and 6 months after the first consultation.

All patients gave written informed consent to the study which was approved by the ethics committee of the University of Regensburg (13-101-0160).

All patients presented twice in the hospital—for the first consultation and a first follow-up 3 months thereafter. The first contact took place in emergency settings. Three months after the second visit, patients received questionnaires by mail. We recorded different categories of data (i.e., demographic, tinnitus-related, audiology, psychopathological, health-related, treatment and life-style data). Most of the data were ratings or subjective reported variables. Audiology was recorded by the investigator team (pure tone audiogram; frequencies 125 Hz, 250 Hz, 500 Hz, 1 kHz, 2 kHz, 3 kHz, 4 kHz, 6 kHz, and 8 kHz). Standardized ratings included the Tinnitus Sample Case History Questionnaire (18) for tinnitus characteristics, numeric ratings scales for different aspects of tinnitus (19), the Mini Tinnitus Questionnaire (20) for measurement of tinnitus distress, the Big-Five-Inventory-10 (21) for measurement of five personality traits, the Life Orientation Test (LOT-R) (22) for measurement of optimism and pessimism, and the Generalized Anxiety Disorder 7 (GAD-7) of the Patient Health Questionnaire (PHQ) (23).

For group comparisons of categorial variables we used chi-square tests of independence, and of metric variables Student *t*-tests. Longitudinal analyses were done with Student *t*-test for dependent samples or, in the case of three observations, with analyses of variance with the within-subjects factor time. Significance threshold was set to 5%. Analyses were done with SPSS 24 (IBM SPSS Statistics).

RESULTS

Sample Description

Fifty patients presented from October 2013 to December 2016 with a tinnitus onset of up to 28 days. Due to a high number of missing values, one patient had to be excluded from the study. The analysis sample consisted of 49 patients presenting in either one of two clinics for Otorhinolaryngology in Eastern Bavaria (Regensburg: $n = 14$; Straubing: $n = 35$). The recruitment time interval was from October 2013 to December 2016.

Demographics

Twenty-one out of these 49 patients were females. Mean age was 46 ± 14 years (range: 21–81 years). Seventeen reported A-levels or equivalently high education. Thirty-one were married, seven with and 11 without partnership. Mean height was 1.73 ± 0.76 m and mean weight was 79 ± 14 kg. The mean number of alcoholic

drinks per week was 2.8 ± 3.6. Eight patients reported regular smoking. Mean hearing (dB HL) loss was 27 ± 29 on the right and 24 ± 22 on the left side.

Tinnitus Characteristics

Tinnitus duration was 8.5 ± 5.3 days (range: 1–25 days), tinnitus loudness was 44 ± 25, tinnitus awareness 61 ± 31, and tinnitus annoyance 54 ± 34 (all three variables with a scale from 0 to 100). Numeric ratings showed values for severity of 3.2 ± 1.1 (on a scale from 0 to 5). Numeric ratings with a scale from 0 to 10 showed 4.3 ± 2.7 for loudness, 5.1 ± 3.0 for discomfort, 5.3 ± 3.2 for annoyance, 5.5 ± 3.4 for ignorability, and 5.2 ± 3.1 for unpleasantness. The Mini Tinnitus Questionnaire showed a mean value of 11.6 ± 6.5 (range 0–23) indicating moderate distress in average. Eighteen (37%) patients reported tinnitus in relatives, 12 reported a gradual and 37 a sudden beginning of tinnitus. All patients experienced non-pulsatile tinnitus. Nineteen (39%) reported fluctuations of their tinnitus over time. Twenty patients had tinnitus purely on the right, 18 purely on the left side. Three reported a right-dominant tinnitus, five a left-dominant, and three patients equal distributed tinnitus over both ears. Most patients reported a tonal tinnitus (n = 39), two noise-like, one crickets-like, and seven other sounds. With respect to pitch, tinnitus was rated very high in six, high in 24, middle in 14, and low in five patients. Thirty-one reported maskability of tinnitus by sounds, 10 patients reported it not maskable, and eight were unable to answer this question. Modulation of tinnitus by somatic maneuvers was possible in 16 (33%) patients.

Comorbidities

Half of patients (n = 23; 46.9%) reported worsening of tinnitus by stress and the remaining patients reported no impact of stress on their tinnitus. Only one patient was equipped with hearing aids. Thirteen patients reported painful hyperacusis, 27 had no hyperacusis, and nine patients did not answer this question. Fear-related hyperacusis was 2.8 ± 1.0 on a scale from 1 to 5.

Headache was prevalent in 14 patients, temporomandibular joint problems in 11 patients, neck pain in 22 patients, and general pain in six patients. Two patients reported concomitant psychiatric treatment.

With respect to putative tinnitus-causing factors, five patients reported to have a noisy hobby, 29 reported stress in the last weeks, five an acute and two long lasting noise exposition. Ear infections in the previous weeks were present in three patients, a common cold in nine patients, a recent hearing loss in 18 and a long-lasting hearing loss in eight patients. Ear pressure was prevalent in 28 patients and vertigo in 12 patients. Two patients reported a diving accident, six patients ear surgery, one patient acute and six patients earlier cervical spine injury. One patient reported head injury in the last weeks before tinnitus onset and two in the past.

With respect to diseases, we asked for diabetes (n = 2), stroke (n = 1), heart attack (n = 1), hypertension (n = 16), hypotension (n = 2), diseases of the immune system (n = 4), high cholesterol (n = 11), and gout (n = 3). No patient had any kidney disease or an infectious disease.

TABLE 1 | Significant differences in patients with full remission vs. patients with chronic course of tinnitus.

	Remitted tinnitus (n = 9)	Chronic tinnitus (n = 40)	
Sex (female/male)	7/2	14/26	$\chi^2 = 5.490$; df = 1; $p = 0.019$
Tinnitus duration (days)	4.78 ± 12.74	9.38 ± 5.36	$T = 2.501$; df = 47; $p = 0.016$
Loudness hyperacusis (never/rarely/sometimes/usually/always)	2.00 ± 1.00	2.98 ± 0.95	$T = 2.764$; df = 47; $p = 0.008$
Drinks per week (500 ml beer or 250 ml wine)	0.44 ± 0.88	3.33 ± 3.85	$T = 2.217$; df = 47; $p = 0.032$
Ear pressure (yes/no)	8/1	20/20	$\chi^2 = 4.537$; df = 1; $p = 0.033$

Concerning regular medication, five patients took anticoagulants, four diuretics, 15 blood pressure medication, eight antibiotics, and three contraceptives. No patient was undergoing chemotherapy.

Treatment

During the observation period 30 patients (61.2%) received tinnitus treatment. Nineteen received steroid hormones (cortisone, prednisolone, and dexamethasone), five local anesthetics (lidocaine, procaine, and novocaine), six antihistamines (betahistine, dimenhydrinate), eight cardiac medication (several different medications), and nine herbal drugs (different herbal drugs and vitamines). Eleven underwent physiotherapy, two psychosomatic interventions (rehabilitation, autogenic training), one hyperbaric oxygen therapy. No ear surgery was reported. Four patients could not specify the treatment they received.

Psychological Measures

The evaluation of personality traits with the Big-Five Personality Inventory (scale from 1 to 5), revealed extraversion to be 3.4 ± 1.0, neuroticism 3.2 ± 0.9, openness 3.5 ± 0.9, conscientiousness 4.3 ± 0.6, and agreeableness 3.1 ± 0.8. Pessimism was 11.1 ± 2.2 and optimism 6.6 ± 2.4, both measured on a scale from 1 to 15. Depressivity on a scale from 0 to 2 was 0.7 ± 0.9, and anxiety on a scale from 0 to 15 was 6.5 ± 4.4.

Predictor Analysis

Nine out of 49 patients (18.4%) showed a full remission of tinnitus after 3 and 6 months. All measured variables were tested for group differences. Patients with full remission differed from patients with "chronic tinnitus" with respect to tinnitus duration, fear-related hyperacusis, drinks per week, gender, and ear pressure (i.e., tinnitus remission was associated with the following characteristics at baseline: shorter tinnitus duration, lower fear-related hyperacusis, lower consumption of alcoholic drinks, higher incidence of increased ear pressure and a higher proportion of women). For statistical values see **Table 1**. All other variables turned out not to differ significantly between groups.

TABLE 2 | Course of tinnitus related variables over time in patients with chronic tinnitus.

	Visit 1	Visit 2 (3 months)	Visit 3 (6 months)	Statistics
Tinnitus loudness (0–100)	46.6 ± 25.0	43.7 ± 25.7	46.5 ± 23.7	$F = 0.545$; df = 2,70; $p = 0.582$
Tinnitus loudness (0–10)	4.6 ± 2.9	3.9 ± 2.9	3.9 ± 2.9	$F = 2.581$; df = 2,68; $p = 0.083$
Tinnitus awareness (0–100)	62.8 ± 30.1	50.0 ± 32.3	76.5 ± 140.8	$F = 0.872$; df = 2,70; $p = 0.423$
Tinnitus annoyance (0–100)	57.4 ± 32.9	49.1 ± 35.5	43.8 ± 31.0	$F = 4.981$; df = 2,68; $p = 0.010$
Tinnitus severity (0–5)	3.3 ± 1.1	2.7 ± 1.1	2.5 ± 1.1	$F = 18.964$; df = 2,68; $p < 0.001$
Tinnitus discomfort (0–10)	5.4 ± 3.0	4.4 ± 3.2	4.3 ± 3.2	$F = 3.547$; df = 2,68; $p = 0.034$
Tinnitus annoyance (0–10)	5.7 ± 3.2	4.1 ± 3.4	3.9 ± 3.2	$F = 10.214$; df = 2,68; $p < 0.001$
Tinnitus ignorability (0–10)	6.2 ± 3.4	4.8 ± 3.5	4.1 ± 3.2	$F = 11.032$; df = 2,68; $p < 0.001$
Tinnitus unpleasantness (0–10)	5.7 ± 3.1	4.3 ± 3.2	3.8 ± 3.2	$F = 10.693$; df = 2,68; $p < 0.001$
Mini tinnitus questionnaire (0-24; distress)	12.5 ± 6.5	10.3 ± 6.3	9.3 ± 6.3	$F = 11.816$; df = 2,66; $p < 0.001$
Tinnitus laterality (right/left/ left>right/right>left/ equal)	16/13/4/2/2	14/10/5/6/2	n.a.	$\chi^2 = 34.585$; $p < 0.001$
Tinnitus laterality (right/left/ left>right/right>left/ equal/inside head)	15/13/3/2/2	n.a.	9/11/4/4/5/2	$\chi^2 = 40.558$; $p < 0.001$
Tinnitus type (tone/noise/ crickets/other)	28/2/1/6	29/1/4/3	n.a.	$\chi^2 = 17.196$; $p = 0.047$
Tinnitus type (tone/noise/ crickets/other)	27/2/1/6	n.a.	29/3/1/3	$\chi^2 = 17.200$; $p = 0.053$
Tinnitus frequency (very high/high/middle/low)	5/17/10/5	9/16/9/3	n.a.	$\chi^2 = 16.355$; $p = 0.016$
Tinnitus frequency (very high/high/middle/low)	4/17/10/5	n.a.	5/20/8/3	$\chi^2 = 18.147$; $p = 0.005$
Mean hearing right (dB HL)	32 ± 32	26 ± 29	n.a.	$T = 3.855$; df = 33; $p = 0.001$
Mean hearing left (dB HL)	27 ± 25	23 ± 23	n.a.	$T = 2.890$; df = 33; $p = 0.007$

Please note that for χ^2 statistics statistical significance means that there is no change over time.

Longitudinal Analysis

For 37 out of the 40 patients with chronic tinnitus complete data sets of both follow-up visits were available. These patients showed no significant changes over time for tinnitus loudness or tinnitus awareness, but for tinnitus annoyance, discomfort, ignorability, unpleasantness, and distress. The reduction of the Mini TQ score over the observation period of 6 months was in the range of a medium effect size (Cohen's d(?) 0.691). Tinnitus laterality, type, and subjective reported frequency were similar for both visits as indicated by (near) significant chi-square tests. For details see **Table 2**. Hearing functions improved from visit 1 to visit 2, but there was no significant correlation between changes in hearing and changes in annoyance, discomfort, ignorability, unpleasantness, and distress. Correlations analyses were not significant (all $r < 0.296$; all $p > 0.094$).

DISCUSSION

Discussion of Our Results

The aim of our study was to observe the transition from acute to chronic tinnitus and to identify predictors for the remission and trajectory of tinnitus. Our main results are (1) that among patients who present with a tinnitus duration of <4 weeks at the clinic only a small amount (18%) lose their tinnitus and show full remission, (2) that putative predictors for remission may be shorter tinnitus duration, female sex, lower consumption of alcoholic drinks, lower fear-related hyperacusis, and increased subjective ear pressure, and (3) that among those patients who develop chronic tinnitus, the perceptual tinnitus characteristics remain unchanged, whereas tinnitus distress improves over time.

To our knowledge, two studies with a comparable approach exist (14, 15). Particularly similar was the investigation by Wallhausser-Franke. Patients were also recruited between 2013 and 2016, the sample size and inclusion criteria (tinnitus onset below 4 weeks) were similar, the observation period equally was 6 months, and some rating instruments were identical. Our findings confirm the main findings of the two previous publications. Both studies indicate a high heterogeneity with respect to tinnitus etiology and applied treatments, both suggest remission rates below 20% and both converge in the observation that tinnitus characteristics (localization, sound quality) tend to stay stable, whereas the average tinnitus distress improves moderately over time. Predictor analysis was done with respect to variables of tinnitus distress as an outcome variable and not with respect to the complete remission of tinnitus. By this means, higher tinnitus distress and depressivity in the acute phase of tinnitus were identified as predictors for a worsening of tinnitus over time.

Limitations

These three small studies highlight the need for further investigations of larger samples. The design of these investigations should consider the experiences and the limitations of the available studies. One lesson from previous undertakings is the need of a uniform definition of variables. For example, Wallhausser-Franke and colleagues find changes

in tinnitus awareness over time that we weren't able to, which may be related to the operationalisation of this variable (15). Wallhausser-Franke coded this variable as "permanent" and "intermittent," and we asked for percentage values (0–100%).

Another limitation of the available studies is the heterogeneity of performed interventions. These studies investigating the natural course of tinnitus over time should be complemented by interventional research. Even if we gathered data prospectively, it is not possible to draw causal conclusions as long as treatments are not controlled and randomized. For example, we can only speculate if a therapeutic intervention targeting the identified risk factors will improve the course of tinnitus. For example, consumption of alcoholic drinks was identified as one predictor. Only an interventional study could tell whether a corresponding intervention (e.g., decrease of alcohol consumption may help to increase the chance of remission or whether alcohol consumption is not a cause, but rather the consequence of a more affected chronic and decompensated tinnitus). Another limitation is the short period of a 6 months of follow-up and a missing question for thyroid disease.

Perspective for Future Studies

In the future, increasing the validity of data by collecting a highly operationalized case history, interview, and diagnosis of patients as well as medical records, instead of relying solely on subjective reports as has been done in the present study, should be considered. In order to avoid a selection bias, one should aim not only to recruit from hospital clinics but also from ENT- and GP-practices. Moreover, one should aim at an early assessment of tinnitus patients as soon as possible after tinnitus onset. As heterogeneity of etiology and treatment is high, large-scale multi-center trials will be necessary to create a sufficiently large data basis.

The remission rate for acute tinnitus in our study is quite low. It is not clear whether the results are representative. One might assume a selection bias, as those patients in which the tinnitus did disappear spontaneously a few days after tinnitus onset did not present in the clinic. This selection bias is particularly relevant for those patients who present at a later timepoint after tinnitus onset. Accordingly, we observed that a longer tinnitus duration at presentation in the clinic was a predictor for a chronic manifestation of tinnitus.

The remission rate identified in our study and in comparable previous investigations (14, 15) was lower than remission rates for conditions such as sudden hearing loss and acoustic trauma [for overview see (15)]. Even if hearing recovery is a predictor for tinnitus improvement (6), our finding of a lower remission rate of tinnitus when compared to hearing recovery after sudden hearing loss suggests that the chances for hearing recovery after acute hearing loss are higher than the chances for tinnitus disappearance after acute tinnitus onset. Indeed, in clinical practice patients frequently report about good hearing recovery but ongoing tinnitus after sudden hearing loss.

These preliminary data will help in deducing hypotheses about which aspects might be relevant for the chronification of tinnitus. The finding that female sex is associated with a higher chance for tinnitus disappearance might explain why chronic tinnitus is more prevalent in men. Hyperacusis was speculated to be a precursor for tinnitus (9). It might be necessary to screen for hyperacusis in acute tinnitus patients and to find out which aspects of hyperacusis are relevant (in our sample this was fear-related, even if general anxiety did not predict remission). Interestingly, we did no see a significant effect of personality or anxiety even if there is evidence that these variables are involved in decompensated tinnitus (24, 25). It would be highly interesting to see whether ear pressure could be validated by means of diagnostic tests. One could speculate that the subjectively reported increased ear pressure might be an indicator of endolymphatic hydrops, which in turn might characterize a subtype of tinnitus with more fluctuations (26). For this purpose, a more exact definition of ear pressure is also necessary.

In conclusion, acute tinnitus is a highly heterogeneous phenomenon with up to 20% full recovery after 6 months and is taking a moderately positive trajectory in terms of tinnitus distress over time, despite unchanged tinnitus characteristics.

DATA AVAILABILITY STATEMENT

The raw data supporting the conclusions of this article will be made available by the authors, without undue reservation.

ETHICS STATEMENT

The studies involving human participants were reviewed and approved by University of Regensburg, Germany. The patients/participants provided their written informed consent to participate in this study.

AUTHOR CONTRIBUTIONS

VV study concept, patient recruitment, manuscript, and statistics. RS patient recruitment. PK study concept and manuscript. BL study concept, patient recruitment, and manuscript. MS study concept, manuscript, and statistics. All authors contributed to the article and approved the submitted version.

REFERENCES

1. Langguth B. Treatment of tinnitus. *Curr Opin Otolaryngol Head Neck Surg.* (2015) 23:361–8. doi: 10.1097/MOO.0000000000000185
2. Henry JA, Reavis KM, Griest SE, Thielman EJ, Theodoroff SM, Grush LD, et al. Tinnitus: an epidemiologic perspective. *Otolaryngol Clin North Am.* (2020) 53:481–99. doi: 10.1016/j.otc.2020.03.002
3. Maes IH, Cima RF, Vlaeyen JW, Anteunis LJ, Joore MA. Tinnitus: a cost study. *Ear Hear.* (2013) 34:508–14. doi: 10.1097/AUD.0b013e31827d113a
4. Schaette R, Kempter R. Development of tinnitus-related neuronal hyperactivity through homeostatic plasticity after hearing loss: a computational model. *Eur J Neurosci.* (2006) 23:3124–38. doi: 10.1111/j.1460-9568.2006.04774.x

5. Gopinath B, McMahon CM, Rochtchina E, Karpa MJ, Mitchell P. Risk factors and impacts of incident tinnitus in older adults. *Ann Epidemiol*. (2010) 20:129–35. doi: 10.1016/j.annepidem.2009.09.002
6. Muhlmeier G, Baguley D, Cox T, Suckfull M, Meyer T. Characteristics and spontaneous recovery of tinnitus related to idiopathic sudden sensorineural hearing loss. *Otol Neurotol*. (2016) 37:634–41. doi: 10.1097/MAO.0000000000001081
7. Sanchez TG, Rocha CB. Diagnosis and management of somatosensory tinnitus: review article. *Clinics*. (2011) 66:1089–94. doi: 10.1590/S1807-59322011000600028
8. Park E, Kim H, Choi IH, Han HM, Han K, Jung HH, et al. Psychiatric distress as a common risk factor for tinnitus and joint pain: a National Population-Based Survey. *Clin Exp Otorhinolaryngol*. (2019) 13:234–40. doi: 10.21053/ceo.2019.00563
9. Schecklmann M, Landgrebe M, Langguth B, T.R.I.Group DS. Phenotypic characteristics of hyperacusis in tinnitus. *PLoS ONE*. (2014) 9:e86944. doi: 10.1371/journal.pone.0086944
10. Langguth B, Kleinjung T, Fischer B, Hajak G, Eichhammer P, Sand PG. Tinnitus severity, depression, and the big five personality traits. *Prog Brain Res*. (2007) 166:221–5. doi: 10.1016/S0079-6123(07)66020-8
11. Holgers SZKM, Svedlund K. Predictive factors for development of severe tinnitus suffering-further characterisation. *Int J Audiol*. (2005) 44:584–92. doi: 10.1080/14992020500190235
12. Wallhausser-Franke E, Delb W, Balkenhol T, Hiller W, Hormann K. Tinnitus-related distress and the personality characteristic resilience. *Neural Plast*. (2014) 2014:370307. doi: 10.1155/2014/370307
13. D'Amelio CAR, Scholz S, Falkai P, Plinkert PK, Delb W. Psychological distress associated with acute tinnitus. *HNO*. (2004) 52:599–603. doi: 10.1007/s00106-003-0944-5
14. Olderog M, Langenbach M, Michel O, Brusis T, Kohle K. Predictors and mechanisms of tinnitus distress—a longitudinal analysis. *Laryngorhinootologie*. (2004) 83:5–13. doi: 10.1055/s-2004-814235
15. Wallhausser-Franke E, D'Amelio R, Glauner A, Delb W, Servais JJ, Hormann K, et al. Transition from acute to chronic tinnitus: predictors for the development of chronic distressing tinnitus. *Front Neurol*. (2017) 8:605. doi: 10.3389/fneur.2017.00605
16. Forti S, Ambrosetti U, Crocetti A, Del Bo L. Tinnitus patients lost to follow-up. *Int J Audiol*. (2010) 49:877–80. doi: 10.3109/14992027.2010.505583
17. Cima RFF, Mazurek B, Haider H, Kikidis D, Lapira A, Norena A, et al. A multidisciplinary European guideline for tinnitus: diagnostics, assessment, and treatment. *HNO*. (2019) 67:10–42. doi: 10.1007/s00106-019-0633-7
18. Landgrebe M, Zeman F, Koller M, Eberl Y, Mohr M, Reiter J, et al. The Tinnitus Research Initiative (TRI) database: a new approach for delineation of tinnitus subtypes and generation of predictors for treatment outcome. *BMC Med Inform Decis Mak*. (2010) 10:42. doi: 10.1186/1472-6947-10-42
19. Manning C, Grush L, Thielman E, Roberts L, Henry JA. Comparison of tinnitus loudness measures: matching, rating, and scaling. *Am J Audiol*. (2019) 28:137–43. doi: 10.1044/2018_AJA-17-0115
20. Hesse G. *Tinnitus*. Stuttgart, KG: Georg Thieme Verlag (2008).
21. Rammstedt KCJB, Klein MC, Beierlein C, Kovaleva A. *Eine kurze Skala zur Messung der fünf Dimensionen der Persönlichkeit: Big-Five-Inventory-10 (BFI-10); GESIS-Working Papers 2012|22*. Köln/Mannheim: GESIS-Leibniz-Institut für Sozialwissenschaften (2012).
22. Glaesmer HJH, Klotsche J, Herzberg PJ. *Deutsche Version der Revision des Life-Orientation-Tests (LOT-R)*. Heft: Zeitschrift für Gesundheitspsychologie (2008).
23. Spitzer KMR, Williams J, Löwe B. A brief measure for assessing generalized anxiety disorder: the GAD-7. *Archiv Internal Med*. (2006) 166:1092–7. doi: 10.1001/archinte.166.10.1092
24. Fuller TE, Cima RFF, Van den Bussche E, Vlaeyen JWS. The fear of tinnitus questionnaire: toward a reliable and valid means of assessing fear in adults with tinnitus. *Ear Hear*. (2019) 40:1467–77. doi: 10.1097/AUD.0000000000000728
25. Simoes J, Schlee W, Schecklmann M, Langguth B, Farahmand D, Neff P. Big five personality traits are associated with tinnitus improvement over time. *Sci Rep*. (2019) 9:18234. doi: 10.1038/s41598-019-53845-4
26. De Luca P, Cassandro C, Ralli M, Gioacchini FM, Turchetta R, Orlando MP, et al. Dietary restriction for the treatment of Meniere's disease. *Transl Med UniSa*. (2020) 22:5–9.

Conflict of Interest: The authors declare that the research was conducted in the absence of any commercial or financial relationships that could be construed as a potential conflict of interest.

frontiers in Neurology

ORIGINAL RESEARCH
published: 22 October 2020
doi: 10.3389/fneur.2020.591602

Positioning Velocity Matters in Central Paroxysmal Positional Vertigo: Implication for the Mechanism

Xia Ling[1], *Hyo-Jung Kim*[2], *Jong-Hee Lee*[3], *Jeong-Yoon Choi*[3,4], *Xu Yang*[5] *and Ji-Soo Kim*[3,4]*

[1] Department of Medicine, Seoul National University College of Medicine, Seoul, South Korea, [2] Research Administration Team, Seoul National University Bundang Hospital, Seongnam, South Korea, [3] Dizziness Center, Seoul National University Bundang Hospital, Seongnam, South Korea, [4] Department of Neurology, Seoul National University College of Medicine, Seoul, South Korea, [5] Department of Neurology, Aerospace Center Hospital, Peking University Aerospace School of Clinical Medicine, Beijing, China

OPEN ACCESS

Edited by:
Hideo Shojaku,
University of Toyama, Japan

Reviewed by:
Yasuo Ogawa,
Tokyo Medical University Hachioji Medical Center, Japan
Tjasse Bruintjes,
Gelre Hospitals, Netherlands

***Correspondence:**
Ji-Soo Kim
jisookim@snu.ac.kr

Specialty section:
This article was submitted to Neuro-Otology, a section of the journal Frontiers in Neurology

Received: 04 August 2020
Accepted: 15 September 2020
Published: 22 October 2020

Citation:
Ling X, Kim H-J, Lee J-H, Choi J-Y, Yang X and Kim J-S (2020) Positioning Velocity Matters in Central Paroxysmal Positional Vertigo: Implication for the Mechanism.
Front. Neurol. 11:591602.
doi: 10.3389/fneur.2020.591602

Objectives: To elucidate the mechanism of paroxysmal central positional nystagmus (CPN) by determining the effects of head rotation velocity on the intensity of paroxysmal downbeat nystagmus induced during straight head hanging (SHH).

Methods: We recruited 21 patients with paroxysmal downbeat CPN induced during SHH at the Dizziness Center of Seoul National University Bundang Hospital from September 2018 to July 2019. Twenty-one patients had manual SHH at two different lying velocities, the fast (routine) and slow, and they also underwent SHH at different rotation velocities of 10, 20, 30, and 40 °/s using a motorized rotation chair. Induced nystagmus was recorded using video-oculography and the maximum slow phase velocity (SPV) and time constant (TC) of the induced paroxysmal nystagmus were analyzed.

Results: During manual SHH, paroxysmal downbeat nystagmus was invariably induced during routine SHH (fast lying down), but absent or minimal during slow positioning. During motorized SHH, the median of maximum intensity of downbeat nystagmus increased from 7.6 °/s (0–16.9) to 14.0 °/s (0–32.5), 16.5 °/s (0–44.6), and 19.1 °/s (0–55.2) as the rotation velocity increased from 10 to 20, 30, and 40°/s ($P < 0.001$, $P < 0.001$, $P = 0.004$; linear mixed models). In contrast, the TCs of paroxysmal downbeat CPN remained unchanged ($P = 0.558$, $P = 0.881$, $P = 0.384$, linear mixed models).

Conclusions: The dependence of nystagmus intensity on head rotation velocity supports a disinhibited and exaggerated inhibitory rebound of the canal signals as the mechanism of paroxysmal CPN.

Keywords: vertigo, nystagmus, central positional nystagmus, downbeat nystagmus, mechanism

INTRODUCTION

Either paroxysmal or persistent form of positional vertigo and nystagmus may occur in central as well as peripheral vestibular disorders (1). In peripheral disorders, paroxysmal vertigo and nystagmus are mostly explained by migration of the otolithic debris dislodged from the utricular macule into the semicircular canals or by alteration in the specific gravity of the cupula relative to endolymph (2). Central positional nystagmus (CPN) mostly takes the form of apogeotropic (3) or geotropic (4) nystagmus when the head is turned to either side while supine, or downbeat nystagmus after lying down (5).

Persistent CPN has been explained by erroneous neural processing within the velocity-storage circuit located in the brainstem and cerebellum that functions in estimating the angular head velocity, gravity direction, and inertial acceleration (3). Paroxysmal CPN is also featured by transient geotropic or apogeotropic nystagmus after head-turning to either side while supine, and upbeat or downbeat nystagmus after lying down, straight head hanging (SHH) or sitting up (6). Of those, paroxysmal downbeat nystagmus while lying down or SHH is most common (7). The mechanism of paroxysmal CPN requires further exploration. In our previous study, the paroxysmal form of CPN mostly occurred in the planes of semicircular canals inhibited during the positioning, and showed the features suggestive of a semicircular canal origin regarding the latency, duration, and direction of nystagmus (7). Based on those findings, paroxysmal CPN was attributed to disinhibition and enhanced responses of the secondary vestibular neurons during the positioning due to lesions involving the nodulus and uvula (7). In this instance, increment of the post-rotatory signals is invoked to generate paroxysmal CPN (7). For example, paroxysmal downbeat nystagmus observed during lying down or SHH is explained by transient over-activation of the anterior and/or horizontal canals on both sides (7). According to this explanation, the intensity of paroxysmal CPN would depend on stimulation intensity of the semicircular canals during the positioning, and thus lying velocity (acceleration) in paroxysmal downbeat CPN.

This study aimed to determine the effect of lying (head rotation) velocity (acceleration) on the intensity of paroxysmal downbeat CPN induced during SHH by adopting a stepwise increase in the rotation velocity. We hypothesized that the intensity of induced nystagmus would increase in proportion to the lying velocity.

MATERIALS AND METHODS

Patients

We recruited 27 patients with paroxysmal downbeat CPN at the Dizziness Center of Seoul National University Bundang Hospital from September 2018 to July 2019. All experiments followed the tenets of the Declaration of Helsinki and this study was approved by the Institutional Review Board of Seoul National University Bundang Hospital (IRB No. B-1908/558-103).

All patients underwent detailed neuro-otologic evaluation by the senior author (J.S.K). The diagnosis of paroxysmal downbeat CPN was based on (1) paroxysmal downbeat nystagmus (<1 min) induced during SHH, (2) presence of other symptoms and signs indicative of brainstem or cerebellar dysfunction, or brainstem or cerebellar lesions documented on MRIs, and (3) no resolution of paroxysmal downbeat nystagmus with repeated canalith repositioning maneuvers for benign paroxysmal positional vertigo involving the anterior semicircular canals. Of the 27 patients, 21 (12 men, mean age $\pm$ SD = 54.4 $\pm$ 14.9 years) were finally included for analyses after excluding six patients due to (1) a duration of the paroxysmal nystagmus <5 s (n = 1), (2) concomitant periodic alternating nystagmus that interfered accurate analyses of downbeat nystagmus (n = 1), (3) an inconsistency; direction-changing or alternating with horizontal nystagmus (intermittent, n = 2), and (4) incomplete evaluation (n = 2).

Oculography

Eye movements were recorded binocularly using 3-dimensional video-oculography (VOG, SLVNG®, SLMED, Seoul, South Korea). Spontaneous nystagmus was recorded both with and without visual fixation in the sitting position. Gaze-evoked nystagmus, horizontal smooth pursuit, horizontal saccades, and horizontal head-shaking nystagmus were also evaluated.

Positioning Maneuvers

All patients had manual SHH at both fast (routine) and slow lying velocities. During the fast SHH, patients were laid from the sitting position onto the lying down position with the head extended about 30° below the table. During the fast SHH, this positioning was performed at a routine velocity and was completed usually within 3 s (2–4 s). Thus, the mean head rotation velocity was about 40°/s during the fast SHH test. During the slow SHH, the patients assumed the same position over about 35 s (from 25 to 51 s) with an assistance by the examiner. Thus, the mean head rotation velocity was ∼3–4 °/s during the slow SHH (**Figure 1**, **Supplementary Video 1**).

All patients also underwent SHH at different rotation velocities of 10, 20, 30, and 40 °/s using a 3-dimensional motorized rotation chair (SLRVT®, SLMED, Seoul, South Korea, **Figure 2**, **Supplementary Video 2**). During this maneuver, the patients were tilted backward 100° from the sitting position without extending the neck at each rotation velocity.

In each testing condition, the SHH position was maintained until the positional nystagmus disappeared or at least for 1 min. The positional nystagmus was recorded at a sampling rate of 120 Hz without visual fixation in darkness using video-oculography (VOG, SLVNG®, SLMED, Seoul, South Korea).

Analyses of Nystagmus

Digitized eye position data were analyzed with MATLAB software (version R2019b, The MathWorks, Inc., MA,

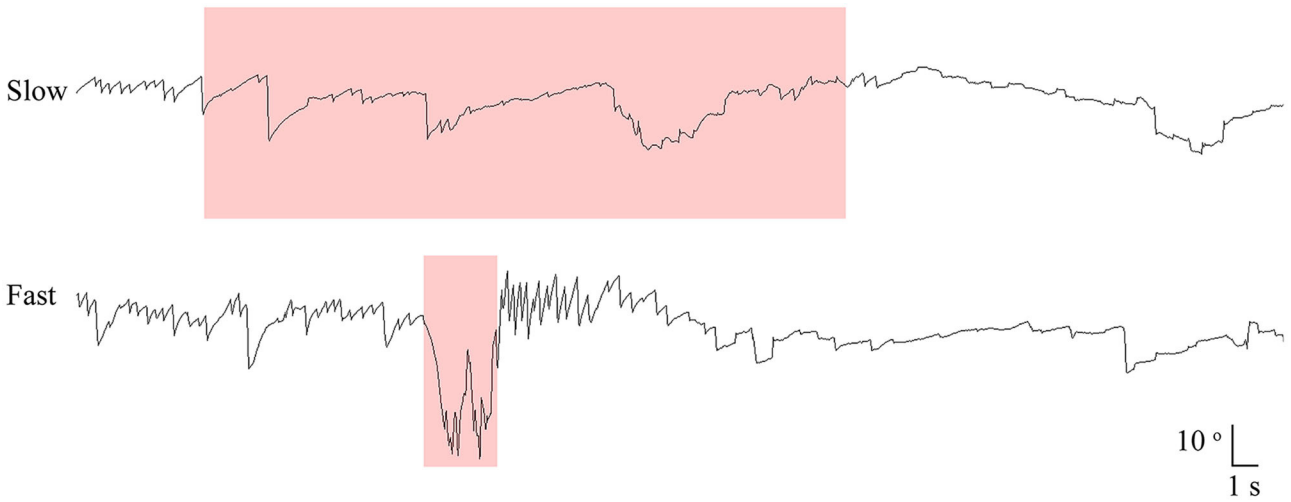

FIGURE 1 | Recording of paroxysmal downbeat nystagmus during manual straight head hanging in patient 21. With slow positioning, no discernable nystagmus was induced, and the pre-existing spontaneous downbeat nystagmus was even suppressed. During fast positioning, in contrast, paroxysmal downbeat nystagmus was induced for several seconds. Only the vertical eye motion is presented and the shaded areas in pink indicate the period of positioning. Upward deflection denotes upward eye motion in each recording.

USA). For each paroxysmal CPN, the intensity (maximum slow phase velocity, SPV) and time constant (TC) were calculated. When persistent CPN was combined with the paroxysmal one, we calculated the maximum SPV and TC of paroxysmal CPN after subtracting the persistent component from the velocity profile of induced positional nystagmus.

Statistical Analyses

Statistical analyses were performed using SPSS software (version 20.0, IBM SPSS Statistics, N.Y., USA). Continuous variables were expressed as a mean ± *SD* for parametric values or as a median (range) for non-parametric ones. Counting variables were expressed as a percentage. Normality of the data was determined using the Shapiro-Wilk test. Linear mixed model analysis was used to determine any difference in the maximum SPV and TC of paroxysmal downbeat CPN among the test conditions that had adopted different rotation velocities using a motorized rotation chair. The level of statistical significance for the linear mixed model analyses was corrected using the Bonferroni method, and the corrected level of significance was set at 0.0083 (0.05/6) since the comparisons were performed six times in each group. The Wilcoxon signed ranks test were used to determine any difference in the maximum SPVs of paroxysmal downbeat CPN induced during the fast and slow SHH and maximum SPVs of paroxysmal downbeat CPN induced during the fast SHH and motorized positioning test at a rotation velocity of 40.0°/s, and the paired *t*-test was used to determine any difference in the TCs of paroxysmal downbeat CPN induced during the fast SHH and motorized positioning test at a rotation velocity of 40.0 °/s. The significance threshold was set at a 2-sided $P < 0.05$.

RESULTS

Clinical Characteristics

Underlying disorders included spinocerebellar ataxia ($n = 14$), episodic ataxia ($n = 4$), Chiari malformation ($n = 1$), and no etiology was identified in the remaining two patients.

During visual fixation, eight patients (38.1%) showed spontaneous nystagmus that was pure downbeat in seven, and mixed horizontal and downbeat in the remaining one. The SPV of downbeat nystagmus ranged from 0.7 to 8.2°/s (median = 2.0). Without visual fixation in darkness, 15 patients (71.4%) showed spontaneous nystagmus that was pure downbeat in eight, mixed horizontal-downbeat in five, pure horizontal in one, and mixed horizontal-upbeat in the remaining one. The SPV of downbeat nystagmus ranged from 1.1 to 8.7°/s (median = 3.1) without visual fixation in darkness. After horizontal head-shaking, 18 patients (85.7%) showed nystagmus that was mixed horizontal-downbeat in 11, pure downbeat in five, and pure horizontal in two. Gaze-evoked nystagmus was found in 14 patients (66.7%), and eight of them also showed rebound nystagmus. Horizontal smooth pursuit was impaired in 14 patients (66.7%). Horizontal saccades were abnormal in 11 patients (52.4%); hypermetric in six, hypometric in four, and slow in one (**Table 1**).

Manual SHH

All 21 patients showed paroxysmal downbeat CPN during the routine (fast) positioning, and only two of them showed downbeat nystagmus during the slow SHH (**Table 1**). During the routine SHH, the downbeat CPN was pure paroxysmal in 16 and mixed paroxysmal and persistent in five patients. The paroxysmal downbeat CPN showed a peak initially in 19 patients (90.5%) and reached its peak within 2.5 s in the remaining two. After then, the nystagmus decreased exponentially. The maximum SPV of positional downbeat nystagmus ranged from

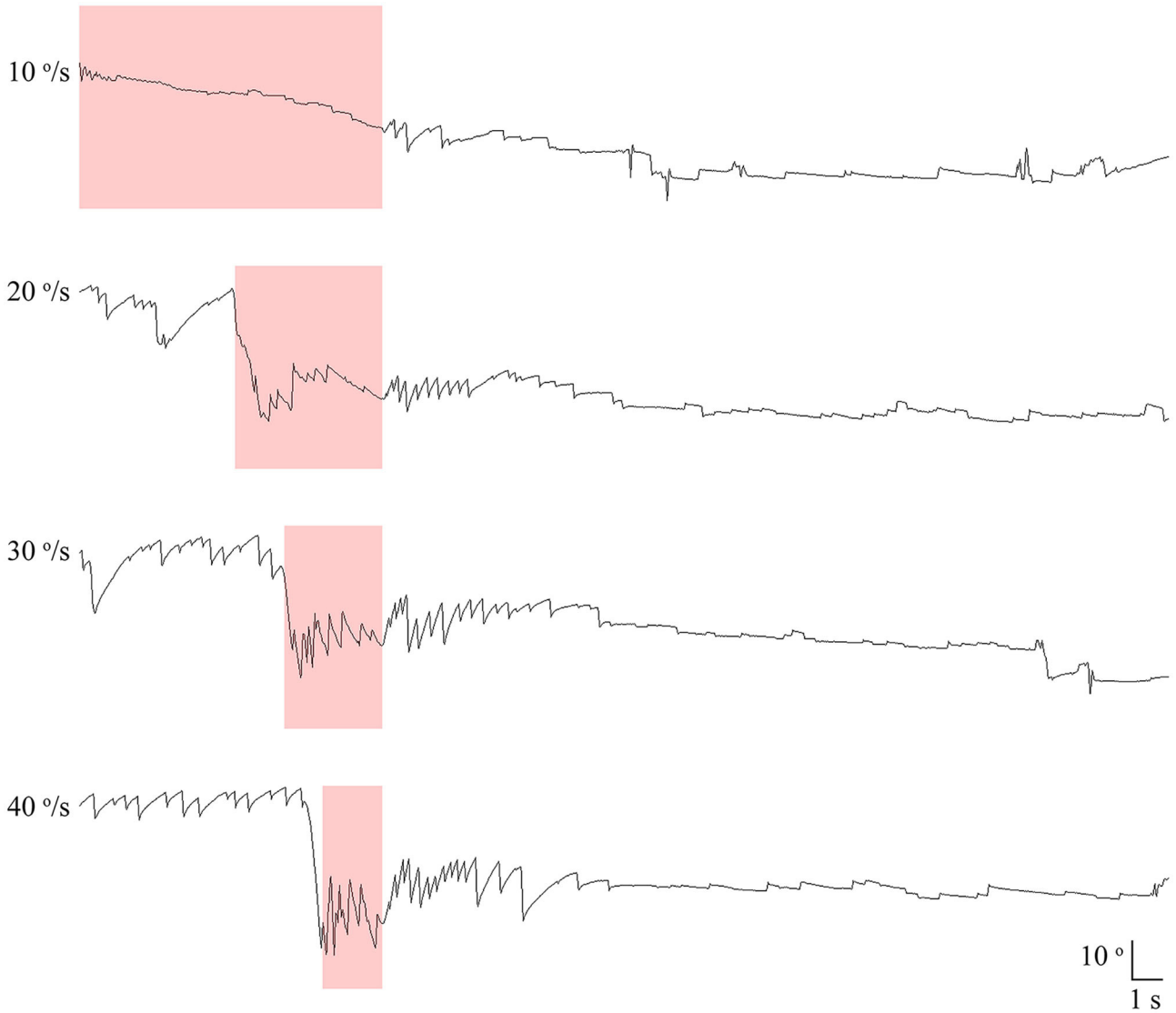

FIGURE 2 | Recording of paroxysmal downbeat nystagmus induced during motorized rotation chair test at four different rotation velocities in patient 21. The intensity of induced downbeat nystagmus increased as the rotation velocity was escalated from 10 to 40°/s. The paroxysmal downbeat nystagmus was followed by a small upbeat nystagmus. Only the vertical eye motion is presented and the shaded areas in pink indicate the period of positioning. Upward deflection denotes upward eye motion in each recording.

4.6 to 65.6°/s (median = 19.8, mean ± *SD* = 23.4 ± 14.7), and the TC ranged from 1.1 to 7.4 s (median = 3.5, mean ± *SD* = 3.8 ± 1.8) during the fast SHH. During the slow SHH, the maximum SPVs for the two patients with discernable positional downbeat nystagmus were 10.4 and 12.3°/s with the TCs at 1.3 and 3.7 s. Thus, there was a significant rise in the maximum SPV of paroxysmal downbeat CPN as the lying velocity increased ($Z = -4.02$, Wilcoxon signed ranks test, $P < 0.001$ (**Table 1**, **Figure 3**).

Motorized Rotation Chair Test

The median of maximum SPV of paroxysmal downbeat CPN was 7.6 °/s (range: 0–16.9; mean ± *SD* = 7.2 ± 5.7) at the rotation velocity of 10°/s, which increased to 14.0 °/s (range: 0–32.5; mean ± *SD* =14.6 ± 8.1) at 20°/s, 16.5°/s (range: 0–44.6; mean ± *SD* = 17.6 ± 9.5) at 30°/s, and 19.1°/s (range: 0–55.2; mean ± *SD* = 20.5 ± 12.1) at 40°/s. Thus, there was a significant rise in the maximum SPV of paroxysmal downbeat CPN as the lying velocity increased [(95% CI, −18.42 to −8.19), $P < 0.001$; (95% CI, −8.95 to −3.00), $P < 0.001$; (95% CI, −4.84 to −1.06), $P = 0.004$; Linear mixed model; **Figure 4A**]. In contrast, the TCs of paroxysmal downbeat nystagmus remained at about 3.5 s without a difference among the four testing conditions [(95% CI, −1.12 to 0.62), $P = 0.558$; (95% CI, −0.51 to 0.60), $P = 0.881$; (95% CI, −0.29 to 0.70), $P = 0.384$, Linear mixed model, **Figure 4B**].

Six patients showed both paroxysmal and persistent components of positional nystagmus, and the persistent

TABLE 1 | Findings in patients with paroxysmal downbeat central positional nystagmus.

Pt	Etiology	Sex/Age	SN fix	SN non-fix	GEN	HSN	Manual				Rotatory chair							
							Max SPV		TC		Max SPV				TC			
							Slow	Fast	Slow	Fast	10° /s	20° /s	30° /s	40° /s	10° /s	20° /s	30° /s	40° /s
1	SCA 6	M/56	-	D	-	R+D	0.0	14.5	-	3.4	8.7	14.6	14.7	16.5	7.1	7.8	6.3	4.5
2	ACM	F/66	D	R+D	+(REB)	R→ L+D	0.0	30.0	-	4.3	6.7	11.2	15.8	21.9	7.7	4.1	4.3	4.3
3	SCA	F/45	D	R+D	+(REB)	R+D	0.0	16.0	-	7.4	11.4	16.4	20.3	18.2	2.9	4.0	3.8	4.1
4	CA	F/70	-	L	+(REB)	-	10.4	25.7	1.3	1.4	8.0	16.5	22.1	23.3	2.3	2.8	1.5	1.1
5	CA	F/72	-	-	+(REB)	R→ L	12.3	23.1	3.7	6.2	9.2	12.1	12.1	13.5	3.0	4.9	4.3	5.7
6	SCA 1	M/62	-	D	-	R→ L+D	0.0	16.2	-	2.0	6.4	11.3	14.2	18.5	2.9	1.9	1.5	1.5
7	EA2	F/22	D	R+D	-	L→ R+D	0.0	19.8	-	2.0	0.0	6.5	17.4	24.1	-	3.0	2.6	2.4
8	CA	M/48	-	-	+	D	0.0	11.6	-	5.3	15.7	23.8	22.8	16.3	4.0	3.2	4.6	5.9
9	CA	F/43	-	D	-	R+D	0.0	19.5	-	4.5	8.5	14.0	16.5	19.5	2.6	4.0	4.2	3.7
10	CA	M/72	-	L+D	-	L+D	0.0	26.7	-	3.5	5.5	8.0	8.4	6.7	3.1	3.1	3.2	3.8
11	CA	M/47	-	U+OF	+	-	0.0	35.9	-	2.7	16.8	17.0	19.4	22.4	1.0	2.8	2.7	2.7
12	CVUE	M/67	D	D	+	D	0.0	19.4	-	3.7	0.0	13.9	16.3	19.1	-	1.4	3.4	2.3
13	EA2	M/16	D	D	+(REB)	L+D	0.0	26.1	-	3.5	7.6	8.3	10.4	13.8	3.6	3.3	5.7	2.0
14	EA	M/48	-	D	-	D	0.0	4.6	-	6.8	0.0	0.0	3.8	4.1	-	-	6.5	6.8
15	CA	F/55	-	-	+(REB)	-	0.0	23.6	-	1.1	0.0	23.2	27.4	35.1	-	0.8	1.4	1.3
16	SCA	M/66	D	D	+	R→ L+D	0.0	22.2	-	4.7	10.8	24.7	25.6	28.8	2.8	3.6	4.4	4.2
17	SCA	F/48	-	-	+(REB)	D	0.0	17.5	-	2.7	13.8	21.2	26.0	30.2	2.3	2.4	2.1	1.9
18	OPCA	F/56	-	-	-	D	0.0	9.3	-	6.5	6.5	9.5	9.7	9.8	3.7	4.2	4.1	4.4
19	EA	M/63	-	-	+	R+D	0.0	6.8	-	3.3	0	0	0	0	-	-	-	-
20	CVUE	M/55	D	D	+	R	0.0	56.7	-	1.8	0	20.9	21.7	34.1	-	1.8	1.8	1.9
21	SCA	M/65	D+SWJ	D+SO	+(REB)	L→ R+D	0.0	65.6	-	2.7	16.9	32.5	44.6	55.2	1.4	2.7	2.9	2.7

ACM, Arnold-Chiari malformation; APAN, aperiodic alternating nystagmus; CA, cerebellar ataxia; CVUE, central vertigo with unknown etiology; D, downbeat nystagmus; EA, episodic ataxia; F, female; GEN, gaze-evoked nystagmus; HSN, head shaking nystagmus; L, left beating nystagmus; M, male; Max, maximum; MSO, macro saccadic oscillation; OF, ocular flutter; OPCA, olivopontocerebellar atrophy; Pt, patient; R, right beating nystagmus; REB, rebound; SCA, spinocerebellar ataxia; SPV, slow phase velocity; SN, spontaneous nystagmus; SN fix, spontaneous nystagmus with visual fixation; SN non-fix, spontaneous nystagmus without visual fixation; SO, saccadic oscillation; SWJ, square wave jerk; TC, time constant; +, present or plus; −, normal or absent; →, change to.

nystagmus was upbeat (0.2–3.1°/s) in five and downbeat (3.1°/s) in one.

Comparison of Manual and Motorized SHH

We compared the maximum SPVs and TCs of the paroxysmal downbeat nystagmus between the manual fast SHH and motorized SHH test at the rotation velocity of 40 °/s since the head rotation velocities were similar for those testing conditions, and found that the maximum SPVs [19.1 (0–55.2) vs. 19.8 (4.6–65.6) °/s, $Z = -1.06$, Wilcoxon signed ranks test, $P = 0.29$] and TCs [3.8 ± 1.9 vs. 3.4 ± 1.6 s, (95% CI, −0.02–0.92), paired t-test, $P = 0.06$] of the paroxysmal downbeat CPN induced during both tests were similar.

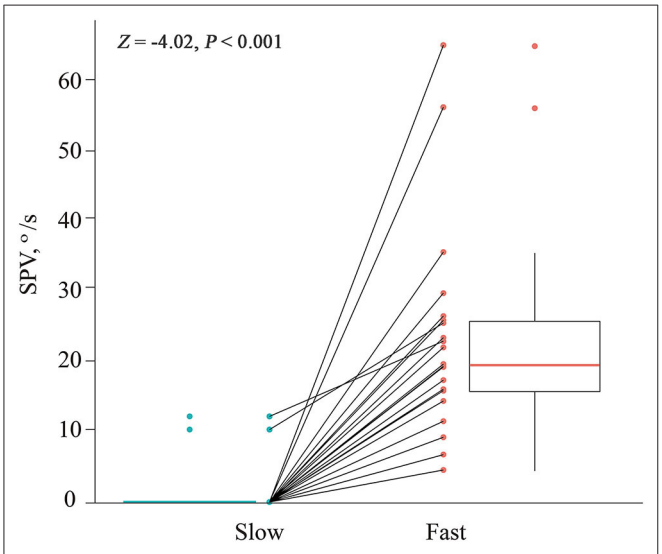

FIGURE 3 | Comparison of the maximum slow phase velocity (SPV) of paroxysmal downbeat nystagmus induced during slow and fast manual straight head hanging tests in each patient. During slow positioning, only two patients showed paroxysmal downbeat CPN, which became larger during fast positioning. In contrast, paroxysmal downbeat nystagmus was observed in all patients after fast positioning.

DISCUSSION

We found that the intensity of paroxysmal downbeat CPN during SHH depends on the rotation velocity (acceleration) of the head during the positioning while the TC was not affected by the rotation velocity. Furthermore, the intensity of positional downbeat nystagmus increases in proportion to the positioning velocity during the motorized rotatory chair tests.

In this study, most patients showed diffuse cerebellar dysfunction in association with the hereditary or acquired forms of ataxia. However, the associated ocular motor findings of spontaneous downbeat nystagmus, gaze-evoked nystagmus, perverted head-shaking nystagmus, and impaired smooth pursuit all indicate dysfunction of the vestibulocerebellum (8–10). In our previous studies, circumscribed lesions responsible for CPN, either the paroxysmal or persistent form, also were mostly overlapped in the nodulus and uvula (7).

In this study, the intensity of paroxysmal downbeat CPN induced during SHH depended on the positioning velocity during either manual SHH or the whole-body rotation using a motorized chair. Indeed, most patients showed no or minimal downbeat nystagmus during SHH when the positioning was performed at a very slow speed. This was also observed in a previous study on spontaneous downbeat nystagmus even though the detailed findings or mechanisms were not explored (11). The TCs of paroxysmal downbeat CPN were mostly around

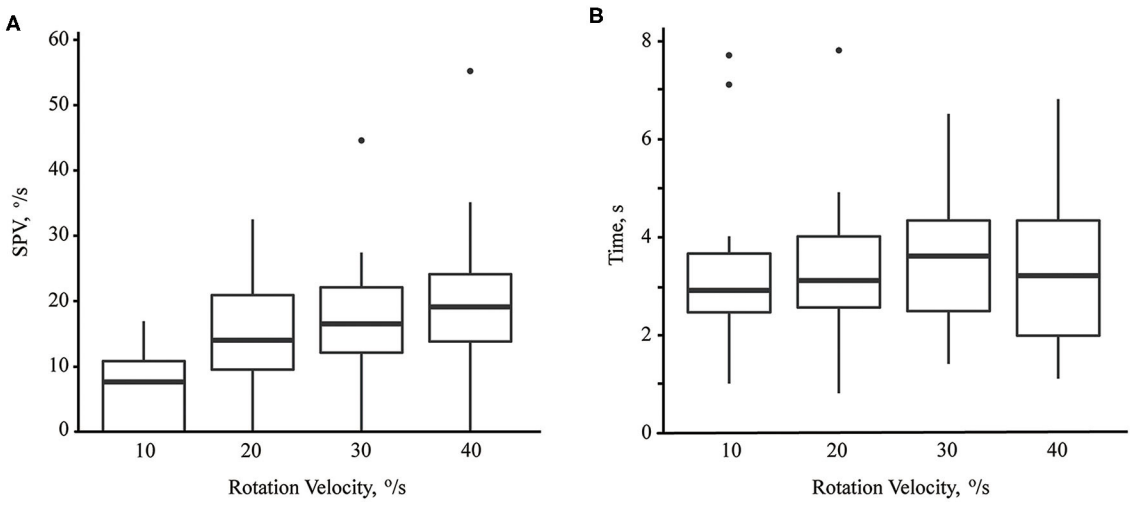

FIGURE 4 | The maximum slow phase velocity (SPV, **A**) and time constant **(B)** of paroxysmal downbeat nystagmus induced during motorized rotation chair test at four different rotation velocities. As the rotation velocity was escalated from 10 to 40°/s, the maximum slow phase velocity of induced downbeat nystagmus increased while the time constant remained unchanged.

3.5 s with some variations among the patients and different testing conditions, which are similar to the TCs of the vertical semicircular canals (12–14). These characteristics of paroxysmal downbeat nystagmus observed in this study are consistent with those found in our previous study on paroxysmal CPN regarding its maximum at onset, short duration with a TC around 4 s, and alignment of the nystagmus direction with the vector sum of the rotational axes of the semicircular canals that are normally inhibited during the positioning (7). Based on these findings, we previously proposed that paroxysmal CPN is generated by disinhibition and enhanced responses of the secondary vestibular neurons during positioning due to cerebellar dysfunction (7). The similar TCs regardless of different nystagmus intensity in each testing condition are consistent with the findings observed in previous studies on the attenuation of nystagmus but constant TC during rotations having adopted a stepwise increase in the head rotation velocity (15, 16).

The first-order neurons from the horizontal semicircular canal have a resting discharge and the firing rate increases during head rotation that induces an ampullopetal flow of the endolymph and decreases during head motion that produces an ampullofugal flow of the endolymph. The reverse holds for the vertical semicircular canals (17, 18). Within a specific dynamic range, this increase or decrease of action potentials is directly proportional to the magnitude of head acceleration or deceleration (17). The primary vestibular afferents are classified into the regular and irregular according to their discharge properties (17). The irregular afferents are responsible for the adaptation responses and velocity-storage mechanism. The adaptation responses include a rapid decline in the discharge with a rebound when the discharge goes below the resting rate and a following gradual return to the resting level (post-acceleratory secondary phenomenon) (17). We postulate that the lesions involving the vestibulocerebellum disinhibit the irregular afferents and result in exaggerated post-acceleratory secondary phenomenon (7). One of the functions of the velocity-storage mechanism is to estimate the gravitational direction by integrating the rotation cues from the semicircular signals. Since there is a rotation feedback loop inside the velocity-storage mechanism, which acts to adjust the estimated gravitational direction to the real gravitational direction (7), vestibulocerebellar lesions and resultant disinhibition of the irregular afferents would lead to an exaggerated post-acceleratory secondary response and a difference between the estimated and real gravitational directions. This difference would generate the post-rotatory nystagmus (7). During SHH, the irregular vestibular fibers from both posterior semicircular canals are mostly activated and this activation is followed by transient inhibitory rebound (17). When this secondary inhibition becomes prominent due to dysfunction of the vestibulocerebellum, the exaggerated inhibitory signals conveyed to the vestibular storage mechanism may generate nystagmus through the rotational feedback mechanism (7). In this scenario, the degree of post-acceleratory depression would depend on the strength of head acceleration during positioning, which forms the basis of this study. Indeed, the intensity of paroxysmal downbeat CPN induced during SHH depended on the positioning head velocity.

Several studies showed that transient compression of the vertebral arteries during neck rotation or extension may reduce the blood supply to the peripheral or the central parts of the vestibular system and give rise to paroxysmal downbeat nystagmus along with vertigo and tinnitus (19–21). The presumed mechanism was excitation of unilateral or bilateral anterior semicircular canals (19–21). Thus, paroxysmal downbeat nystagmus may be induced by head extension during SHH. However, in our study, only two patients (9.5%) showed paroxysmal downbeat CPN during the manual slow SHH test, and all patients showed paroxysmal downbeat CPN during the SHH using a rotation chair, which did not allow any neck motion during the positioning. Thus, the role of head extension, if any, in generating paroxysmal downbeat nystagmus could have been minimal in our study.

Four patients showed an evolution of initial positional downbeat into upbeat nystagmus over 4–15 s. This reversal in the direction of induced nystagmus is observed in various conditions including benign paroxysmal positional vertigo (22–24), head-shaking nystagmus (25), caloric stimulation (26), and vertebral artery occlusion syndrome (21), and may be ascribed to short-term adaption of the vestibular imbalance.

LIMITATIONS

There are several limitations in our study. First, we only quantified paroxysmal downbeat CPN, and did not include other types of paroxysmal CPN such as geotropic or apogeotropic horizontal nystagmus during head turning to either side while supine. However, our observation was also similar in apogeotropic CPN (**Supplementary Video 3**). Second, for the patient's safety, we set the maximum rotation velocity at 40 °/s during the motorized chair rotations. Thus, the characteristics of paroxysmal CPN during the head rotation at higher velocities remain to be determined. Third, due to severe vertigo, some patients involuntarily closed their eyes just after the positioning, and this might have biased the maximal SPV and TC. Finally, we couldn't measure the accurate acceleration and deceleration of the head motion during the SHH tests, so it was not possible to further elucidate the effects of velocity and acceleration on paroxysmal CPN.

DATA AVAILABILITY STATEMENT

The raw data supporting the conclusions of this article will be made available by the authors, without undue reservation.

ETHICS STATEMENT

The studies involving human participants were reviewed and approved by Institutional Review Board of Seoul National University Bundang Hospital (IRB No. B-1908/558-103). Written informed consent to participate in this study was provided by the participants. Written informed consent was obtained from the individual(s) for the publication of any potentially identifiable images or data included in this article.

AUTHOR CONTRIBUTIONS

XL acquired and analyzed the data and wrote the manuscript. H-JK, J-HL, J-YC, and XY analyzed and interpreted the data and revised the manuscript. J-SK designed and conceptualized the study, interpreted the data, and revised the manuscript. All authors contributed to the article and approved the submitted version.

FUNDING

This study was supported by MYUNG-IN PHARM.CO., LTD. (no. 06-2019-224). The funder had no role in study design, data collection and analysis, decision to publish, and preparation of the manuscript.

SUPPLEMENTARY MATERIAL

The Supplementary Material for this article can be found online at: https://www.frontiersin.org/articles/10.3389/fneur.2020.591602/full#supplementary-material

Supplementary Video 1 | Paroxysmal downbeat nystagmus induced during slow and fast manual straight head hanging in patient 21. With slow positioning, no nystagmus was induced, and the pre-existing spontaneous downbeat nystagmus was even suppressed. During fast positioning, in contrast, paroxysmal downbeat nystagmus was induced for several seconds.

Supplementary Video 2 | Paroxysmal downbeat nystagmus induced during straight head hanging using a motorized rotation chair in patient 21. During rotation at a velocity of 10°/s, only small downbeat nystagmus was observed for a couple of seconds. During rotation at a velocity of 40°/s, in contrast, strong downbeat nystagmus was induced for about 7 s, which was followed by a small upbeat nystagmus.

Supplementary Video 3 | Effect of positioning velocity on paroxysmal apogeotropic central positional nystagmus during head turning to either side while supine. During fast head rotation, strong paroxysmal apogeotropic nystagmus was induced with the maximum slow phase velocity (SPV) at 28.1°/s and the time constant of 3.7 s, and was followed by a persistent nystagmus (mean SPV:1.9°/s). In contrast, the induced paroxysmal nystagmus was absent or minimal after slow head rotation, but the persistent nystagmus was still observed at the mean SPV of 2.1°/s.

REFERENCES

1. Choi JY, Kim JS. Central positional nystagmus: characteristics and model-based explanations. *Prog Brain Res.* (2019) 249:211–25. doi: 10.1016/bs.pbr.2019.04.012
2. Choi JY, Kim JS. Nystagmus and central vestibular disorders. *Curr Opin Neurol.* (2017) 30:98–106. doi: 10.1097/WCO.0000000000000416
3. Choi JY, Glasauer S, Kim JH, Zee DS, Kim JS. Characteristics and mechanism of apogeotropic central positional nystagmus. *Brain.* (2018) 141:762–75. doi: 10.1093/brain/awx381
4. Choi SY, Jang JY, Oh EH, Choi JH, Park JY, Lee SH, et al. Persistent geotropic positional nystagmus in unilateral cerebellar lesions. *Neurology.* (2018) 91:e1053–e7. doi: 10.1212/WNL.0000000000006167
5. Choi J-Y, Kim J-S. Positional downbeat nystagmus. In: Shaikh A, Ghasia F, editors. *Advances in Translational Neuroscience of Eye Movement Disorders*. Cham: Springer International Publishing. (2019). p. 191–201. doi: 10.1007/978-3-030-31407-1_10
6. De Schutter E, Adham ZO, Kattah JC. Central positional vertigo: a clinical-imaging study. *Prog Brain Res.* (2019) 249:345–60. doi: 10.1016/bs.pbr.2019.04.022
7. Choi JY, Kim JH, Kim HJ, Glasauer S, Kim JS. Central paroxysmal positional nystagmus: characteristics and possible mechanisms. *Neurology.* (2015) 84:2238–46. doi: 10.1212/WNL.0000000000001640
8. Huh YE, Koo JW, Lee H, Kim JS. Head-shaking aids in the diagnosis of acute audiovestibular loss due to anterior inferior cerebellar artery infarction. *Audiol Neurootol.* (2013) 18:114–24. doi: 10.1159/000345643
9. Patel VR, Zee DS. The cerebellum in eye movement control: nystagmus, coordinate frames and disconjugacy. *Eye.* (2015) 29:191–5. doi: 10.1038/eye.2014.271
10. Kheradmand A, Zee DS. Cerebellum and ocular motor control. *Front Neurol.* (2011) 2:53. doi: 10.3389/fneur.2011.00053
11. Baloh RW, Spooner JW. Downbeat nystagmus: a type of central vestibular nystagmus. *Neurology.* (1981) 31:304–10. doi: 10.1212/WNL.31.3.304
12. Morita M, Imai T, Kazunori S, Takeda N, Koizuka I, Uno A, et al. A new rotational test for vertical semicircular canal function. *Auris Nasus Larynx.* (2003) 30:233–7. doi: 10.1016/S0385-8146(03)00098-1
13. Bertolini G, Bockisch CJ, Straumann D, Zee DS, Ramat S. Do humans show velocity-storage in the vertical rVOR? *Prog Brain Res.* (2008) 171:207–10. doi: 10.1016/S0079-6123(08)00628-6
14. Bertolini G, Ramat S. Velocity storage in the human vertical rotational vestibulo-ocular reflex. *Exp Brain Res.* (2011) 209:51–63. doi: 10.1007/s00221-010-2518-6
15. Sills AW, Honrubia V. A new method for determining impulsive time constants and their application to clinical data. *Otolaryngology.* (1978) 86:ORL-81-9. doi: 10.1177/019459987808600118
16. Sills AW, Honrubia V, Baloh RW. Is the adaptation model a valid description of the vestibulo-ocular reflex? *Biol Cybern.* (1978) 30:209–20. doi: 10.1007/BF00361042
17. Goldberg JM, Fernandez C. Physiology of peripheral neurons innervating semicircular canals of the squirrel monkey. I. Resting discharge and response to constant angular accelerations. *J Neurophysiol.* (1971) 34:635–60. doi: 10.1152/jn.1971.34.4.676
18. Baloh RW, Honrubia V, Konrad HR. Ewald's second law re-evaluated. *Acta Otolaryngol.* (1977) 83:475–9. doi: 10.3109/00016487709128874
19. Yun SY, Lee JY, Kwon EJ, Jung C, Yang X, Kim JS. Compression of both vertebral arteries during neck extension: a new type of vertebral artery compression syndrome. *J Neurol.* (2019) 267:276–8. doi: 10.1007/s00415-019-09576-7
20. Marti S, Hegemann S, von Budingen HC, Baumgartner RW, Straumann D. Rotational vertebral artery syndrome: 3D kinematics of nystagmus suggest bilateral labyrinthine dysfunction. *J Neurol.* (2008) 255:663–7. doi: 10.1007/s00415-008-0773-2
21. Choi KD, Shin HY, Kim JS, Kim SH, Kwon OK, Koo JW, et al. Rotational vertebral artery syndrome: oculographic analysis of nystagmus. *Neurology.* (2005) 65:1287–90. doi: 10.1212/01.wnl.0000180405.00560.51
22. Lee SH, Kim MK, Cho KH, Kim JS. Reversal of initial positioning nystagmus in benign paroxysmal positional vertigo involving the horizontal canal. *Ann N Y Acad Sci USA.* (2009) 1164:406–8. doi: 10.1111/j.1749-6632.2008.03739.x

23. Baloh RW, Jacobson K, Honrubia V. Horizontal semicircular canal variant of benign positional vertigo. *Neurology*. (1993) 43:2542–9. doi: 10.1212/WNL.43.12.2542
24. Choi SY, Lee MJ, Oh EH, Choi JH, Choi KD. Short-term central adaptation in benign paroxysmal positional vertigo. *Front Neurol*. (2020) 11:260. doi: 10.3389/fneur.2020.00260
25. Hain TC, Fetter M, Zee DS. Head-shaking nystagmus in patients with unilateral peripheral vestibular lesions. *Am J Otolaryngol*. (1987) 8:36–47. doi: 10.1016/S0196-0709(87)80017-0
26. Bock O, von Koschitzky H, Zangemeister WH. Vestibular adaptation to long-term stimuli. *Biol Cybern*. (1979) 33:77–9. doi: 10.1007/BF00355256

Conflict of Interest: The authors declare that the research was conducted in the absence of any commercial or financial relationships that could be construed as a potential conflict of interest.

frontiers in Neurology

ORIGINAL RESEARCH
published: 21 January 2021
doi: 10.3389/fneur.2020.601883

Assessment of Potential Risk Factors for the Development of Persistent Postural-Perceptual Dizziness: A Case-Control Pilot Study

Aaron Trinidade[1]*, *Paula Harman*[1], *Jon Stone*[2], *Jeffrey P. Staab*[3] and *Joel A. Goebel*[4]

[1] Southend University Hospital NHS Foundation Trust, Southend-on-Sea, United Kingdom, [2] Centre for Clinical Brain Sciences, University of Edinburgh, Edinburgh, United Kingdom, [3] Mayo Clinic, Rochester, MN, United States, [4] Washington University in St. Louis School of Medicine, St. Louis, MO, United States

OPEN ACCESS

Edited by:
Dominik Straumann,
University of Zurich, Switzerland

Reviewed by:
Habib Georges Rizk,
Medical University of South Carolina, United States
Nese Celebisoy,
Ege University, Turkey

***Correspondence:**
Aaron Trinidade
aaron.trinidade@southend.nhs.uk

Specialty section:
This article was submitted to Neuro-Otology, a section of the journal Frontiers in Neurology

Received: 01 September 2020
Accepted: 29 December 2020
Published: 21 January 2021

Citation:
Trinidade A, Harman P, Stone J, Staab JP and Goebel JA (2021) Assessment of Potential Risk Factors for the Development of Persistent Postural-Perceptual Dizziness: A Case-Control Pilot Study. Front. Neurol. 11:601883. doi: 10.3389/fneur.2020.601883

Objectives: (1) To assess whether neuroticism, state anxiety, and body vigilance are higher in patients with persistent postural-perceptual dizziness (PPPD) compared to a recovered vestibular patient group and a non-dizzy patient group; (2) To gather pilot data on illness perceptions of patients with PPPD.

Materials and Methods: 15 cases with PPPD and two control groups: (1) recovered vestibular patients ($n = 12$) and (2) non-dizzy patients (no previous vestibular insult, $n = 12$). Main outcome measures: Scores from the Big Five Inventory (BFI) of personality traits, Generalized Anxiety Disorder - 7 (GAD-7) scale, Body Vigilance Scale (BVS), Dizziness Handicap Inventory (DHI), modified Vertigo Symptom Scale (VSS) and Brief Illness Perception Questionnaire (BIPQ).

Results: Compared to non-dizzy patients, PPPD cases had higher neuroticism ($p = 0.02$), higher introversion ($p = 0.008$), lower conscientiousness ($p = 0.03$) and higher anxiety ($p = 0.02$). There were no differences between PPPD cases and recovered vestibular patients in BFI and GAD-7. PPPD cases had higher body vigilance to dizziness than both control groups and their illness perceptions indicated higher levels of threat than recovered vestibular patients.

Conclusion: PPPD patients showed statistically significant differences to non-dizzy patients, but not recovered vestibular controls in areas such as neuroticism and anxiety. Body vigilance was increased in PPPD patients when compared with both recovered vestibular and non-dizzy patient groups. PPPD patients also exhibited elements of negative illness perception suggesting that this may be the key element driving the development of PPPD. Large scale studies focusing on this area in the early stages following vestibular insult are needed.

Keywords: state anxiety, neuroticism, body vigilance, illness perceptions, PPPD

INTRODUCTION

The diagnosis *persistent postural-perceptual dizziness (PPPD)* entered the 11th edition of the World Health Organization's International Classification of Diseases (ICD-11 beta draft) in 2015 following a consensus document on its diagnostic criteria created by Bárány Society for the International Classification of Vestibular Disorders (ICVD) and the criteria for its dignosis are outlined in **Table 1** (1–3).

PPPD is a relatively new diagnosis and to date it is still not clear what predisposes some people to it following known triggers such as acute, episodic, or chronic vestibular syndromes, other neurological or medical illnesses, or psychological distress. Several authors have shown that acute anxiety and body vigilance predicted chronic dizziness after acute vestibulopathies (4–8). A prospective study found that psychological distress predicted severity of dizziness-related handicap among patients with various vestibular disorders in the 12 months following tertiary consultation (9). Neuroticism, the personality trait tendency to experience negative emotions or psychological distress in response to life events, has also been identified as a possible predisposing risk factor in both PPPD and chronic subjective dizziness (CSD), one of PPPD's precursors (10–12). In addition patients' appraisals and perceptions of their illness have been shown to influence outcomes in a range of other medical conditions including vestibular disorders (13, 14). (**Figure 1**). Apart from one study of neuroticism, however (10), these investigations were conducted prior to publication of the ICD-11 and ICVD definitions of PPPD or included patients with combinations of structural, metabolic, psychiatric, and functional causes of vestibular symptoms. As such, they offer data to formulate hypotheses about roles that psychological variables and illness perceptions may play in the developement of PPPD. Confirmation or refutation of those hypotheses requires investigations that include patients explicitly diagnosed with PPPD and carefully selected comparison groups. In addition, it is yet to be deterimined if any of these factors are associated strongly and uniquely enough with the onset of PPPD to be useful for early detection of the disorder.

As a first step in validating hypotheses about the relationship of psychological variables specifically to PPPD and with the intent of designing a prospective trial to predict patients at risk for developing this disorder, the primary aim of this current study was to gather pilot data to test the hypothesis that the frequency of anxiety-related variables is higher in patients who meet ICVD criteria for PPPD compared to those who suffered acute vestibulopathies but did not develop PPPD and patients without a history of dizziness who were receiving treatment for other medical conditions. The second aim was to gather pilot data on illness perceptions in patients with PPPD. Findings of an increased prevalence or severity of anxiety-related variables or adverse illness perceptions would provide an impetus for conducting fully-powered, prospective studies with the aim of identifying a risk profile for PPPD that could guide early interventions for patients susceptible to developing this burdensome chronic dizziness condition.

TABLE 1 | Criteria for the diagnosis of persistent postural-perceptual dizziness (PPPD) as outlined by the Committee for the Classification of Vestibular Disorders of the Bárány Society (CCBS) (1).

Criteria*	Description	Qualifiers
A	One or more symptoms of dizziness, unsteadiness, or non-spinning vertigo are present on most days for 3 months or more	1. Symptoms last for prolonged (hours long) periods of time but may wax and wane in severity 2. Symptoms need not be present continuously throughout the entire day
B	Persistent symptoms occur without specific provocation, but are exacerbated by three factors:	1. Upright posture, 2. Active or passive motion without regard to direction or position, or 3. Exposure to moving visual stimuli or complex visual patterns
C	The disorder is precipitated by conditions that cause vertigo, unsteadiness, dizziness, or problems with balance including acute, episodic, or chronic vestibular syndromes, other neurological or medical illnesses, or psychological distress	1. When the precipitant is an acute or episodic condition, symptoms settle into the pattern of criterion A as the precipitant resolves, but they may occur intermittently at first, and then consolidate into a persistent course 2. When the precipitant is a chronic syndrome, symptoms may develop slowly at first and worsen gradually
D	Symptoms cause significant distress or functional impairment	
E	Symptoms are not better accounted for by another disease or disorder	

**All five criteria A–E must be fulfilled to make the diagnosis of PPPD.*

METHODOLOGY

The study was conducted as a case-control observational study (www.clinicaltrials.gov, reference NCTO3930485, with ethical approval from South West—Cornwall & Plymouth Research Ethics Committee). All participants (both cases and controls) were aged ≥18 years old and were able to provide informed consent. Any participants who were <18 years old and unable to provide informed consent were excluded from the study.

Data Collected

All participants (cases, recovered group and healthy group) provided written informed consent before then being asked to complete the Big Five Inventory (BFI) of personality traits, the Generalized Anxiety Disorders-7 (GAD-7) Scale, the Body Vigilance Scale (BVS), the Dizziness Handicap Inventory (DHI), the short form of the Vertigo Symptom Scale (VSS), and the Brief Illness Perception Questionnaire (BIPQ). The BFI consists of 44 questions that assess the five core human personality traits of neuroticism (tendency toward pessimistic worry), extraversion (outgoing nature), openness (to new ideas and experiences),

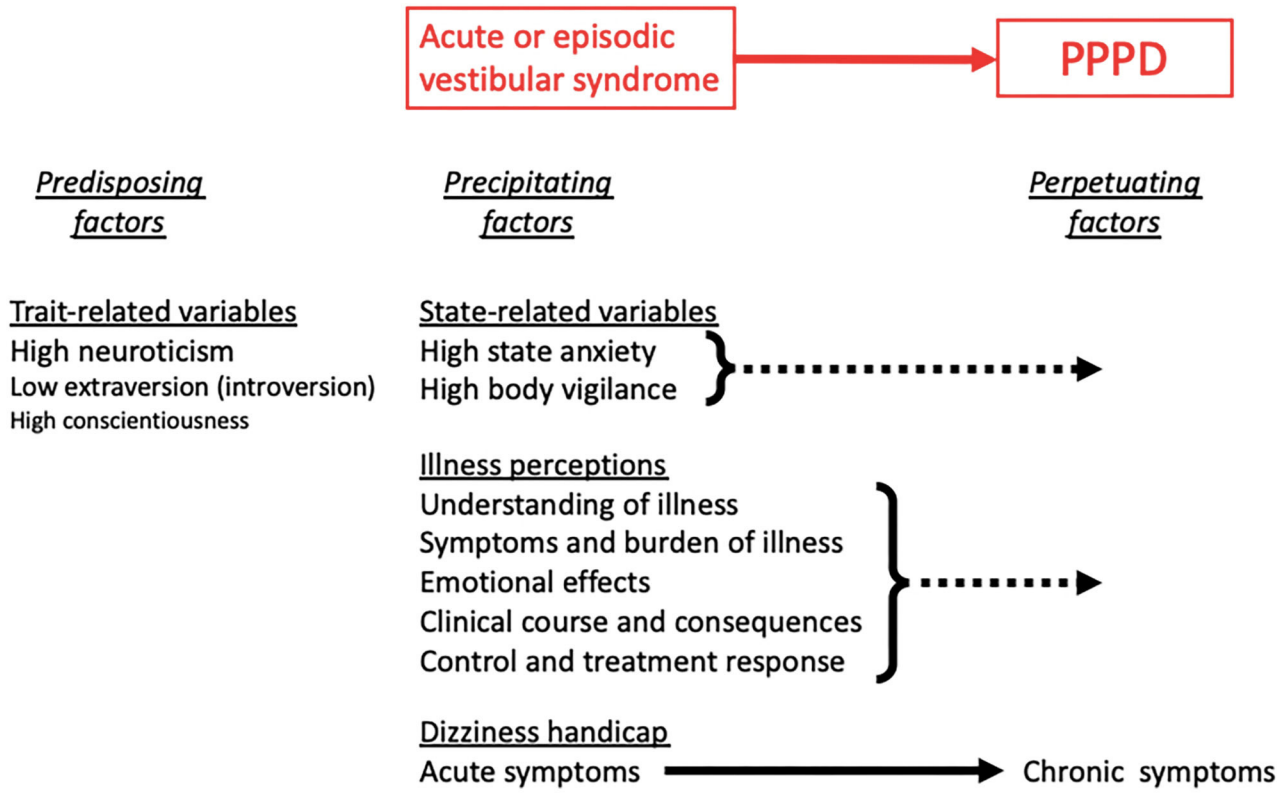

FIGURE 1 | Potential risk factors for PPPD include, from left to right, anxiety-related personality traits (primarily neuroticism and introversion) that predate the onset of vestibular symptoms, high levels of state anxiety and body vigilance that coincide with the onset of vestibular symptoms, and adverse illness perceptions and dizziness-related handicap that emerge as the course of illness progresses toward PPPD rather than recovery.

agreeableness (affability and warmth), and conscientiousness (diligence and dutifulness) and provides standardized scores against population norms. Testers respond to the questions with degrees of agreement or disagreement on a five-point Likert scale. For each personality trait, a mean score of higher than 2.5 suggests a tendency toward that trait. The GAD-7 consists of seven questions that measure the severity of state anxiety. The BVS consists of four questions: the first three measure sensitivity and attentiveness to bodily sensations in general; the fourth question measures attentiveness to 15 specific somatic symptoms, including five that are germane to patients with vestibular disorders (dizziness, nausea, faintness, feelings of unreality, and feelings detached from one's self). Testers respond to the questions on an 11 point Likert-like scale ranging from 0 (Not at all like me) to 10 (Extremely like me). A mean score higher than 5.0 suggests a tendency toward strong agreement with the question. The BVS total score is the sum of the answers to questions one to four. The DHI contains 25 questions that measure the severity of handicap due to dizziness-related physical and emotional symptoms and interference with functioning. The short form VSS includes 15 questions, eight that measure severity of vertiginous symptoms and seven that measure severity of associated autonomic/anxiety symptoms. The BIPQ consists of nine questions that assess respondents' understanding, emotional response, and sense of control of their illness, as well as concerns about its causes, consequences, clinical course, and likelihood of treatment response. The DHI, VSS, and BIPQ were administered to the PPPD group only as they were the only ones with active dizziness symptoms required to make sense of the questionnaires.

Statistical Analysis (Performed Using SPSS Statistics v26)

Statistical analyses were confined to valid outputs from the questionnaires that tested our hypotheses. As the DHI, VSS, and GAD-7 have not been validated for item-by-item analyses and the BIPQ has no total score, analyses were limited to: BFI—scores for the 5 factors; GAD-7—total score only; BVS—individual item scores; DHI—total score only; VSS—total and two subscale scores; BIPQ—individual items only.

BFI, GAD-7, and BVS

Each variable was checked for normality (skewness, kurtosis, Shapiro-Wilk's test), however very few of the variables were normally distributed. Due to this, and the low sample size, non-parametric tests were used. Due to having three independent variables (cases, recovered group, healthy group), an Independent-Samples Kruskal-Wallis test was performed. If a statistically significant result was found, then a *post hoc* pairwise

comparison was conducted to determine which of the study groups were statistically different from each other. Statistical significance was determined at $p < 0.05$. Significance values for pairwise comparisons were adjusted using Bonferroni correction for multiple tests and were reported as their adjusted values. Effect sizes, η^2, were calculated from the Kruskal-Wallis H-value and were interpreted per usual convention as $\eta^2 < 0.06$ (small), $0.06 \leq \eta^2 < 0.14$ (medium), and $\eta^2 \geq 0.14$ (large).

RESULTS

Recruitment

Cases

The clinical care team at the Department of Otolaryngology, Southend University Hospital NHS Foundation Trust reviewed medical records of current and past patients who were evaluated between January 2019 and January 2020. Eighteen patients who had been given a diagnosis of PPPD in accordance with ICVD criteria (**Table 1**) during that time period were consecutively asked to take part in the study. All 18 agreed to participate but only 15 completed and returned the questionnaire (see below). These 15 patients were included in the PPPD group with the three non-responders being excluded from the study.

Controls

Two sex- and age-matched (±5 years) comparison groups were identified. The first group consisted of patients who had sustained a peripheral vestibular insult but did not develop PPPD (recovered vestibular patient controls). Participants in this group were all consecutively recruited from the dizziness and balance clinic, deemed to have recovered from their vestibular insult and not progressed to PPPD. To be included as a recovered vestibular patient control, patients had to confirm that they had not experienced any vertigo or dizziness within the last year and were currently asymptomatic. As labyrinthine function and symptoms in recovered vestibular patients correlate poorly (15, 16), it was not deemed necessary to subject controls within this group to further vestibular function testing. Confirmation of an asymptomatic state was taken as evidence of full compensation from previous vestibular insult.

The second group consisted of patients from both the general ENT clinic and other non-ENT clinics who had never sustained a vestibular insult (non-dizzy patient controls). This group included any patient who was being followed up for a non-vestibular condition. Patients were asked whether they had ever experienced vertigo and dysequilibrium in the past or whether they had ever been diagnosed with a condition that could cause vertigo and only those who had not were asked to participate. The conditions that these patients were being followed up for included rhinitis ($n = 2$), otitis externa ($n = 1$), tinnitus ($n = 1$), epistaxis ($n = 1$), tympanic membrane perforation ($n = 1$), single-sided deafness ($n = 1$), chronic back pain ($n = 1$), knee osteoarthritis ($n = 1$), deep vein thrombosis ($n = 1$), anal polyps ($n = 1$) and COPD ($n = 1$). The purpose of the non-dizzy comparison group was to control for the state of being ill vs. being healthy. The psychological measures that were investigated are potentially affected by overall health status but vary little with respect to specific types of medical illness.

Demographics

Fifteen PPPD cases (13 (86.7%) females and two males, with a mean age was 63.7 years) were matched with 12 recovered vestibular controls (10 females (83.3%), mean age 63.8 years) and 12 non-dizzy controls (10 females (83.3%), mean age 62.6 years). The mean duration from diagnosis of PPPD was 5.7 months (range: 0−13 months) and the mean duration of PPPD symptoms was 79.5 months (range: 8−300 months). In the PPPD group vestibular neuronitis (VN) and benign paroxysmal positional vertigo (BPPV) were the two most common triggers (both: $n = 4$, 26.7%), followed by Ménière's disease ($n = 3$, 20%), psychological distress ($n = 3$, 20%) and gentamicin-induced vestibular failure ($n = 1$, 6.7%). Of the three patients who developed PPPD following psychological distress, all three cited bereavement of a spouse ($n = 2$) or parent ($n = 1$) as the trigger of their symptoms. One third of the group were on psychiatric medication. (See **Table 2**) The vestibular insults in the recovered vestibular group were BPPV ($n = 6$, 50%), VN ($n = 4$, 33.3%), Ménière's disease (treated with intratympanic gentamicin therapy; $n = 1$) and vestibular schwannoma (managed with stereotactic radiotherapy; $n = 1$).

Big Five Inventory

There was a statistically significant difference between the three study groups in neuroticism ($p = 0.01$; $\eta^2 = 0.16$, large effect), extroversion ($p = 0.01$, $\eta^2 = 0.20$, large effect), and conscientiousness ($p = 0.03$; $\eta^2 = 0.14$, large effect), but not openness ($p = 0.4$). Agreeableness trended toward a significant difference ($p = 0.09$) with a low medium effect; $\eta^2 = 0.08$. Pairwise comparison revealed that these results were largely due to differences between patients with PPPD and non-dizzy controls. Patients with PPPD had higher neuroticism than non-dizzy controls ($p = 0.02$; $\eta^2 = 0.43$, large effect) whilst non-dizzy controls were more extroverted ($p = 0.008$; $\eta^2 = 0.49$, large effect) and more conscientious ($p = 0.03$; $\eta^2 = 0.41$, large effect) than patients with PPPD. A pairwise comparison between patients with PPPD and recovered vestibular controls for neuroticism approached significance ($p = 0.05$). The effect size, $\eta^2 = 0.38$, was large indicating a clinically meaningful difference that a larger sample would have revealed as statistically significant) (See **Table 3**).

Generalized Anxiety Disorders-7

With respect to the overall GAD-7 score, there was a statistically significant difference among groups ($p < 0.02$; $\eta^2 = 0.18$, large effect). The mean score for PPPD cases was 10.6; for recovered vestibular controls was 4.6; for non-dizzy controls was 4.1. Pairwise analysis showed that PPPD cases were statistically significantly more anxious than non-dizzy controls ($p = 0.02$; $\eta^2 = 0.43$, large effect) and trended toward a difference from recovered vestibular controls ($p = 0.07$); Again, a large effect size, $\eta^2 = 0.49$, suggested a clinically meaningful difference that missed statistical significance due to the sample size.

TABLE 2 | Demographic data of cases with PPPD.

Cases	Age	Sex	Duration of PPPD symptoms (months)	Precitipating condition	Psychiatric medications
1	78	F	300	BPPV	None
2	34	F	10	Vestibular neuronitis	None
3	67	F	14	Vestibular neuronitis	Fluoxetine
4	69	M	21	Psychological distress	None
5	69	F	8	Psychological distress	Sertraline
6	82	F	14	BPPV	None
7	73	F	9	Gentamicin-induced vestibular failure	None
8	69	F	18	Ménière's disease	None
9	61	F	21	Vestibular neuronitis	None
10	59	F	300	Ménière's disease	Amitriptyline, duloxetine, quetiapine
11	63	F	132	Psychological distress	None
12	49	F	108	Ménière's disease	None
13	47	F	216	BPPV	Fluoxetine
14	70	M	14	BPPV	Sertraline
15	65	F	8	Vestibular neuronitis	None
Mean	**62.6**		**79.5**		

TABLE 3 | Big Five Inventory–Patients with PPPD patients and comparison groups.

Domain	Group	Mean	Std. Error	Mean Ranks	Kruskal-Wallis test Sig. (*p*)	Pairwise Sample	Sig. (*p*)	Adj. sig* (*p*)
Agreeableness	PPPD (15)	3.9	0.13	15.63	0.09	RC[a]-HC[b]	–	–
	RC (12)	4.1	0.15	20.2		RC-PPPD	–	–
	HC (12)	4.4	0.2	27.1		HC-PPPD	–	–
Extraversion	PPPD (15)	2.7	0.2	13.9	0.01	RC-HC	0.15	0.46
	RC (12)	3.4	0.2	20.5		RC-PPPD	0.13	0.4
	HC (12)	3.8	0.1	27.1		HC-PPPD	**0.003**	**0.008**
Conscientiousness	PPPD (15)	3.6	0.2	14.2	0.03	RC-HC	0.5	1.0
	RC (12)	4.1	0.1	22.0		RC-PPPD	0.08	0.23
	HC (12)	4.2	0.1	25.3		HC-PPPD	**0.01**	**0.03**
Openness	PPPD (15)	3.2	0.2	17.3	0.4	RC-HC	–	–
	RC (12)	3.4	0.2	19.9		RC-PPPD	–	–
	HC (12)	3.6	0.2	23.5		HC-PPPD	–	–
Neuroticism	PPPD (15)	3.5	0.2	26.8	0.01	RC-HC	0.8	1.0
	RC (12)	2.6	0.2	16.4		RC-PPPD	**0.02**	**0.05**
	HC (12)	2.5	0.2	15.1		HC-PPPD	**0.008**	**0.02**

**significance values adjusted by Bonferroni correction for multiple tests.*
[a]RC–Recovered Controls (recovered vestibular patients).
[b]HC–Healthy Controls (non-dizzy patients).
The bold values represent statistically significant results.

Body Vigilance Scale

There was a statistically significant difference among the study groups in the scores of two subsets of question 4 of the BVS pertaining to how much attention was paid to specific body sensations: feelings of dizziness ($p < 0.0001$; $\eta^2 = 0.58$, large effect) and unreality ($p = 0.02$; $\eta^2 = 0.15$, large effect). In pairwise comparisons, PPPD cases were found to pay more attention to feelings of dizziness than both control group (vs. recovered vestibular controls: $p = 0.002$, $\eta^2 = 0.53$, large effect; vs. non-dizzy controls: $p < 0.0001$, $\eta^2 = 0.72$, large effect) and to feelings of unreality than non-dizzy controls: $p = 0.02$, $\eta^2 = 0.36$, large effect) (See **Table 4**).

Brief Illness Perception Questionnaire

Patients with PPPD agreed quite strongly that PPPD affected their life severely and generally felt that it would last a long time. There was a slightly weaker tendency for patients to indicate feeling like they had no control over their illness and that the treatment they were on for PPPD was unlikely to help their symptoms. There were stronger tendencies for patients with PPPD to consider that their symptoms were severe, concerning, and affecting them emotionally. However, they tended to agree that they understood their illness. When asked to rank the three most likely factors causing their problem, only one third of the patients listed psychological problems, although the wording

TABLE 4 | Body Vigilance Scale (BVS)–Patients with PPPD patients and comparison groups.

	Group	Mean	Std. Error	Mean Ranks	Kruskal-Wallis test Sig. (*p*)	Pairwise Sample	Sig. (*p*)	Adj. sig* (*p*)
Q1. "I am the kind of person who pays close attention to internal body sensations."	PPPD (15)	6.1	0.5	25.9	0.04	RC-HC	0.92	1.0
	RC[a] (12)	3.5	0.9	16.1		RC-PPPD	0.03	0.08
	HC[b] (12)	3.6	1.0	16.5		HC-PPPD	0.03	0.1
Q2. "I am very sensitive to **changes** in my internal body sensations."	PPPD (15)	5.5	0.7	23.7	0.3	RC-HC	–	–
	RC (12)	3.5	0.9	17.0		RC-PPPD	–	–
	HC (12)	4.0	1.2	18.4		HC-PPPD	–	–
Q3. On average, **how much time** do you spend each day scanning your body for sensations?	PPPD (15)	29.3	7.3	25.5	0.03	RC-HC	0.9	1.0
	RC (12)	6.7	3.6	16.8		RC-PPPD	0.03	0.09
	HC (12)	9.2	6.1	16.3		HC-PPPD	0.02	0.07
Q4. Rate how much attention you pay to each of the following sensations using this scale:								
Q4.1. heart palpitations	PPPD (15)	3.3	1.0	21.7	0.6	RC-HC	–	–
	RC (12)	2.9	1.0	20.7		RC-PPPD	–	–
	HC (12)	2.2	0.9	17.3		HC-PPPD	–	–
Q4.2. chest pain/discomfort	PPPD (15)	3.5	1.0	23.4	0.2	RC-HC	–	–
	RC (12)	2.4	1.0	19.6		RC-PPPD	–	–
	HC (12)	1.3	0.7	16.2		HC-PPPD	–	–
Q4.3. numbness	PPPD (15)	3.5	1.0	22.9	0.3	RC-HC	–	–
	RC (12)	2.3	0.7	20.3		RC-PPPD	–	–
	HC (12)	1.4	0.8	16.1		HC-PPPD	–	–
Q4.4. tingling	PPPD (15)	3.5	1.0	23.9	0.2	RC-HC	–	–
	RC (12)	1.7	0.6	17.6		RC-PPPD	–	–
	HC (12)	1.7	0.8	17.5		HC-PPPD	–	–
Q4.5. shortness of breath/smothering	PPPD (15)	4.2	1.1	22.2	0.6	RC-HC	–	–
	RC (12)	2.8	1.0	18.3		RC-PPPD	–	–
	HC (12)	3.0	1.0	19.0		HC-PPPD	–	–
Q4.6. faintness	PPPD (15)	3.6	1.0	23.5	0.2	RC-HC	–	–
	RC (12)	2.0	0.7	19.7		RC-PPPD	–	–
	HC (12)	1.4	0.9	16.0		HC-PPPD	–	–
Q4.7. vision changes	PPPD (15)	4.7	0.8	23.5	0.3	RC-HC	–	–
	RC (12)	2.9	0.8	17.3		RC-PPPD	–	–
	HC (12)	3.2	1.1	18.3		HC-PPPD	–	–
Q4.8. feelings of unreality	PPPD (15)	3.1	0.9	25.1	0.02	RC-HC	0.4	1.0
	RC (12)	0.8	0.4	18.5		RC-PPPD	0.08	0.2
	HC (12)	0.8	0.8	15.1		HC-PPPD	**0.008**	**0.02**
Q4.9. feeling detached from self	PPPD (15)	3.2	0.9	24.6	0.1	RC-HC	–	–
	RC (12)	0.7	0.3	17.3		RC-PPPD	–	–
	HC (12)	1.7	1.0	17.0		HC-PPPD	–	–
Q4.10. dizziness	PPPD (15)	8.2	0.5	30.2	0.0	RC-HC	0.3	0.8
	RC (12)	2.2	0.9	16.0		RC-PPPD	**0.001**	**0.002**
	HC (12)	0.8	0.8	11.2		HC-PPPD	**0.0**	**0.0**
Q4.11. hot flash	PPPD (15)	3.7	1.0	22.9	0.2	RC-HC	–	–
	RC (12)	1.3	0.8	15.8		RC-PPPD	–	–
	HC (12)	3.1	1.0	20.6		HC-PPPD	–	–
Q4.12. sweating/clammy hands	PPPD (15)	2.7	0.9	21.7	0.7	RC-HC	–	–
	RC (12)	1.5	0.8	18.1		RC-PPPD	–	–
	HC (12)	2.3	0.9	19.8		HC-PPPD	–	–

(Continued)

TABLE 4 | Continued

	Group	Mean	Std. Error	Mean Ranks	Kruskal-Wallis test Sig. (*p*)	Pairwise Sample	Sig. (*p*)	Adj. sig* (*p*)
Q4.13. upset stomach	PPPD (15)	4.1	0.9	23.7	0.2	RC-HC	–	–
	RC (12)	1.9	0.8	15.7		RC-PPPD	–	–
	HC (12)	3.2	1.0	19.6		HC-PPPD	–	–
Q4.14. nausea	PPPD (15)	3.5	0.8	24.1	0.1	RC-HC	–	–
	RC (12)	2.8	1.0	20.2		RC-PPPD	–	–
	HC (12)	1.1	0.7	14.6		HC-PPPD	–	–
Q4.13. choking/throat closing	PPPD (15)	4.0	1.0	24.8	0.1	RC-HC	–	–
	RC (12)	1.8	0.9	17.9		RC-PPPD	–	–
	HC (12)	1.3	0.8	16.1		HC-PPPD	–	–

**significance values adjusted by Bonferroni correction for multiple tests.*
[a]RC–Recovered Controls (recovered vestibular patients).
[b]HC–Healthy Controls (non–dizzy patients).
The bold values represent statistically significant results.

TABLE 5 | Brief Illness Perception Questionnaire (BIPQ)–descriptive statistics for PPPD cases.

	N	Mean	Std. Deviation
Q1. How much does your illness affect your life? (0 = no affect at all, 10 = severely affects my life)	15	7.4	2.6
Q2. How long do you think your illness will continue? (0 = a very short time,; 10 = forever)	14	8.5	2.4
Q3. How much control do you feel you have over your illness? (0 = absolutely no control, 10 = extreme amount of control)	15	4.1	4.0
Q4. How much do you think your treatment can help your illness? (0 = not at all; 10 = extremely helpful)	14	4.2	3.0
Q5. How much do you experience symptoms from your illness? (0 = no symptoms at all; 10 = many severe symptoms)	15	6.3	2.9
Q6. How concerned are you about your illness? (0 = not at all concerned; 10 = extremely concerned)	15	6.8	3.3
Q7. How well do you feel you undertand your illness? (0 = don't understand at all, 10 = understand very clearly)	15	6.1	3.2
Q8. How much does your illness affect you emotionally? (0 = not at all affected emotionally; 10 = extremely affected emotionally)	15	6.9	2.9
Q9. List in rank order the three most important factors that you believe caused your illness	Factor 1	Factor 2	Factor 3
Case 1	Blocked ears	Vertigo	–
Case 2	Heart problem	Low BP	Head injury
Case 3	Labyrinthitis	–	–
Case 4	Anxiety	Poor hearing	Anger
Case 5	Grief	Depression	Anxiety
Case 6	–	–	–
Case 7	Gentamicin	–	–
Case 8	Stress	Tiredness	Migraines
Case 9	Viral infections	Labyrinthitis	Stress
Case 10	Head trauma	Disastrous life	–
Case 11	Mother's death	Father's cancer	Quit smoking
Case 12	Ménière's disease	–	–
Case 13	Labyrinthitis	–	–
Case 14	–	–	–
Case 15	Thunderclap headaches	Delay in BPPV treatment	–

could have been interpreted as the initial trigger rather than the current mechanism of the symptoms (**Table 5**).

DHI and VSS

The mean total DHI score was 29.3/100 (range: 11−43, s.d. = 9.8), which is at the upper border of the mild range (0−30) on this questionnaire [Whitney et al. (17)]. The mean total VSS score was 28.7 (range: 10−49; s.d. = 10.8).

Post-hoc Analysis

A *post-hoc* analysis was performed on the data set for BFI, GAD-7, and BVS after removing cases who developed PPPD following psychological trauma ($n = 3$), leaving a more homogeneous subgroup of 12 patients who developed PPPD following peripheral vestibular illnesses, in total (11 females, one male; mean age 62.8 years; mean months from diagnosis, six; mean duration of symptoms, 86 months). All controls (12 recovered vestibular controls and 12 non-dizzy controls) were kept in the data set. The focus of this sub-analysis was therefore on structural vestibular triggers of PPPD likely to present to the ENT surgeon. The statistical treatment of this data set was identical to that of the original data set. The *post-hoc* analysis showed a statistically significant result in one question of the BVS only: PPPD patients were found to pay more attention to feelings of dizziness than both control groups (vs. recovered vestibular controls: $p = 0.007$; vs. non-dizzy controls: $p < 0.0001$). There were no statistically significant differences between patients who developed PPPD after a vestibular illness and either control group with respect to the BFI or GAD-7 questionnaires.

DISCUSSION

The processes thought to give rise to and then drive PPPD are a combination of those described for its precursors, namely phobic postural vertigo, space-motion discomfort, visual vertigo and chronic subjective dizziness (1). Anxiety and anxiety-related personality traits, in particular neuroticism, have been described as possible predisposing factors, making the affected individual prone to a hypervigilant state of increased introspective self-monitoring that arises from fear of further attacks of vertigo or the consequences of being dizzy during or following the episode of acute vestibular disease (7, 10, 11, 18–25). Yagi et al. (26) have recently developed a PPPD severity questionnaire (the Niigata PPPD Questionnaire) that reflects the diagnostic criteria of PPPD (26). Even more recently, Powell et al. (27) describe PPPD as a complex neurological condition that includes broad perceptual factors and suggest that some individuals' brains are predisposed to generalized cross-modal sensory-overload, giving rise to vulnerability to severe PPPD should a vestibular insult occur (27). What remains to be determined is whether pre-existing psychological risk factors can help in predicting who might be at risk of developing PPPD after an acute vestibular injury, thus allowing for the institution of early treatment (3).

Neuroticism is thought to be one of the key risk factors for the development of PPPD and refers to relatively stable tendencies to respond with negative emotions to threat, frustration or loss (28). Individuals who score highly on the BFI for neuroticism are more prone to anxiety amongst other negative emotions. In a functional MRI (fMRI) study by Indovina et al. (29) it was shown that reduced activation in human analogs of the parieto-insular vestibular cortex (PIVC), hippocampus, anterior insula, inferior frontal gyrus and anterior cingulate cortex, as well as connectivity changes among these regions, may be linked to long-term vestibular symptoms in patients with CSD (29). Also in a fMRI study, Ricelli et al. (30) showed that individual differences in neuroticism were significantly associated with changes in the activity and functional connectivity patterns within visuo-vestibular and anxiety-related systems during simulated vertical self-motion (30). Similarly, Passamonti et al. (31) have shown neuroticism to increase the activity and connectivity of neural networks that mediate attention to visual motion cues during vertical motion. They suggest that this mechanism may mediate visual control of balance in neurotic patients with PPPD (31). In our study, PPPD patients were found to be more neurotic than healthy controls. When compared with recovered controls, the result approached significance only, though the effect size calculation indicated that this negative finding many have been a Type II error given our small sample size. Our study also showed PPPD patients to be more introverted and less conscientious than non-dizzy controls, in keeping with previous research findings by Staab et al. (10) with respect to chronic subjective dizziness (10).

Anxiety is a crucial factor in persisting dizziness (4). The prevalence of anxiety in PPPD has been the focus of one of the treatment modalities, namely cognitive behavioral therapy (CBT) (32). Toshishige et al. (33) have recently demonstrated in a study of 34 patients with PPPD that the presence of comorbid anxiety disorders predicted a considerable improvement of DHI scores from pre-treatment to 6-month following CBT (33). Our data showed a significant difference in anxiety levels between PPPD cases and non-dizzy controls. The comparison with recovered vestibular controls did not reach statistical significance, but again the effect size pointed to a Type II error.

It is interesting that the primary comparisons of all PPPD cases to recovered vestibular controls and the *post-hoc* analysis limited to cases of PPPD following vestibular illnesses found no significantly greater neuroticism or anxiety in those with PPPD. It may be that in a larger cohort, both factors would be significantly higher in PPPD.

Alongside anxiety, a high BVS in the setting of acute vestibular disorders has been shown to predict persistent PPPD-like dizziness far better than measures of structural vestibular deficits (4–7, 32). In a prospective longitudinal study, Heinrichs et al. (5) assessed fear of bodily sensations and cognitions related to anxiety at the time of hospital admission and 3 months later in 43 patients with an episode of VN or BPPV. They showed that the interaction between fear of bodily sensations within the first 2 weeks after admission and the type of vestibular disorder predicted the extent of dizzy complaints 3 months later (5). Our study reflects these findings, with attention to a feeling of dizziness being found to be highly statistically significant in PPPD with respect to the BVS when compared with both control groups. Our *post-hoc* analysis also supports this notion by demonstrating the importance of heightened body vigilance even in a group of patients developing PPPD after vestibular insult.

There is evidence in other areas of medicine that supports the notion that negative illness perception is independently linked to all-cause mortality and can strongly influence recovery from illness which can be slower than in other patients (34–36). Illness perception is seen as an important and potentially modifiable risk factor to target in future disease interventions and intervention has already been shown to reduce illness anxiety, which has relevance in this study (35, 37). One interesting finding in our study is that despite PPPD patients being found to be more neurotic and anxious than healthy controls, only one third of them felt that psychological factors were contributing to their symptoms. This shows similarities to other functional disorders. In a controlled study of 107 patients with functional weakness, Stone et al. (38) showed that these patients tend to reject psychological factors as potentially causal factors (38). They also demonstrated similar findings, though to a lesser degree, in patients with non-epileptic seizures (39). In PPPD, one potential for this finding may be due to the fact that whilst patients experience their dizziness most of the time, they may not necessarily attribute their symptoms to anxiety-related factors or may consider anxiety to be a secondary consequence rather than a contributor to their symptoms. Stigmatization of mental health issues could also play a role, especially in male patients. Targeted patient education on the central role anxiety plays in PPPD could help in addressing this misperception and improving illness perception.

The results of this study support hypotheses derived from investigations of the predecessors of PPPD that anxiety-related factors play important roles in promoting the development of the disorder following conditions that cause vestibular symptoms or disturb balance function, including acute vestibular disorders. However, these results offer a sharper focus, suggesting specifically that heighted body vigilance about dizziness and adverse perceptions of illness may distinguish patients likely to develop PPPD from those more likely to recover from acute illnesses without clinically significant sequelae.The ultimate goal of this line of research is to develop a risk profile that can be used reliably to identify patients susceptible to PPPD so that they may receive early and hopefully preventative interventions. Such a profile is likely to consist of clinical variables present at the time of an acute vestibulopathy (e.g., anxiety-related personality traits, state anxiety) and ones that emerge in the immediate aftermath of acute illness before the onset of chronic morbidity (e.g., adverse illness perceptions).

Study Limitations

The participant numbers in this exploratory study were small, so no conclusions may be drawn from the results. However, the investigation accomplished its stated objective by gathering pilot data from patients explicitly diagnosed with PPPD to inform the design of more definitive investigations of risk factors and potential early indicators of the disorder.

The study was retrospective and carried with it the inherent problems associated with retrospective studies. Whilst a systematic data collection method was employed, it was collected from patients after they had developed PPPD and at differing times from the onset, thus representing a heterogeneous group.

In our main analysis, PPPD cases were included regardless of their initiating insult, vestibular or otherwise, despite all members of the recovered group having a history of vestibular insult only. This is because the ICVD criteria do not sub-categorize PPPD by type of precipitating event. Our *post-hoc* analysis suggested that this may have had an effect on our results as the comparisons limited to patients who developed PPPD following a vestibular disorder identified a narrower range of differences than the full PPPD cohort compared to recovered controls. Potential differences in risk factors for the development of PPPD following different precipitants merits future study.

Interestingly, our PPPD group was older and consisted of more women than most other reports of PPPD and CSD. This may reflect differences in referrals patterns to various clinical centers around the world and might make our data uncomparable with other studies.

CONCLUSION

The data gathered in this pilot study support the design and conduct of fully powered prospective investigations of neuroticism, state anxiety, body vigilance and aberrant illness perceptions as risk factors and contributors to the onset of PPPD that could be formulated into a risk profile to be used for early detection of the disorder in clinical practice.

DATA AVAILABILITY STATEMENT

The raw data supporting the conclusions of this article will be made available by the authors, without undue reservation.

ETHICS STATEMENT

The studies involving human participants were reviewed and approved by South West – Cornwall & Plymouth Research Ethics Committee. The patients/participants provided their written informed consent to participate in this study.

AUTHOR CONTRIBUTIONS

AT was the principal investigator and responsible for the study design, conducting the study, data collection, and preparation of the manuscript. PH was responsible for liaison with study participants, liaising with research and development and ethics departments, conducting the study, supervision of study flow, data processing and analysis and manuscript editing, and proofreading. JS, JPS, and JG were responsible for study design, supervision of the study and manuscript editing, and proofreading. All authors contributed to the article and approved the submitted version.

REFERENCES

1. Staab JP, Eckhardt-Henn A, Horii A, Jacob R, Strupp M, Brandt T, et al. Diagnostic criteria for persistent postural-perceptual dizziness (PPPD): consensus document of the committee for the Classification of Vestibular Disorders of the Bárány Society. *J Vestib Res*. (2017) 27:191–208. doi: 10.3233/VES-170622
2. World Health Organization. *International Classification of Diseases, 11th Edition Beta Version Draft (ICD-11 Beta), Definition of Persistent Postural-Perceptual Dizziness*. Available online at: https://icd.who.int/dev11/l-m/en#/http%3a%2f%2fid.who.int%2ficd%2fentity%2f2005792829 (accessed March 11, 2018).
3. Trinidade A, Goebel JA. Persistent postural-perceptual dizziness (PPPD) – a systematic review of the literature for the balance specialist. *Otol Neurotol*. (2018) 39:1291–303. doi: 10.1097/MAO.0000000000002010
4. Godemann F, Siefert K, Hantschke-Brüggemann M, Neu P, Seidl R, Ströhle A. What accounts for vertigo one year after neuritis vestibularis - anxiety or a dysfunctional vestibular organ? *J Psychiatr Res*. (2005) 39:529–34. doi: 10.1016/j.jpsychires.2004.12.006
5. Heinrichs N, Edler C, Eskens S, Mielczarek MM, Moschner C. Predicting continued dizziness after an acute peripheral vestibular disorder. *Psychosom Med*. (2007) 69:700–7. doi: 10.1097/PSY.0b013e318151a4dd
6. Cousins S, Kaski D, Cutfield N, Arshad Q, Ahmad H, Gresty MA, et al. Predictors of clinical recovery from vestibular neuritis: a prospective study. *Ann Clin Transl Neurol*. (2017) 4:340–6. doi: 10.1002/acn3.386
7. Best C, Tschan R, Eckhardt-Henn A, Dieterich M. Who is at risk for ongoing dizziness and psychological strain after a vestibular disorder? *Neuroscience*. (2009) 164:1579–87. doi: 10.1016/j.neuroscience.2009.09.034
8. Staab JP. Persistent postural-perceptual dizziness. *Semin Neurol*. (2020) 40:130–7. doi: 10.1055/s-0039-3402736
9. Probst T, Dinkel A, Schmid-Mühlbauer G, Radziej K, Limburg K, Pieh C, et al. Psychological distress longitudinally mediates the effect of vertigo symptoms on vertigo-related handicap. *J Psychosom Res*. (2017) 93:62–8. doi: 10.1016/j.jpsychores.2016.11.013
10. Staab JP, Rohe DE, Eggers SD, Shepard NT. Anxious, introverted personality traits in patients with chronic subjective dizziness. *J Psychosom Res*. (2014) 76:80–3. doi: 10.1016/j.jpsychores.2013.11.008
11. Yan Z, Cui L, Yu T, Liang H, Wang Y, Chen C. Analysis of the characteristics of persistent postural-perceptual dizziness: a clinical-based study in China. *Int J Audiol*. (2017) 56:33–7. doi: 10.1080/14992027.2016.1211763
12. Chiarella G, Petrolo C, Riccelli R, Giofrè L, Olivadese G, Gioacchini FM, et al. Chronic subjective dizziness: analysis of underlying personality factors. *J Vestib Res*. (2016) 26:403–8. doi: 10.3233/VES-160590
13. Broadbent E, Petrie KJ, Main J, Weinman J. The brief illness perception questionnaire. *J Psychosom Res*. (2006) 60:631–7. doi: 10.1016/j.jpsychores.2005.10.020
14. Wolf J, Sattel H, Limburg K, Lahmann C. From illness perceptions to illness reality? Perceived consequences and emotional representations relate to handicap in patients with vertigo and dizziness. *J Psychosom Res*. (2020) 130:109934. doi: 10.1016/j.jpsychores.2020.109934
15. Manzari L, Burgess AM, MacDougall HG, Curthoys IS. Vestibular function after vestibular neuritis. *Int J Audiol*. (2013) 52:713–8. doi: 10.3109/14992027.2013.809485
16. Kim YH, Kim KS, Kim KJ, Choi H, Choi JS, Hwang IK. Recurrence of vertigo in patients with vestibular neuritis. *Acta Otolaryngol*. (2011) 131:1172–7. doi: 10.3109/00016489.2011.593551
17. Whitney SL, Wrisley DM, Brown KE, Furman JM. Is perception of handicap related to functional performance in persons with vestibular dysfunction? *Otol Neurotol*. (2004) 25:139–43. doi: 10.1097/00129492-200403000-00010
18. Whalley MG, Cane DA. A cognitive-behavioral model of persistent postural-perceptual dizziness. *Cogn Bahav Pract*. (2017) 24:72–89. doi: 10.1016/j.cbpra.2016.03.003
19. Dieterich M, Staab JP. Functional dizziness: from phobic postural vertigo and chronic subjective dizziness to persistent postural-perceptual dizziness. *Curr Opin Neurol*. (2017) 30:107–13. doi: 10.1097/WCO.0000000000000417
20. Popkirov S, Staab JP, Stone J. Persistent postural-perceptual dizziness (PPPD): a common, characteristic and treatable cause of chronic dizziness. *Pract Neurol*. (2018) 18:5–13. doi: 10.1136/practneurol-2017-001809
21. Horii A. Anxiety, depression and persistent perceptual postural dizziness: international classification of vestibular disorders by Bárány Society. *Equilibrium Res*. (2017) 76:316–22. doi: 10.3757/jser.76.316
22. Yu Y, Xue H, Zhang Y, Zhou J. Cognitive behaviour therapy as augmentation for sertraline for treating patients with persistent postural-perceptual dizziness. *BioMed Res Int*. (2018)2018:8518631. doi: 10.1155/2018/8518631
23. Holmberg J, Karlberg M, Harlacher U, Magnusson M. Experience of handicap and anxiety in phobic postural vertigo. *Acta Otolaryngol*. (2005) 125:270–5. doi: 10.1080/00016480410023001
24. Balaban CD, Jacob RG. Background and history of the interface between anxiety and vertigo. *J Anxiety Disord*. (2001) 15:27–51. doi: 10.1016/S0887-6185(00)00041-4
25. Zur O, Schoen G, Dickstein R, Feldman J, Berner Y, Dannenbaum E, et al. Anxiety among individuals with visual vertigo and vestibulopathy. *Disabil Rehabil*. (2015) 37:2197–202. doi: 10.3109/09638288.2014.1002577
26. Yagi C, Morita Y, Kitazawa M, Nonomura Y, Yamagishi T, Ohshima S, et al. A validated questionnaire to assess the severity of Persistent Postural-Perceptual Dizziness (PPPD): the Niigata PPPD Questionnaire (NPQ). *Otol Neurotol*. (2019) 40:e747–52. doi: 10.1097/MAO.0000000000002325
27. Powell G, Derry-Sumner H, Shelton K, Rushton S, Hedge C, Rajenderkumar D, et al. Visually-induced dizziness is associated with sensitivity and avoidance across all senses. *J Neurol*. (2020) 267:2260–71. doi: 10.1007/s00415-020-09817-0
28. Lahey BB. Public health significance of neuroticism. *Am Psychol*. (2009) 64:241–56. doi: 10.1037/a0015309
29. Indovina I, Riccelli R, Chiarella G, Petrolo C, Augimeri A, Giofrè L, et al. Role of the insula and vestibular system in patients with chronic subjective dizziness: an fMRI study using sound-evoked vestibular stimulation. *Front Behav Neurosci*. (2015) 9:334. doi: 10.3389/fnbeh.2015.00334
30. Riccelli R, Indovina I, Staab JP, Nigro S, Augimeri A, Lacquaniti F, et al. Neuroticism modulates brain visuo-vestibular and anxiety systems during a virtual rollercoaster task. *Hum Brain Mapp*. (2017) 38:715–26. doi: 10.1002/hbm.23411
31. Passamonti L, Riccelli R, Lacquaniti F, Staab JP, Indovina I. Brain responses to virtual reality visual motion stimulation are affected by neurotic personality traits in patients with persistent postural-perceptual dizziness. *J Vestib Res*. (2018) 28:369–78. doi: 10.3233/VES-190653
32. Edelman S, Mahoney AE, Cremer PD. Cognitive behavior therapy for chronic subjective dizziness: a randomized, controlled trial. *Am J Otolaryngol*. (2012) 33:395–401. doi: 10.1016/j.amjoto.2011.10.009
33. Toshishige Y, Kondo M, Kabaya K, Watanabe W, Fukui A, Kuwabara J, et al. Cognitive-behavioural therapy for chronic subjective dizziness: predictors of improvement in Dizziness Handicap Inventory at 6 months posttreatment. *Acta Otolaryngol*. (2020) 1-6. doi: 10.1080/00016489.2020.1772994
34. Petrie KJ, Weinman J. Why illness perceptions matter. *Clin Med (Lond)*. (2006) 6:536–9. doi: 10.7861/clinmedicine.6-6-536
35. Serlachius A, Gamble G, House M, Vincent ZL, Knight J, Horne A, et al. Illness perceptions and mortality in patients with gout: a prospective observational study. *Arthritis Care Res (Hoboken)*. (2017) 69:1444–8. doi: 10.1002/acr.23147
36. Juergens MC, Seekatz B, Moosdorf RG, Petrie KJ, Rief W. Illness beliefs before cardiac surgery predict disability, quality of life, and depression 3 months later. *J Psychosom Res*. (2010) 68:553–60. doi: 10.1016/j.jpsychores.2009.10.004

37. Broadbent E, Ellis CJ, Thomas J, Gamble G, Petrie KJ. Can an illness perception intervention reduce illness anxiety in spouses of myocardial infarction patients? A randomized controlled trial. *J Psychosom Res*. (2009) 67:11–5. doi: 10.1016/j.jpsychores.2008.11.006
38. Stone J, Warlow C, Sharpe M. The symptom of functional weakness: a controlled study of 107 patients. *Brain*. (2010) 133:1537–51. doi: 10.1093/brain/awq068
39. Ludwig L, Whitehead K, Sharpe M, Reuber M, Stone J. Differences in illness perceptions between patients with non-epileptic seizures and functional limb weakness. *J Psychosom Res*. (2015) 79:246–9. doi: 10.1016/j.jpsychores.2015.05.010

Conflict of Interest: The authors declare that the research was conducted in the absence of any commercial or financial relationships that could be construed as a potential conflict of interest.

frontiers in Neurology

REVIEW
published: 19 February 2021
doi: 10.3389/fneur.2021.643634

Vestibular Thresholds: A Review of Advances and Challenges in Clinical Applications

Megan J. Kobel[1,2]*, *Andrew R. Wagner*[1,3], *Daniel M. Merfeld*[1] and *Jameson K. Mattingly*[1]

[1] Department of Otolaryngology – Head and Neck Surgery, The Ohio State University Wexner Medical Center, Columbus, OH, United States, [2] Department of Speech and Hearing Science, The Ohio State University, Columbus, OH, United States, [3] Department of Health and Rehabilitation Sciences, The Ohio State University, Columbus, OH, United States

Vestibular disorders pose a substantial burden on the healthcare system due to a high prevalence and the severity of symptoms. Currently, a large portion of patients experiencing vestibular symptoms receive an ambiguous diagnosis or one that is based solely on history, unconfirmed by any objective measures. As patients primarily experience perceptual symptoms (e.g., dizziness), recent studies have investigated the use of vestibular perceptual thresholds, a quantitative measure of vestibular perception, in clinical populations. This review provides an overview of vestibular perceptual thresholds and the current literature assessing use in clinical populations as a potential diagnostic tool. Patients with peripheral and central vestibular pathologies, including bilateral vestibulopathy and vestibular migraine, show characteristic changes in vestibular thresholds. Vestibular perceptual thresholds have also been found to detect subtle, sub-clinical declines in vestibular function in asymptomatic older adults, suggesting a potential use of vestibular thresholds to augment or complement existing diagnostic methods in multiple populations. Vestibular thresholds are a reliable, sensitive, and specific assay of vestibular precision, however, continued research is needed to better understand the possible applications and limitations, especially with regard to the diagnosis of vestibular disorders.

Keywords: vestibular system, self-motion perception, vestibular thresholds, psychophysics, vestibular disorders

OPEN ACCESS

Edited by:
Herman Kingma,
Maastricht University, Netherlands

Reviewed by:
Erin Gillikin Piker,
James Madison University, United States
Vincenzo Marcelli,
Local Health Authority Naples 1 Center, Italy

***Correspondence:**
Megan J. Kobel
kobel.6@osu.edu

Specialty section:
This article was submitted to Neuro-Otology, a section of the journal Frontiers in Neurology

Received: *18 December 2020*
Accepted: *01 February 2021*
Published: *19 February 2021*

Citation:
Kobel MJ, Wagner AR, Merfeld DM and Mattingly JK (2021) Vestibular Thresholds: A Review of Advances and Challenges in Clinical Applications. Front. Neurol. 12:643634. doi: 10.3389/fneur.2021.643634

INTRODUCTION

The vestibular system senses head motion, including rotation, translation and orientation relative to gravity, via input from the semicircular canals (SCC), otolith organs, and their subsequent central integration. Signals from the vestibular periphery have a wide range of reflexive functions, including gaze stabilization via the vestibulo-ocular reflex (VOR), postural control, and autonomic regulation. The vestibular system also contributes to percepts of head motion and spatial orientation, along with contributions from vision, somatosensation, and proprioception. When an injury occurs to the peripheral end organs or central vestibular structures, patients may report abnormal perception of self-motion, imbalance, blurring of vision, and oscillopsia.

Diagnosis and management of patients with vestibular disorders can be challenging due to poor understanding of the underlying pathology, and the lack of reliable objective tests capable of fully evaluating peripheral and/or central vestibular function. Standard physiological assessment of the vestibular system focuses on reflexes including the VOR (i.e., caloric testing, rotary chair, head

impulse testing) as an assay of SCC function and vestibulospinal reflexes (VSR) (i.e., vestibular evoked myogenic potentials – VEMPs) as an assay of otolith function. In general, these measures can be effective at localizing lesions or supporting/refuting certain pathologies; however, the results of such tests are often nonspecific to common vestibular pathologies (e.g., vestibular migraine) (1), have poor correlation to patient reported symptoms or perceived disability (2–5), cannot assess the central integration of canal and otolith inputs (6, 7), and have limited physiological relevance (e.g., VEMPs, caloric testing). Furthermore, approximately one-third of patients will have normal or non-localizing results with these tests, suggesting that these tests are inadequate for a thorough evaluation of many vestibular disorders (1).

There is evidence that vestibular perception has qualitatively different underlying mechanisms than vestibular reflexes (8–10), thus serving as a potential source of novel or additive information for those affected by vestibular disorders. This may be particularly important for central disorders (e.g., vestibular migraine), as perceptual tasks have been shown to reflect a higher level of central processing that is otherwise neglected in reflexive assessments (8, 9, 11). Compared with clinical testing of the VOR, which has been widely studied and implemented, much less is known about vestibular perceptual thresholds. Vestibular perceptual thresholds provide a quantitative measure of the smallest self-motion stimulus that can be reliably perceived by an observer (this somewhat terse definition will be expanded upon further below). Although vestibular (i.e., self-motion) perception has been studied for decades, original studies have focused more on studying the non-dynamical aspects of these responses in healthy, rather than symptomatic, populations (e.g., pilots, astronauts) (12–15).

Vestibular thresholds can also describe each of the peripheral vestibular organs using a single methodology, both independently – yaw rotation for the horizontal SCC, roll or pitch rotations about an earth vertical axis for the vertical canals (**Figure 1**), z-axis translation for the saccule, y-axis translation for the utricle, x-axis translations for both the utricle and saccule (**Figure 2**)—and when SCC and otolith cues interact during rotations (i.e., tilts) about an earth horizontal axis (**Figure 3**) (6–9). This is a significant advantage over conventional vestibular tests that require multiple devices to thoroughly evaluate the vestibular system - e.g., calorics and rotary chair to evaluate the horizontal SCC and VEMPs to evaluate otolith mediated reflexes (16, 17). Furthermore, from a practical standpoint, testing of the VOR can be quite bothersome to patients, as it can be associated with motion sickness including severe nausea and vomiting, which often limits the ability or willingness to complete testing (18, 19).

While the theoretical benefits of studying vestibular perceptual thresholds is clear, their specific utility with respect to clinical medicine has only recently been examined. Thus, our goal with this review article is to highlight the methodology and clinical contributions that have been published and discuss how these findings may be useful to clinicians in the future, particularly as it pertains to the diagnosis of vestibular disorders.

OVERVIEW OF VESTIBULAR PERCEPTUAL THRESHOLDS

Vestibular perceptual thresholds refer to the smallest appreciable stimulus, or in this case motion, detected by the participant in some proportion of trials set by the investigator (20, 21). Similarly, in signal detection theory terminology (22), a threshold is the level at which a signal becomes distinguishable relative to noise (21). Studies reviewed herein were limited to those which reported thresholds and not those studying vestibular perception using other supra-threshold stimuli. A brief overview of methods will be provided, but a full review, including application of signal detection theory, adaptive methods, and fitting psychometric functions, is outside the scope of this review and interested readers are directed to Merfeld (21), Lim and Merfeld (23), Chaudhuri and Merfeld (24), and Karmali et al. (25). When measuring thresholds, a recognition task (i.e., left vs. right) is used more commonly than a detection task (i.e., no motion vs. motion) due to the influence of vibration and other cues on detection tasks (21, 26–28). Techniques are common to other psychophysical tasks used to assess other sensory domains, with the participant being provided with a large number of trials traversing a wide range of magnitudes; binary responses (e.g., present/absent, left/right) are then fit to a psychometric function to determine an estimate of threshold based off of pre-determined criteria (e.g., 79.4% correct). To determine magnitude of the test stimuli, a variety of non-adaptive (i.e., predetermined levels) and adaptive (i.e., stimulus changes based on participant responses) have been used. An adaptive staircase, where the subject is required to answer correctly on a predefined number of consecutive trials in order to reduce the stimulus level, is a common paradigm in self-motion perception tasks due to the capacity to accurately and efficiently estimate thresholds (25, 29).

An important aspect to consider is that motion detection is inherently dependent upon multisensory cues, with many extra-vestibular senses contributing to self-motion perception, including vision, somatosensation, proprioception, and audition (6, 30, 31). While whole-body motion thresholds are referred to as "vestibular" thresholds, other modalities have an impact on perceptual thresholds as evidenced by the fact that patients with complete vestibular surgical ablation are able to complete threshold tasks, albeit at thresholds significantly higher (∼1.3–56 times) than those without vestibular pathology (32). This obviously complicates evaluation of vestibular perception, and most studies go to great lengths to prevent contributions by non-vestibular cues – including testing in complete darkness, using noise-canceling headphones or active noise cancellation, and taking precautions to minimize localizing tactile feedback (e.g., skin coverage, padding). Methodologic considerations such as the choice of performing recognition, rather than detection, tasks have been emphasized to minimize extra-vestibular vibratory cues (21, 33).

The units of measure used to report vestibular perceptual thresholds has varied between studies; this choice is largely dependent on the test stimuli employed and the targeted end-organ. Many studies report vestibular perceptual thresholds

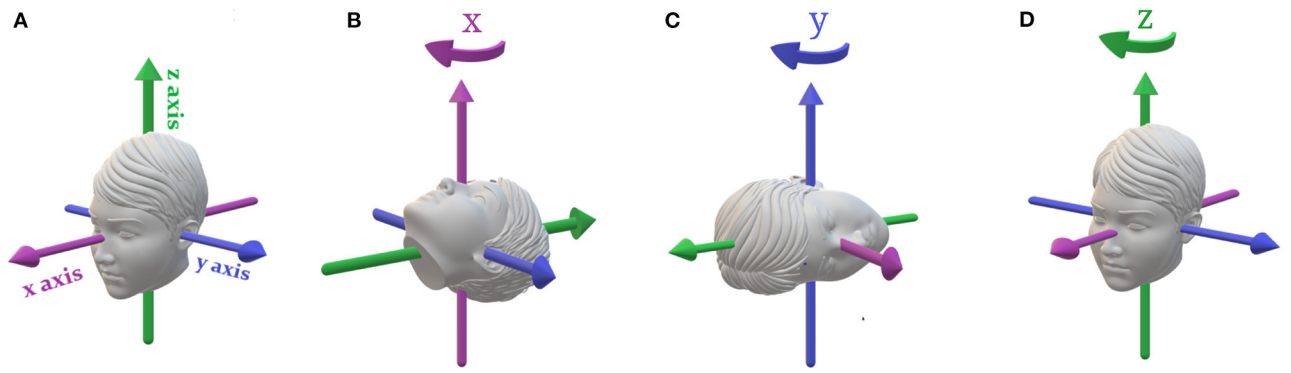

FIGURE 1 | Primary rotations of the head. **(A)** Movement is described in a head-fixed coordinate system. The x-axis is naso-occipital, y-axis is inter-aural, and the z-axis is head-vertical. **(B)** Roll rotation about the x-axis stimulating the vertical SCCs. **(C)** Pitch rotation about the y-axis stimulating primarily the vertical SCCs. **(D)** Yaw rotation about the z-axis stimulating the horizontal SCCs.

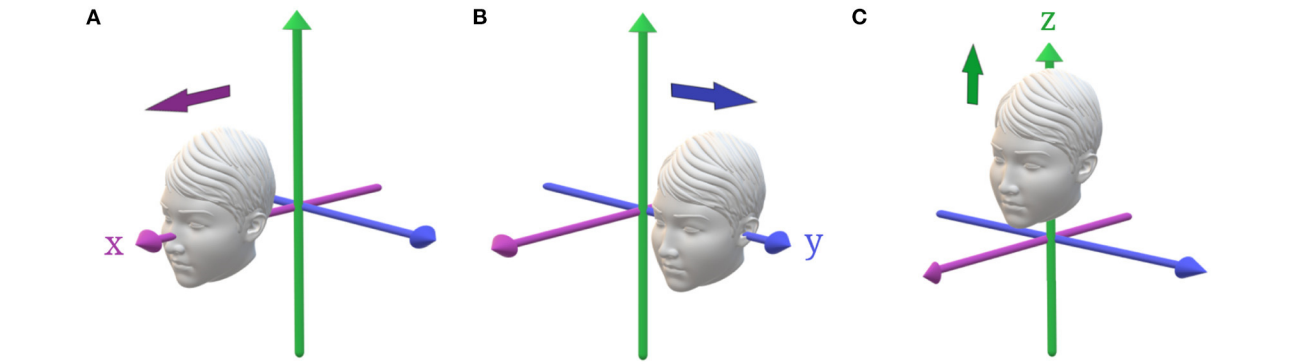

FIGURE 2 | Primary head translations. **(A)** Positive x-translation, along the naso-occipital axis, stimulating predominantly the utricle with saccular contributions. **(B)** Positive y-translation, along the inter-aural axis, stimulating the utricles. **(C)** Positive z-translation, along the head-vertical axis, stimulating the saccules.

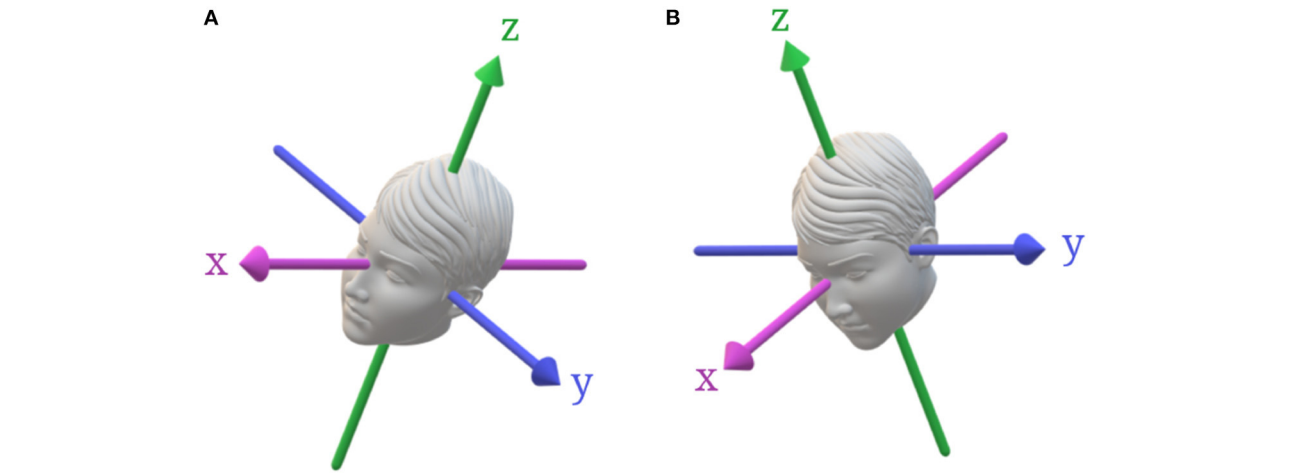

FIGURE 3 | Head tilts from upright with respect to gravity. **(A)** Roll tilt about an earth-vertical axis, which stimulates both the vertical SCCs and the utricle. **(B)** Pitch-tilt about an earth-vertical axis, which stimulates both the vertical SCCs and the otoliths.

in terms of peak velocity of the motion stimulus [e.g., (27, 34, 35)]; this is common in studies of the SCCs, since the SCC's act as integrating angular accelerometers and the afferent canal signal is proportional to angular velocity (10, 27, 32, 36). Similarly, thresholds for motions stimulating the otoliths are often reported in terms of peak acceleration of the test stimulus [e.g., (20, 26, 37)] since the otolith afferent signal is proportional to net gravitoinertial acceleration [e.g., (38, 39)]. Yet, peak velocity has been reported for translation thresholds [e.g., (32, 35, 40)] and peak acceleration has been reported for rotational stimuli meant to assess canal function [e.g., (41, 42)]. Although standardized units will be beneficial for clinical implementation, many experimental paradigms use stimuli [e.g., single cycles of sinusoidal acceleration; (27, 43)] that allow simple mathematical conversion between reported units permitting direct comparison between studies or between clinics.

VESTIBULAR PERCEPTUAL THRESHOLDS AS A MEASURE OF VESTIBULAR FUNCTION

Evaluation of SCC Function

Yaw rotation about an earth-vertical axis has been the most widely studied motion trajectory and primarily reflects horizontal SCC function (**Figure 1**). Yaw perceptual thresholds reported in the literature have demonstrated significant variability, and this is thought to be related to the type of psychophysical procedure, frequency of the motion stimuli, and differences in equipment used to generate the motion stimulus (26, 27, 44–46). Recently, however, test-retest reliability has been shown to be excellent (intraclass correlation = 0.92) suggesting minimal within subject variation (46). Vertical SCC function is more difficult to measure as this involves applying a roll rotation while avoiding concurrent otolith stimulation during tilts relative to gravity (e.g., roll rotation with the subject in supine, pitch rotations with the subject in ear down; **Figure 1**) (47). Additionally, vertical canals can be assessed using rotations about an earth vertical axis in the plane of the vertical canals [right-anterior left posterior (RALP) or left-anterior right-posterior (LARP)]; however, this methodology has not been routinely implemented.

Yaw rotation velocity thresholds have been found to display high-pass characters with a characteristic increase below 0.2 Hz and a plateau between 0.5 and 5.0 Hz (7, 27, 40). Benson et al. revealed similar results for yaw rotation, in which thresholds decreased with frequency, but their testing was limited to lower frequency motions (<1.11 Hz) limiting assessment of a high frequency plateau (48). With the frequency range extended to capture the high-pass characteristics, the average cutoff frequency was 0.23–0.44 Hz corresponding to time constants of 0.3–0.15 s, which is significantly shorter than even that of the peripheral vestibular afferents (27, 40). This time constant reduction has been referred to as "velocity leakage," which is in contrast with the behavioral time constant increase which is commonly referred to as "velocity storage" (27, 32). This velocity plateau suggests that the brain performs the recognition task using velocity rather than position or acceleration information, which is consistent with the assertion that SCC act as integrating angular accelerometers (10, 27, 32, 36). Yaw VOR thresholds, measured using similar techniques as perceptual experiments but measuring eye movements, found that VOR thresholds were not high pass filtered and relatively constant between 0.2 and 5 Hz (10). This de-coupling of the VOR and perception is similarly found in motion paradigms that stimulate the otoliths (8–10) and gives insight into the disparate behavior of the perceptual and motor (i.e., VOR) pathways.

Evaluation of Otolith Function

The otoliths (saccule and utricle) encode the net gravitoinertial force, the sum of linear acceleration and gravity. Vestibular perceptual thresholds assess otolith function using translations in the naso-occipital or x-axis (predominantly utricle), interaural or y-axis (utricle), and superior-inferior or z-axis (saccule) planes (see **Figure 2**). Additionally, the otoliths can be assessed using quasi-static roll tilt in which the otoliths are stimulated in isolation as the patient is tilted at a velocity below SCC thresholds and the subject is asked to report the direction of the static tilt cue (see **Figure 3**) (7). Similar to yaw rotation, translation thresholds typically display high-pass characteristics with an increase in thresholds below ∼1 Hz (32, 40). Additionally, evidence suggests that saccular afferents are less sensitive than utricular afferents, which has been demonstrated by lower thresholds during interaural compared to superior-inferior translations (20, 33, 35, 49). Evaluation of the saccule also poses unique technical challenges in comparison to the utricle due to issues with ceiling effects of vertical motion and equipment limitations (20, 32).

Vestibular pathology has been shown to exert a greater impact on earth-vertical translations (i.e., parallel to gravity) compared to earth-horizontal translations (i.e., perpendicular to gravity) (32, 35); in contrast, in healthy controls, earth-horizontal and earth-vertical translations have been found to be similar (33). As well, perceptual precision has been shown to be reduced when thresholds are assayed in a non-upright position (e.g., supine or side-lying), atypical of routine human motion (33). Additional research is needed to determine the impact of gravitational cues, body/head orientation, and axis of translation (i.e., interaural and superior-inferior) in order to ascertain the factors that impact assays of otolith function in disease and health.

SCC-Otolith Interactions

One unique aspect of vestibular perceptual testing is the capability to assess the central integration of SCC and otoliths cues. Internal models parse the net gravitoinertial force, encoded by the otoliths, into separate estimates of tilt and translation, using the SCC inputs to estimate head orientation relative to gravity during tilt (8, 50–52). Lim et al. found that dynamic roll tilt thresholds, which require canal-otolith integration, measured at 0.2–0.5 Hz were significantly lower than (1) thresholds measuring SCC (via supine roll) or otolith (via quasi-static roll tilt) precision in isolation and (2) a maximum likelihood estimate; this finding was interpreted as evidence that the perception of dynamic roll tilt stimuli requires both direct sensory inputs and indirect information obtained from the dynamic interaction between the canals and otoliths (7). As

will be discussed more below, evidence of an abnormal central integration of canal and otolith cues, as indicated by isolated changes in dynamic roll tilt thresholds, may be useful in the diagnosis of certain central vestibular disorders, particularly vestibular migraine (53, 54).

USE OF VESTIBULAR THRESHOLDS IN PATIENT POPULATIONS

Vestibular Hypofunction

Vestibular hypofunction can result from a broad array of pathologies. Etiologies include medication side effects, post-surgical, neoplastic, autoimmune, Meniere's disease and idiopathic hypofunction. Bilateral vestibular hypofunction (BVH) causes progressive symptoms of imbalance, and in severe cases, oscillopsia; BVH is of particular interest in clinical medicine as it remains a poorly defined chronic disorder, with an unknown etiology (55). The current literature concerning perceptual testing in patients with vestibular hypofunction describe the performance of patients encompassing a range of disease severity, including partial and complete bilateral loss (i.e., post-surgical ablation) (11, 12, 20, 32, 40, 40, 56–59) (see **Table 1**). Early perceptual assessments in patients with labyrinthine dysfunction used a parallel swing and showed a 10-fold increase in linear motion thresholds in a group of hard of hearing children deemed to have bilateral SCC dysfunction (12). These results have been supported by other studies in both unilateral and bilateral vestibular hypofunction, although the methodology and patient populations have differed dramatically (11, 20, 32, 40, 58, 59, 61, 62). Valko et al. performed the only study to date in patients with complete bilateral vestibular loss (i.e., neurofibromatosis type 2 with bilateral surgical ablation to treat vestibular schwannomas) and assessed motion paradigms assaying multiple end-organs across a wide frequency range (0.5–5 Hz) (32). Overall, the results confirmed that vestibular cues were dominant for self-motion tasks, as thresholds for yaw rotation, superior-inferior (z-axis) translation, inter-aural (y-axis) translation, and head-centered roll tilt about a naso-occipital axis were significantly higher (1.3–56.8 times) in patients than in healthy controls. Threshold changes were smallest for motions with more prominent non-vestibular cues (i.e., roll tilt and inter-aural translation) and greatest for superior-inferior (z-axis) translation, suggesting an impaired ability to differentiate transient self-motion cues from constant gravitational acceleration (32).

While this is the only study to date to include patients with complete vestibular loss, several studies have assessed vestibular perceptual thresholds in patients with incomplete bilateral vestibulopathy and have identified deficits in perception consistent with varying degrees of end organ dysfunction (11, 20, 40). Yaw rotation thresholds were found to be significantly increased in patients with idiopathic or ototoxic bilateral horizontal SCC dysfunction, as identified by a decrease in gain on caloric testing (40, 60). Priesol et al. (40) also found a modest but statistically significant elevation in inter-aural translation (y-translation) thresholds, possibly reflecting the shared innervation of the horizontal SCC and utricle; however, no significant differences were noted in superior-inferior translations or dynamic roll tilt thresholds. Importantly, these data suggest that end organ pathology in conditions such as idiopathic bilateral hypofunction is non-uniform, and conventional testing in many scenarios may incompletely characterize end-organ pathology. However, generalizability of these results may be limited due to the small sample size and the absence of a comparison test of utricular dysfunction (i.e., VEMPs) (40).

Translation thresholds were also assessed by Agrawal et al. in a group of patients with bilateral horizontal SCC weakness identified via calorics and/or head impulse testing (20). Thresholds for 0.5 Hz naso-occipital (x-axis), interaural (y-axis), and superior-inferior (z-axis) translations were significantly higher in patients than in healthy controls. An association was also noted between vibration-evoked ocular vestibular evoked myogenic potentials (oVEMP) and 0.5 Hz naso-occipital and inter-aural thresholds, suggesting that both tests assay underlying utricular function. Significant associations were not seen between cVEMP findings with any translation threshold, suggesting a dissociation between measures of presumed saccular function (20). However, Bremova et al. noted an opposite pattern in patients with Meniere's disease, showing an association between cVEMPs and 1 Hz superior-inferior (z-axis) and naso-occipital thresholds (x-axis), but no relationship between oVEMPs and any linear translation thresholds (37). The lack of agreement between these studies may reflect differences in the frequency of the test stimulus (0.5 vs. 1 Hz) or differences in the study populations; however, more testing is needed in these areas to further understand these relationships in both healthy and patient populations. It should be noted that other studies have refuted these findings, finding no or minimal difference between labyrinthine defective individuals and normal controls (56, 61). All of these studies have however demonstrated significant methodological heterogeneity, including different motion stimuli, testing frequencies, etiologies and severities of labyrinthine dysfunction.

Notably, determining laterality of vestibular responses in those with a vestibular injury is obscured by the fact that motion stimuli stimulate both labyrinths simultaneously, thus limiting application of published methodologies when lateralization of pathology is needed. Vestibular detection thresholds using yaw acceleration steps revealed asymmetrically elevated thresholds for ipsi-lesionally directed stimuli when testing in the acute stage (1–5 days post onset of vestibular neuritis); however, these thresholds become symmetric within weeks of onset, despite lack of recovery of calorics, revealing a persistent asymmetry in peripheral function (58). As well, while ipsi-lesional rotations may reveal acute changes in perception, this may reflect the central processing of both ipsi- and contra-lesional vestibular systems rather than a signal from the damaged labyrinth in isolation (58, 59).

Episodic Vestibular Disorders

Several studies have investigated changes in vestibular thresholds seen in episodic vestibular disorders, namely vestibular migraine (VM) and Meniere's Disease (MD) (see **Table 2**). Vestibular

TABLE 1 | Summary of studies investigating the impact of vestibular hypofunction on perceptual thresholds.

Study	Subjects	Stimuli	Findings
Valko et al. (32)	• 3 complete bilateral loss (aged 24–58) • 14 healthy controls (mean age 36, SD: 10)	Single cycle of sinusoidal acceleration	• Yaw rotations (1, 2, and 5 Hz), z-translations (0.3, 0.5, 1, 2, and 5 Hz), y-translations (1, 2, and 5 Hz), and roll tilt (0.05, 0.1, 0.2, 0.5, 1, 2, 5 Hz) thresholds were significantly higher in vestibular loss patients. • Yaw rotations at 0.2 and 0.5 Hz and y-translations at 0.3 and 0.5 Hz could not be completed by loss patients at the highest level generated by the motion platform.
Priesol et al. (40)	• 4 bilateral weakness (reduced calorics, reduced time constant) • 14 healthy controls (mean age 36, SD: 10)	Single cycle of sinusoidal acceleration	• Yaw rotation thresholds (0.2, 0.5, 1, 2, and 5 Hz) were significantly higher in bilateral hypofunction; y-translation: (0.3, 0.5, 1, 2, and 5 Hz) were statistically higher, however, the effect was limited to unspecified "lower frequencies." • Z-translation (0.3, 0.5, 1, 2, and 5 Hz) and roll tilt (0.05, 0.1, 0.2, 0.5, 1, 2, 5 Hz) thresholds were not significantly different between groups.
Shayman et al. (60)	• 3 bilateral weakness (reduced calorics, 35–55 years) • 13 healthy controls (23–49 years)	Single cycles of raised cosine velocity	• Yaw rotation (1 Hz) thresholds were significantly higher in patiens with bilateral weakness.
Agrawal et al. (20)	• 33 bilateral weakness (reduced calorics or HIT, 24–83 years) • 42 healthy controls (15–72 years)	Raised cosine velocity profile	• Z-translation (0.5 Hz), y-translation (0.5 Hz), x-translation (0.5 Hz) thresholds were significantly higher in patients with bilateral vestibular loss.
Bringoux et al. (61)	• 4 bilateral vestibular loss (37–60 years) • 12 healthy controls (mean age: 29 ± 6 years)	Tilts from upright at 0.05 deg/s	• Roll and pitch tilt thresholds were not significantly different between groups.
Gianna et al. (56)	• 5 bilateral vestibular loss (31–64 years) • 8 health controls (24–49 years)	Acceleration steps	• Y-translation thresholds were not significantly different between groups.
Cousins et al. (58)	• 25 VN patients, (mean age: 46) • 30 healthy controls (mean age: 42)	Acceleration at 0.5 deg/s/s, increasing 0.5 deg/s/s every 3 s	• Ipsilesional and contralesional yaw rotation thresholds were significantly higher in VN patients at acute (1–5 days) and recovered (6–16 weeks) time points.
Cutfield et al. (59)	• 12 patients with VN (mean age: 50.0) • 12 healthy controls (mean age: 46.0)	Acceleration at 0.5 deg/s/s, increasing 0.5 deg/s/s every 3 s	• Ipsilesional and contralesional yaw rotation thresholds were significantly higher in VN patients.

HIT, head impulse test; VN, vestibular neuritis.

migraine (VM) is estimated to be the most common cause of recurrent episodic vertigo (64, 65), with a prevalence between 1 and 2.7% of the adult population (66). VM is characterized by recurrent episodes of vestibular symptoms in association with signs and symptoms of migraine, including headache, visual aura, photophobia, and phonophobia (67). Due to the frequent reports of positional and head-motion induced symptoms in VM and the characteristic hypersensitivity to sensory stimuli in migraine, possible abnormalities in vestibular sensory perception have been investigated as a putative biomarker (23, 37, 53, 54, 63, 68). Overall, increases in vestibular sensitivity and abnormalities across motion profiles are inconsistent (37, 53, 54, 63, 68); increased sensitivity to motions stimulating both the SCC and otoliths have instead been consistently reported (53, 54, 63, 68).

Translation thresholds for naso-occipital (x-axis), inter-aural (y-axis) and superior-inferior (z-axis) motions were not significantly different between patients with VM and healthy controls (37). Consistent with this finding, thresholds were similar between healthy controls, migraineurs without vestibular symptoms, and VM subjects for supine roll rotation (vertical SCCs) and a "quasi-static" roll tilt (otoliths) (53, 54, 63). However, in an experiment using six trials of progressively accelerating rotational stimuli, Bednarczuk et al. reported an increased time (i.e., increased temporal threshold) to perceive yaw angular acceleration in patients with VM and in those with non-migrainous vertigo compared to healthy controls and non-vertiginous migraineurs (42).

In an apparently contradictory finding, a significant decrease in roll tilt thresholds has been demonstrated for VM patients in comparison to both healthy and non-vertiginous migraine controls (53, 54, 63). This reduction in thresholds was only seen with low to mid-frequency stimuli, reflecting an increased sensitivity to combined activation of SCC and otolith cues, given normal thresholds at higher frequencies, where the response reflects predominantly SCC cues (6, 7, 53, 54, 63). King et al. (63) also identified two populations of VM patients with low roll

TABLE 2 | Summary of studies investigating the impact of episodic vertigo on perceptual thresholds.

Study	Subjects	Stimuli	Findings
Bremova et al. (37)	• 27 Meniere's disease (mean age: 58) • 20 vestibular migraine (mean age: 40.9) • 34 healthy controls (mean age: 44.6)	Raised cosine velocity profile	• Z-translation (1 Hz), and x-translation (1 Hz) thresholds were significantly higher in MD in comparison to both VM and healthy controls. • Y-translation (1 Hz) thresholds were significantly higher in MD in comparison to VM, but not significantly different in comparison to healthy controls.
King et al. (63)	• 12 vestibular migraine (35.5 ± 2.7 years) • 12 migraine (34.0 ± 3.1 years) • 12 healthy control (38.1 ± 3.1 years) • 8 Meniere's disease	Single cycle of sinusoidal acceleration	• Roll tilt thresholds were significantly lower in VM patients in comparison to healthy controls, migraine (0.03, 0.05, 0.1 Hz) and MD (0.2 Hz); no differences were seen at higher frequencies (0.2, 0.5, 1, 2, 5 Hz). • Y-translation (0.2, 0.3, and 0.5 Hz) and roll rotation (0.2 and 0.5 Hz) thresholds not significantly different between VM, migraine, and healthy controls.
Lewis et al. (53, 54)	• 8 vestibular migraine (35.5 ± 2.7 years) • 8 migraine (34.0 ± 3.1 years) • 8 healthy control (38.1 ± 3.1 years)	Single cycle of sinusoidal acceleration	• Roll tilt thresholds (0.1 Hz) were significantly lower in VM in comparison to migraine and healthy controls. • Quasi-static roll tilt (constant ramp of 0.125 deg/s) and roll-rotation thresholds (0.1 and 1 Hz) were not significantly different between patients with VM and healthy controls.
Bednarcazuk et al. (42)	• 15 vestibular migraine (mean age, 42.0) • 15 migraine (mean age: 38.7) • 15 BPPV (mean age: 44.7) • 15 healthy controls (mean age: 44.7)	Acceleration at 0.3 deg/s/s, increasing by 0.3 deg/s/s every 3 s	• Yaw rotation thresholds were significantly higher in VM and BPPV in comparison to patients with migraine and healthy controls.

BPPV, benign paroxysmal positional vertigo; HIT, head impulse test; MD, Meniere's Disease; VM, vestibular migraine; VN, vestibular neuritis.

tilt thresholds, with one subset showing a positive correlation between tilt threshold and symptom severity, and the other with thresholds being independent of symptoms. Lower roll tilt thresholds were also shown to correlate with a decrease in VOR time constant in a subset of patients, suggesting sensitization of the cerebellar nodulus and uvula, the presumed site of SCC and otolith integration (63, 69). Abnormal central integration of otolith and SCC cues in VM patients was also found using a centrifugation paradigm, where patients with VM were found to have a slowed perception of roll tilt when presented with conflicting SCC and otolith cues (68, 70). Currently, no pathognomonic finding exists for VM, thus the potential use of low to mid-frequency roll tilt vestibular thresholds to assess midline cerebellar structures is a promising avenue for clinical diagnosis and management.

Vestibular thresholds have also been assessed in Meniere's disease (MD), another frequently encountered episodic vestibular disorder. MD is characterized by episodic vertigo and auditory symptoms, which include fluctuating hearing loss, aural fullness, and tinnitus (71). Histopathological studies have shown that MD can cause damage throughout the cochlea and labyrinth, particularly within the saccule (72). Currently, there is a paucity of research assessing perceptual thresholds in MD. At this time, only two studies have assessed vestibular thresholds in patients with MD (37, 63). Bremova et al. (37) found that MD patients displayed elevated translation thresholds for naso-occipital (x-axis) and superior-inferior (z-axis) translations when compared to healthy controls, suggesting saccular damage. In the study by King et al. (63) patients with MD were found to have normal roll tilt thresholds at 0.2 Hz, contrasting the selective reduction in low to mid-frequency roll tilt thresholds in patients with VM. In addition, Bremova et al. (37) found that translation thresholds in all axes were significantly higher in MD than VM patients, with the largest difference for superior-inferior and naso-occipital axes, even after accounting for age as a covariate. Receiver operating characteristic curve (ROC) analyses assessing differentiation of VM and MD revealed fair to good area under the curve (AUC) values (0.775–0.848) for all three axes of translation, suggesting that vestibular thresholds assessing otolith function may allow separation of these two episodic vestibular disorders (37).

VESTIBULAR THRESHOLDS AS A MAKER OF AGE-RELATED VESTIBULAR DECLINE

Degradation of vestibular function with age has been well documented in the literature (73–78); such declines occur alongside an age-associated reduction in the number of vestibular hair cells (79, 80) and vestibular afferent neurons (81). However, the impact of age on rotation and translation perceptual thresholds is less clear (summarized in **Table 3**). Overall, changes in rotation thresholds reflecting SCC function have been less consistently reported than translation thresholds. The largest study to date assessed vestibular perceptual thresholds in 105

TABLE 3 | Summary of studies investigating the impact of aging on perceptual thresholds.

Study	Subjects	Stimuli	Findings
Seemungal et al. (41)	• 14 young (19–37 years) • 9 older (56–75 years)	Triangular velocity profile, 10 s	• Yaw rotation thresholds were not significantly different between young and older adults.
Chang et al. (82)	• 19 young (20–26 years) • 16 older (63–84 years)	5 s of sinusoidal rotations	• Yaw rotation thresholds were not significantly different between young and older adults.
Kingma (83)	• 28 subjects (22–60; seven/decade)	Raised sinusoids (5 periods maximum)	• X-translation thresholds (1 Hz) showed a significant increase with age. • Y-translation thresholds (1 Hz) did not show a significant increase with age.
Roditi and Crane (34)	• 16 younger adults (21–49) • 8 older adults (50–8 years)	Single cycle of sinusoidal acceleration	• Z-translation (0.5 and 1 Hz), y-translation (0.5 and 1 Hz) and x-translation (0.5 Hz) thresholds were significantly higher in older adults compared to younger adults. • Yaw rotation (0.5 and 1 Hz) and x-translation (1 Hz) thresholds were not significantly different between younger and older adults.
Agrawal et al. (20)	• 42 healthy controls (15–72 years)	Raised cosine velocity profile	• Z-translation (0.5 Hz), y-translation (0.5 Hz) and x-translation (0.5 Hz) thresholds showed a significant positive correlation with age.
Bremova et al. (37)	• 34 healthy controls (mean: 44.6 years, SD: 15.2)	Raised cosine velocity profile	• Z-translation (1 Hz), y-translation (1 Hz) and x-translation (1 Hz) thresholds showed a significant positive correlation with age.
Bermudez et al. (37), Karmali et al. (84), and Beylergil et al. (85)[a]	• 105 subjects (18–80 years)	Single cycle of sinusoidal acceleration	• Z-translation (1 Hz), y-translation (1 Hz), and roll tilt (0.2 and 1 Hz) thresholds were constant below ∼42 years of age and displayed a significant monotonic increase between 42 and 80. • Yaw rotation thresholds (1 Hz) did not show significant increases with age when examined in isolation by Karmali et al. (84).

[a] *The dataset in Bermudez et al. (35) was subsequently further examined by Karmali et al. (84) and Beylergil et al. (85), thus studies are summarized together.*

adults across a large age range (aged 18–80) (35). The main finding was that thresholds for 0.2 Hz roll tilt and 1 Hz inter-aural translation (y-axis), superior-inferior (z-axis) translation, roll tilt, and yaw rotation were stable below the age of 42 but showed a significant, monotonic increase above 42 years of age. While all thresholds increased, the largest increase was seen in z-translation thresholds, which increased ∼83% above baseline per decade, followed by 1 Hz roll tilt (increase of 56% per decade), y-translation (increase of 46% per decade), 0.2 Hz roll tilt (increase of 32% per decade), and yaw rotation (increase of 15% per decade) (35). Principal component analysis of this dataset revealed that ∼20% of the variation in the population was explained by aging and 40% by a single component that included similar contributions from all thresholds (84). This single component was suggested by the authors to represent higher or lower thresholds as an individual trait that may represent physiologic age or anatomic variation across the population (84). It should also be noted that upon re-analysis in which fits were made for each motion trajectory, yaw thresholds no longer demonstrated a statistically significant age effect (84).

Similarly, several other studies have failed to detect a significant increase in yaw rotation thresholds with age. Seemungal et al. found similar yaw acceleration thresholds between healthy young adults (aged 19–37) and older adults (aged 56–75) using a triangular velocity trajectory (86). Likewise, no differences were noted in 0.5 Hz yaw detection and discrimination thresholds between younger (aged 20–26 years) and older (aged 63–84) adults (82), and for 0.5 Hz recognition thresholds in younger (age < 50) and older adults (age > 50) (34). These findings suggest that yaw rotation may be impacted differently by aging than other profiles which display clear aging effects. While moderate correlation coefficients have been demonstrated between all five motion profile thresholds, even after adjusting for age, the lowest coefficients were between yaw and any translation or roll tilt threshold (84). This provides additional evidence that yaw earth-vertical rotational cues are processed differently than other motion paradigms. For example, yaw rotations about an earth-vertical axis only receive useful information from the horizontal SCC, while translations and tilt require central integration of SCC and otolith cues to disambiguate tilt from translation cues (8, 9, 84). Additionally, there is evidence that yaw rotation and horizontal SCC stimulation may undergo more extensive or unique central processing due to the longer time constant when compared to the vertical SCCs (87) and the reduced impact of otolith cues on velocity storage (88).

The preferential impact of age on thresholds stimulating the otoliths demonstrated by Bermúdez Rey et al. (35) is also reflected in a number of studies that have detected age-related changes in translation thresholds, specifically for trajectories assaying saccular function (20, 34, 37, 83). In subjects aged 15–83,

0.5 Hz naso-occipital (x-axis) and superior-inferior (z-axis) perceptual thresholds were found to be significantly correlated with age, but inter-aural thresholds did not demonstrate this same relationship (20). Similarly, Kingma (83) reported that in contrast to naso-occipital axis thresholds, 1 Hz inter-aural translation thresholds did not correlate with age. However, Roditi and Crane (34) compared adults below and above the age of 50, and saw a significant difference in 0.5 and 1 Hz inter-aural and superior-inferior thresholds and 0.5 Hz naso-occipital thresholds. While 1 Hz naso-occipital thresholds failed to reach a statistically significant difference between younger and older adults, this may have been reflective of the small sample of older adults in this study ($n = 3$), as another study of 34 healthy subjects saw a significant positive correlation with age for 1 Hz naso-occipital, inter-aural, and head vertical translation thresholds (37).

While studies measuring yaw and translational thresholds have shown mixed findings, assessment of roll tilt thresholds have revealed unique insights into the influence of vestibular function on age-related balance impairment (35, 84, 85). An increase in 0.2 Hz roll tilt thresholds was shown to be accompanied by a significant increase in the risk of balance impairment as assessed by the inability to complete a foam surface eyes closed balance task (35, 84, 85), a finding previously shown to predict more than a six-fold increase in fall risk (35, 78, 84, 85). Subsequent mediation analyses found that 0.2 Hz roll tilt thresholds mediated approximately 46% of the relationship between age and balance impairment (85). While this relationship needs to be further explored, these results suggest a potential future clinical application of roll tilt thresholds as a mechanism to identify age-related balance declines and fall risk.

DISCUSSION

The study of vestibular perception traverses many scientific domains, spanning from the study of spatial disorientation in pilots to the differential diagnosis of vestibular disorders. This review, however, employs an intentionally narrow focus. The inherent limitations of current vestibular function tests have prompted this review to explore the state of the evidence as it pertains to the use of vestibular perceptual thresholds in clinical medicine.

Vestibular perceptual thresholds have the capacity to quantify the integrity of each vestibular end organ (otoliths and canals), a substantial improvement upon current vestibular assessments. As an example of possible clinical utility, Priesol et al. was able to show a specific pattern of end-organ damage in individuals with idiopathic bilateral vestibular hypofunction, which included elevated thresholds during yaw rotation and low frequency interaural translation (40). Routine clinical testing would have incompletely characterized the specific pattern of end-organ dysfunction in these individuals due to an inability to individually survey the peripheral vestibular apparatus independent of the extra-vestibular factors that influence VOR and VEMP responses. The natural vestibular stimulus, head rotation and/or translation, used by threshold assessment may also explain the finding that thresholds, but not standard vestibular function tests, correlate with patient symptoms (2, 63).

Vestibular thresholds may also be useful to assess treatment response or disease progression for those with unilateral or bilateral vestibular hypofunction (20, 58). Standard metrics, such as VOR gain, are limited in their ability to closely monitor vestibular function due to the compensatory recruitment of oculomotor strategies (89–91). Recently, test re-test reliability for vestibular threshold testing was shown to be very reliable, suggesting a potential to use thresholds to track vestibular function over time (46, 92). Furthermore, the results of traditional vestibular function tests often do not correlate with the extent of one's perceived dizziness related handicap (2). Positive correlations have however been identified between perceptual thresholds and dizziness handicap inventory (DHI) scores in subjects with vestibular migraine and bilateral vestibular hypofunction (20, 63). The independence of thresholds on oculomotor function may also prove particularly useful in measuring vestibular function in those with oculomotor disorders (e.g., congenital nystagmus), as these conditions impact traditional vestibular tests of the VOR (62).

Differentiation between other, more ambiguous vestibular disorders (e.g., MD and VM) appears particularly promising. Many patients with vestibular disorders present with symptoms that result from an unknown etiology, without clear indication of a specific disease process or of an individually culpable vestibular organ. Traditional diagnostic methods are typically exclusionary, excluding the more obvious etiologies prior to confirming a diagnosis based upon patient symptoms (67, 71). However, recent findings suggest that mid to low frequency roll tilt perceptual thresholds may serve as a biomarker for VM, suggesting that vestibular thresholds may provide an objective metric to differentiate VM from other episodic vestibular disorders with similar symptom profiles, namely MD (53, 54, 63). Considering the findings both in VM and in vestibular hypofunction, these results suggest a broadened capacity for thresholds to be used as a critical piece to the diagnostic puzzle in patients with ambiguous symptoms of central or peripheral etiology (53, 54, 63).

The comprehensive nature of vestibular thresholds also allows for potential improvements in our understanding of how age influences vestibular function. This point is not trivial, given the well-documented association between aging, vestibular decline, and fall risk (73–78). Roll tilt thresholds at 0.2 Hz in particular have been shown to predict the likelihood of failing condition four of the modified Romberg balance test (eyes closed, compliant stance balance task), an outcome previously shown to be associated with a 6.3-fold increase in the odds of falling (78) in older adults. As mentioned above, a standard mediation analysis of the same data set found that 0.2 Hz roll tilt thresholds, accounted for nearly half of the well-known association between aging and fall risk (85). Although we agree that this does not imply causation, this finding does suggest that if one were to consider all of the alternative factors likely to contribute to age-related balance dysfunction (e.g., proprioception, cognition, strength), the combined effect of these factors would be approximately equal to the contribution of a single variable,

roll tilt perceptual thresholds. Although these results are in need of confirmation in additional samples of older adults, at a minimum, vestibular noise, assayed by roll tilt perceptual thresholds, appears to be one of the primary contributors to age-related balance decline and fall risk. It is worth noting that the aforementioned findings were made in *asymptomatic* adults without complaints of vestibular impairment, suggesting that roll tilt thresholds may prove to be a sensitive screening tool to detect sub-clinical vestibular impairment and fall risk in asymptomatic adults over age 40.

From a logistical standpoint, an advantage of vestibular perceptual testing is the relative ease of testing, the task is simple and intuitive and can be readily learned by most, if not all, patients. This testing is similar to a standard hearing test, which may be the most commonly performed threshold procedure. Furthermore, algorithms that yield efficient data collection and precise data analysis have already been automated, making it possible for non-specialists to perform testing with minimal training. Unlike the heterogeneity in some other vestibular tests, this automation may serve to help standardize procedures across laboratories.

Several methodological limitations do however influence the potential clinical use of vestibular thresholds. The principal limitation with vestibular perceptual threshold testing is the time and equipment required to perform an accurate assessment. This is particularly an issue with lower frequency testing where each individual motion can require a significant amount of time (e.g., 0.1 Hz takes 10 s for 1 cycle). Automatic computer-based threshold environments and adaptive methodological approaches (e.g., staircase paradigms) have reduced test durations, yet the average assessment still requires between 10 and 20 min (∼100 trials) per test motion. We cannot directly observe one's internal perception of a sensory stimulus, and instead we are forced to rely upon a subjective report of their perceived world state (e.g., "I feel that I moved left"). Thus, aside from logistical concerns, the increased time for threshold testing introduces potential errors related to subject inattention and fatigue. This problem can be mitigated by ensuring the subject receives adequate rest, that testing occurs at a time of day where the subject is more alert, and by using statistical techniques that exclude attentional lapses from the threshold analysis (93, 94).

In addition, particular care must be taken to avoid the introduction of potentially confounding extra-vestibular cues [auditory, visual, and somatic (e.g., vibration)]. Veridical visual cues (6) and earth fixed auditory cues (30) have each been shown to reduce perceptual thresholds, and thus can influence vestibular thresholds if visual and auditory cues are not adequately controlled. When using a motion platform to deliver stimuli, somatic cues such as vibration are unavoidable. However, using a direction recognition task (e.g., did I move right or left?) rather than a detection task (e.g., did I move) can mitigate the effect of vibration on vestibular thresholds (21, 26, 28).

From an equipment standpoint, vestibular perceptual threshold measurements require only a few simple components (i.e., a motorized chair, a tablet or subject response buttons, and a computer for device control and data acquisition). Yaw perceptual thresholds could be performed using a rotary chair, which is found in most tertiary care vestibular referral centers and audiology clinics. However, immediate implementation is not feasible with most commercially available systems and will be dependent upon thedevelopment of appropriate software and hardware by the device manufacturers. The primary limitation of the rotary chair in comparison to a 6DOF motion platform is the limitation in test conditions, as the rotary chair can only be used to assess yaw thresholds within a limited frequency range. Therefore, a motion platform with multiple degrees of freedom is likely necessary for a comprehensive assessment of vestibular thresholds. While currently 6DOF motion platforms (e.g., Moog) are not commonly available, we feel that their implementation would be very straightforward. This equipment could fit in a small room and the total cost is estimated to be $< \$200$ K, an estimate that is based upon our own lab set-up. We emphasize that all aspects of both central and peripheral vestibular function would be tested using the single motion device, and as a result this equipment would almost certainly cost less than the total cost of the devices currently used today (rotary chair, caloric irrigator, evoked potentials equipment, head impulse goggles, etc.).

SUMMARY

Vestibular thresholds are arguably the most direct, sensitive, and specific assay of vestibular noise currently available (20, 63, 95). The ability to test all end-organs and their central integration, the correlation to patient symptoms, the possible role in differentiating certain vestibular disorders, and the relative ease of testing make thresholds a promising clinical measure. Continued research is needed to better understand the possible applications and limitations, especially with regard to the differential diagnosis of vestibular disorders. Such disorders continue to be a challenge to manage clinically and the absence of reliable diagnostic testing is a critical barrier to improving the day-to-day management of these patients.

AUTHOR CONTRIBUTIONS

MK, AW, DM, and JM wrote the manuscript and approved the final version prior to publication. MK created all tables and figures presented herein. All authors contributed to the article and approved the submitted version.

FUNDING

MK, AW, and DM were funded by an NIH/NIDCD R01 (DC014924); AW was funded in part by a Promotion of Doctoral Studies (PODS) I Scholarship from the Foundation for Physical Therapy Research.

REFERENCES

1. Gordon CR, Shupak A, Spitzer O, Doweck I, Melamed Y. Nonspecific vertigo with normal otoneurological examination. The role of vestibular laboratory tests. *J Laryngol Otol.* (1996) 110:1133–7. doi: 10.1017/S0022215100135947
2. Yip CW, Strupp M. The dizziness handicap inventory does not correlate with vestibular function tests: a prospective study. *J Neurol.* (2018) 265:1210–8. doi: 10.1007/s00415-018-8834-7
3. Perez N, Martin E, Garcia-Tapia R. Dizziness: relating the severity of vertigo to the degree of handicap by measuring vestibular impairment. *Otolaryngol Head Neck Surg.* (2003) 128:372–81. doi: 10.1067/mhn.2003.102
4. Kanayama R, Bronstein AM, Gresty MA, Brookes GB, Faldon ME, Nakamura T. Perceptual studies in patients with vestibular neurectomy. *Acta Otolaryngol Suppl.* (1995) 520 (Pt 2):408–11. doi: 10.3109/00016489509125284
5. Kammerlind AS, Ledin TE, Skargren EI, Odkvist LM. Long-term follow-up after acute unilateral vestibular loss and comparison between subjects with and without remaining symptoms. *Acta Otolaryngol.* (2005) 125:946–53. doi: 10.1080/00016480510043477
6. Karmali F, Lim K, Merfeld DM. Visual and vestibular perceptual thresholds each demonstrate better precision at specific frequencies and also exhibit optimal integration. *J Neurophysiol.* (2014) 111:2393–403. doi: 10.1152/jn.00332.2013
7. Lim K, Karmali F, Nicoucar K, Merfeld DM. Perceptual precision of passive body tilt is consistent with statistically optimal cue integration. *J Neurophysiol.* (2017) 117:2037–52. doi: 10.1152/jn.00073.2016
8. Merfeld DM, Park S, Gianna-Poulin C, Black FO, Wood S. Vestibular perception and action employ qualitatively different mechanisms. I. Frequency response of VOR and perceptual responses during translation and tilt. *J Neurophysiol.* (2005) 94:186–98. doi: 10.1152/jn.00904.2004
9. Merfeld DM, Park S, Gianna-Poulin C, Black FO, Wood S. Vestibular perception and action employ qualitatively different mechanisms. II. VOR and perceptual responses during combined tilt&translation. *J Neurophysiol.* (2005) 94:199–205. doi: 10.1152/jn.00905.2004
10. Haburcakova C, Lewis RF, Merfeld DM. Frequency dependence of vestibuloocular reflex thresholds. *J Neurophysiol.* (2012) 107:973–83. doi: 10.1152/jn.00451.2011
11. Mallery RM, Olomu OU, Uchanski RM, Militchin VA, Hullar TE. Human discrimination of rotational velocities. *Exp Brain Res Exp Hirnforschung.* (2010) 204:11–20. doi: 10.1007/s00221-010-2288-1
12. Walsh EG. Role of the vestibular apparatus in the perception of motion on a parallel swing. *J Physiol.* (1961) 155:506–13. doi: 10.1113/jphysiol.1961.sp006643
13. Graybiel A, Hupp DI, Patterson JL Jr. The law of the otolith organs. *Fed Proc.* (1946) 5:35.
14. Mann CW, Berthelot-Berry NH, Dauterive HJ Jr. The perception of the vertical; visual and non-labyrinthine cues. *J Exp Psychol.* (1949) 39:538–47. doi: 10.1037/h0063533
15. Clark B, Graybiel A. Perception of the postural vertical in normals and subjects with labyrinthine defects. *J Exp Psychol.* (1963) 65:490–4. doi: 10.1037/h0045606
16. Baloh RW, Honrubia V, Yee RD, Hess K. Changes in the human vestibulo-ocular reflex after loss of peripheral sensitivity. *Ann Neurol.* (1984) 16:222–8. doi: 10.1002/ana.410160209
17. Curthoys IS. A critical review of the neurophysiological evidence underlying clinical vestibular testing using sound, vibration and galvanic stimuli. *Clin Neurophysiol.* (2010) 121:132–44. doi: 10.1016/j.clinph.2009.09.027
18. Schaefer SD, Post JD, Close LG, Wright CG. Ototoxicity of low- and moderate-dose cisplatin. *Cancer.* (1985) 56:1934–9. doi: 10.1002/1097-0142(19851015)56:8<1934::AID-CNCR2820560807>3.0.CO;2-F
19. Kelly EA, Stocker C, Kempton CM, Dierking DM, Fehlberg HE, Adams ME. Vestibular testing: patient perceptions, morbidity, and opportunity costs. *Otol Neurotol.* (2018) 39:1222–8. doi: 10.1097/MAO.0000000000002025
20. Agrawal Y, Bremova T, Kremmyda O, Strupp M, MacNeilage PR. Clinical testing of otolith function: perceptual thresholds and myogenic potentials. *J Assoc Res Otolaryngol.* (2013) 14:905–15. doi: 10.1007/s10162-013-0416-x
21. Merfeld DM. Signal detection theory and vestibular thresholds: I. Basic theory and practical considerations. *Exp Brain Res Exp Hirnforschung.* (2011) 210:389–405. doi: 10.1007/s00221-011-2557-7
22. Green DM, Swets JA. *Signal Detection Theory and Psychophysics*. New York, NY: John Wiley (1966).
23. Lim K, Merfeld DM. Signal detection theory and vestibular perception: II. Fitting perceptual thresholds as a function of frequency. *Exp Brain Res.* (2012) 222:303–20. doi: 10.1007/s00221-012-3217-2
24. Chaudhuri SE, Merfeld DM. Signal detection theory and vestibular perception: III. Estimating unbiased fit parameters for psychometric functions. *Exp Brain Res.* (2013) 225:133–46. doi: 10.1007/s00221-012-3354-7
25. Karmali F, Chaudhuri SE, Yi Y, Merfeld DM. Determining thresholds using adaptive procedures and psychometric fits: evaluating efficiency using theory, simulations, and human experiments. *Exp Brain Res.* (2016) 234:773–89. doi: 10.1007/s00221-015-4501-8
26. MacNeilage PR, Turner AH, Angelaki DE. Canal-otolith interactions and detection thresholds of linear and angular components during curved-path self-motion. *J Neurophysiol.* (2010) 104:765–73. doi: 10.1152/jn.01067.2009
27. Grabherr L, Nicoucar K, Mast FW, Merfeld DM. Vestibular thresholds for yaw rotation about an earth-vertical axis as a function of frequency. *Exp Brain Res Exp Hirnforschung.* (2008) 186:677–81. doi: 10.1007/s00221-008-1350-8
28. Chaudhuri SE, Karmali F, Merfeld DM. Whole body motion-detection tasks can yield much lower thresholds than direction-recognition tasks: implications for the role of vibration. *J Neurophysiol.* (2013) 110:2764–72. doi: 10.1152/jn.00091.2013
29. Leek MR. Adaptive procedures in psychophysical research. *Percep Psychophys.* (2001) 63:1279–92. doi: 10.3758/BF03194543
30. Shayman CS, Peterka RJ, Gallun FJ, Oh Y, Chang NN, Hullar TE. Frequency-dependent integration of auditory and vestibular cues for self-motion perception. *J Neurophysiol.* (2020) 123:936–44. doi: 10.1152/jn.00307.2019
31. Hlavacka F, Mergner T, Bolha B. Human self-motion perception during translatory vestibular and proprioceptive stimulation. *Neurosci Lett.* (1996) 210:83–6. doi: 10.1016/0304-3940(96)12667-7
32. Valko Y, Lewis RF, Priesol AJ, Merfeld DM. Vestibular labyrinth contributions to human whole-body motion discrimination. *J Neurosci.* (2012) 32:13537–42. doi: 10.1523/JNEUROSCI.2157-12.2012
33. MacNeilage PR, Banks MS, DeAngelis GC, Angelaki DE. Vestibular heading discrimination and sensitivity to linear acceleration in head and world coordinates. *J Neurosci.* (2010) 30:9084–94. doi: 10.1523/JNEUROSCI.1304-10.2010
34. Roditi RE, Crane BT. Directional asymmetries and age effects in human self-motion perception. *J Assoc Res Otolaryngol.* (2012) 13:381–401. doi: 10.1007/s10162-012-0318-3
35. Bermudez Rey MC, Clark TK, Wang W, Leeder T, Bian Y, Merfeld DM. Vestibular perceptual thresholds increase above the age of 40. *Front Neurol.* (2016) 7:162. doi: 10.3389/fneur.2016.00162
36. Goldberg JM, Fernandez C. Physiology of peripheral neurons innervating semicircular canals of the squirrel monkey. I. Resting discharge and response to constant angular accelerations. *J Neurophysiol.* (1971) 34:635–60. doi: 10.1152/jn.1971.34.4.676
37. Bremova T, Caushaj A, Ertl M, Strobl R, Bottcher N, Strupp M, et al. Comparison of linear motion perception thresholds in vestibular migraine and Meniere's disease. *Eur Arch Otorhinolaryngol.* (2016) 273:2931–9. doi: 10.1007/s00405-015-3835-y
38. Fernandez C, Goldberg JM. Physiology of peripheral neurons innervating otolith organs of the squirrel monkey. I. Response to static tilts and to long duration centrifugal force. *J Neurophysiol.* (1976) 39:970–84. doi: 10.1152/jn.1976.39.5.970
39. Fernández C, Goldberg JM. Physiology of peripheral neurons innervating otolith organs of the squirrel monkey. III. Response dynamics. *J Neurophysiol.* (1976) 39:996–1008. doi: 10.1152/jn.1976.39.5.996
40. Priesol AJ, Valko Y, Merfeld DM, Lewis RF. Motion perception in patients with idiopathic bilateral vestibular hypofunction. *Otolaryngol Head Neck Surg.* (2014) 150:1040–2. doi: 10.1177/0194599814526557
41. Seemungal BM, Gunaratne IA, Fleming IO, Gresty MA, Bronstein AM. Perceptual and nystagmic thresholds of vestibular function in yaw. *J Vestib Res.* (2004) 14:461–6.

42. Bednarczuk NF, Bonsu A, Ortega MC, Fluri AS, Chan J, Rust H, et al. Abnormal visuo-vestibular interactions in vestibular migraine: a cross sectional study. *Brain.* (2019) 142:606–16. doi: 10.1093/brain/awy355
43. Benson AJ, Spencer MB, Stott JRR. Thresholds for the detection of the direction of whole-body, linear movement in the horizontal plane. *Aviat Space Environ Med.* (1986) 57:1088–96.
44. Clark B. Thresholds for the perception of angular acceleration in man. *Aerosp Med.* (1967) 38:443–50.
45. Jones GM, Young LR. Subjective detection of vertical acceleration: a velocity-dependent response? *Acta Otolaryngol.* (1978) 85:45–53. doi: 10.3109/00016487809121422
46. Lee TL, Shayman CS, Oh Y, Peterka RJ, Hullar TE. Reliability of vestibular perceptual threshold testing about the Yaw Axis. *Ear Hear.* (2020) 1:1772–4. doi: 10.1097/AUD.0000000000000859
47. Merfeld DM, Priesol A, Lee D, Lewis RF. Potential solutions to several vestibular challenges facing clinicians. *J Vestib Res.* (2010) 20:71–7. doi: 10.3233/VES-2010-0347
48. Benson AJ, Hutt EC, Brown SF. Thresholds for the perception of whole body angular movement about a vertical axis. *Aviat Space Environ Med.* (1989) 60:205–13.
49. Benson AJ, Spencer MB, Stott JR. Thresholds for the detection of the direction of whole-body, linear movement in the horizontal plane. *Aviat Space Environ Med.* (1986) 57:1088–96.
50. Merfeld DM, Zupan L, Peterka RJ. Humans use internal models to estimate gravity and linear acceleration. *Nature.* (1999) 398:615–8. doi: 10.1038/19303
51. Angelaki DE, McHenry MQ, Dickman JD, Newlands SD, Hess BJ. Computation of inertial motion: neural strategies to resolve ambiguous otolith information. *J Neurosci.* (1999) 19:316–27. doi: 10.1523/JNEUROSCI.19-01-00316.1999
52. Angelaki DE, Shaikh AG, Green AM, Dickman JD. Neurons compute internal models of the physical laws of motion. *Nature.* (2004) 430:560–4. doi: 10.1038/nature02754
53. Lewis RF, Priesol AJ, Nicoucar K, Lim K, Merfeld DM. Dynamic tilt thresholds are reduced in vestibular migraine. *J Vestib Res.* (2011) 21:323–30. doi: 10.3233/VES-2011-0422
54. Lewis RF, Priesol AJ, Nicoucar K, Lim K, Merfeld DM. Abnormal motion perception in vestibular migraine. *Laryngoscope.* (2011) 121:1124–5. doi: 10.1002/lary.21723
55. Strupp M, Kim JS, Murofushi T, Straumann D, Jen JC, Rosengren SM, et al. Bilateral vestibulopathy: diagnostic criteria consensus document of the classification committee of the barany society. *J Vestib Res.* (2017) 27:177–89. doi: 10.3233/VES-170619
56. Gianna C, Heimbrand S, Gresty M. Thresholds for detection of motion direction during passive lateral whole-body acceleration in normal subjects and patients with bilateral loss of labyrinthine function. *Brain Res Bull.* (1996) 40:443–7. discussion: 8–9. doi: 10.1016/0361-9230(96)00140-2
57. Walsh EG. Perception of linear motion following unilateral labyrinthectomy: variation of threshold according to the orientation of the head. *J Physiol.* (1960) 153:350–7. doi: 10.1113/jphysiol.1960.sp006538
58. Cousins S, Kaski D, Cutfield N, Seemungal B, Golding JF, Gresty M, et al. Vestibular perception following acute unilateral vestibular lesions. *PLoS ONE.* (2013) 8:e61862. doi: 10.1371/journal.pone.0061862
59. Cutfield NJ, Cousins S, Seemungal BM, Gresty MA, Bronstein AM. Vestibular perceptual thresholds to angular rotation in acute unilateral vestibular paresis and with galvanic stimulation. *Ann N Y Acad Sci.* (2011) 1233:256–62. doi: 10.1111/j.1749-6632.2011.06159.x
60. Shayman CS, Seo J-H, Oh Y, Lewis RF, Peterka RJ, Hullar TE. Relationship between vestibular sensitivity and multisensory temporal integration. *J Neurophysiol.* (2018) 120:1572–7. doi: 10.1152/jn.00379.2018
61. Bringoux L, Schmerber S, Nougier V, Dumas G, Barraud PA, Raphel C. Perception of slow pitch and roll body tilts in bilateral labyrinthine-defective subjects. *Neuropsychologia.* (2002) 40:367–72. doi: 10.1016/S0028-3932(01)00103-8
62. Okada T, Grunfeld E, Shallo-Hoffmann J, Bronstein AM. Vestibular perception of angular velocity in normal subjects and in patients with congenital nystagmus. *Brain.* (1999) 122 (Pt 7):1293–303. doi: 10.1093/brain/122.7.1293
63. King S, Priesol AJ, Davidi SE, Merfeld DM, Ehtemam F, Lewis RF. Self-motion perception is sensitized in vestibular migraine: pathophysiologic and clinical implications. *Sci Rep.* (2019) 9:14323. doi: 10.1038/s41598-019-50803-y
64. Neuhauser HK. Epidemiology of vertigo. *Curr Opin Neurol.* (2007) 20:40–6. doi: 10.1097/WCO.0b013e328013f432
65. Van Ombergen A, Van Rompaey V, Van de Heyning P, Wuyts F. Vestibular migraine in an otolaryngology clinic. *Otol Neurotol.* (2014) 36:133–8. doi: 10.1097/MAO.0000000000000596
66. Neuhauser HK, Radtke A, von Brevern M, Feldmann M, Lezius F, Ziese T, et al. Migrainous vertigo: prevalence and impact on quality of life. *Neurology.* (2006) 67:1028–33. doi: 10.1212/01.wnl.0000237539.09942.06
67. Lempert T, Olesen J, Furman J, Waterston J, Seemungal B, Carey J, et al. Vestibular migraine: diagnostic criteria. *J Vestib Res.* (2012) 22:167–72. doi: 10.3233/VES-2012-0453
68. King S, Wang J, Priesol AJ, Lewis RF. Central integration of canal and otolith signals is abnormal in vestibular migraine. *Front Neurol.* (2014) 5:1–7. doi: 10.3389/fneur.2014.00233
69. Wearne S, Raphan T, Cohen B. Control of spatial orientation of the angular vestibuloocular reflex by the nodulus and uvula. *J Neurophysiol.* (1998) 79:2690–715. doi: 10.1152/jn.1998.79.5.2690
70. Wang J, Lewis RF. Abnormal tilt perception during centrifugation in patients with vestibular migraine. *J Assoc Res Otolaryngol.* (2016) 17:253–8. doi: 10.1007/s10162-016-0559-7
71. Lopez-Escamez JA, Carey J, Chung WH, Goebel JA, Magnusson M, Mandala M, et al. Diagnostic criteria for Meniere's disease. *J Vestib Res.* (2015) 25:1–7. doi: 10.3233/VES-150549
72. Okuno T, Sando I. Localization, frequency, and severity of endolymphatic hydrops and the pathology of the labyrinthine membrane in Meniere's disease. *Ann Otol Rhinol Laryngol.* (1987) 96:438–45. doi: 10.1177/000348948709600418
73. Peterka RJ, Black FO. Age-Related Changes in Human Posture Control: Sensory Organization Tests. *J Vestib Res.* (1990) 1:73–85.
74. Baloh RW, Enrietto J, Jacobson KM, Lin A. Age-related changes in vestibular function: a longitudinal study. *Ann N Y Acad Sci.* (2001) 942:210–9. doi: 10.1111/j.1749-6632.2001.tb03747.x
75. Serrador JM, Lipsitz LA, Gopalakrishnan GS, Black FO, Wood SJ. Loss of otolith function with age is associated with increased postural sway measures. *Neurosci Lett.* (2009) 465:10–5. doi: 10.1016/j.neulet.2009.08.057
76. Agrawal Y, Zuniga MG, Davalos-Bichara M, Schubert MC, Walston JD, Hughes J, et al. Decline in semicircular canal and otolith function with age. *Otol Neurotol.* (2012) 33:832–9. doi: 10.1097/MAO.0b013e3182545061
77. Agrawal Y, Van de Berg R, Wuyts F, Walther L, Magnusson M, Oh E, et al. Presbyvestibulopathy: diagnostic criteria consensus document of the classification committee of the Bárány Society. *J Vestib Res.* (2019) 29:161–70. doi: 10.3233/VES-190672
78. Agrawal Y, Carey JP, Della Santina CC, Schubert MC, Minor LB. Disorders of balance and vestibular function in US adults: data from the National Health and Nutrition Examination Survey, 2001-2004. *Arch Intern Med.* (2009) 169:938–44. doi: 10.1001/archinternmed.2009.66
79. Merchant SN, Tsuji K, Wall C, Velázquez-Villaseñor L, Glynn RJ, Rauch SD. Temporal bone studies of the human peripheral vestibular system. *Ann Otol Rhinol Laryngol.* (2000) 109 (5_Suppl.):3–13. doi: 10.1177/00034894001090S502
80. Rauch SD, Velázquez-Villaseñor L, Dimitri P, Merchant SN. Decreasing hair cell counts in aging humans. *Ann N Y Acad Sci.* (2006) 942:220–7. doi: 10.1111/j.1749-6632.2001.tb03748.x
81. Makary CA, Shin J, Kujawa SG, Liberman MC, Merchant SN. Age-related primary cochlear neuronal degeneration in human temporal bones. *J Assoc Res Otolaryngol.* (2011) 12:711–7. doi: 10.1007/s10162-011-0283-2
82. Chang NYN, Hiss MM, Sanders MC, Olomu OU, MacNeilage PR, Uchanski RM, et al. Vestibular perception and the vestibulo-ocular reflex in young and older adults. *Ear Hear.* (2014) 35:565–70. doi: 10.1097/AUD.0000000000000052
83. Kingma H. Thresholds for perception of direction of linear acceleration as a possible evaluation of the otolith function. *BMC Ear Nose Throat Disord.* (2005) 5:5. doi: 10.1186/1472-6815-5-5

84. Karmali F, Bermudez Rey MC, Clark TK, Wang W, Merfeld DM. Multivariate analyses of balance test performance, vestibular thresholds, and age. *Front Neurol.* (2017) 8:578. doi: 10.3389/fneur.2017.00578
85. Beylergil SB, Karmali F, Wang W, Bermudez Rey MC, Merfeld DM. Vestibular roll tilt thresholds partially mediate age-related effects on balance. *Prog Brain Res.* (2019) 248:249–67. doi: 10.1016/bs.pbr.2019.04.019
86. Seemungal BM, Gunaratne IA, Fleming IO, Gresty MA, Bronstein AM. Perceptual and nystagmic thresholds of vestibular function in yaw. *J Vestib Res.* (2004) 14:461–6.
87. Bertolini G, Ramat S, Ramat GBS. Velocity storage in the human vertical rotational vestibulo-ocular reflex. *Exp Brain Res.* (2011) 209:51–63. doi: 10.1007/s00221-010-2518-6
88. Bockisch CJ, Straumann D, Haslwanter T. Human 3-D aVOR with and without otolith stimulation. *Exp Brain Res.* (2005) 161:358–67. doi: 10.1007/s00221-004-2080-1
89. Dichgans J, Bizzi E, Morasso P, Tagliasco V. Mechanisms underlying recovery of eye-head coordination following bilateral labyrinthectomy in monkeys. *Exp Brain Res.* (1973) 18:548–62. doi: 10.1007/BF00234137
90. Herdman SJ, Schubert MC, Tusa RJ. Role of central preprogramming in dynamic visual acuity with vestibular loss. *Arch Otolaryngol Head Neck Surg.* (2001) 127:1205–10. doi: 10.1001/archotol.127.10.1205
91. Schubert MC, Hall CD, Das V, Tusa RJ, Herdman SJ. Oculomotor strategies and their effect on reducing gaze position error. *Otol Neurotol.* (2010) 31:228–31. doi: 10.1097/MAO.0b013e3181c2dbae
92. Wagner A MD, Klaus M, Mast F. *Training Roll Tilit Self-Motion Perception. Vestibular Oriented Research Meeting.* Toronto, Canada: Journal of Vestibular Research (2020).
93. Wichmann FA, Hill NJ. The psychometric function: I. Fitting, sampling, and goodness of fit. *Percep Psychophys.* (2001) 63:1293–313. doi: 10.3758/BF03194544
94. Wichmann FA, Hill NJ. The psychometric function: II. Bootstrap-based confidence intervals and sampling. *Percep Psychophys.* (2001) 63:1314–29. doi: 10.3758/BF03194545
95. Jacobson GP, Newman CW. The development of the dizziness handicap inventory. *Arch Otolaryngol Head Neck Surg.* (1990) 116:424–7. doi: 10.1001/archotol.1990.01870040046011

Conflict of Interest: The authors declare that the research was conducted in the absence of any commercial or financial relationships that could be construed as a potential conflict of interest.

frontiers in Neurology

METHODS
published: 03 March 2021
doi: 10.3389/fneur.2021.627294

Applications of Multivariate Statistical and Data Mining Analyses to the Search for Biomarkers of Sensorineural Hearing Loss, Tinnitus, and Vestibular Dysfunction

Paul F. Smith [1,2,3]* *and Yiwen Zheng* [1,2,3]

[1] *Department of Pharmacology and Toxicology, Brain Health Research Centre, School of Biomedical Sciences, University of Otago, Dunedin, New Zealand,* [2] *Brain Research New Zealand Centre of Research Excellence, University of Auckland, Auckland, New Zealand,* [3] *The Eisdell Moore Centre for Hearing and Balance Research, University of Auckland, Auckland, New Zealand*

Disorders of sensory systems, as with most disorders of the nervous system, usually involve the interaction of multiple variables to cause some change, and yet often basic sensory neuroscience data are analyzed using univariate statistical analyses only. The exclusive use of univariate statistical procedures, analyzing one variable at a time, may limit the potential of studies to determine how interactions between variables may, as a network, determine a particular result. The use of multivariate statistical and data mining methods provides the opportunity to analyse many variables together, in order to appreciate how they may function as a system of interacting variables, and how this system or network may change as a result of sensory disorders such as sensorineural hearing loss, tinnitus or different types of vestibular dysfunction. Here we provide an overview of the potential applications of multivariate statistical and data mining techniques, such as principal component and factor analysis, cluster analysis, multiple linear regression, random forest regression, linear discriminant analysis, support vector machines, random forest classification, Bayesian classification, and orthogonal partial least squares discriminant analysis, to the study of auditory and vestibular dysfunction, with an emphasis on classification analytic methods that may be used in the search for biomarkers of disease.

Keywords: multivariate statistical analysis, data mining, orthogonal partial least squares discriminant analysis, hearing loss, tinnitus, vestibular dysfunction

OPEN ACCESS

Edited by:
Andreas Zwergal, Ludwig Maximilian University of Munich, Germany

Reviewed by:
Seyed-Ahmad Ahmadi, LMU Munich, Germany
Sung Huhn Kim, Yonsei University, South Korea

***Correspondence:**
Paul F. Smith
paul.smith@otago.ac.nz

Specialty section:
This article was submitted to Neuro-Otology, a section of the journal Frontiers in Neurology

Received: *09 November 2020*
Accepted: *01 February 2021*
Published: *03 March 2021*

Citation:
Smith PF and Zheng Y (2021) Applications of Multivariate Statistical and Data Mining Analyses to the Search for Biomarkers of Sensorineural Hearing Loss, Tinnitus, and Vestibular Dysfunction. Front. Neurol. 12:627294. doi: 10.3389/fneur.2021.627294

INTRODUCTION

Experimental phenomena in neuroscience often involve the complex, sometimes non-linear interaction, of multiple variables. In the context of sensorineural hearing loss (SNHL), tinnitus or vestibular disorders, a number of independent variables may interact with one another, such as age, sex, drug use, and genetic predispositions; similarly, many biochemical systems may interact with one another to cause such disorders (see **Figure 1** for an example in the context of age-related neurochemical changes in the brainstem vestibular nucleus and cerebellum). Despite this, the majority of statistical analyses in basic auditory and vestibular neuroscience have tended

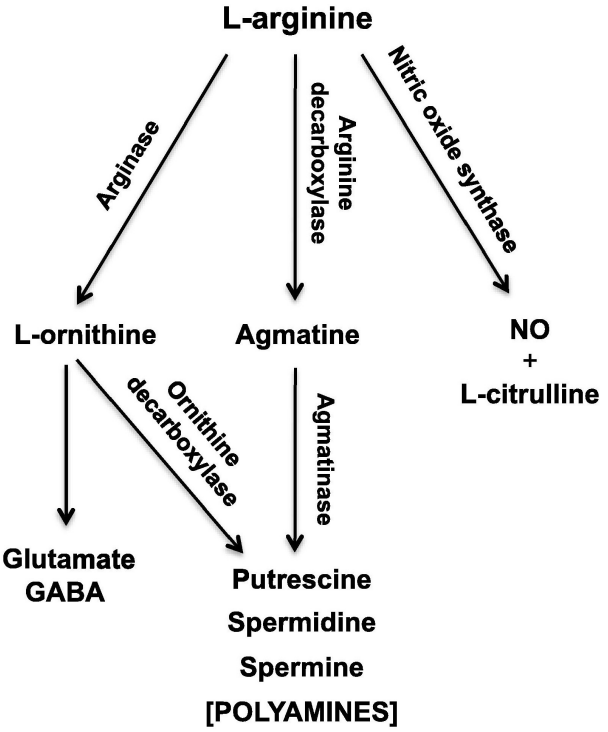

FIGURE 1 | Schematic diagram of the L-arginine metabolic pathways in the vestibular nucleus and cerebellum, which change during the brain aging process. NO, nitric oxide; GABA, γ-aminobutyric acid. From Liu et al. (4) with permission.

to focus on comparisons between treatment groups, analyzing one variable at a time. In many areas of sensory neuroscience in general, univariate statistical analyses have been used almost exclusively. This approach neglects the fact that changes may occur at the level of the interaction within a network or system of variables, that cannot be detected in any individual variable alone (1–6) (see **Figure 1** for an example). In addition, the use of multiple univariate statistical analyses may inflate the type 1 error rate, or the probability of rejecting the null hypothesis when it is true, as a result of a large number of individual analyses (1, 2, 7) (**Figure 2**). In situations in which there are a large number of variables, for example, gene microarray, proteomic and metabolomic data, and more recently, medical diagnostics, multivariate statistical analyses and data mining approaches have been increasingly employed in order to understand the complex interactions that can occur between systems of variables, as well as to avoid increasing the type I error rate [e.g., (6, 8–30)].

Multivariate statistical analyses (MVAs) and data mining analyses can be broadly divided into those that are "supervised" and those that are "unsupervised". A "supervised" method of analysis is directed at a specific dependent variable, in order to determine the relationship between a set of independent variables and one or more dependent variables, (e.g., to make a prediction; e.g., multiple linear regression). By contrast, in "unsupervised" methods, there is no specific dependent variable; instead, the objective is to explore associations between variables (e.g., cluster analyses) (see **Table 1**). Furthermore, some MVAs and data mining methods are concerned with predicting categorical variables ("classification," e.g., linear discriminant analysis), and some concerned with predicting continuous variables ("regression," e.g., multiple linear regression). Some of these methods involve only one dependent variable, e.g., multiple linear regression, while others may involve multiple dependent variables, e.g., canonical correlation analysis; however, for the purposes of this paper, MVAs will be defined as a collection of methods that involve *multiple variables*, either independent or dependent, or both. Clearly, regression methods such as multiple linear regression can be extended to include more than one dependent variable [e.g., multivariate multiple regression; (1, 2)].

Some unsupervised MVAs are not focussed on a specific dependent variable or the implication of causality, but more the degree of co-variation amongst multiple variables, as an indicator of association. For example, cluster analyses could be used to investigate the degree to which different variables related to SNHL co-vary with one another. Cluster analyses have been used extensively in genomics and proteomics research as a means of exploring the association between variables. Still other MVAs are concerned with investigating the way that groups of variables with different weightings, explain most of the variation in a system of variables (e.g., **Figure 1**; e.g., principal component analysis). Data mining analyses are related to MVAs; however, some have arisen out of computer science rather than conventional statistics. Data mining analyses include procedures such as random forest regression, random forest classification and support vector machines.

The aim of this paper is to provide a succinct guide to some MVAs and data mining analytic methods that can be applied to auditory and vestibular neuroscience data related to SNHL, tinnitus, and vestibular dysfunction, at both the basic experimental and clinical levels. Particular emphasis will be placed on "classification methods" that are relevant to the search for biomarkers of auditory and vestibular dysfunction, i.e., linear discriminant analysis, support vector machines, random forest classification, Bayesian classification, and orthogonal partial least squares discriminant analysis. However, classification and regression methods are related statistically, and for this reason, regression methods, in which there is no categorical dependent variable, will also be addressed. The review is intended to exemplify the application of MVA and data mining methods to problems in vestibular and auditory neuroscience, and is not meant to be exhaustive in terms of the specific methods described; procedures such as artificial neural network modeling (ANN), structural equation modeling, multivariate regression, canonical correlation analysis and many others, are also important, but are outside the scope of this review.

Abbreviations: GC/MS, gas chromatography/mass spectrometry; MVA, multivariate statistical analysis; OLPSDA, orthogonal partial least squares discriminant analysis; SNHL, sensorineural hearing loss.

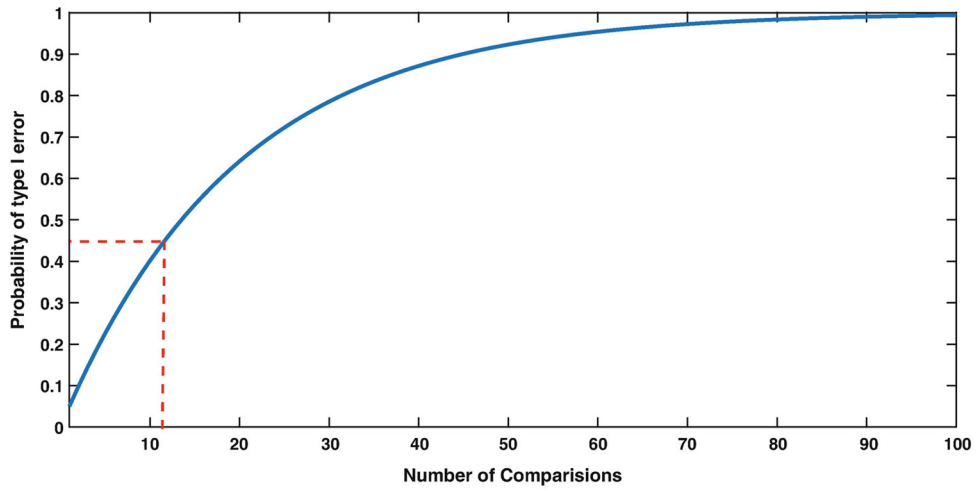

FIGURE 2 | The Type I error rate (False Alarm rate) strongly depends on the number of comparisons. For example, with 12 comparisons (red dashed lines), the probability of making at least one False Alarm is 0.46, i.e., much increased compared to 0.05 with only 1 comparison. From Herzog et al. (7) with permission.

UNSUPERVISED METHODS

Principal Component Analysis and Factor Analysis

Principal Component Analysis (PCA) attempts to explain variation in data using linear combinations of variables. It is a "dimension reduction" procedure, often used to reduce the number of variables to a smaller number of "components," which account for most of the variation in the data. In contexts such as metabolomics, where hundreds of metabolites may be investigated for their relationship to some disease state, it can be difficult to conceptualize their role just because of their sheer number. PCA looks for underlying latent components or factors, which represent linear combinations of variables, but without predicting a dependent variable. The objective is to find linear combinations of variables that explain most of the variation in the data, in the process reducing the number of separate variables in the data ("reducing dimensionality") (1, 32–34). These components or factors are expressed as "eigenvalues," which in PCA are represented as linear combinations of the original variables, each with a coefficient or "eigenvector" that indicates the "direction" of that particular variable for each component. An important attribute is that the different PCs are uncorrelated or "orthogonal" (32–34), and this property means that they can be used in other statistical techniques such as discriminant analysis, where correlation between independent variables can be a problem (see orthogonal partial least squares discriminant analysis below in Orthogonal Partial-Least Squares Discriminant Analysis).

For each PC, each of the original independent variables is expressed in a linear equation with specific coefficients that represent the "weighting" of the variable in that component. The number of PCs, which can be large, is usually displayed in decreasing order of importance in explaining the variability in the data matrix, often shown graphically as a "Scree plot." PCA is often performed using the correlation matrix for the data, in which case the data have to be standardized, i.e., each value subtracted from the mean for that variable and divided by the standard deviation (i.e., "z scores"). This prevents extreme differences in variance, e.g., due to different measurement scales, disproportionately affecting the analysis. While PCA is an exploratory method that does not make very many assumptions, the related method, Factor Analysis, has a formal statistical model, and assumptions such as multivariate normality (see below in Linear Discriminant Analysis) become important.

The interpretation of the PCs relies on the magnitude of the eigenvalues, and the contrasts between the eigenvectors for the variables relating to that eigenvalue. There is no specific criterion for how many PCs should be used; however, ideally, there should be a small number of PCs that explain most of the variation of the data. Loading plots, which represent the variance or magnitude of the variables within a PC, are often used to compare the different variables in the first two or three components. Because the interpretation of the PCs relies on the loadings, sometimes "rotations" are used to maximize the contrasts between them while maintaining the relationship between the variables in the components. Examples include "varimax" and "quartimax" rotations (1, 32–34).

Whether PCA is of any use in the analysis of multiple variables, depends on whether considering the different variables together, as a component, makes sense in the context of the research question, and also on what meaning can be attributed to the differences between the loadings. For example, if changes in free radicals are related to SNHL, does it make sense to reduce chemicals related to free radical generation to single components that combine the individual variables, or does this lose information? This problem of interpretability, which undermines many MVAs, will be addressed in a later section (see section Data pre-processing and imputation, overfitting

TABLE 1 | Different types of MVA and Data Mining Methods categorized according to whether they involve a categorical or continuous (quantitative) dependent variable and whether they specify a dependent variable (i.e., Supervised) or not (i.e., Unsupervised).

Supervised
Qualitative or categorical variables
Linear discriminant analysis
Logistic regression
Partial least squares discriminant analysis
Structural equation modeling
Support vector machines (DM)
Random forest classification (DM)
Neural networks (DM)
K nearest neighbors
Quantitative variables
Multiple linear regression
Canonical correlation analysis
Multivariate multiple regression
Structural equation modeling
Random forest regression (DM)
Gradient boosted decision trees (DM)
Neural networks (DM)
K nearest neighbors
Unsupervised
Qualitative or categorical variables
Correspondence analysis
Quantitative variables
Principal component analysis
Factor analysis
Cluster analysis
Multidimensional scaling
Ordination

"DM" denotes those methods that emerged out of dating mining research in computer science. From Smith (31) with permission.

and the problem of interpretability). PCA is often useful in a context where there are hundreds of variables, e.g., genomics, metabolomics, where it is useful to determine whether there is a change in the overall pattern of genes or metabolites [e.g., (35)].

Cluster Analysis

Another MVA method that has not been used extensively in the context of auditory or vestibular neuroscience, is cluster analysis. Cluster analyses are a type of non-parametric statistical analysis that is used to explore the natural groupings of variables in a data set (1). Therefore, assumptions such as multivariate normality and equality of the variance-covariance matrices (see below in Linear Discriminant Analysis) are not required (1, 36). Different measurements of the distance between the variables, such as squared Euclidean or Mahalanobis distance, are used to relate them to one another, and specific algorithms (e.g., Ward Minimal Variance Linkage) are used to determine the clusters (36). As with PCA, the standardized data (i.e., z scores) are usually used in order to prevent bias introduced by differences in scales of measurement. The results are usually displayed using a "dendrogram." Some cluster analysis algorithms, such as single linkage, are susceptible to producing long strings of clusters ("chaining") (1, 36). Ward's Minimal Variance Linkage method, based on the objective of obtaining the smallest within-cluster sum of squares (the "minimal variance principle"), is often a good option (1, 36). The results of PCA and cluster analysis are often related, and it can be observed that many of the original independent variables that co-vary closely together in the dendrogram, also appear to have similar eigenvectors in the dominant PCs. In this way, PCA and cluster analysis provide similar information regarding which variables "work together," but in different ways.

K-Nearest Neighbors Algorithm

The K-Nearest Neighbors ("*k*-NN") Algorithm can be used for regression or classification purposes. It is a non-parametric procedure in which either a category (in the case of classification) or a continuous variable value (in the case of regression) is estimated on the basis of its "nearest neighbours," where "*k*" is usually a small positive integer (2, 37). The data are usually standardized (see above) before the analysis is performed. The main challenges of this method include determining the appropriate value for k (i.e., how many neighbors?) and how the distance between neighbors should be quantified [see (37) for a discussion]. It is possible to use the *k*-NN algorithm in unsupervised or supervised forms.

SUPERVISED METHODS

Regression

Multiple Linear Regression

Another statistical method that has been under-employed in auditory and vestibular neuroscience is multiple linear regression (MLR). MLR is a part of the general linear model (GLM), that is useful for determining whether one continuous variable can be predicted from a combination of other variables. Simple linear regression can be expanded to include more than one predictor variable to become MLR, which has the general form: $Y = \beta_0 + \beta_1 X_1 + \beta_2 X_2 + ... \beta_p X_p + \varepsilon$, where Y = the continuous dependent variable; X_1, X_2,...X_p are independent variables; β_1, β_2... β_p are coefficients; β_0 is the intercept and ε is the error term (2, 36–41).

Canonical correlation analysis is an extension of MLR in which multiple Y variables are related to multiple X variables (1).

Formal statistical hypothesis tests for MLR, like those for simple linear regression, make assumptions regarding the distribution of the data, which cannot always be fulfilled (see section Data pre-processing and imputation, overfitting and the problem of interpretability). These assumptions are the same as those for other methods that are part of the GLM, such as analysis of variance (ANOVA): that the residuals are normally distributed, with homogeneity of variance, and that they are independent of one another (e.g., not autocorrelated) (31, 36–43). Furthermore, the predictor variables should be numerical, although indicator variables can be used in order to include nominal variables (e.g., binary coding to represent male and female). The violation of the assumption of normality can sometimes be redressed using data transformation, which may also correct heterogeneity of variance, but other issues such as autocorrelation, are not

easily dealt with and may require methods such as time series regression (31, 36–43).

Unlike simple linear regression, MLR is more complicated in terms of avoiding potential artifacts. Because the coefficient of determination, the R^2, which indicates as a percentage or fraction, how much of the variation in the dependent variable is explained by the independent variables, will increase as more independent variables are incorporated into the regression model, an "adjusted R^2" must be used in order to compensate for the number of variables included. The adjusted R^2 = [R^2-(k/n−1)][(n−1)(n−(k + 1))]. For k = 1 variables, the R^2 and adjusted R^2 are approximately equal.

There are various forms of MLR: forward regression, backward regression, stepwise regression and best subsets regression. In forward regression, predictors are added into the model one at a time (if α is set to 1.0, then all of them will be included, in ascending order of significance). In backward regression, predictors are taken out one at a time (if α is set to 0, all of them will be taken out, in descending order of significance). Backward regression tends to be preferred over forward regression because it allows examination of the interaction between variables (31, 36–43). In stepwise regression, the program stops at each step and checks whether the variables, either in the model or not, are the best combination for that step. The adjusted R^2 will change as different variables are included in a model and an ANOVA can be done at each step to determine whether it has made a significant difference. Best subsets regression, however, computes all possible MLR models from which the researcher must choose the best, based on the adjusted R^2 and various diagnostic information regarding the validity of the regression model (31, 36–43). One of the greatest problems in MLR is "over-fitting" and "multicollinearity" (31, 36–39, 44–46). If the regression variables are highly inter-correlated, multicollinearity occurs. This inflates the variance of the least square estimates and therefore the coefficients will be inaccurate, which can lead to the situation in which the ANOVA for the regression is significant without any single *t*-test for an individual variable being significant. In this case, one or more of the highly correlated variables needs to be removed from the regression model. One way of controlling for multicollinearity is using an index such as the Mallow's Cp index. The adjusted R^2 should be high but the Mallow's Cp index [= (the sum of squares for the error at the current step/mean square error for the full regression)–(n−2p), where n = total number of observations and p = number of estimated coefficients], should be as small as possible. Ideally, it should be one more than the number of parameters in the current step. Other indices of multicollinearity include the variance inflation factor and tolerance (1/variance inflation factor) (36–39, 45, 46). Different software packages (e.g., SPSS and Minitab) offer different options. Autocorrelation in the data can be tested using the Durban-Watson statistic (36–39, 45, 46). Like most other multivariate statistical procedures, MLR is prone to artifacts and researchers need to be cautious when using it [see (44) for a rigorous discussion of this issue].

Random Forest Regression

Although modeling using regression trees has been used for over 25 years, its use in auditory and vestibular neuroscience has been very limited. In regression tree modeling, a flow-like series of questions is asked about each variable ("recursive partitioning"), subdividing a sample into groups that are as homogeneous as possible by minimizing the within-group variance, in order to determine a numerical response variable (47, 48). The predictor variables can be continuous variables also, or they can be categorical. By contrast with MLR, which makes assumptions about the distribution of the data, regression trees make no distributional assumptions. The data are sometimes split into training and test data sets (e.g., 70:30) and the mean square error between the model based on the training data and the test data, is calculated as a measure of the model's success. Variables are chosen to split the data based on the reduction in the mean square error achieved after a split (i.e., the information gained). Unlike MLR, interactions between different predictor variables are automatically incorporated into the regression tree model and variable selection is unnecessary because irrelevant predictors are excluded from the model. This makes complex, non-linear interactions between variables easier to accommodate than in linear regression modeling (47, 48). Breiman et al. (48) extended the concept of regression trees by exploiting the power of computers to simultaneously generate hundreds of trees ("bagging"), known as "random forests," which were based on a random selection of a subset of data from the training set. The various regression tree solutions are averaged in order to predict the target variable with the smallest mean square error (47–52). An alternative form of cross-validation of the random forest model, which does not require splitting the data set and therefore is particularly useful in the context of small sample sizes, is the leave-one-out ("LOO") procedure. Here, each subject is removed from the sample, in turn, and the model based on the remaining data is used to predict for that subject; then, another subject is removed, and the procedure repeated, until the entire data set has been cross-validated (47–51).

Gradient boosted decision trees (GBDTs) are an alternative to the random forest procedure in which learning algorithms are combined ("boosting") so that each decision tree tries to minimize the error of the previous tree (37, 52).

Classification

Logistic Regression

Logistic regression is similar to linear regression but applied to the prediction of a binary outcome (37, 39). Rather than fitting a linear function to the prediction of a continuous dependent variable, logistic regression employs the logistic function, logistic(η) = 1/(1 + exp(-η)), to generate an outcome between 0 and 1. The logistic function is then incorporated into the probability function, $P(y^{(i)} = 1) = 1/(1 + exp\ (-(\beta_0 + \beta_1\ x_1^{(i)} + \ldots.\ \beta_p\ x_p^{(i)})))$, where P is a probability, x are predictor variables, the β's represent coefficients and β_0 is the intercept (37). The output of this function is then a probability of classification to one of two groups, although logistic regression can also be extended to multinomial regression (39).

Linear Discriminant Analysis

Linear discriminant analysis is a statistical method that is often used to predict the membership of two or more groups from a linear combination of independent variables (1, 2). A linear

discriminant function (LDF) has the general form: $Z = a_1X_1 + a_2X_2 + ...a_pX_p$, where Z refers to the group, X, X_2,...X_p are independent variables, and a_1, a_2,...a_p are coefficients (1). Linear discriminant analysis is similar in aim, but different in approach, to logistic regression, in which the dependent variable is binary (0/1) and consists of positive (a "success") and negative responses (a "failure") only (1). An example in the context of auditory neuroscience might be the prediction of SNHL by a linear combination of neurochemical variables in the peripheral or central auditory systems [e.g., (35)]. The statistical significance of the LDF can be assessed using statistics such as Wilk's λ and its success in separating the groups can be evaluated using cross-validation (e.g., a LOO procedure), in which the linear equation is used to classify the data, one observation at a time, without knowledge of the actual group membership. It is possible to use a stepwise linear discriminant analysis. However, some authors [e.g., (1, 45, 46)] suggest that stepwise methods can result in suppressor effects and an increase in type II error. Linear discriminant analysis is readily available in programs such as SPSS and Minitab. It is part of the GLM, and therefore makes similar assumptions to MLR, but other forms of discriminant analysis, which do not make all of these assumptions, include quadratic discriminant analysis, where the data are assumed to be normally distributed but the variance-covariance matrices need not be identical. Orthogonal partial least squares discriminant analysis is another type of discriminant analysis in which the discriminant function consists of PCs from a PCA (see below in Orthogonal Partial-Least Squares Discriminant Analysis).

As mentioned, MVA methods that are part of the GLM, such as linear discriminant analysis, do make assumptions. The first is that, for formal tests of statistical significance to be valid, the data within groups should have a multivariate normal distribution (1). Unlike univariate statistical analyses such as ANOVA, linear discriminant analysis is quite sensitive to the violation of the assumption of multivariate normality (1, 2, 36, 53). It is difficult to test for multivariate normality, because most programs such as SPSS do not offer such an assumption test (1). Because univariate normality, i.e., the normality of the individual variables, is necessary but not sufficient for multivariate normality, it is possible for each individual variable to be normally distributed without the multivariate distribution being normally distributed. Stevens (2) points out that because a multivariate normal distribution entails that all subsets of variables have normal distributions, one way to assess multivariate normality is to determine whether all pairs of variables are bivariate normal. Box's test for the homogeneity of the covariance matrices (see below) is sensitive to violation of multivariate normality; therefore, in order to obtain results from that test that are valid, whether the assumption of multivariate normality is fulfilled, must be of concern (2). However, there is a multivariate formulation of the central limit theorem and sample sizes of 10–20 per group appear to be sufficient to afford protection against the consequences of violating multivariate normality (2, 45, 46). It should be noted that linear discriminant analysis may still discriminate between groups even if the assumption of multivariate normality does not hold. On the other hand, multivariate normality does not necessarily mean that it will effectively discriminate between the groups.

A second assumption of linear discriminant analysis, but not quadratic discriminant analysis, is that the population covariance matrices are equal for all groups, usually tested using Box's *M*-test (1, 36). If this assumption is violated, a quadratic discriminant analysis, can be used instead. In a review of several Monte Carlo studies, Stevens (2) concluded that, provided that the sample sizes are equal, even moderate heterogeneity of the covariances does not substantially affect type I error. Unequal sample sizes, on the other hand, are potentially very problematic if the covariances are unequal (2). While Box's *M*-test is often used, its null hypothesis may be rejected only because the multivariate normality assumption is violated (2). Therefore, it is important to determine whether this is the reason for a significant Box's *M*-test. Box's *M*-test is also very sensitive to departure from homogeneity of the covariances (45, 46). Both Stevens (2), Field (45), and Field et al. (46) suggest that even if Box's *M*-test is significant, the type I error rate will be only slightly affected provided that there are equal sample sizes, although the power may be somewhat reduced.

One of the common problems in many MVAs is the sample size for each variable, n, relative to the number of variables, *p*. While unequal sample sizes can be problematic, as described above, when *p* is greater than *n*, statistical analyses such as linear discriminant analysis can become invalid. Stevens (2), Field (45), and Field et al. (46) suggest that, unless the n is large, $p \leq 10$. Monte Carlo studies have shown that if the sample size is not large compared to the number of variables, the standardized discriminant function coefficients and correlations obtained in a linear discriminant analysis, are unstable (2). By "large," Stevens (2) suggests a ratio of *n* (total sample size):*p* (number of variables) of 20:1. He further cautions that a small *n:p* ratio (i.e., $\leq$5) can be problematic for stepwise linear discriminant analysis in particular, because the significance tests are used to determine which variables are included in the solution (2).

These methods, and others related to them such as orthogonal partial least squares discriminant analysis, should be applicable to many situations in auditory and vestibular neuroscience in which multiple variables interact to determine a categorical dependent variable, e.g., SNHL, tinnitus, Meniere's Disease, vestibular neuritis, and benign paroxysmal positional vertigo, provided that the sample sizes are sufficient and the cross-validations demonstrate the predictive accuracy of the LDFs. Given that Box's *M*-test of the equality of the covariance matrices assumes multivariate normality, one way to proceed is to determine whether all pairs of variables appear to be bivariate normal. If so, Box's *M*-test can be used as a guide to whether the assumption of the equality of the covariance matrices is fulfilled. However, the cross-validation procedure can be used as the ultimate arbiter of the effectiveness of the LDF (31).

Random Forest Classification

The random forest method that is used for regression, can also be used for classification purposes, in which case the solution is based on the number of "votes" from the different trees for a particular category (48, 49). The effect of variable removal on

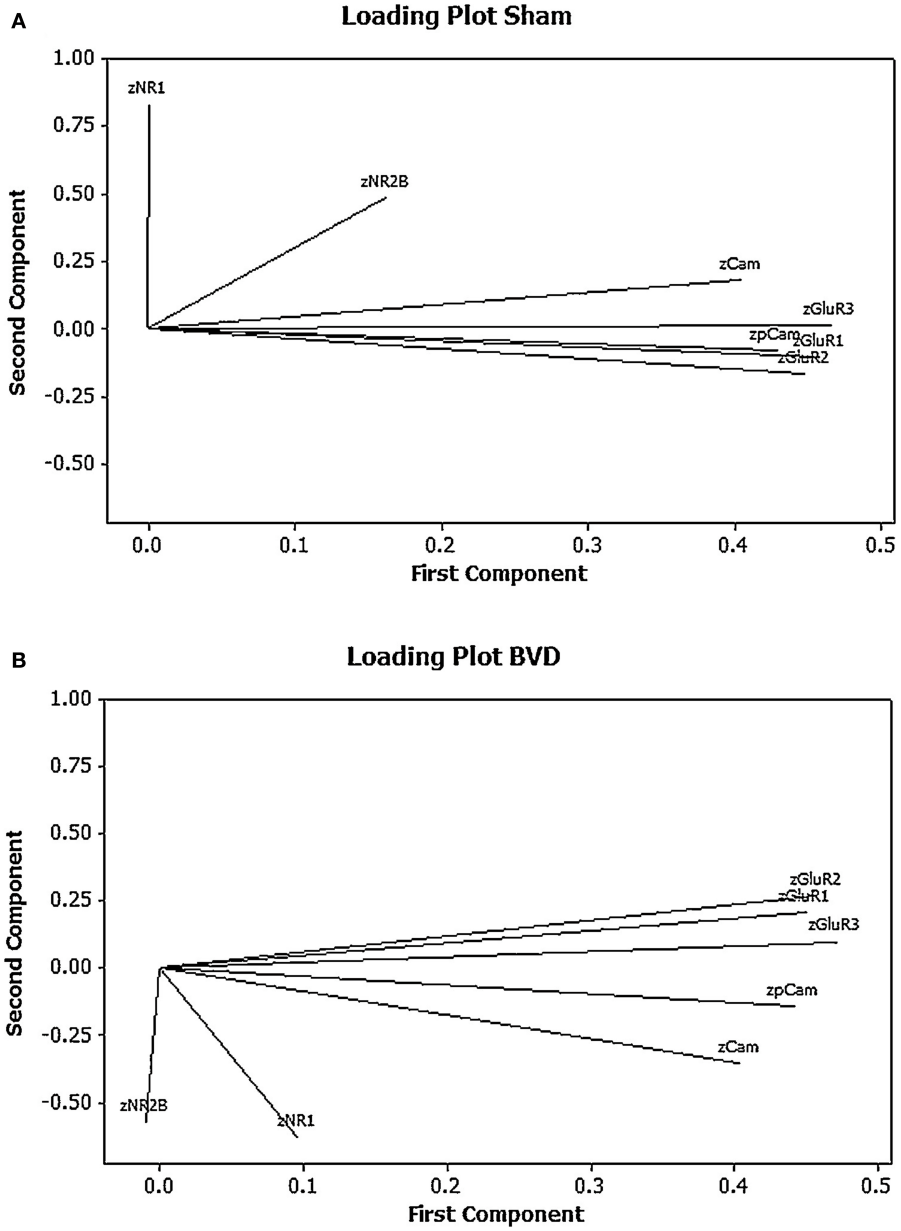

FIGURE 3 | Loading plots for the first 2 principal components for the mean normalized density of expression of NR1, NR2B, GluR1, GluR2, GluR3, CaMKII, and pCaMKII in the CA1, CA2/3, and dentate gyrus (DG) regions of the hippocampus at 6 months following sham **(A)** or BVD **(B)** surgery. Note the inverted pattern of loadings for the BVD group compared to the sham group. From Smith and Zheng (6) with permission.

the mean decrease in accuracy, the "out of bag" ("OOB") error, and the overall classification matrix error ("confusion matrix error"), are used to evaluate the success of the classification. The OOB error is the error based on the observations that were excluded from the subset of the training data (the "bag") used to generate the decision tree (47, 48). Unlike linear discriminant analysis, random forest classification makes no distributional assumptions and therefore can be applied to situations in which the sample sizes are small relative to the number of variables (47, 48). Random forest classification, along with support vector machines, can be carried out using specific packages in the statistics program, R (47, 54–57). For those who do not wish to use code in R, there is a data mining graphics user interface available, called "Rattle," which is menu-driven and easy to use (55).

Support Vector Machines

Support vector machines are an alternative method for classification, which employ "support vectors," observations that form the spatial boundary between different classes (47–49, 54).

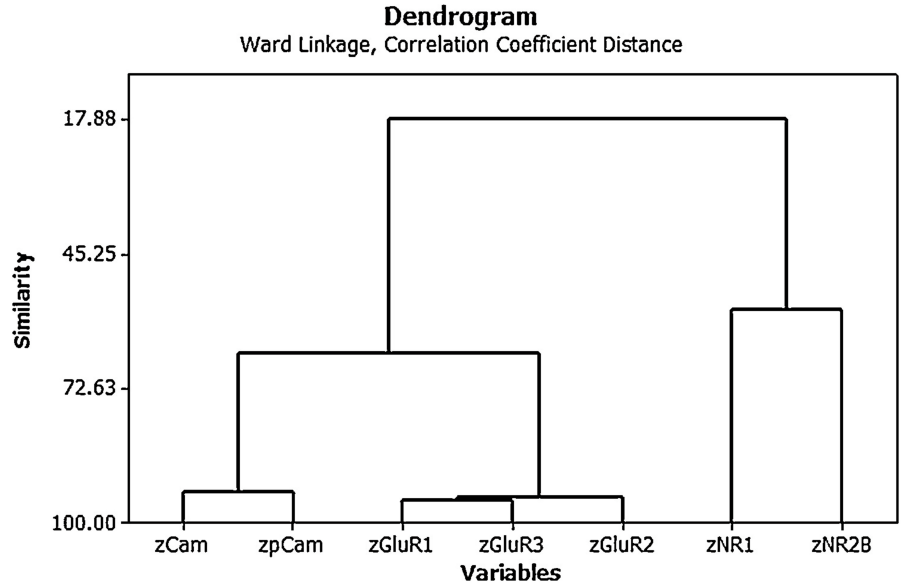

FIGURE 4 | Ward's minimal variance cluster analysis on the correlation coefficient distance for the mean normalized density of expression of NR1, NR2B, GluR1, GluR2, GluR3, CaMKII, and pCaMKII in the CA1, CA2/3, and dentate gyrus (DG) regions of the hippocampus at 6 months following BVD or sham surgery (i.e., both groups shown together). The *y* axis shows degrees of similarity, where 100.00 is the highest similarity and 17.88 is the lowest. Note that the NMDA receptor subunits vary together, as do the AMPA receptor subunits, as well as the CaMKII isoforms. From Smith and Zheng (6) with permission.

TABLE 2 | Results of the multiple linear regression analysis of the data from Smith et al. (51), showing the adjusted R^2-values, the residual standard errors (RSEs) and the significant input variables.

	GABA	put	spd	spm	arg	glut	agm	orn	cit
R^2	0.811	0.675	0.861	0.938	0.936	0.698	0.796	0.623	0.958
MSE	846.57	0.23	203.29	34.89	225.48	50064.54	0.12	189.54	119.52
Significant predictor variables	cit***	ag***	spm***	spd***	cit***	GABA***	put***	age***	arg***
	glut***	orn*	age***	cit***	orn*	spm***	cit***	cit***	GABA**
	spd*		orn**	glut***		orn**	age***	glut**	age**
			glut*					spd**	spm**
								enrich*	orn**

****P ≤ 0.0001, ** P ≤ 0.001, * P ≤ 0.05. From Smith et al. (51) with permission.*

These support vectors are then used to determine a hyperplane that defines the boundary between the classes (46–54). Support vector machines can employ a variety of functions, such as radial kernel and Laplace functions, to remap the data and generate new variables that can separate the different categories (47–54). The data are usually split into training and test data sets (e.g., 70:30) and the difference between the model based on the support vectors in the training data set, and the test data set, is calculated as a measure of the model's success. As with linear discriminant analysis, classification error matrices can be used to evaluate the success of the classification, as well as receiver operating characteristic ("ROC") curves, that quantify the relationship between the true positive rate of classification ("sensitivity") and the false positive rate of classification ("1—the specificity") (47).

One of the major advantages of support vector machines is that they do not make distributional assumptions like linear discriminant analysis, other than that the data are independent and identically distributed. Wilson (54) suggests that for this reason, even small sample sizes can provide accurate estimates of prediction error when there are a large number of variables.

Bayesian Classifiers

Bayesian classification methods are based on Bayes' Theorem, which relates a posterior probability of an event to a prior probability: P(H/X) = P(X/H)(P(H)/P(X), where X represents the data and H represents the hypothesis; P(H/X) = the probability of H given X (the posterior probability), P(X/H) = the probability of X given H, P(H) = the probability of H (the prior probability), and P(X) = the probability of X, which cannot = zero. P(H/X) and P(X/H) are known as "conditional probabilities" and P(X) and P(H) as "marginal probabilities"

TABLE 3 | Results of the random forest regression models of the data from Smith et al. (51), showing the proportion of variance explained values, the residual standard errors (RSEs) and the input variables chosen using the stepwise process.

	GABA	put	spd	spm	arg	glut	agm	orn	cit
R^2	0.939	0.868	0.947	0.989	0.986	0.914	0.910	0.861	0.983
MSE	271.63	0.09	77.38	6.14	47.96	14,285.84	0.05	69.75	48.63
Most important predictor variables	cit	agm	spm	arg	cit	spm	arg	age	arg
	glut	arg	arg	cit	spm	GABA	put	glut	spm
	arg		agm	agm		cit	spm	cit	agm
			cit					GABA	GABA
								arg	spd

From Smith et al. (51) with permission.

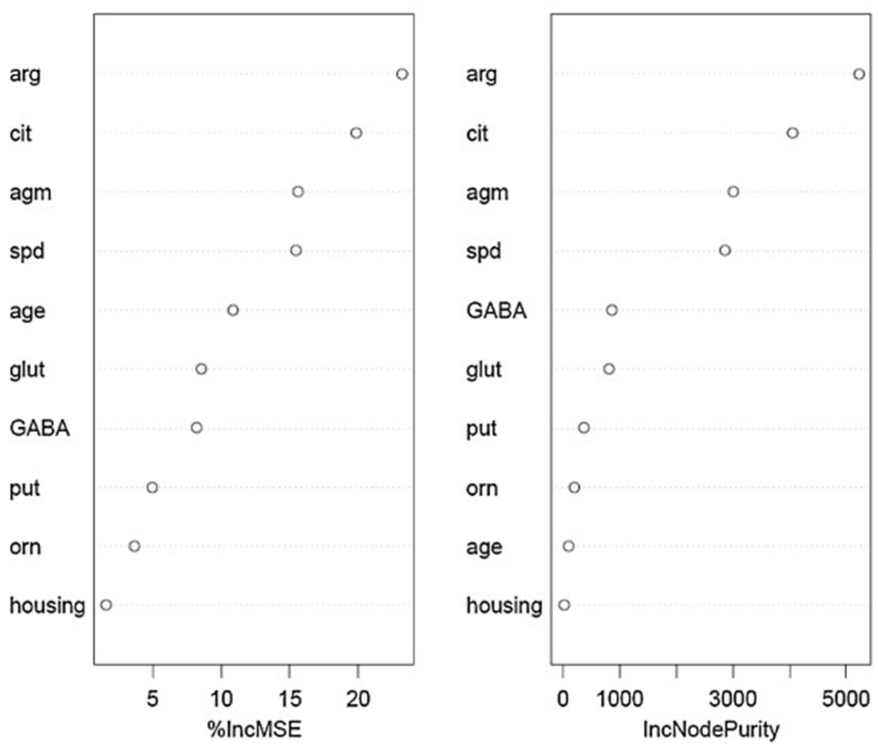

FIGURE 5 | Variables in order of importance for the random forest regression analysis for spermine, which had the highest proportion of variance explained (0.94). From Smith et al. (51) with permission.

(58–61). In simple terms, Bayes' Theorem relates the degree of belief in an hypothesis before accounting for the data, to that after accounting for the data, so that the probability of the hypothesis being true given the data, equals (the probability of obtaining the data given that the hypothesis is true, multiplied by the probability that the hypothesis is true), divided by the probability of obtaining the data (58–61). The calculation of the conditional and marginal probabilities can be used to generate a Bayesian Network, which can be displayed in graphical form such as directed acyclic graphs (61).

Orthogonal Partial-Least Squares Discriminant Analysis

Also known as orthogonal projection to latent structures discriminant analysis, orthogonal partial-least squares discriminant analysis (OPLS-DA) is a method of discriminant analysis that cleverly combines PCA with discriminant analysis and partial least squares regression, in order to classify subjects (62). Therefore, it can be seen as an alternative to methods such as linear discriminant analysis, support vector machines and random forest classification. OPLS-DA is an ideal method to use in the search for biomarkers

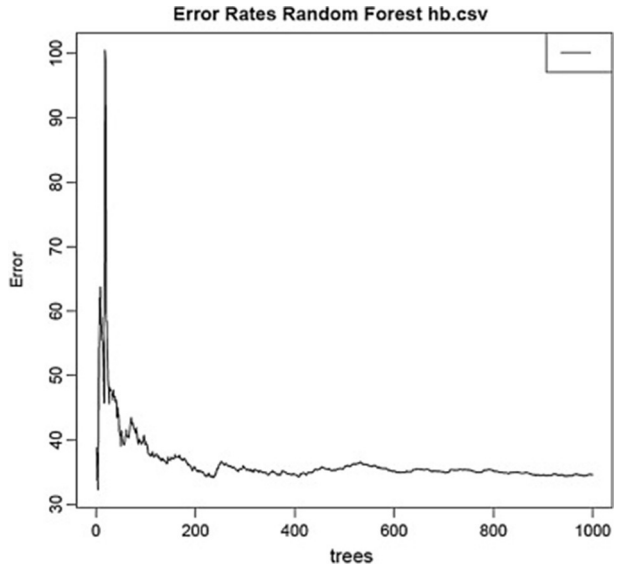

FIGURE 6 | Decrease in error as a function of the number of trees for the random forest regression model for spermine, which had the highest proportion of variance explained (0.94). From Smith et al. (51) with permission.

of SNHL, tinnitus or vestibular disorders, for e.g., using metabolomic data from animals or humans with those conditions. In partial least squares regression, which is an extension of MLR, factors are extracted from the $Y'XX'Y$ matrix in order to generate prediction functions, only in the case of partial least squares discriminant analysis, the dependent variable is categorical. One major advantage of partial least squares discriminant analysis is that it is minimally restrictive because it allows for fewer observations than variables (i.e., less n than p), a problem that is significant for linear discriminant analysis (62). As with PCA and cluster analysis, the data would normally be standardized to z scores before proceeding.

In OPLS-DA, the X variables are latent variables that maximize the separation between the groups, ranked according to how much variation in Y that they explain. OPLS-DA separates the systematic variation in X into 2 parts: (1) that which is linearly related to Y; and (2) that which is unrelated or "orthogonal" to Y (62). The OPLS method uses a modification of the non-linear iterative partial least squares algorithm (62). An orthogonal signal correction procedure, developed by Trygg and Wold (62), employs an iterative process to find orthogonal components in the X matrix. For this it depends on a starting vector, which can use PCs from a PCA. The main problem with discriminant analysis is over-fitting, particularly where the $p >$ the n, so that the model works well on the training data but not on new data, and where there is multicollinearity. However, this possibility can be addressed using permutation testing (63). In permutation testing, variables are assigned randomly to the different samples, and new models are generated many times, e.g., 2,000. A null distribution of classifications is created, which is expected to be non-significant. The results obtained from the original data should be outside the 95 or 99% confidence intervals for the null distribution, in order to be statistically significant, i.e., not part of the null distribution (63).

Biplots can be used to show some of the results of an OPLS-DA, where the x axis is labeled "t[1]," which are the X scores predictive of Y, and the y axis is labeled "to[2]," which are the X scores that are not predictive of Y. Therefore, the x axis represents the between group variation and the y axis represents the within group variation. OPLS-DA calculates various indices of the success of the model. R^2X (cum) is the sum of the predictive and orthogonal variation in X that is explained by the model, which can be split into the predictive and orthogonal components. R^2Y (cum) is the total sum of variation in Y explained by the model. Q^2 is the effectiveness of the prediction, based on the OPLS-DA equation, using cross-validation, e.g., using a LOO procedure, where 0.9 would be excellent.

S plots are often used to help interpret the OPLS-DA results. In the S plot, the x axis "p[1]" is the magnitude of each variable in the x axis. The y axis "p(corr)[1]" is the reliability (obtained with confidence intervals using jack-knifing and cross-validation). Values close to zero on both axes are close to noise, i.e., they have almost zero magnitude and reliability. OPLS-DA can be carried out in R, or using the programs Metaboanalyst and Metscape 3.1 (35, 64).

Pathway impact analyses can also be carried out on the OPLS-DA. Using the prior knowledge of pathways, these methods look for over-representation of specific pathways in the data. They calculate the sum of the importance measures of the matched metabolites normalized by the sum of the importance measures of all metabolites in each pathway. Over-representation analysis, quantitative enrichment analysis, and single sample profiling are three different types of pathway analysis that can be used in the program Cytoscape 3.30 (35, 64, 65).

DATA PRE-PROCESSING AND IMPUTATION, OVERFITTING, AND THE PROBLEM OF INTERPRETABILITY

When using MVA and data mining methods to analyse data, some pre-processing of the data is often necessary. In the case of MVA, methods that are part of the General Linear Model (GLM), such as multiple linear regression, multivariate multiple linear regression, linear discriminant analysis, structural equation modeling, and canonical correlation analysis, require that the assumption of multivariate normality be met (see section Linear Discriminant Analysis). Therefore, data need to be checked to determine whether they are normally distributed or even whether they have a multivariate normal distribution (see Linear Discriminant Analysis). Normality (Q–Q) plots and plots of residuals vs. fitted values usually need to be obtained and formal assumption tests conducted, such as the Anderson-Darling, Shapiro-Wilk or Kolmogorov-Smirnov tests for univariate normality, and Bartlett's or Levene's tests for homogeneity of variance. If these tests are statistically significant (i.e., $P \leq 0.05$), a decision may be made to transform variables in order to achieve fulfillment of the normality and homogeneity of

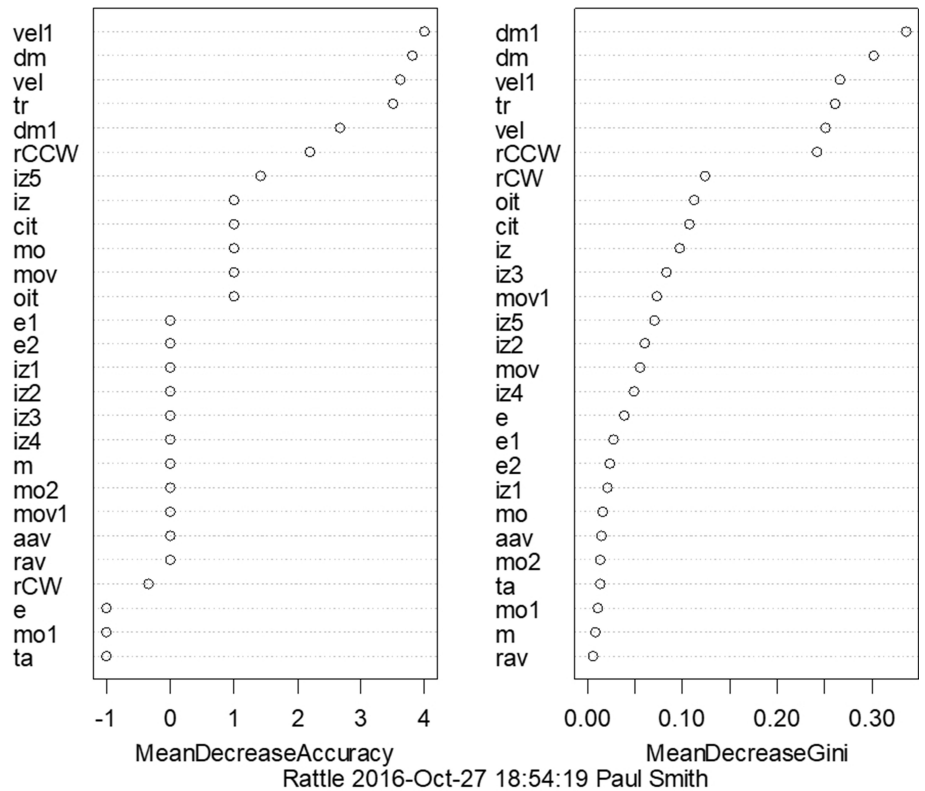

FIGURE 7 | Order of variable importance for the random forest classification for day 3 following BVD, showing the decrease in the accuracy of the prediction as the variables are removed. The mean decrease in Gini coefficient is an indication of the extent to which each variable contributes to the homogeneity of the nodes and leaves in the random forest. dm, distance moved nose-point; dm1, distance moved center-point; e, contracted; e1, elongation normal; e2, elongation stretched; iz, in zone outer zone, nose-point; iz1, in zone inner zone, nose-point; iz2, in zone mid zone, nose-point; iz3, in zone outer zone center-point; iz4, in zone inner zone center-point; iz5, in zone mid zone center-point; m, meander center-point; cit, center inter-transition center-point; mo, mobility immobile; mo1, mobility mobile; mo2, mobility highly mobile; mov, movement center-point/moving; mov1, movement center-point/not moving; rCCW, rotation counter-clockwise center-nose; rCW, rotation clockwise center-nose; ta, turn angle center-point; vel, velocity nose-point; vel1, velocity center-point; aav, absolute angular velocity center-point; oit, outer inter-transition center-point; rav, relative angular velocity; tr, total rotations. From Aitken et al. (72) with permission.

variance assumptions; however, great care needs to be taken in transforming non-linear dependent variables into linear ones, as in Scatchard plots, because of the way that it can distort the error around the line of best fit (66). For receptor binding data, non-linear regression is now considered preferable to linear regression following transformation (66). In the case of other methods such as PCA, OPLS-DA and cluster analysis, pre-processing may involve standardizing the data (see Principal Component Analysis and Factor Analysis), in order to ensure that differences in measurement scales do not bias the analysis.

Even for univariate statistical analyses, many statistical programs delete experimental subjects if they have missing data for procedures such as repeated measures ANOVAs (43, 45). Many animal studies in auditory and vestibular neuroscience already have small and unequal sample sizes; therefore, simply deleting data in the case of missing values will result in lower statistical power and may bias the results (67). For alternatives to repeated measures ANOVAs such as linear mixed model analysis, "imputation" procedures are employed in order to estimate the missing values ("Missing Values Analysis or MVA") (43, 67, 68). A maximum likelihood (ML) and expectation-maximization (EM) approach (a combination of imputation and ML) can be used (68). However, only some programs (e.g., SPSS) offer the EM algorithm and for the ML and EM methods to be used, the missing data must be "missing at random" (MAR, i.e., the probability that an observation is missing must not depend on the unobserved missing value but may depend on the group to which it would have belonged) or "missing completely at random" (MCAR, i.e., the probability that an observation is missing must not depend on the observed or missing values) (67, 68). In other words, there can be no bias to the way that data are missing, a condition that is sometimes difficult to satisfy. The

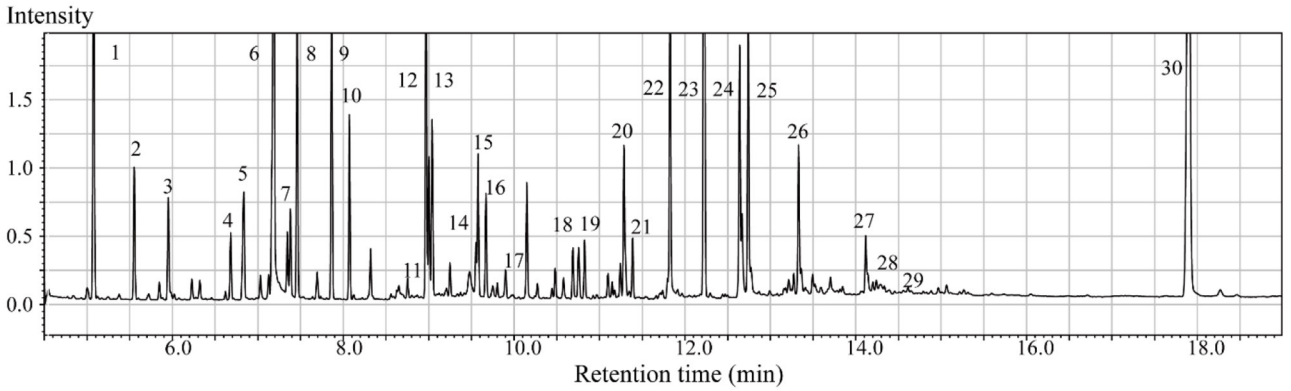

FIGURE 8 | Typical GC/MS chromatograms of extracts from brain tissue of a sham animal. The compounds were identified as: 1. Lactic Acid, 2. Alanine, 3. Oxalic acid, 4. Valine, 5. Urea, 6. Phosphoric acid, 7. Proline, 8. Glycine, 9. Serine, 10. Threonine, 11. Malic acid, 12. Aspartic acid, 13. γ-Aminobutanoic acid, 14. Creatinine, 15. Glutamic acid, 16. Phenylalanine, 17. N-Acetylaspartic acid, 18. Hypoxanthine, 19. Citric acid, 20. Lysine, 21. Tyrosine, 22. Palmitic acid, 23. Myo-Inositol, 24. Oleic acid, 25. Stearic acid, 26. Arachidonic acid, 27. Docosahexaenoic acid, 28. Inosine, 29. Glycerol monostearate, 30. Cholesterol. From He et al. (35) with permission.

K-NN algorithm discussed in K-Nearest Neighbors Algorithm can be used for imputation and there is a variety of multivariate imputation procedures [see (69) for a review].

"Overfitting" is an enormous problem in MVA and data mining methods which involve regression modeling. Overfitting occurs when a model for prediction is based so closely on a particular data set that it has little predictive value for other, similar data sets, often a result of including too many parameters in the model (44). As a result, a regression model based on a training data set may have no predictive value for the test data set. Although the problem is well-recognized in MLR (44), Breiman et al. (48) have suggested that random forest methods do not overfit, a view that has been challenged (70). Solutions to overfitting include collecting more data so that there is a larger n for each predictor variable, p, combining predictors in order to reduce correlation between them and the use of "shrinkage and penalization" procedures (44). The adjusted R^2 in MLR is one type of shrinkage estimator because it takes into account the number of predictor variables. "Lasso" regression ("least absolute shrinkage and selection operator") is a method that generates a linear regression model with greater "sparsity" [see (37) for a review].

One of the advantages of univariate statistical methods is that they are relatively easy to understand and this is partly why they are so popular. Researchers turn to multivariate statistical and data mining (or machine learning) methods because they have to deal with many variables, sometimes hundreds or thousands, but in the process of using such procedures, they sacrifice simplicity and interpretability. Molnar (37) has written extensively about the problem of "interpretability" with MVA and data mining methods, which involve complex modeling. Even if they provide good predictive value, they may be difficult to understand. Simpler models, by definition, such as shorter decision trees, are more easily interpreted than longer ones. Molnar (37) has suggested that "model agnostic interpretation methods" be used for machine learning in preference to "model-specific ones." These are methods that can be applied to any machine learning model, are not restricted to a certain form of explanation (e.g., a linear formula vs. a graphic representation) and should have flexibility in the way that the explanation is represented. Examples include partial dependence plots (PDP), feature importance and Shapley values [see (37) for a review].

EXAMPLES OF APPLICATIONS OF MULTIVARIATE STATISTICAL AND DATA MINING METHODS TO THE ANALYSIS OF OTOLOGICAL DATA

Principal Component Analysis and Cluster Analysis

One of our research interests has been the role of neurochemical changes in the hippocampus in the cognitive deficits that occur following peripheral bilateral vestibular damage. In this process we have used western blotting to analyse the expression of various glutamate receptor subtypes in the rat hippocampus, given the importance of glutamate receptors to memory processes such as long-term potentiation [see (71) for a review]. Due to the fact that we quantified 5 different glutamate receptor subunit subtypes (GluR1, GluR2, GluR3, NR1, and NR2) and 2 forms of calmodulin kinase II (CaMII and phosphorylated CaMII), related to glutamate receptor activation, we decided to use PCA and cluster analysis to analyse the results, particularly so that we could understand the co-variation and interactions of any changes in the expression of the proteins. Using univariate statistical analysis, there were no significant differences in the expression of any individual protein between the bilateral vestibular deafferentation (BVD) group and the sham controls (15); however, PCA suggested that when the 1st and 2nd components were plotted against one another using a loading plot, the relationship between the expression of the different proteins had changed [see **Figure 3**; (6)]. Although the meaning

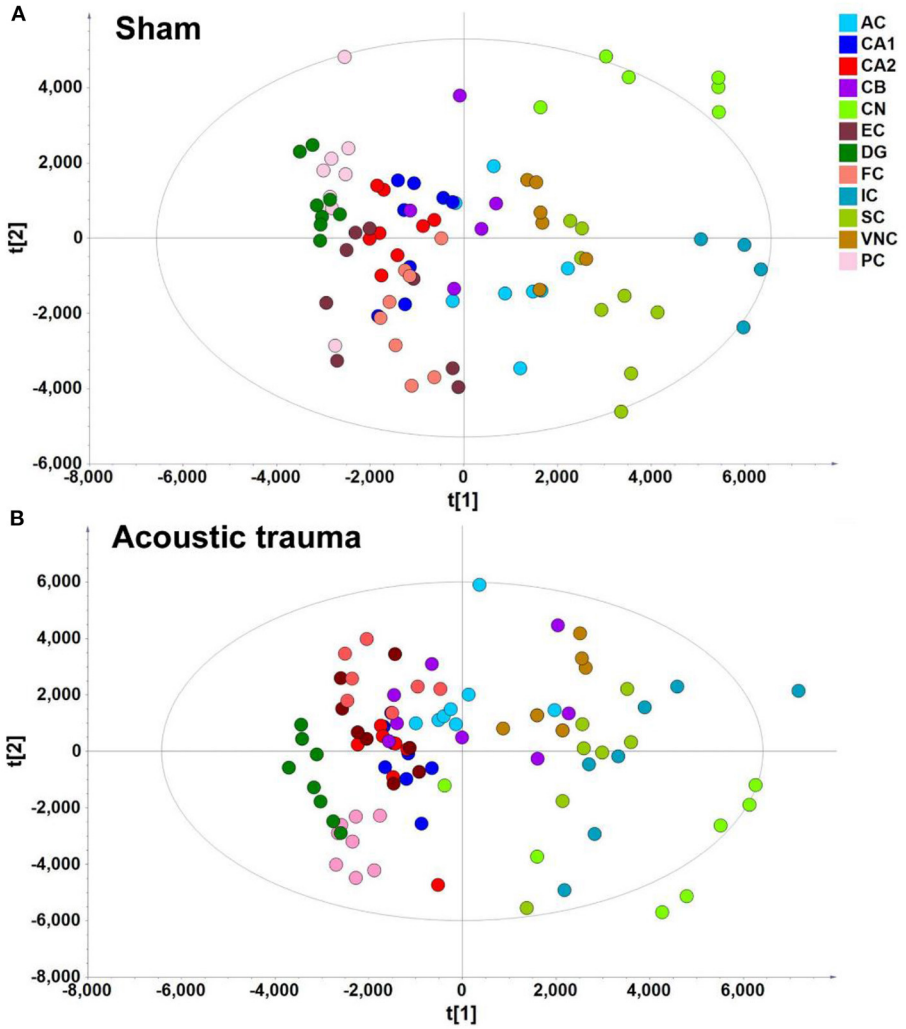

FIGURE 9 | PLS-DA score plot of different brain regions from sham **(A)** and acoustic trauma **(B)** groups. **(A)** sham [PC1: *R2X* = 0.344, *R2Y* = 0.0842, Q^2 =0.0726; PC2: *R2X* = 0.249, *R2Y* = 0.0525, Q^2 = 0.0373; All 6 PCs: *R2X* (cum) = 0.84, *R2Y* (cum) = 0.381, Q^2 (cum) = 0.286]; **(B)** acoustic trauma [PC1: *R2X* = 0.336, *R2Y* = 0.0759, Q^2 = 0.0683; PC2: *R2X* = 0.307, *R2Y* = 0.0513, Q^2 = 0.0407; All 6 PCs: *R2X* (cum) = 0.875, *R2Y* (cum) = 0. 384, Q^2 (cum) = 0.325]. AC, auditory cortex; CB, cerebellum; IC, inferior colliculus; CN, cochlear nucleus; VNC, vestibular nucleus complex; SC, superior colliculus; CA1 and CA2 of the hippocampus; DG, dentate gyrus; FC, frontal cortex; PC, perirhinal cortex; EC, entorhinal cortex. From He et al. (35) with permission.

of this shift is not easy to interpret—one of the perennial problems of PCA—this MVA revealed a change in the pattern of interaction between the different proteins which the univariate analysis could not. Note that all of the data were transformed to z scores.

Cluster analysis of the individual protein variables showed that they co-varied in a predictable way [see **Figure 4**; (15)]. Note again the use of z scores and the fact that the AMPA (GluR1, 2, and 3) and NMDA (NR1 and 2) receptor subunits tended to co-vary closely with one another.

Multiple Linear Regression

Another area of interest for us has been the L-arginine cycle and its role in producing nitric oxide synthase, polyamines and glutamate in the brainstem vestibular nucleus and cerebellum (**Figure 1**). This complex pathway is involved in brain aging in the central vestibular system and has been the target for drug treatments aimed at interfering with neurodegenerative diseases such as Alzheimer's Disease (3, 4). Because these neurochemicals interact in a network, it is important to understand how each part of the system affects the other parts. We have used MLR in an attempt to predict different neurochemicals in this pathway from one another, with adjusted R^2 values ranging from 0.50 (ornithine) to 0.95 (citrulline) (51). The best predictions were for citrulline (0.95), spermine (0.93) and arginine (0.92) (see **Table 2**). Assumptions were tested using normal Q–Q plots and residuals vs. fitted values plots, and were fulfilled. In this study, MLR was compared directly with random forest regression on the same data set (51) (see below).

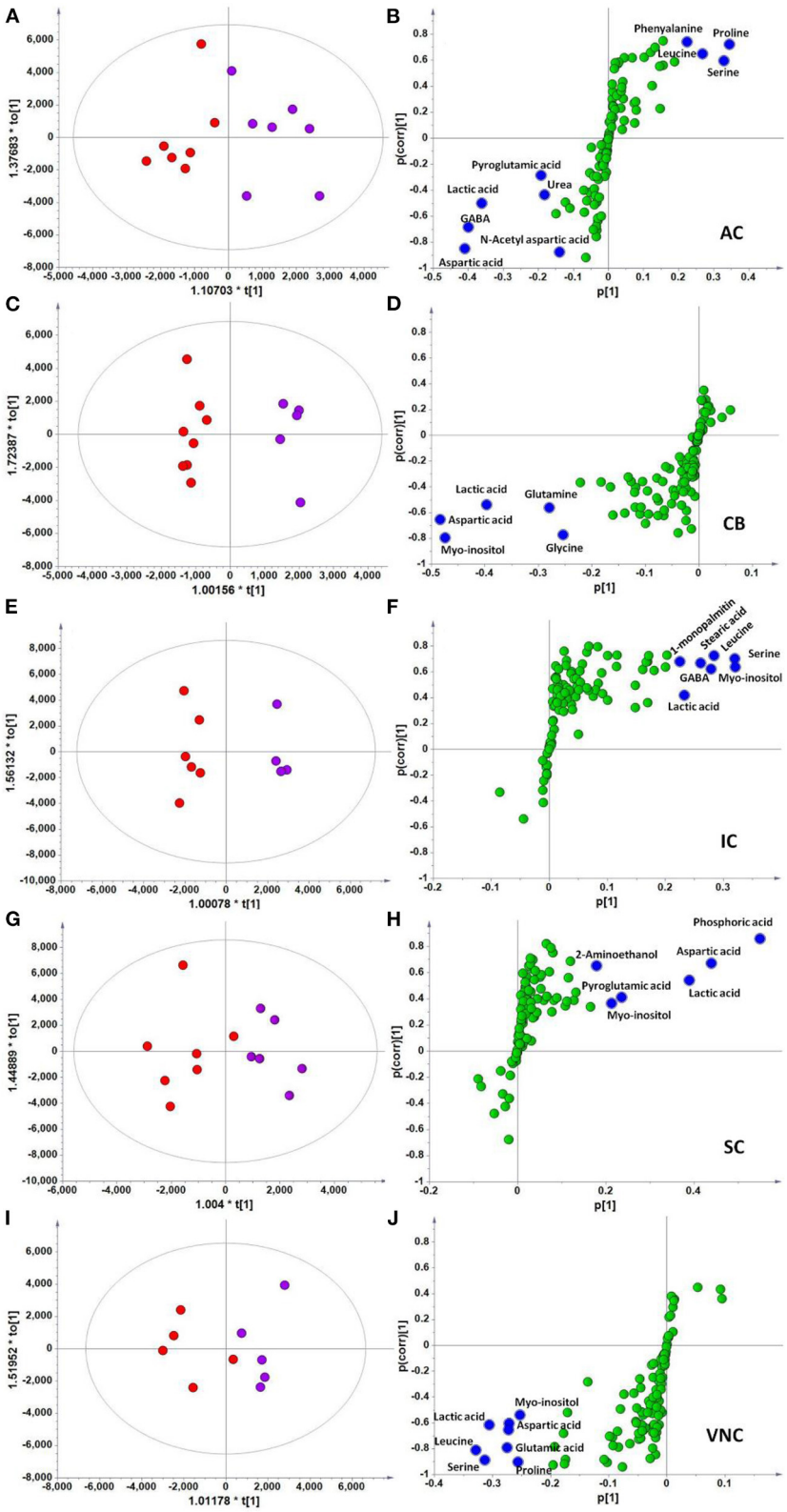

FIGURE 10 | OPLS-DA and S-plot analysis comparing the OPLSDA scores between sham and acoustic trauma animals in different brain regions. Left panel, OPLSDA scores plots, red dots: Sham, purple dots: Acoustic trauma; Right panel, S-plots. **(A,B)** AC [Predictive component: $R2X = 0.194$, $R2Y = 0.76$, $Q^2 = 0.45$;

(Continued)

FIGURE 10 | Orthogonal component 1: *R2X* = 0.446; All components: *R2X* (cum) = 0.64]; **(C,D)** CB [Predictive component: *R2X* = 0.152, *R2Y* = 0.973, Q^2 = 0.68; Orthogonal component 1: *R2X* = 0.364; All components: *R2X* (cum) = 0.927]; **(E,F)** IC [Predictive component: *R2X* = 0.293, *R2Y* = 0.978, Q^2 = 0.702; Orthogonal component 1: *R2X* = 0.417; All components: *R2X* (cum) = 0.905]; **(G,H)** SC [Predictive component: *R2X* = 0.238, *R2Y* = 0.791, Q^2 = 0.691; Orthogonal component: *R2X* = 0.562; All components: *R2X* (cum) = 0.8]; **(I,J)** VNC [Predictive component: *R2X* = 0.403, *R2Y* = 0.779, Q^2 = 0.445; Orthogonal component: *R2X* = 0.389; All components: *R2X* (cum) = 0.792]. In the right panel, the blue dots show variables with high negative magnitude and reliability scores (everything is scaled and relative) or high positive magnitude and reliability scores, i.e., potential biomarkers. AC, auditory cortex; CB, cerebellum; IC, inferior colliculus; CN, cochlear nucleus; VCN, vestibular nucleus complex. From He et al. (35) with permission.

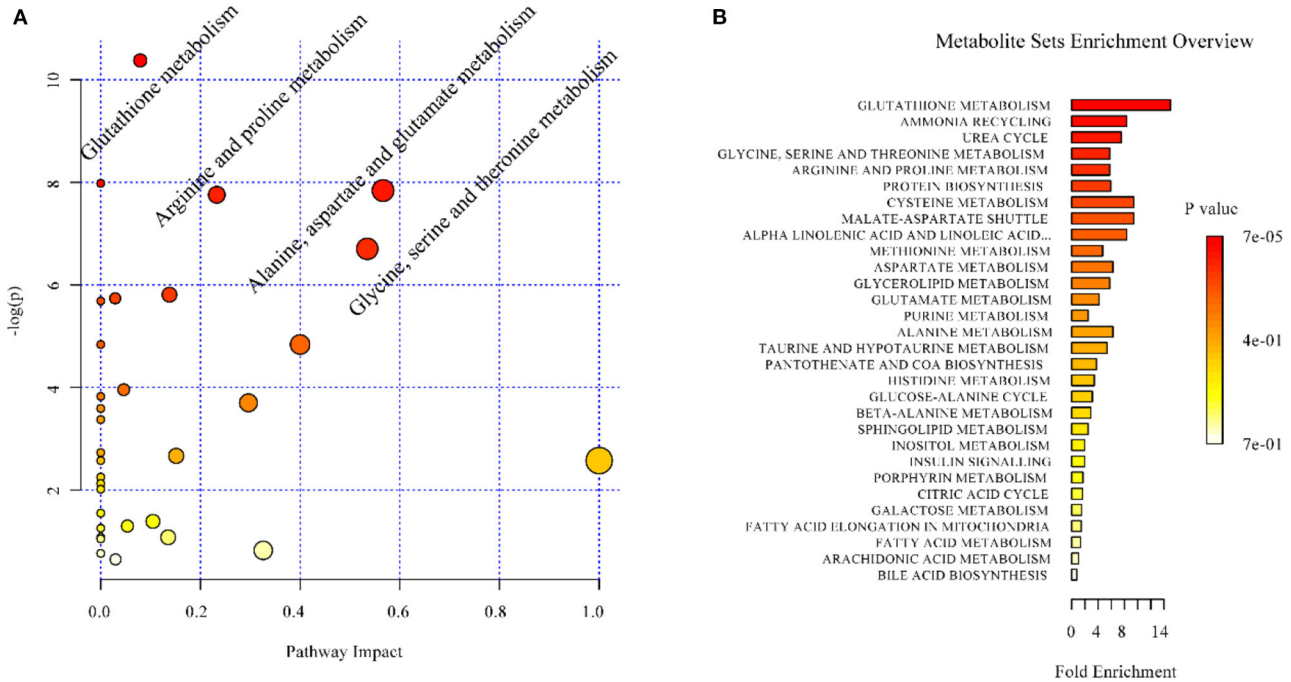

FIGURE 11 | Overview of the impact of acoustic trauma on brain metabolites. **(A)** The pathway impact of acoustic trauma on metabolites. The y axis shows the *p*-values and the x axis, the pathway impact values; the node color is based on its *p*-value and the node size reflects the pathway impact values. **(B)** The enrichment overview of the pathway-associated metabolite sets perturbed by acoustic trauma. From He et al. (35) with permission.

Random Forest Regression

Using the same data set, we found that random forest regression was also successful in predicting the neurochemical concentrations in the L-arginine pathway, with the best values for the proportion of variance explained, 0.94 (spermine), 0.92 (arginine), and 0.90 (citrulline) [see **Table 3**; (51)]. However, for this data set, random forest regression was somewhat less successful than MLR in predicting some of the variables (e.g., 0.27 for ornithine; see **Table 3**). Variable importance plots (VIPs) were obtained and **Figure 5** shows the variables in order of importance for the prediction of spermine, where arginine and citrulline were clearly the most important variables (51). **Figure 6** shows the degree of error in the prediction of spermine as a function of the number of trees generated. It can be seen that the error decreases rapidly after the first 150–200 trees (51).

Linear Discriminant Analysis

We have also used linear discriminant analysis to predict the age of animals based on the concentrations of neurochemicals in the L-arginine pathway (**Figure 1**). This research is directly applicable to the identification of biomarkers that might be used to predict pathological changes that occur in brain aging in vestibular areas of the brain. In Liu et al. (3), we identified an LDF that could predict whether rats were young (4 months old) or aged (24 months old). The LDF based on putrescine, spermidine, spermine, citrulline, glutamate and GABA in the vestibular nucleus (note the z transformation), could predict age with 100% accuracy using cross-validation (P = 0.000, Wilks'λ). Using the cerebellum, age could be predicted with 93% accuracy (P = 0.000, Wilks'λ), using only spermine and spermidine. Similar results were reported by Liu et al. (4), who found 90% accuracy in classifying animals to the aged group based on neurochemicals in the vestibular nucleus and 80% accuracy in classifying them based on neurochemicals in the cerebellum. We have also applied linear discriminant analysis to the prediction of whether rats have had a BVD or a sham procedure based on a combination of their behavioral symptoms, such as unsupported rearing, locomotor activity in the inner vs. outer zones of the open field maze and performance in the spatial alternation in a T maze task, and

found that whether the animals had received a BVD could be predicted with 100% accuracy ($P = 0.000$, Wilks'λ) (5). These kinds of methods may be applicable to the differential diagnosis of vestibular and auditory disorders.

Random Forest Classification

With a similar aim to the use of linear discriminant analysis to predict whether animals have BVD on the basis of their behavioral symptoms, we have also employed random forest classification using a range of symptoms measured using the Ethovision tracking system (72). For days 3 and 23 post-BVD, we found that random forest classification could predict which rats had received BVD and which were sham animals with 100% accuracy. **Figure 7** shows the variables in order of importance for day 3 and indicates that the most important variables were the animals' locomotor velocity (hyperactivity is a common symptom of BVD in rats), distance moved and rotation (72).

Ahmadi et al. (26, 27) have recently used logistic regression and random forest classification, as well as artificial neural networks, to support differential diagnosis of peripheral and central vestibular disorders in humans. In general, they observed that machine learning methods outperformed univariate scores. Karmali et al. (28) also used logistic regression to predict the probability of falling based on age and thresholds for the perception of 0.2 Hz roll head tilt.

OPLS-DA

In the context of auditory neuroscience, we have used OPLS-DA on metabolomics data from brain samples to successfully predict whether rats have been exposed to acoustic trauma or a sham procedure (35, 65). The ultimate aim here is to use metabolomic analysis of blood samples to predict whether humans might develop tinnitus or whether they might respond to particular tinnitus treatments (65). In what we believe to be the first study of its kind, we analyzed brain samples from 12 different brain regions in rats that had been exposed to either acoustic trauma or a sham procedure, and used GC-MS to isolate a total of 107 distinct peaks in the chromatogram, with 88 authentically identified as amino acids, small organic acids, carbohydrates, fatty acids, lipids and amines (see **Figure 8**). PCA and OPLS-DA were performed on the data. In **Figure 9**, each dot represents the summarized information from the 88 authentically identified molecules for a particular brain region. The distance between the dots indicates the similarity of the metabolic composition of the samples. Brain regions with similar functions appeared to have a similar metabolic composition in both sham and acoustic-trauma exposed animals. However, OPLS-DA in specific brain regions such as the auditory cortex, cerebellum, inferior colliculus, superior colliculus and vestibular nucleus, showed that the metabolic profile was separated for the sham and acoustic-trauma-exposed animals (35). This suggested that a shift in the metabolic pattern had occurred in these brain regions in the animals exposed to acoustic trauma. The associated S plots (**Figure 10**) indicated that potential biomarkers of acoustic trauma in these brain regions included urea, amino acids, fatty acids, sugar acids, nucleosides and organic acids, in a region-specific fashion. For example, GABA was significantly increased only in the auditory cortex. The overall impact of the acoustic trauma on brain metabolites is summarized in a pathway analysis in **Figure 11** (35).

SUMMARY

Phenomena in vestibular and auditory neuroscience, as in other areas of neuroscience, almost always involve the complex interaction of multiple variables, and yet many areas of basic vestibular and auditory neuroscience, in particular, employ univariate statistical analyses almost exclusively. This may limit the ability of studies to reveal how the interactions between different variables may determine a particular outcome. We have used MVAs and data mining methods to explore the way that combinations of variables can account for neurochemical and behavioral changes following the loss of vestibular function (3–6, 15, 72, 73) and auditory function [e.g., (35, 65)]. In clinical neuroscience research, MVAs and data mining methods have been used to predict the progression of patients from one neurological disorder to another [e.g., (9, 12)] and the probability that the early adolescent use of *Cannabis* can lead to the development of psychotic symptoms in later life [e.g., (74)]. These methods are now in routine use in areas such as genomics, proteomics, metabolomics (10, 11), and the analysis of fMRI data [e.g., (75)]. Electrophysiological research in neuroscience is increasingly moving to the use of multi-electrode arrays using dozens or more micro-electrodes simultaneously, and in this situation one of the main objectives is to determine how different brain regions change in relation to one another, which requires MVA [e.g., (76, 77)].

MVAs and data mining methods can be applied to every aspect of vestibular and auditory neuroscience in order to gain a better understanding of the way in which networks or systems of variables affect otological function. In the search for biomarkers of SNHL, tinnitus and vestibular dysfunction, classification methods such as linear discriminant analysis, support vector machines, random forest classification, Bayesian classifiers and OPLS-DA, can be applied to behavioral, neurophysiological and neurochemical data to predict the probability of a disease or disorder developing, in order to intervene and provide treatments that will prevent or impede the pathological changes. In the context of metabolomics, MVAs and data mining methods have already been proven to be useful in the prediction of disease [e.g., (8, 9, 11–13, 78–80)]. OPLS-DA is an example of an MVA that has successfully been applied to metabolomic data in order to predict hearing loss in rats (35, 65) and may be particularly useful in the search for biomarkers of SNHL, tinnitus, and vestibular dysfunction [e.g., (81)].

DATA AVAILABILITY STATEMENT

The raw data supporting the conclusions of this article will be made available by the authors, without undue reservation.

AUTHOR CONTRIBUTIONS

PS and YZ: conceptualization and writing—review and editing. PS: writing—original draft preparation.

FUNDING

This research has been supported by grants from the Health Research Council of New Zealand, the New Zealand Neurological Foundation and the Brain Research New Zealand Center for Research Excellence.

ACKNOWLEDGMENTS

The content of this manuscript has been published in part as part of the MApplStat thesis of Smith (73).

REFERENCES

1. Manly BFJ. *Multivariate Statistical Analyses. A Primer*. 3rd ed. London: Chapman and Hall/CRC (2005).
2. Stevens, J.P. *Applied Multivariate Statistics for the Social Sciences*. 5th ed. Hillsdale NJ, Lawrence Erlbaum (2009).
3. Liu P, Zhang H, Devaraj R, Ganesalingam G, Smith PF. A multivariate analysis of the effects of aging on glutamate, GABA and arginine metabolites in the rat vestibular nucleus. *Hear Res.* (2010) 269:122–33. doi: 10.1016/j.heares.2010.06.019
4. Liu P, Gupta N, Jing Y, Collie ND, Zhang H, Smith PF. Further studies of age-related changes in arginine metabolites in the rat vestibular nucleus and cerebellum. *Neuroscience.* (2017) 348:273–87. doi: 10.1016/j.neuroscience.2017.02.033
5. Smith PF, Haslett SJ, Zheng, Y. A multivariate statistical and data mining analysis of spatial memory-related behaviour following bilateral vestibular deafferentation in the rat. *Behav Brain Res.* (2013) 246:15–23. doi: 10.1016/j.bbr.2013.02.033
6. Smith PF, Zheng, Y. Principal component analysis suggests subtle changes in glutamate receptor subunit expression in the rat hippocampus following bilateral vestibular deafferentation in the rat. *Neurosci Lett.* (2013) 548:265–8. doi: 10.1016/j.neulet.2013.05.036
7. Herzog MH, Francis G, Clarke A (editors). The multiple testing problem. In: Understanding Statistics and Experimental Design. Learning Materials in Biosciences. Cham: Springer (2009). doi: 10.1007/978-3-030-03499-3_5
8. Pang H, Lin A, Holford M, Enerson BE, Lu B, Lawton MP, et al. Pathway analysis using random forests classification and regression. *Bioinformatics.* (2006) 22:2028–36. doi: 10.1093/bioinformatics/btl344
9. Krafczyk S, Tietze S, Swoboda W, Valkovic P, Brandt, T. Artificial neural network: A new diagnostic posturographic tool for disorders of stance. *Clin Neurophysiol.* (2006) 117:1692–8. doi: 10.1016/j.clinph.2006.04.022
10. Dziuda DM. *Data Mining for Genomics and Proteomics.* Hoboken, NJ: Wiley (2010).
11. Ryan M, Mason-Parker SE, Tate WP, Abraham WC, Williams, JM. Rapidly induced gene networks following induction of long-term potentiation at perforant synapses *in vivo*. *Hippocampus.* (2011) 21:541–53. doi: 10.1002/hipo.20770
12. Brandt T, Strupp M, Novozhilov S, Krafczyk, S. Artificial neural network posturography detects the transition of vestibular neuritis to phobic postural vertigo. *J Neurol.* (2012) 259:182–4. doi: 10.1007/s00415-011-6124-8
13. Prochazka A, Vysata O, Valis M, Tupa, O, Schatz M, Marík V, et al. Bayesian classification and analysis of gait disorders using image and depth sensors of Microsoft Kinect. *Digital Signal Proc.* (2015) 47:169–77. doi: 10.1016/j.dsp.2015.05.011
14. Smith PF. Statistical analysis in pharmacology is not always BO. *Trends Pharmacol Sci.* (2012) 33:565–6. doi: 10.1016/j.tips.2012.08.006
15. Zheng Y, Wilson G, Stiles L, Smith PF. Glutamate receptor subunit and calmodulin kinase II expression in the rat hippocampus, with and without T maze experience, following bilateral vestibular deafferentation. *PLOS ONE.* (2013) 8:e54527. doi: 10.1371/journal.pone.0054527
16. Agrawal Y, Carey JP, Della Santina CC, Schubert MC, Minor LB. Diabetes, vestibular dysfunction, and falls: analyses from the National Health and Nutrition Examination Survey. *Otol Neurotol.* (2010) 31:1445–50. doi: 10.1097/MAO.0b013e3181f2f035
17. Semenov YR, Bigelow RT, Xue QL, du Lac S, Agrawal Y. Association between vestibular and cognitive function in U.S. Adults: data from the national health and nutrition examination survey. *J Gerontol A Biol Sci Med Sci.* (2016) 71:243–50. doi: 10.1093/gerona/glv069
18. Düwel P, Ilgner J, Engelke JC, Westhofen M. Subclassification of vestibular disorders by means of statistical analysis in caloric labyrinth testing. *Acta Otolaryngol.* (2004) 124:595–602. doi: 10.1080/00016480310015182
19. Dimitri PS, Wall C 3rd, Oas JG, Rauch SD. Application of multivariate statistics to vestibular testing: discriminating between Menière's disease and migraine associated dizziness. *J Vestib Res.* (2001) 11:53–65.
20. Dimitri PS, Wall C III, Oas JG. Classification of human rotation test results using parametric modeling and multivariate statistics. *Acta Otolaryngol.* (1996) 116:497–506. doi: 10.3109/00016489609137880
21. Chien WW, Janky K, Minor LB, Carey JP. Superior canal dehiscence size: multivariate assessment of clinical impact. *Otol Neurotol.* (2012) 33:810–5. doi: 10.1097/MAO.0b013e318248eac4
22. Rossi-Izquierdo M, Basta D, Rubio-Rodríguez JP, Santos-Pérez S, Ernst A, Sesar-Ignacio Á, et al. Is posturography able to identify fallers in patients with Parkinson's disease? *Gait Posture.* (2014) 40:53–7 doi: 10.1016/j.gaitpost.2014.02.003
23. Gabelić T, Krbot Skorić M, Adamec I, Barun B, Zadro I, Habek M. The vestibular evoked myogenic potentials (VEMP) score: a promising tool for evaluation of brainstem involvement in multiple sclerosis. *Eur J Neurol.* (2015) 22:261–9. doi: 10.1111/ene.12557
24. Abouzari M, Goshtasbi K, Sarna B, Khosravi P, Reutershan T, Mostaghni N, et al. Prediction of vestibular schwannoma recurrence using artificial neural network. *Laryngoscope Investig Otolaryngol.* (2020) 5:278–85. doi: 10.1002/lio2.362
25. Vibert N, Hoang T, Gilchrist DP, MacDougall HG, Burgess AM, Roberts RD, et al. Psychophysiological correlates of the inter-individual variability of head movement control in seated humans. *Gait Posture.* (2006) 23:355–63. doi: 10.1016/j.gaitpost.2005.04.006
26. Ahmadi SA, Vivar G, Navab N, Möhwald K, Maier A, Hadzhikolev H, et al. Modern machine-learning can support diagnostic differentiation of central and peripheral acute vestibular disorders. *J. Neurol.* (2020) 267:143–52. doi: 10.1007/s00415-020-09931-z
27. Ahmadi SA, Vivar G, Frei J, Nowoshilow S, Bardins S, Brandt T, et al. Towards computerized diagnosis of neurological stance disorders: data mining and machine learning of posturography and sway. *J Neurol.* (2019) 266 (Suppl. 1):108–17. doi: 10.1007/s00415-019-09458-y
28. Karmali F, Bermudez MC, Clark TK, Wang W, Merfeld DM. Multivariate analyses of balance test performance, vestibular thresholds, and age. *Front Neurol.* (2017) 8:578. doi: 10.3389/fneur.2017.00578
29. Molina ME, Perez A, Valente JP. Classification of auditory brainstem responses through symbolic pattern recovery. *Artif Intell Med.* (2016) 70:12–30. doi: 10.1016/j.artmed.2016.05.001
30. Exarchos TP, Rigas G, Bibas A, Kikidis D, Nikitas C, Wuyts FL, et al. Mining balance disorders' data for the development of diagnostic decision support systems. *Comput Biol Med.* (2016) 77:240–8. doi: 10.1016/j.compbiomed.2016.08.016
31. Smith PF. On the application of multivariate statistical and data mining analyses to data in neuroscience. *J Undergrad Neurosci Educ.* (2018) 16:R20–32.

32. Kline P. *An Easy Guide to Factor Analysis*. London: Routledge (2002).
33. Lattin J, Carroll JD, Green PE. *Analyzing Multivariate Data*. Pacific Grove, CA: Duxbury (2003).
34. Jolliffe, I.T. *Principal Component Analysis*. 2nd ed. New York, NY: Springer (2004).
35. He J, Zhu Y, Aa J, Smith PF, De Ridder D, Wang G, et al. Brain metabolic changes in rats following acoustic trauma. *Front. Neurosci.* (2017) 11:148. doi: 10.3389/fnins.2017.00148
36. Marcoulides GA, Hershberger SL. *Multivariate Statistical Methods. A First Course*. Mahwah, NJ: Lawrence Erlbaum Associatio (1997).
37. Molnar, C. *Interpretable Machine Learning. A Guide for Making Black Box Models Explainable*. Victoria, BC: Lean Publishing (2019).
38. Brook RJ, Arnold GC. *Applied Regression Analysis and Experimental Design*. Boca Raton, FL: Chapman and Hall/CRC (1985).
39. Ryan TP. *Modern Regression Methods*. New Jersey, NY: Wiley (2009). doi: 10.1002/9780470382806
40. Rutherford, A. *Introducing ANOVA and ANCOVA. A GLM Approach*. London: Sage Publications (2001).
41. Vittinghoff E, Glidden DV, Shiboski SC, McCulloch CE. *Regression Methods in Statistics: Linear, Logistic, Survival and Repeated Measures Models*. New York, NY: Springer (2005).
42. Doncaster CP, Davey AJH. *Analysis of Variance and Covariance*. Cambridge: Cambridge University Press (2007).
43. Gamst G, Meyers LS, Guarino, A.J. *Analysis of Variance Designs. A Conceptual and Computational Approach with SPSS and SAS*. New York, NY: Cambridge University Press (2008). doi: 10.1017/CBO9780511801648
44. Babayak MA. What you see may not be what you get: a brief, non-technical introduction to over-fitting in regression-type models. *Psychosomat Med*. (2004) 66:411–21. doi: 10.1097/00006842-200405000-00021
45. Field A. *Discovering Statistics Using SPSS*. Los Angeles, CA: Sage (2011).
46. Field A, Miles J, Field Z. *Discovering Statistics Using R*. Los Angeles, CA: Sage (2012).
47. Hastie T, Tibshirani R, Friedman, J. *Elements of Statistical Learning: Data Mining, Inference and Prediction*. 2nd ed. Heidelberg: Springer Verlag (2009).
48. Breiman L, Friedman J, Stone CJ, Olshen RA. *Classification and Regression Trees*. 1st ed. Boca Raton, FL: CRC Press (1984).
49. Marsland, S. *Machine Learning. An Algorithmic Perspective*. Boca Raton, FL: CRC Press (2019).
50. Williams, G.J. *Data Mining With Rattle And R*. New York, NY: Springer (2011). doi: 10.1007/978-1-4419-9890-3
51. Smith PF, Ganesh S, Liu P. A comparison of random forest regression and multiple linear regression for prediction in neuroscience. *J Neurosci Methods*. (2013) 220:85–91. doi: 10.1016/j.jneumeth.2013.08.024
52. Friedman JH. Greedy function approximation: a gradient boosting machine. *Ann. Stats*. (2001) 29:1189–232. doi: 10.1214/aos/1013203451
53. Tabachnick BG, Fidell LS. *Using Multivariate Statistics*. 5th ed. Boston, MA: Pearson Education Inc (2007).
54. Wilson MD. Support vector machines. In: Jorgensen SE, Fath BD, editors. Encyclopedia of Ecology. New York, NY: Elsevier (2008). p. 3431–7. doi: 10.1016/B978-008045405-4.00168-3
55. Williams GJ. Rattle: a data mining GUI for R. *R J*. (2009) 1/2:45–55. doi: 10.32614/RJ-2009-016
56. Crawley MJ. *The R Book*. Chichester: Wiley (2007). doi: 10.1002/9780470515075
57. Davies TM. *The Book of R*. San Francisco, CA: No Starch Press (2017).
58. Bolstad WM. *Introduction to Bayesian Statistics*. 2nd ed. New York, NY: Wiley (2007).
59. Lesaffre E, Lawson LB. *Bayesian Biostatistics*. New York, NY: Wiley (2012). doi: 10.1002/9781119942412
60. Link WA, Barker RJ. *Bayesian Inference*. New York, NY: Elsevier (2010).
61. Junker BH, Koschutzki D, Schreiber F. Exploration of biological network centralities with CentiBiN. *BMC Bioinform*. (2006) 7:219. doi: 10.1186/1471-2105-7-219
62. Trygg T, Wold S. (2002) Orthogonal projections to latent structures (O-PLS). *J Chemomet*. (2002) 16:119–28. doi: 10.1002/cem.695
63. Westerhuis JA, Hoefslott HCJ, Smit S, Vis DJ, Smilde AK, van Velzen EJJ, et al. Assessment of PLSDA cross validation. *Metabolom*. (2008) 4:81–9. doi: 10.1007/s11306-007-0099-6
64. Chong J, Wishard DS, Xia J. Using metaboanalyst 4.0 for comprehensive and integrative metabolics data analysis. *Curr Protoc Bioinform*. (2019) 68:e86. doi: 10.1002/cpbi.86
65. He J, Aa J, Sun J, Smith PF, De Ridder D, Wang G, et al. Metabolic changes in the blood and brain following acoustic trauma, tinnitus and hyperacusis. *Prog Brain Res*. (2021) (in press). doi: 10.1016/bs.pbr.2020.09.002
66. Motulsky H. *Intuitive Biostatistics*. Oxford: Oxford University Press (1995).
67. Smith PF. A guerrilla guide to common problems in 'neurostatistics': essential statistical topics in neuroscience. *J Undergrad Neurosci Educ*. (2017) 16:R1–12.
68. Quinn GP, Keough MJ. *Experimental Design and Data Analysis for Biologists*. Cambridge: Cambridge University Press (2002). doi: 10.1017/CBO9780511806384
69. De Waale T, Pannekoek J, Scholtus S. Multivariate imputation. In: *Handbook of Statistical Data Editing and Imputation*. New York, NY: Wiley (2011). doi: 10.1002/9780470904848
70. Cueto-Lopez N, Garcia-Ordas MT, Davila-Batista V, Moreno V, Aragones N, Alaiz-Rodríguez R, et al. A comparative study of feature selection for a risk prediction model for colorectal cancer. *Comput Methods Programs Biomed*. (2019) 177:219–29. doi: 10.1016/j.cmpb.2019.06.001
71. Smith PF, Truchet B, Challain F, Zheng Y, Besnard S. Vestibular modulation of long-term potentiation and NMDA receptor expression in the hippocampus. *Front Mol Neurosci*. (2020) 13:140. doi: 10.3389/fnmol.2020.00140
72. Aitken P, Zheng Y, Smith P.F. Ethovision^{TM} analysis of open field behaviour in rats following bilateral vestibular loss. *J Vestib Res*. (2017) 27:89–101. doi: 10.3233/VES-170612
73. Smith PF. *A Multivariate Analysis of Vestibular Loss*. (MApplStat. Thesis), Massey University, Palmerston North, New Zealand (2014).
74. Caspi A, Moffitt TE, Cannon M, McClay J, Murray R, Harrington H, et al. Moderation of the effect of adolescent-onset cannabis use on adult psychosis by a functional polymorphism in the catechol-O-methyltransferase gene: longitudinal evidence of a gene X environment interaction. *Biol Psychiat*. (2005) 57:1117–27. doi: 10.1016/j.biopsych.2005.01.026
75. Chen H, Cao G, Cohen RA. Multivariate semiparametric spatial methods for imaging data. *Biostatistics*. (2017) 18:386–401. doi: 10.1093/biostatistics/kxw052
76. Staude B, Rotter S, Grün S. CuBIC: cumulant based inference of higher-order correlations in massively parallel spike trains. *J Comput Neurosci*. (2010) 29:327–50. doi: 10.1007/s10827-009-0195-x
77. Hitier M, Zhang Y, Sato G, Besnard S, Zheng Y, Smith PF. Effects of selective electrical stimulation of the rat cochlea on hippocampal field potentials. *Hear Res*. (2020) 395:108023. doi: 10.1016/j.heares.2020.108023
78. Sun L, Diao X, Gang X, Lv Y, Zhao X, Yang S, et al. Risk factors for cognitive impairment in patients with Type 2 Diabetes. *J Diabetes Res*. (2020) 2020:4591938. doi: 10.1155/2020/4591938
79. Hong X, Zhang B, Liang L, Zhang Y, Ji Y, Wang G, et al. Postpartum plasma metabolomic profile among women with preeclampsia and preterm delivery: implications for long-term health. *BMC Med*. (2020) 18:277. doi: 10.1186/s12916-020-01741-4
80. Wang J, Zheng J, Ren X, Wang S, Wang G, Hu, et al. Integrative analysis of hepatic metabolomic and transcriptomic data reveals potential mechanism of non-alcoholic steatohepatitis in high-fat diet-fed mice. *J Diabetes*. (2020) (in press). doi: 10.1111/1753-0407.13120
81. Gomaa NA, Jimoh Z, Campbell S, Zenke JJ, Szczepek AJ. Biomarkers for inner ear disorders: scoping review on the role of biomarkers in hearing and balance disorders. *Diagnostics*. (2020) 11:E42. doi: 10.3390/diagnostics11010042

Conflict of Interest: The authors declare that the research was conducted in the absence of any commercial or financial relationships that could be construed as a potential conflict of interest.

frontiers in Neurology

ORIGINAL RESEARCH
published: 14 April 2021
doi: 10.3389/fneur.2021.658419

Independent Measures of Utricular Function: Ocular Vestibular Evoked Myogenic Potentials Do Not Correlate With Subjective Visual Vertical or Fundus Photographic Binocular Cyclorotation

Sarah Hösli [1,2]* *and Dominik Straumann* [1,2]

[1] Department of Neurology, University Hospital Zurich and University of Zurich, Zurich, Switzerland, [2] Clinical Neuroscience Center, University Hospital Zurich, Zurich, Switzerland

OPEN ACCESS

Edited by:
Sun-Young Oh,
Jeonbuk National University,
South Korea

Reviewed by:
Ian S. Curthoys,
The University of Sydney, Australia
Sendhil Govender,
Prince of Wales Hospital, Australia

***Correspondence:**
Sarah Hösli
sarah.hoesli@usz.ch

Specialty section:
This article was submitted to Neuro-Otology, a section of the journal Frontiers in Neurology

Received: 25 January 2021
Accepted: 10 March 2021
Published: 14 April 2021

Citation:
Hösli S and Straumann D (2021) Independent Measures of Utricular Function: Ocular Vestibular Evoked Myogenic Potentials Do Not Correlate With Subjective Visual Vertical or Fundus Photographic Binocular Cyclorotation. Front. Neurol. 12:658419. doi: 10.3389/fneur.2021.658419

Ocular vestibular evoked myogenic potentials (oVEMPs), subjective visual vertical (SVV), and fundus photographically measured binocular cyclorotation (BCR) are diagnostic tests to assess utricular function in patients with vertigo or dizziness. In 138 patients with chronic vertigo or dizziness, we asked whether the asymmetry ratio of oVEMP (normal, right side pathological, left side pathological) could predict the SVV deviation (normal, rightward deviation, leftward deviation) or BCR (normal, cyclorotation to the right, cyclorotation to the left). There was no correlation between oVEMP and SVV and between oVEMP and BCR, while SVV and BCR correlated highly. Although both oVEMP and SVV measure aspects of utricular function, our findings demonstrate that oVEMP and SVV are not redundant and may reflect different utricular pathologies. The role of fundus photographic BCR may be relegated to only confirm unclear SVV results in vestibular diagnostic workup.

Keywords: ocular vestibular evoked myogenic potentials, subjective visual vertical, binocular cyclorotation, otolith organs, utricle, vertigo, dizziness

INTRODUCTION

In patients with vertigo or dizziness, it is common to apply a comprehensive battery of auxiliary tests that help identify underlying disorders within the vestibular labyrinth, the vestibular nerve, or central vestibular networks. These vestibular tests include assessments of both semicircular canal and otolith functions (1). Frequently used otolith tests are vestibular evoked myogenic potentials (VEMPs), subjective visual vertical (SVV), and fundus photography of static binocular cyclorotation (BCR). While VEMPs are elicited by dynamic stimulation (vibration or sound) of utricular (ocular VEMPs) or saccular (cervical VEMPs) hair cells, SVV and BCR reflect the orientation of the sensed static gravito-inertial vector relative to the head in the coronal plane (2–4). Theoretically, a global hypofunction of the utricle or its afferents on one side should lead to a reduction of ocular VEMPs (oVEMPs) on the contralateral side (crossed reflex), an ipsilateral tilt of SVV, and an ipsitorsional BCR.

Test results of oVEMPs, SVV, and BCR reflect the function of different types of hair cells situated in the utricular macula. Type 1 cells are located mainly in the striola and respond to dynamic stimulation by vibration or sound. Type 2 cells are in the peripheral zones of the macula and respond to static stimulation such as constant orientation of the gravito-inertial vector relative to the head (5). While the readout of oVEMP and BCR is eye position, SVV is a psychophysical measure of the perceived earth-vertical, which subjects indicate by orienting a luminous line in otherwise complete darkness.

It was shown that SVV tilt from true earth-vertical is largest in the acute phase of a vestibular deficit, while on subsequent measurements, SVV gradually becomes close to normal again over the course of several months (6–8). This normalization of SVV is most likely due to central compensation mechanisms (9–11). The normalization of the SVV together with the unchanged oVEMP pathology may reflect the well-known pattern that high-frequency vestibular reflexes, which are transmitted along short-latency pathways with few synapses (e.g., the head-impulse vestibulo-ocular reflex), are less compensated in the chronic stage than low-frequency vestibular reflexes (e.g., caloric nystagmus) (12).

Nevertheless, asymmetries of static utricular function might still be apparent in the chronic state: When chronic patients after vestibular neuritis with normal SVV values with the head upright are roll-tilted with their heads toward the affected ear or eccentrically rotated about an earth-vertical axis passing through the unaffected ear, SVV deviations from earth-vertical are significantly larger than in healthy subjects (13–15).

In this study, we set out to analyze the association of SVV, oVEMP, and fundus photographic BCR data in a population of unselected vertigo patients who were consecutively seen in a tertiary vertigo center. We specifically asked whether there was a direct correlation between normal and side-specific pathological SVV, oVEMP, and BCR data. We also explored whether compensated SVV and BCR together with remaining oVEMP asymmetry are common patterns in chronic vertigo patients.

MATERIALS AND METHODS

Patients

In total, 318 patients who were seen at the Center for Vertigo and Neurological Vision Disorders, University Hospital Zurich, during the years 2017 and 2018 were screened for the study. The inclusion criteria for patients were as follows: (i) complete testing of the SVV, (ii) complete testing of oVEMP, and (iii) a signed general consent form from the hospital to use their personal data for research purposes. Among them, 178 patients were excluded because of missing general consent form and two patients were excluded because of incomplete data. Then, 138 consecutive patients (mean age: 52.8 years ± 16 SD) who fulfilled the inclusion data were selected. Here, 76 (56%) patients were male, 60 (44%) female. The diagnostic workup took place in the subacute or chronic stage after the beginning of vestibular symptoms. Final diagnosis was made after taking patient history, clinical findings, diagnostic vestibular workup, and (if obtained) MRI into consideration. The most common diagnoses were vestibular schwannomas, vestibular migraines, dizziness of unknown origin, and Menière's disease (**Figure 1**). If patients additionally underwent fundus photography, BCR data were also included in the analysis. The protocol was approved by the Ethics Committee Zürich (BASEC-Nr. 2017-020119).

Subjective Visual Vertical

SVV was measured with an in-house constructed apparatus (built and programmed by U. Scheifele). For SVV measurements, patients were asked to sit on a chair in complete darkness to exclude a visual reference for upright. All data were acquired with binocular vision. A luminous arrow was projected on a circular screen (diameter: 0.4 m) in front of the patient (distance: 1.20 m). At the beginning of every trial, the luminous arrow pointed in a random direction. Patients were then asked to move the arrow into an orientation that was perceived as the perfectly earth-vertical with the arrowhead directed upward. Patients changed the orientation of the arrow by turning on the knob of a potentiometer. By pressing a button, patients confirmed the final orientation of the arrow at the end of every trial. The difference between the perceived and the true vertical was digitally recorded. Each session consisted of six trials over which the data were averaged. Based on normative data (1.2 ± 0.4 SD), an SVV deviation of more than 2.2 degrees from true vertical was considered pathological. The sign of SVV deviations to the right was defined positive.

Ocular Vestibular Evoked Myogenic Potentials

oVEMPs were measured with a Viking V system (Nicolet Biomedical, USA) and elicited with a mini-shaker (4,810, amplifier 2,706; Bruel and Kjaer, Naerum, Denmark). Patients in supine position were visually fixing on a small object (a small model of the Earth) hanging from the ceiling (eye-to-object distance: 1.30 m). The object was positioned such that patients had to elevate the eyes by about 20 degrees relative to the straight-ahead position. The handheld mini-shaker provided bone-conducted vibration stimuli to the forehead. Here, 500-Hz stimulus vibrations with a repetition of 3.1 times per second were conducted for ∼32 s. The rise/fall time was 0 ms. Muscle activity was measured with surface electrodes placed underneath each eye. Reference electrodes were placed below the active electrodes, while a grounding electrode was placed on the patient's chin. After a set of 100 repetitive stimuli, the average amplitude of the oVEMP was calculated and determined by the difference of the negative potential peak 10 ms after stimulus onset (N10) and the positive potential peak 15 ms after stimulus onset (P15). The average amplitude (A) over two sets of measurements for each eye was used to calculate the asymmetry ratio (AR) using the Jongkees formula:

$$AR = \frac{A\ right\ eye\ - A\ left\ eye}{A\ right\ eye + A\ left\ eye} \times\ 100 \qquad (1)$$

When the response to a stimulus was absent, the size of the amplitude was defined as 0, leading to an AR of 100% to the side of the pathology. By definition, a positive value reflects a

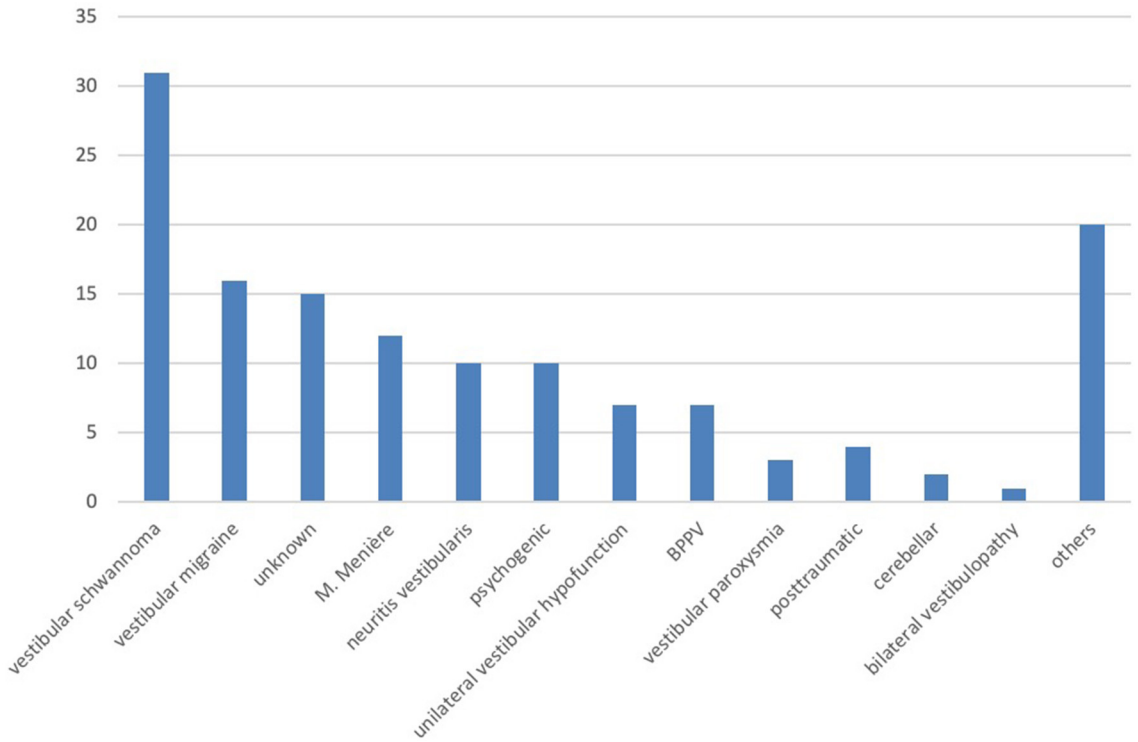

FIGURE 1 | Distribution of diagnosis among patients who fulfilled the inclusion criteria. Others: polyneuropathy, ocular vertigo, mal de debarquement, orthostatic dizziness, cerebral bleeding, meningioma, Wernicke's encephalopathy.

hypofunction of the right utricle. Based on normative data (15.5 ± 11% SD), AR equal to or > 30% was defined as pathological. Since all data were acquired in the subacute or chronic stage, we considered the effect of pathologies with an increase in oVEMP amplitude in the hyperacute setting [e.g., Menière's disease as described by Young et al. (16)] to have a minimal effect in our study population.

Binocular Cyclorotation

To measure the cyclorotation (CR), a non-mydriatic retinal camera was used (Topcon TRC-NW400, Japan). Fundus photographs of each eye were taken during a period of fixating a central target while the head was placed in a perfectly upright position. Using a computer program, a straight line was drawn through the center of the papilla and the macula. By measuring the angle between this line and an earth-horizontal line, the CR of each eye was determined. The BCR of the fundus was calculated using the following formula:

$$BCR = \frac{CR\ right\ eye\ -\ CR\ left\ eye}{2} \quad (2)$$

By definition, positive values represent a vestibular hypofunction of the right side. Based on normative data in the literature, a fundus rotation equal to or > 1.9 degrees from zero was defined as pathological (17).

Data Analysis

The data were extracted from the clinic information system on local hospital servers. For anonymization, the personal data of subjects were coded, and any personal data, such as names or birthdates, were not included. Results of diagnostic tests were analyzed with Pearson's chi-square test and Pearson's correlation using SPSS statistics program (IBM, Armonk, USA). Matlab (MathWorks, Natick, MA, USA) was used for age-matching, bootstrapping, and calculating mean distributions between two groups.

RESULTS

Ocular Vestibular Evoked Myogenic Potentials vs. Subjective Visual Vertical

Among the patients, 43 patients showed pathological SVV test results, 16 of them paired with pathological oVEMP asymmetries to either side. SVV was normal in 95 patients; 61 of these patients also had normal, i.e., symmetric, oVEMP. Considering the laterality of the pathology, there was no correlation ($p > 0.05$, Fisher's exact test; **Table 1**) between normal and pathological SVV and oVEMP measurements.

There was also no correlation between oVEMP-AR and SVV (**Figure 2**).

TABLE 1 | Cross table of SVV and oVEMP.

			oVEMP		
			Asymmetry to the left	**Normal**	**Asymmetry to the right**
SVV	Tilt to the left	% of SVV (n)	9.7% (3)	64.5% (20)	25.8% (8)
	Normal	% of SVV (n)	22.1% (21)	64.2% (61)	13.7% (13)
	Tilt to the right	% of SVV (n)	33.3% (4)	58.3% (7)	8.3% (1)

SVV, subjective visual vertical; oVEMP, ocular vestibular evoked myogenic potential. Pearson's chi-square test: not significant (p = 0.233). Fisher's exact test (33.3% of cell count <5): 5.382 (p = 0.234).

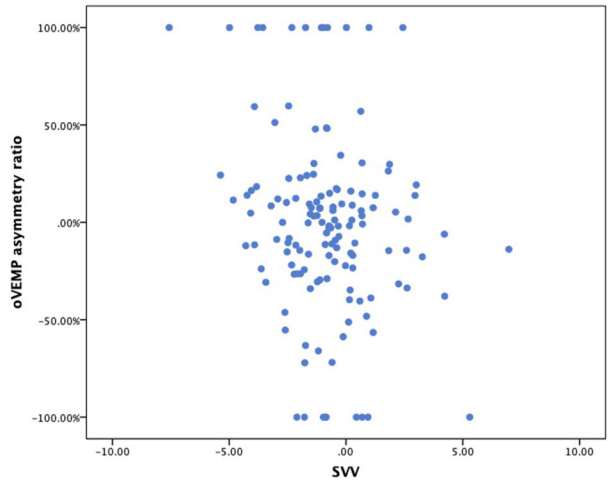

FIGURE 2 | Scatterplot of SVV (x-axis) vs. oVEMP asymmetry ratio (y-axis). SVV, subjective visual vertical; oVEMP, ocular vestibular evoked myogenic potentials.

In a second analysis, the hypothesis of a common chronic pattern with central compensation of SVV and BCR (low frequency), but not of oVEMP (high frequency), was explored. Among the patients, two age-matched groups were selected with an iterative algorithm for minimal age difference, one group with normal oVEMP and one group with pathological oVEMP results. In the first group *(oVEMP p norm)*, normal oVEMP would combine with pathological SVV on either the left (−1) or the right (+1) side, or with normal SVV (0). When bootstrapping the mean of this group, we would therefore expect this value to show a normal distribution around 0. The second group *(oVEMP p path)* contains pathological oVEMP values and the corresponding SVV values. Congruent pathological SVV values were assigned to the value +1, non-congruent SVV to −1, normal SVV to 0. Bootstrapping the mean of this second group, the normal distribution of SVV would be shifted in the positive direction, if pathological oVEMP were to show congruent pathological SVV values. **Figure 3** shows that both groups (patients with normal oVEMP and patients with pathological oVEMP asymmetries) show a normal distribution around 0. Such pattern agrees with the hypothesis that SVV may become normal while oVEMP can still be asymmetric.

The same analysis was also applied to SVV values and their corresponding oVEMP value. Again, among the patients, two age-matched groups were selected with an iterative algorithm for minimal age difference, one group with normal SVV and one group with pathological SVV results. In the first group *(SVV p norm)*, normal SVV results would combine with pathological oVEMP on either the left (−1) or the right (+1) side, or with normal oVEMP (0). When bootstrapping the mean of this group, we would therefore expect this value to show a normal distribution around 0. The second group *(SVV p path)* contains pathological SVV values and the corresponding oVEMP values. Congruent pathological SVV values were assigned to +1, non-congruent SVV values to −1, and normal SVV values to 0. We expected that pathological SVV would generally combine with a congruent oVEMP asymmetry, i.e., a shift in the normal distribution of *SVV p path* toward 1 when compared to *SVV p norm*. **Figure 4** shows that this shift cannot be observed; therefore, the expected congruency between pathological SVV with pathological oVEMP could not be demonstrated in our data (**Figure 4**).

Binocular Cyclorotation vs. Subjective Visual Vertical

Here, 99 out of the 138 patients had also undergone fundus photography to measure BCR. Since both SVV and BCR result from a static, i.e., low-frequency, asymmetry of the utricular signals, we expected to find a direct correlation (18). Among them, 36 patients showed a pathological SVV, 19 of them also showing abnormal results in the fundus rotation. However, 63 patients had normal SVV results, 49 of them also showing normal BCR. The correlation between the SVV results and the fundus rotation was highly significant ($p < 0.001$, Fisher's exact test; **Table 2**).

Figure 5 depicts the scatterplot of the significant correlation between SVV and BCR.

Ocular Vestibular Evoked Myogenic Potentials vs. Binocular Cyclorotation

After finding a direct correlation between SVV and BCR, patients' oVEMP data were also compared with the BCR as a control for the initial SVV and oVEMP comparison. Here, 33 patients were measured with abnormal oVEMP, 12 of them

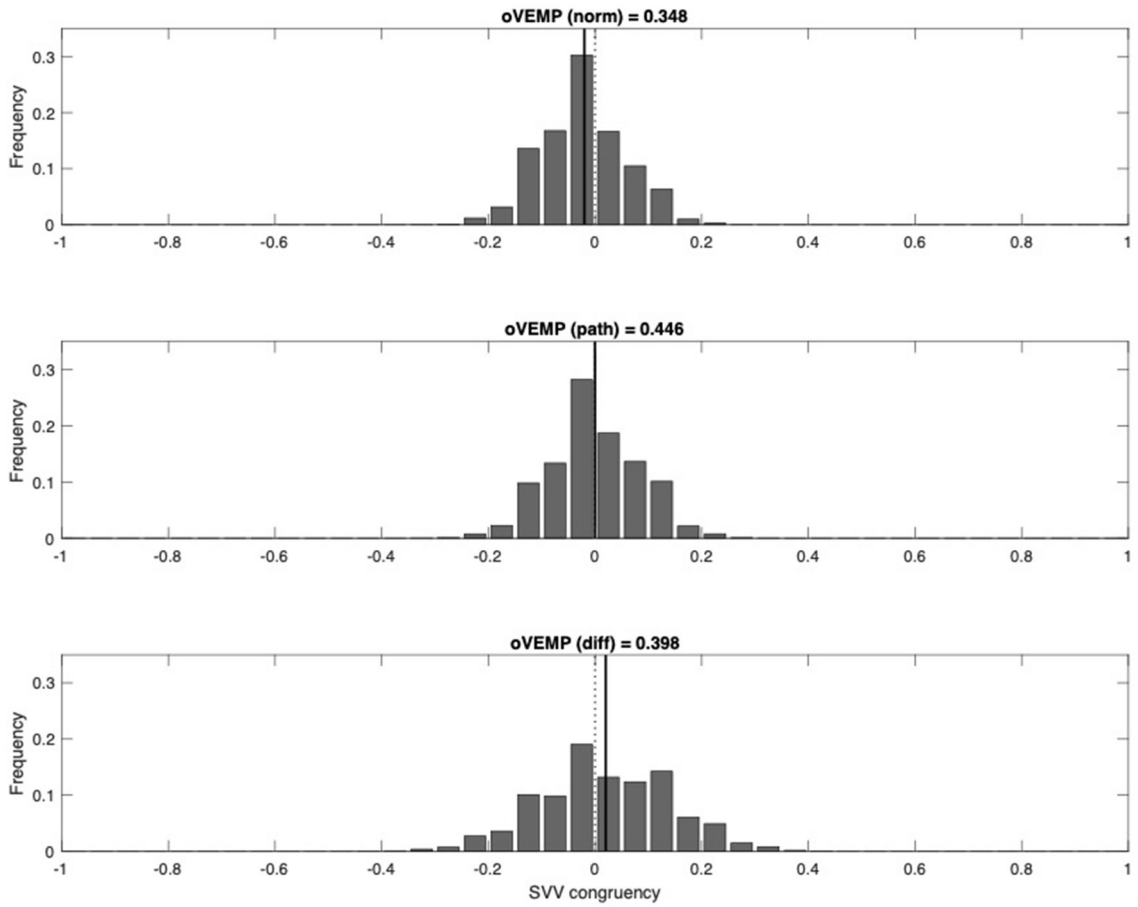

FIGURE 3 | Congruency between oVEMP and SVV (upper panel, patients with normal oVEMP; middle panel, patients with asymmetric oVEMP; lower panel, difference). Groups of patients are age-matched. For each patient, a congruency value for SVV was assigned. Congruency value in patients with normal oVEMP: 0, SVV normal; 1, SVV tilted to the right; −1, SVV tilted to the left. Congruency value in patients with asymmetric oVEMP: 0, SVV normal; 1, SVV congruent with oVEMP asymmetry; −1, SVV not congruent with oVEMP asymmetry. Frequency distributions of means were obtained by bootstrapping. oVEMP, ocular vestibular evoked myogenic potential; SVV, subjective visual vertical.

also showing pathological fundus rotation. Of the 66 patients with normal oVEMP, 46 also measured normal fundus rotation. The direct correlation between oVEMP and BCR (taking into account the laterality of the pathology) was significant ($p < 0.05$, Fisher's exact test; **Table 3**), but with a low Cramer's index. There was no significant correlation between oVEMP and BCR, as shown in **Figure 6** (Spearman-rho correlation coefficient −0.114, $p = 0.261$).

Diagnosis-Specific Measurements

The data were analyzed by each diagnosis separately. Here, it became apparent that for oVEMP and SVV data, there is no significant intervariability between each group and that the range of pathological measurements is large (**Figures 7**, **8**).

DISCUSSION

This study shows that in an unselected sample of patients with vertigo or dizziness, oVEMP results (normal, right side pathological, left side pathological) were not predictive of SVV results (normal, deviated to the right, deviated to the left) or BCR results (normal, CR to the right, CR to the left). There were no correlations between oVEMP and SVV and between oVEMP and BCR. The possible chronic pattern of persistent oVEMP asymmetry and normalized (i.e., compensated) SVV, however, is compatible with our findings. Moreover, SVV and BCR results correlated highly, as it has previously been shown by Curthoys et al. (18) and Schmidt et al. (19).

Putting the study into context with previous work, Nagai et al. (20) had consistent results, not finding SVV and oVEMP results to correlate in patients with different acute pathologies of the inner ear. Ogawa et al. (21) also did not find a significant correlation in the rates of abnormal SVV and abnormal oVEMP results when examining patients over the course of 20 days after the onset of vestibular neuritis. In contrast, the study by Lin and Young (22) did find a significant correlation between SVV and oVEMP in healthy subjects as well as in patients with Menière's disease. In a 2016 conducted study, Taylor et al. (23)

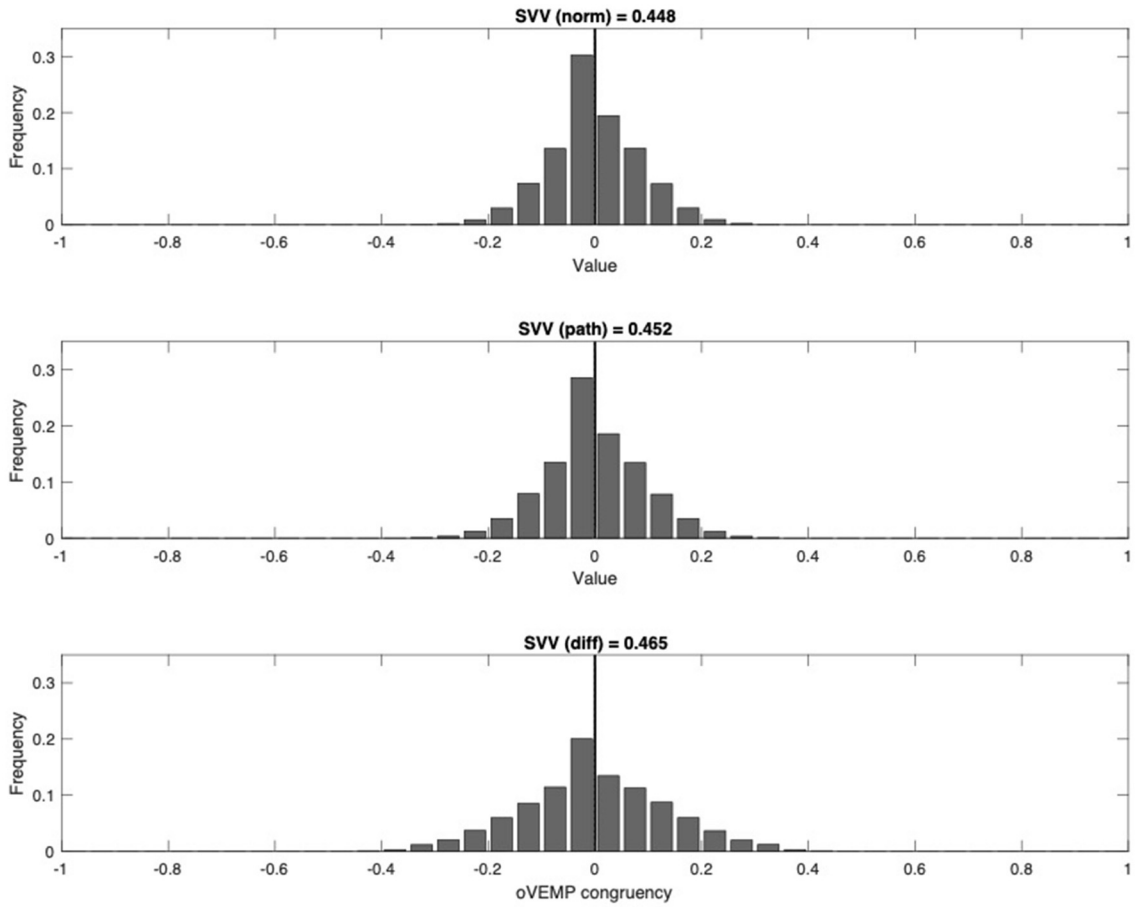

FIGURE 4 | Congruency between SVV and oVEMP (upper panel, patients with normal SVV; middle panel, patients with pathologic SVV; lower panel, difference). Groups of patients are age-matched. For each patient, a congruency value for oVEMP was assigned. Congruency value in patients with normal SVV: 0, oVEMP normal; 1, oVEMP tilted to the right; −1, oVEMP tilted to the left. Congruency value in patients with pathologic SVV: 0, oVEMP normal; 1, oVEMP congruent with pathological SVV; −1, oVEMP not congruent with pathological SVV. Frequency distributions of means were obtained by bootstrapping. oVEMP, ocular vestibular evoked myogenic potential; SVV, subjective visual vertical.

TABLE 2 | Cross table of SVV and BCR.

			BCR		
			Tilt to the left	**Normal**	**Tilt to the right**
SVV	Tilt to the left	% of SVV (n)	51.9% (14)	44.4% (12)	3.7% (1)
	Normal	% of SVV (n)	17.5% (11)	77.8% (49)	4.8% (3)
	Tilt to the right	% of SVV (n)	0.0% (0)	55.6% (5)	44.4% (4)

SVV, subjective visual vertical; BCR, binocular cyclorotation. Pearson's chi-square test: significant (p = 0.000). Fisher's exact test (33.3% of cell count <5): 22.419, p < 0.001. Cramer V = 0.395.

found concordant results between subjective visual horizontal (an alternative static test to the SVV) and oVEMP in the acute setting of vestibular neuritis in 38 patients. In the follow-up of 16 of these patients 12 month later, a similar recovery pattern was reported for the two tests (23). Because of compensation mechanisms that are more effective in static vestibular function tests, Magliulo et al. (24) postulated that oVEMP can be of better use as a prognostic parameter. A lack of correlation for oVEMP and BCR has also been described in healthy controls and in patients with vestibular neuritis by Cherchi (25) and Zalewski et al. (26).

It can be hypothesized that the incongruent SVV and oVEMP results are explained by the different functioning of the two cell types found in otolith organs, one effective for static stimulation, the other for dynamic stimulation (5, 27). This differentiation between the computation of static and dynamic

vestibular signals not only applies to a peripheral level but also is of importance in central vestibular structures (28, 29). As the segregation of static and dynamic vestibular signals carries over to central structures, separate compensation mechanisms could be plausible. Further, it can be hypothesized that pathologies of the utricle could affect the two cell types differently and therefore lead to divergent results when testing the static and dynamic systems. This is supported in the findings that, in humans, the cells of the macula show different involvement after being exposed to external influences. In the study of Lyford-Pike et al. (30), it has been demonstrated that type 1 cells show greater gentamicin accumulation than type 2 cells when exposed to the antibiotic.

In our study, we examined the correlation between oVEMP and SVV in a relatively large number of patients with different diagnoses, which so far has not been reported by others. In contrast to previous studies, the laterality of SVV and oVEMP asymmetries was also taken into account, an important factor when looking for a correlation between the two tests. Moreover, the highly significant correlation between SVV and BCR results provides good evidence that BCR data can usually be used to confirm the SVV results, if they are in doubt. This of course is limited to vestibular diagnostic workup, since BCR remains an important tool in the evaluation of neuro-ophthalmological conditions (31).

The main limitation of the study lies in the singular measurement per patient. To assess the hypothesis of SVV results changing from initial pathological findings to a state of compensation, a prospective study with set examination points after a first measurement during the acute stage would be interesting, as it would give insight to changes from the acute to the chronic stages.

The findings from this study support the use of multiple vestibular tests in patients with vertigo or dizziness. We demonstrated that oVEMPs are an important expansion of the diagnostic workup for utricle function and cannot replace SVV testing. Since there is a strong correlation between SVV and BCR, BCR measurements might be of use in cases of unclear SVV results.

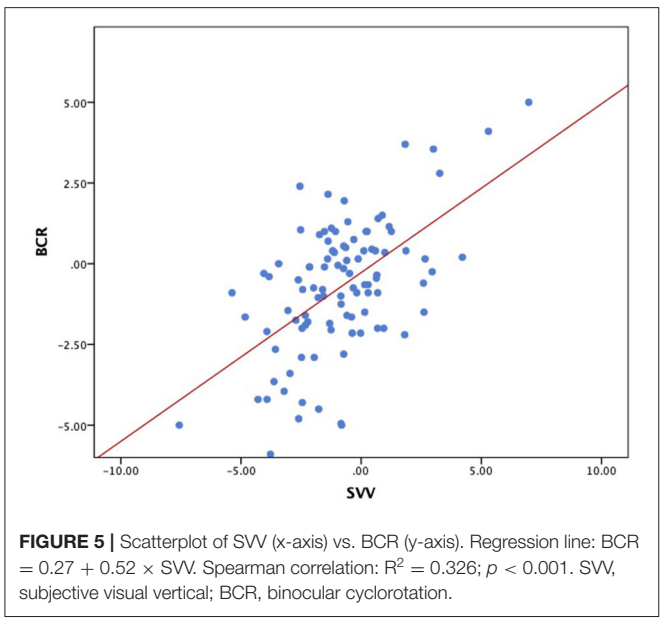

FIGURE 5 | Scatterplot of SVV (x-axis) vs. BCR (y-axis). Regression line: BCR = 0.27 + 0.52 × SVV. Spearman correlation: $R^2 = 0.326$; $p < 0.001$. SVV, subjective visual vertical; BCR, binocular cyclorotation.

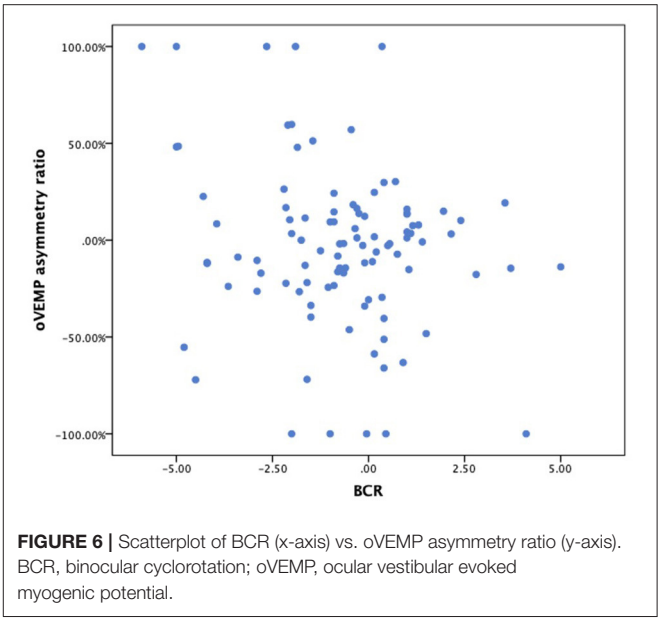

FIGURE 6 | Scatterplot of BCR (x-axis) vs. oVEMP asymmetry ratio (y-axis). BCR, binocular cyclorotation; oVEMP, ocular vestibular evoked myogenic potential.

TABLE 3 | Cross table of oVEMP and BCR.

			BCR		
			Tilt to the left	**Normal**	**Tilt to the right**
oVEMP	Asymmetry to the left	% of oVEMP (n)	15.8% (3)	78.9% (15)	5.3% (1)
	Normal	% of oVEMP (n)	20.9% (14)	68.7% (46)	10.4% (7)
	Asymmetry to the right	% of oVEMP (n)	61.5% (8)	38.5% (5)	0.0% (0)

oVEMP, ocular vestibular evoked myogenic potential; BCR, binocular cyclorotation. Pearson's chi-square test: significant (p = 0.022). Fisher's exact test (44.4% of cells expected count <5): 9.239, p = 0.038. Cramer V = 0.243.

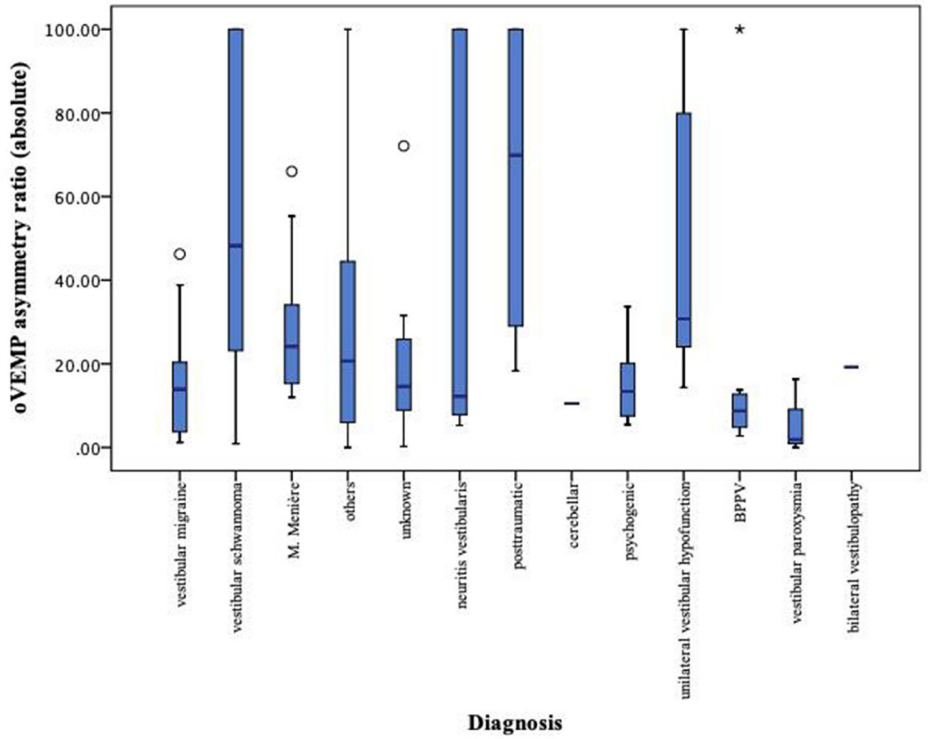

FIGURE 7 | Boxplot of oVEMP measurements for each diagnosis separately. oVEMP, ocular vestibular evoked myogenic potential; left-sided values (original data = <0) and right-sided values (original data = >0) both expressed as positive values. *Extreme value, below quartile 1 or above quartile 3.

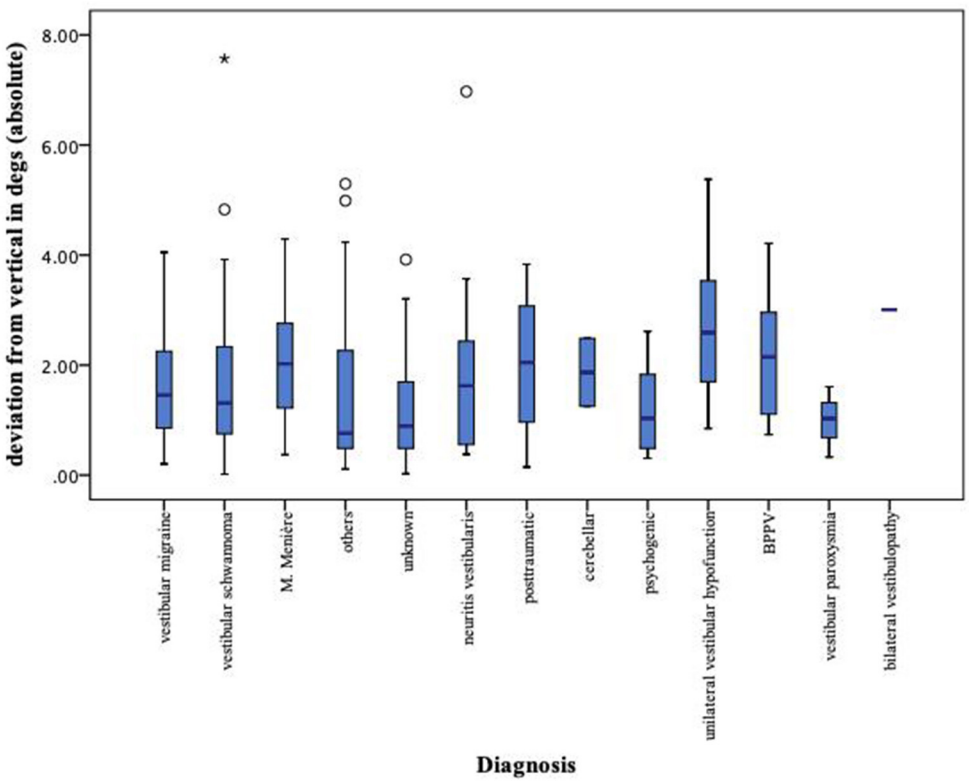

FIGURE 8 | Boxplot of SVV measurements for each diagnosis separately. SVV, subjective visual vertical; left-sided values (original data = <0) and right-sided values (original data = >0) both expressed as positive values. *Extreme value, below quartile 1 or above quartile 3.

DATA AVAILABILITY STATEMENT

The datasets presented in this article are not readily available because this would jeopardize patient confidentiality. Requests to access these datasets should be directed to sarah.hoesli@uzh.ch.

ETHICS STATEMENT

The studies involving human participants were reviewed and approved by Ethics committee Zurich, Switzerland. The patients/participants had provided a written general consent for the use of their data for research purpose.

AUTHOR CONTRIBUTIONS

DS designed and developed the concept of the study. SH gathered and organized the data and wrote the manuscript in consultation with DS. SH and DS contributed to the analysis of the data and interpretation of the results.

FUNDING

This work was supported by the Dr. Dabbous Foundation.

REFERENCES

1. Curthoys IS. The interpretation of clinical tests of peripheral vestibular function. *Laryngoscope.* (2012) 122:1342–52. doi: 10.1002/lary.23258
2. Weber KP, Rosengren SM. Clinical utility of ocular vestibular-evoked myogenic potentials (oVEMPs). *Curr Neurol Neurosci Rep.* (2015) 15:22. doi: 10.1007/s11910-015-0548-y
3. Iwasaki S, Chihara Y, Smulders YE, Burgess AM, Halmagyi GM, Curthoys IS, et al. The role of the superior vestibular nerve in generating ocular vestibular-evoked myogenic potentials to bone conducted vibration at Fz. *Clin Neurophysiol.* (2009) 120:588–93. doi: 10.1016/j.clinph.2008.12.036
4. Rosengren SM, Kingma H. New perspectives on vestibular evoked myogenic potentials. *Curr Opin Neurol.* (2013) 26:74–80. doi: 10.1097/WCO.0b013e32835c5ef3
5. Curthoys IS, Vulovic V. Vestibular primary afferent responses to sound and vibration in the guinea pig. *Exp Brain Res.* (2011) 210:347–52. doi: 10.1007/s00221-010-2499-5
6. Tabak S, Collewijn H, Boumans LJ. Deviation of the subjective vertical in long-standing unilateral vestibular loss. *Acta Otolaryngol.* (1997) 117:1–6. doi: 10.3109/00016489709117982
7. Pinar HS, Ardiç FN, Topuz B, Kara CO. Subjective visual vertical and subjective visual horizontal measures in patients with chronic dizziness. *J Otolaryngol.* (2005) 34:121–5. doi: 10.2310/7070.2005.04014
8. Tribukait A, Bergenius J, Brantberg K. Subjective visual horizontal during follow-up after unilateral vestibular deafferentation with gentamicin. *Acta Otolaryngol.* (1998) 118:479–87. doi: 10.1080/00016489850154595
9. Curthoys IS, Halmagyi GM. Vestibular compensation: a review of the oculomotor, neural, and clinical consequences of unilateral vestibular loss. *J Vestib Res.* (1995) 5:67–107.
10. Strupp M, Arbusow V, Maag KP, Gall C, Brandt T. Vestibular exercises improve central vestibulospinal compensation after vestibular neuritis. *Neurology.* (1998) 51:838–44. doi: 10.1212/WNL.51.3.838
11. Helmchen C, Klinkenstein J, Machner B, Rambold H, Mohr C, Sander T. Structural changes in the human brain following vestibular neuritis indicate central vestibular compensation. *Ann N Y Acad Sci.* (2009) 1164:104–15. doi: 10.1111/j.1749-6632.2008.03745.x
12. Schmid-Priscoveanu A, Böhmer A, Obzina H, Straumann D. Caloric and search-coil head-impulse testing in patients after vestibular neuritis. *J Assoc Res Otolaryngol.* (2001) 2:72–8. doi: 10.1007/s101620010060
13. Hong SM, Yeo SG, Byun JY, Park MS, Park CH, Lee JH. Subjective visual vertical during eccentric rotation in patients with vestibular neuritis. *Eur Arch Otorhinolaryngol.* (2010) 267:357–61. doi: 10.1007/s00405-009-1064-y
14. Valko Y, Hegemann SC, Weber KP, Straumann D, Bockisch CJ. Relative diagnostic value of ocular vestibular evoked potentials and the subjective visual vertical during tilt and eccentric rotation. *Clin Neurophysiol.* (2011) 122:398–404. doi: 10.1016/j.clinph.2010.06.023
15. Schönfeld U, Clarke AH. A clinical study of the subjective visual vertical during unilateral centrifugation and static tilt. *Acta Otolaryngol.* (2011) 131:1040–50. doi: 10.3109/00016489.2011.584902
16. Young YH. Potential application of ocular and cervical vestibular-evoked myogenic potentials in Meniere's disease: a review. *Laryngoscope.* (2013) 123:484–91. doi: 10.1002/lary.23640
17. Dieterich M, Brandt T. Ocular torsion and tilt of subjective visual vertical are sensitive brainstem signs. *Ann Neurol.* (1993) 33:292–9. doi: 10.1002/ana.410330311
18. Curthoys IS, Dai MJ, Halmagyi GM. Human ocular torsional position before and after unilateral vestibular neurectomy. *Exp Brain Res.* (1991) 85:218–25. doi: 10.1007/BF00230003
19. Schmidt T, Hamann KF, Hofmann I, Klopfer M, Kono Kono JO. [Acute peripheral vestibular lesions. Monocular subjective visual vertical and cyclodeviation]. *Ophthalmologe.* (2002) 99:363–6. doi: 10.1007/s00347-001-0565-x
20. Nagai N, Ogawa Y, Hagiwara A, Otsuka K, Inagaki T, Shimizu S, et al. Ocular vestibular evoked myogenic potentials induced by bone-conducted vibration in patients with unilateral inner ear disease. *Acta Otolaryngol.* (2014) 134:151–8. doi: 10.3109/00016489.2013.844361
21. Ogawa Y, Otsuka K, Shimizu S, Inagaki T, Kondo T, Suzuki M. Subjective visual vertical perception in patients with vestibular neuritis and sudden sensorineural hearing loss. *J Vestib Res.* (2012) 22:205–11. doi: 10.3233/VES-2012-0447
22. Lin KY, Young YH. Correlation between subjective visual horizontal test and ocular vestibular-evoked myogenic potential test. *Acta Otolaryngol.* (2011) 131:149–55. doi: 10.3109/00016489.2010.518973
23. Taylor RL, McGarvie LA, Reid N, Young AS, Halmagyi GM, Welgampola MS. Vestibular neuritis affects both superior and inferior vestibular nerves. *Neurology.* (2016) 87:1704–12. doi: 10.1212/WNL.0000000000003223
24. Magliulo G, Gagliardi S, Ciniglio Appiani M, Iannella G, Re M. Vestibular neurolabyrinthitis: a follow-up study with cervical and ocular vestibular evoked myogenic potentials and the video head impulse test. *Ann Otol Rhinol Laryngol.* (2014) 123:162–73. doi: 10.1177/0003489414522974
25. Cherchi M. Utricular function in vestibular neuritis: a pilot study of concordance/discordance between ocular vestibular evoked myogenic potentials and ocular cycloposition. *Exp Brain Res.* (2019) 237:1531–8. doi: 10.1007/s00221-019-05529-8
26. Zalewski CK, Ackley RS, McCaslin DL, Clark MD, Hanks WD, Brewer CC. Examination of utricular response using oVEMP and unilateral centrifugation rotation testing. *Ear Hear.* (2018) 39:910–21. doi: 10.1097/AUD.0000000000000552
27. Curthoys IS. Concepts and physiological aspects of the otolith organ in relation to electrical stimulation. *Audiol Neurootol.* (2020) 25:25–34. doi: 10.1159/000502712
28. Curthoys IS, MacDougall HG, Vidal PP, de Waele C. Sustained and transient vestibular systems: a physiological basis for interpreting vestibular function. *Front Neurol.* (2017) 8:117. doi: 10.3389/fneur.2017.00117
29. Straka H, Beraneck M, Rohregger M, Moore LE, Vidal PP, Vibert N. Second-order vestibular neurons form separate

populations with different membrane and discharge properties. *J Neurophysiol.* (2004) 92:845–61. doi: 10.1152/jn.00107.2004

30. Lyford-Pike S, Vogelheim C, Chu E, Della Santina CC, Carey JP. Gentamicin is primarily localized in vestibular type I hair cells after intratympanic administration. *J Assoc Res Otolaryngol.* (2007) 8:497–508. doi: 10.1007/s10162-007-0093-8
31. Lemos J, Eggenberger E. Clinical utility and assessment of cyclodeviation. *Curr Opin Ophthalmol.* (2013) 24:558–65. doi: 10.1097/ICU.0000000000000003

Conflict of Interest: The authors declare that the research was conducted in the absence of any commercial or financial relationships that could be construed as a potential conflict of interest.

Advantages of publishing in Frontiers

OPEN ACCESS
Articles are free to read for greatest visibility and readership

FAST PUBLICATION
Around 90 days from submission to decision

HIGH QUALITY PEER-REVIEW
Rigorous, collaborative, and constructive peer-review

TRANSPARENT PEER-REVIEW
Editors and reviewers acknowledged by name on published articles

Frontiers
Avenue du Tribunal-Fédéral 34
1005 Lausanne | Switzerland

Visit us: www.frontiersin.org
Contact us: frontiersin.org/about/contact

REPRODUCIBILITY OF RESEARCH
Support open data and methods to enhance research reproducibility

DIGITAL PUBLISHING
Articles designed for optimal readership across devices

FOLLOW US
@frontiersin

IMPACT METRICS
Advanced article metrics track visibility across digital media

EXTENSIVE PROMOTION
Marketing and promotion of impactful research

LOOP RESEARCH NETWORK
Our network increases your article's readership